Advanced Series in Physical Chemistry - Vol. 1

PHYSICAL CHEMISTRY OF SOLIDS

Basic Principles of Symmetry and Stability of Crystalline Solids

H. F. Franzen

World Scientific

This page is intentionally left blank

PHYSICAL CHEMISTRY OF SOLIDS

Basic Principles of Symmetry and Stability of Crystalline Solids

This page is intentionally left blank

Advanced Series in Physical Chemistry - Vol. 1

PHYSICAL CHEMISTRY OF SOLIDS

Basic Principles of Symmetry and Stability of Crystalline Solids

H. F. Franzen
Iowa State University, USA

Editor-in-Charge
C. Y. Ng
Iowa State University, USA

World Scientific
Singapore • New Jersey • London • Hong Kong

Published by

World Scientific Publishing Co. Pte. Ltd.

P O Box 128, Farrer Road, Singapore 9128

USA office: Suite 1B, 1060 Main Street, River Edge, NJ 07661

UK office: 57 Shelton Street, Covent Garden, London WC2H 9HE

Library of Congress Cataloging-in-Publication Data

Franzen, H. F. (Hugo Friedrich), 1934–
Physical chemistry of solids : basic principles of symmetry and stability of crystalline solids / H. F. Franzen ; editor-in-charge, C. Y. Ng
p. cm. -- (Advanced series in physical chemistry ; vol. 1)
Includes bibliographical references and index.
ISBN (invalid) 9810211538. -- ISBN (invalid) 9810211546 (pbk.)
1. Solid state chemistry. I. Ng, C. Y. (Cheuk-Yiu), 1947–
II. Title. III. Series.
QD478.F73 1993
541'.0421--dc20 93-45345
CIP

First published 1994
First reprint 1995

Printed in Singapore.

INTRODUCTION

Many of us who are involved in teaching a special topic graduate course may have experienced difficulty in finding suitable references, especially reference materials put together in a suitable text format. Presently, several excellent book series exist and they have served the scientific community well in reviewing new developments in physical chemistry and chemical physics. However, these existing series publish mostly monographs consisting of review chapters of unrelated subjects. The modern development of theoretical and experimental research has become highly specialized. Even in a small subfield, experimental or theoretical, few reviewers are capable of giving an in-depth review with good balance in various new developments.

A thorough and more useful review should consist of chapters written by specialists covering all aspects of the field. This book series is established with these needs in mind. That is, the goal of this series is to publish selected graduate texts and stand-alone review monographs with specific themes, focusing on modern topics and new developments in experimental and theoretical physical chemistry. In review chapters, the authors are encouraged to provide a section of future developments and needs. We hope that the texts and review monographs of this series will be more useful to new researchers about to enter the field.

Cheuk-Yiu Ng

This page is intentionally left blank

PREFACE

I have written this book with the intention of providing a handbook of some of the major physical-chemical concepts important in the preparation, determination of structure, study of structure change and understanding of elementary band structure of crystalline solids. The book is designed to answer many of the conceptual questions that I have found to arise in my research and that of my students and colleagues. An understanding of the material of undergraduate Physical Chemistry is assumed, and the availability of more advanced texts in specialized areas of symmetry, thermodynamics, crystallography, quantum mechanics and band theory is taken for granted. The book was written in the hope that it will become for many a first source for a deeper understanding of the experiments that many perform in probing crystal chemistry.

Some of the specific areas for which concepts significantly beyond the treatments found in standard Physical Chemistry texts are developed in some detail are: (1) lattices and their interrelations, (2) space group symmetry, (3) irreducible representations of space groups, (4) phase transitions, especially second-order phase transitions, (5) group-subgroup relations, (6) heterogeneous equilibrium and the phase rule, (7) X-ray diffraction (single-crystal and powder), (8) structure determination, (9) order-disorder transitions, (10) incommensurate structure, (11) symmetry aspects of band structure and (12) least squares treatment of data.

Some of the specific analytic tools that are introduced are: (1) the systematic treatment of space lattices, (2) cell reduction, (3) Seitz operators, (4) the determination of full space-group symmetry from a set of generating elements, (5) reciprocal lattice and space, (6) loaded representations,

(7) Landau theory of symmetry and phase transitions, (8) independent net reactions, (9) configurational entropy, (10) the Ewald sphere, (11) the Fresnel construction, (12) statistical analysis of diffraction, (13) Brillouin zones and zone boundary effects (Peierl's distortion) and (14) Fourier analysis.

With such a broad range it is of course necessary that readers be referred to more advanced texts, and reference texts, as well as a few relevant scientific articles are listed in bibliographies at the end of each chapter. Each chapter is followed by a collection of problems for which detailed solutions are provided in an appendix.

It is hoped that the book will find use as a desk-top ready reference to which researchers will turn when confronted by a puzzle in the interpretation of experimental results, and that it will also stimulate further interest to explore the subjects through working the problems and reference to the literature.

Hugo F. Franzen

CONTENTS

CHAPTER 1

INTRODUCTION

1.1. Purpose and Scope

Structure, stability and electronic structure form a basis for the consideration of the properties and reactions of crystalline solids. The underlying concepts of symmetry and thermodynamics provide conceptual frameworks that can effectively guide thinking about solid-state chemistry, but take on a special character when crystalline solids are considered. It is the purpose of this book to provide an elementary overview of applications of group theory, heterogeneous equilibrium, reciprocal space concepts, diffraction theory, nonstoichiometry, phase transitions and band theory in such a way that a research scientist working on solid-state research can refer to it as a handbook of elementary concepts that apply to crystalline solids and to the experimental study of structure and stability of crystalline solids. This first chapter has the purpose of briefly reviewing some of the basic physical chemistry upon which later chapters are based, i.e., the role of irreducible representations in group theory, the role of the phase rule and the Gibbsian equations in thermodynamics, the role of plane waves in diffraction theory, and the role of symmetry in quantum mechanics. For a more complete development of these topics the reader can refer to basic texts such as those listed in the bibliography at the end of the chapter.

1.2. Symmetry Groups

A group[1] consists of a set of members and a binary combination rule. In order to be a group the set and the binary combination must obey the following:

1. all combinations of members under the binary operation must be in the set,
2. the set must contain the identity (combination of any member with the identity yields the member),
3. the set must contain the inverse of each member (combination of an element with its inverse yields the identity),
4. the elements must combine associatively.

The groups under consideration in this book consist of operations which define interchanges of regions of an object, for example interchange what is at x, y, z (in some coordinate system) with what is at $\bar{x}, \bar{y}, \bar{z}$, with the result that the object after interchange is indistinguishable from the object before the interchange. Such operations are called *symmetry operations.* For example, when an object is invariant to exchange of x, y, z, and $\bar{x}, \bar{y}, \bar{z}$ it is said to exhibit *inversion symmetry.* In a Cartesian coordinate system a general proper or improper rotational symmetry operation can be specified by a 3×3 matrix, β, that defines how the regions of the object are interchanged, i.e., if β is a matrix corresponding to a symmetry operation and

$$\beta \begin{pmatrix} x \\ y \\ z \end{pmatrix} = \begin{pmatrix} x' \\ y' \\ z' \end{pmatrix}, \tag{1}$$

then interchanging what is at x, y, z with what is at x', y', z' leaves the object in a state that is indistinguishable from that before the interchange. Such symmetry operations combine under the binary rule of consecutive operation, fulfilling all of the requirements of a group.

Symmetry operations that transform x, y, z also transform functions, i.e., if a symmetry operation takes x, y, z into x', y', z' then it takes $\phi(x, y, z)$ into $\phi(x', y', z')$. A set of *basis functions* is generated by so transforming an initial function or set of functions and adding to the set any generated function that is not a linear combination of functions already in the set. For example, consider the symmetry operations of a four-fold rotation about the z axis: $\varepsilon, C_{4z}, C_{2z}, C_4^3 z$ (Table 1.1). The pair of functions, $\sin 2\pi x, \sin 2\pi y$ form a basis set, as can be seen by the behavior of these functions under the symmetry operations as shown in Table 1.1.

In general, a set of basis functions, $\phi_1, \phi_2, \phi_3 \ldots$, obeys the rule that a linear combination of the functions transforms into itself or a new linear combination under a symmetry operation of the group, i.e., $\Sigma c_i \phi_i$ trans-

Table 1.1. The symmetry operations of C_4 and their effect upon $\sin 2\pi x$.

Operations	Effect upon x, y, z	Effect upon $\sin 2\pi x$
ε	x, y, z	$\sin 2\pi x$
C_{4z}	$\bar{y}, x, z$	$-\sin 2\pi y$
C_{2z}	$\bar{x}, \bar{y}, z$	$-\sin 2\pi x$
C_{4z}^3	$y, \bar{x}, z$	$\sin 2\pi y$

forms into $\Sigma c_i' \phi_i$ under a symmetry operation. It is possible to write down matrices that *represent* the symmetry operations relative to the basis. For example, under C_{4z}:

$$\begin{pmatrix} 0 & \bar{1} \\ 1 & 0 \end{pmatrix} \begin{pmatrix} \sin 2\pi x \\ \sin 2\pi y \end{pmatrix} = \begin{pmatrix} -\sin 2\pi y \\ \sin 2\pi x \end{pmatrix} \tag{2}$$

and under C_{2z}:

$$\begin{pmatrix} \bar{1} & 0 \\ 0 & \bar{1} \end{pmatrix} \begin{pmatrix} \sin 2\pi x \\ \sin 2\pi y \end{pmatrix} = \begin{pmatrix} -\sin 2\pi x \\ -\sin 2\pi y \end{pmatrix} \tag{3}$$

In this way a matrix (not necessarily distinct from other matrices in the set) can represent each symmetry element. The representation matrices have the property that they multiply as do the symmetry operations, e.g., $C_{4z} \cdot C_{2z} = C_4^3 z$ and

$$\begin{pmatrix} 0 & \bar{1} \\ 1 & 0 \end{pmatrix} \begin{pmatrix} \bar{1} & 0 \\ 0 & \bar{1} \end{pmatrix} = \begin{pmatrix} 0 & 1 \\ \bar{1} & 0 \end{pmatrix} \tag{4}$$

gives the matrix representing C_{4z}^3 with the basis functions $\sin 2\pi x$ and $\sin 2\pi y$.

As a second example consider the operations of Table 1.2. These are the operations of a two-fold axis of rotation, an inversion center and a horizontal reflection plane, the *symmetry elements* to which the operations of the set correspond. These symmetry elements combine as shown in Fig. 1.1. Any two of the operations combine to yield a third operation of the set (closure), each element is its own inverse (inverses belong to the set) and the identity operation is included. Such symmetry operations always combine associatively, thus the set $\{\varepsilon, C_{2z}, i, \sigma_z\}$ forms a group (called C_{2h} or $2/m$).

Table 1.2. The symmetry operations of $C_{2h}(2/m)$.

Symmetry operations	Effect upon x, y, z
ε	x, y, z
C_{2z}	$\bar{x}, \bar{y}, z$
i	$\bar{x}, \bar{y}, \bar{z}$
σ_z	$x, y, \bar{z}$

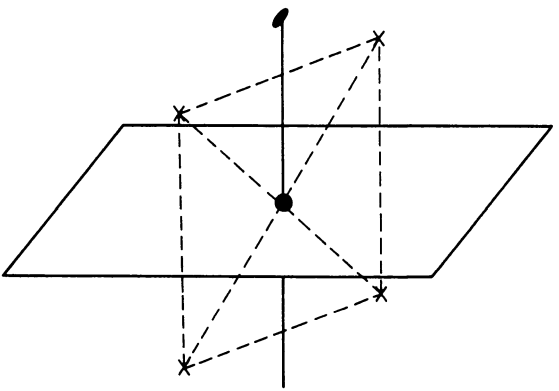

Fig. 1.1. The symmetry elements of C_{2h}.

The set of three functions $\phi_1 = x, \phi_2 = y, \phi_3 = z$ forms a basis and yields the representations:

$$\begin{pmatrix} 1 & 0 & 0 \\ 0 & 1 & 0 \\ 0 & 0 & 1 \end{pmatrix} \begin{pmatrix} x \\ y \\ z \end{pmatrix} = \begin{pmatrix} x \\ y \\ z \end{pmatrix} \tag{5}$$

represents ε,

$$\begin{pmatrix} \bar{1} & 0 & 0 \\ 0 & \bar{1} & 0 \\ 0 & 0 & 1 \end{pmatrix} \begin{pmatrix} x \\ y \\ z \end{pmatrix} = \begin{pmatrix} \bar{x} \\ \bar{y} \\ z \end{pmatrix} \tag{6}$$

represents C_{2z},

$$\begin{pmatrix} \bar{1} & 0 & 0 \\ 0 & \bar{1} & 0 \\ 0 & 0 & \bar{1} \end{pmatrix} \begin{pmatrix} x \\ y \\ z \end{pmatrix} = \begin{pmatrix} \bar{x} \\ \bar{y} \\ \bar{z} \end{pmatrix} \tag{7}$$

represents i, and

$$\begin{pmatrix} 1 & 0 & 0 \\ 0 & 1 & 0 \\ 0 & 0 & \bar{1} \end{pmatrix} \begin{pmatrix} x \\ y \\ z \end{pmatrix} = \begin{pmatrix} x \\ y \\ \bar{z} \end{pmatrix} \tag{8}$$

represents σ_z. Clearly, just as $C_{2z} \cdot i = \sigma_z$,

$$\begin{pmatrix} \bar{1} & 0 & 0 \\ 0 & \bar{1} & 0 \\ 0 & 0 & 1 \end{pmatrix} \begin{pmatrix} \bar{1} & 0 & 0 \\ 0 & \bar{1} & 0 \\ 0 & 0 & \bar{1} \end{pmatrix} = \begin{pmatrix} 1 & 0 & 0 \\ 0 & 1 & 0 \\ 0 & 0 & \bar{1} \end{pmatrix}, \tag{9}$$

and similarly for other combinations, i.e., the matrices multiply as do the operations they represent.

In this case there is no symmetry operation that interchanges the functions (there are no off diagonal elements in the representation matrices). This is a sufficient condition that a multidimensional representation can be *reduced.* That is, it is possible to express the information contained in the 3×3 matrices given above in a greater number of smaller matrices — in this case in sets of 1×1 matrices, and the given three dimensional representation can be reduced to three one-dimensional representations. By examining the 3×3 matrices, it is clear that there are two different 1×1 matrix sets, one of which occurs twice, into which the three-dimensional representation can be decomposed as shown in Table 1.3. The basis functions are listed in the fifth column, where it appears that both x and y are bases for the same one-dimensional representation, and hence this representation appears twice in the three-dimensional representation.

Table 1.3. Decomposition of the vector representation of C_{2h} into one-dimensional representations.

ϵ	C_{2z}	i	σ_z	Basis functions
1	−1	−1	1	x, y
1	1	−1	−1	z

In terms of the basis functions, *reducing* a block diagonalized representation is the process of breaking up the sets of basis functions into subsets. Although it is not obvious from the examples given, it is possible to find a reduction when one exists by rotating the axis system, and thus transforming the basis functions and matrices, and finding a new orientation in

which the transformed matrices all have the same block-diagonal form and the transformed functions form subsets that do not mix under any symmetry operation. Discussions of such *similarity transformations* are a standard part of texts on group theory.[1] When it is no longer possible to reduce a representation (i.e., to find similarity transformations that transform basis functions into closed subsets), then the resultant *irreducible representations* play an important role in the applications of group theory. One important reason for this is that the basis functions for an irreducible representation do not mix with, and are therefore fundamentally symmetrically inequivalent to, the basis functions for other irreducible representations, while the basis functions for a given irreducible representation, when there are more than one, do interchange under symmetry operations.

A complete development of group theory yields a number of properties of irreducible representations that are useful both in reducing a representation and in determining when a set of representations contains one or more reducible representations. One is that the order of a group (the number of symmetry elements) is the sum of the squares of the dimensions of a complete set of distinct irreducible representations. In the case of C_{2h}, two different one-dimensional (and therefore necessarily irreducible) representations are listed in Table 1.3. The group is of order 4. The only possibility is that there are two additional one-dimensional irreducible representations.

Another property of irreducible representations is that they always include the totally symmetric representation, i.e., there exists a totally symmetric basis function that transforms into itself under all operations of the group. Examples here would be x^2, or y^2, or z^2. A third useful characteristic of irreducible representations is that they are pairwise orthogonal. Letting the sum of the diagonal elements of the matrix representing β_i be $\chi(\beta_i)$, this means in part that

$$\sum_i \chi_1(\beta_i)\chi_2^*(\beta_i) = 0 \tag{10}$$

where the subscripts 1 and 2 label two different irreducible representations, the subscript i labels the symmetry elements in the group and χ^* is the complex conjugate of χ. The traces of the matrices, $\chi(\beta_i)$, are called the *characters* of a representation.

Considering the two irreducible representations of Table 1.3 together with the totally symmetric representation, three pairwise orthogonal one-dimensional irreducible representations have been found for C_{2h}. The

fourth irreducible representation follows from the orthogonality condition. A set of irreducible representations of C_{2h} is given in Table 1.4.

Table 1.4. The character table for C_{2h}.

ϵ	C_{2z}	i	σ_z	Basis functions
1	1	1	1	x^2 or y^2 or z^2
1	−1	−1	1	x or y
1	1	−1	−1	z
1	−1	1	−1	xz or yz

The three-dimensional reducible representation found above using the basis functions x, y and z is called the *vector representation* because it provides a description of how vectors in three dimensional space transform under the symmetry operations of the group. The characters of the vector representation of C_{2h} are given in Table 1.5.

Table 1.5. Characters of the vector representation of C_{2h}.

ϵ	C_{2z}	i	σ_z
3	−1	−3	1

In Table 1.3 a reduction into irreducible representations was given for this representation. If this reduction were not known, it would be possible to discover it using only the characters of the reducible representation and those of the irreducible representations. These characters behave like orthogonal components of a vector, i.e., taking n_1 times the characters of the first irreducible representation (Table 1.4), n_2 times those of the second, etc. and combining the characters of Table 1.4 to yield those of Table 1.5:

$$n_1 + n_2 + n_3 + n_4 = 3 \tag{11}$$

$$n_1 - n_2 + n_3 - n_4 = -1 \tag{12}$$

$$n_1 - n_2 - n_3 + n_4 = -3 \tag{13}$$

$$n_1 + n_2 - n_3 - n_4 = 1 \tag{14}$$

yields the result $n_1 = n_4 = 0, n_2 = 2, n_3 = 1$. This confirms the result obtained previously by inspection, i.e., the vector representation can be reduced into representation 2 (which occurs twice) and representation 3.

Table 1.6. One reducible and two irreducible representations of C_4.

ϵ	C_{4z}	C_{2z}	$C_4^3 z$	Basis functions
1	1	1	1	x^2+y^2, z^2
1	−1	1	−1	xy
2	0	−2	0	(x, y)

Returning to C_4, the group of Table 1.1, a two-dimensional representation was found using $\sin 2\pi x$ and $\sin 2\pi y$. Since there are four symmetry operations in the group, and since there must be at least one one-dimensional representation (i.e., the totally symmetric), it follows that there are four one-dimensional irreducible representations, and that this two-dimensional representation is reducible. Two irreducible representations are easily found, the totally symmetric and one that transform as xy. The characters of these are listed in Table 1.6 together with the characters of the two-dimensional representation of Table 1.1. The two-dimensional representation is orthogonal to the two one-dimensional representations given in the table, thus it must be composed of the remaining two one-dimensional representations. The characters of these irreducible representations $(\chi_j(\varepsilon), \chi_j(C_{4z}), \chi_j(C_{2z}), \chi_j(C_{4z}^3), j = 1, 2)$ obey

$$\chi_j(\varepsilon) + \chi_j(C_{4z}) + \chi_j(C_{2z}) + \chi_j(C_{4z}^3) = 0 \tag{15}$$

by orthogonality to the first one-dimensional representation and

$$\chi_j(\varepsilon) - \chi_j(C_{4z}) + \chi_j(C_{2z}) - \chi_j(C_{4z}^3) = 0 \tag{16}$$

by orthogonality to the second one-dimensional representation of Table 1.6. Thus,

$$\chi_j(\varepsilon) = -\chi_j(C_{2z}) \tag{17}$$

and

$$\chi_j(C_{4z}) = -\chi_j(C_{4z}^3)\,. \tag{18}$$

Since the identity operation combined with any operation yields that operation, by definition, it follows that $\chi_j(\varepsilon) = 1$, and thus $\chi_j(C_{2z}) = -1$. Further, since $C_{4z}^2 = C_{2z}$, it follows that

$$\chi_j(C_{4z}) = \pm i\,. \tag{19}$$

Taking i for one irreducible representation and $-i$ for the other yields the results of Table 1.7. Thus, the two-dimensional representation is reducible to complex one-dimensional representations.

Table 1.7. Character table for C_4.

ϵ	C_{4z}	C_{2z}	$C_4^3 z$	Basis functions
1	1	1	1	x^2+y^2, z^2
1	−1	1	−1	xy
1	i	−1	$-i$	$x+iy$
1	$-i$	−1	i	$x-iy$

The groups discussed here (C_{2h} and C_4) are examples of point groups, i.e., groups for which all symmetry elements (axes, planes, centers) have at least one point in common. The crystalline solid state requires the consideration of space groups for which translational symmetry combines with rotational symmetry with the following results: (1) all axes, planes and centers do not meet at a common point, and (2) the operations of plane and axis elements can be generalized to include those of glide-planes and screw-axes. The treatment of these subjects forms a major part of Chapters 2–5.

1.3. Thermodynamics of Condensed Systems

The laws of classical thermodynamics,[2] i.e., the zeroth, first and second laws, establish the existence of the macroscopic properties, U, the internal energy, S, the entropy, and T, the temperature, for macroscopic systems in states of rest. In order to effectively use these properties, it is necessary to also know the number of properties that are required to fix the state of a system (the number of independent variables). This number can be considered for a variety of circumstances, e.g., in the presence or absence of externally applied electric, magnetic or gravitational fields, with or without arbitrary barriers to the flow of heat, the equilibration of pressure or the flow of matter and in systems with or without consequential surface effects. In the various circumstances the number of variables required to fix the state of the system differ. In this book systems of interest will be limited to those in which at most fields are constant in space and are the same before and after processes, those in which there are no arbitrary barriers to internal equilibration and those for which surface effects are negligible. These conditions result in simple systems for which the fundamental postulate that $c+2$ properties, at least p (the number of phases) of which must

be extensive, fix the macroscopic state of a system at rest.[2] The number c is the number of chemical content variables, i.e., the number of quantity variables required to specify the chemical contents of the system. The determination of the quantity c is a major topic of Chapter 7.

This postulate, which is a basic requirement for chemical thermodynamic treatments as they are usually developed, leads immediately to the Gibbs phase rule. Thus, by the postulate, $c + 2$ variables fix the macroscopic state of a system at rest, and, by definition, f independent intensive variables fix the intensive state of each phase, and hence with f intensive variables specified and p quantities fixing the amount of each phase, the state of the system is fixed. Therefore, $f + p$ variables fix the macroscopic state of a simple system at rest, and $c + 2$ do also, and

$$f + p = c + 2 \tag{20}$$

or

$$f = c - p + 2\,. \tag{21}$$

The thermodynamic consideration of chemical equilibrium plays an important role in thinking about solids and their preparation. In particular, as will be developed in Chapter 7, such consideration plays an important part in the determination of the chemical content variable number. The combined first and second laws yield, for reversible processes in closed systems,

$$dU = dq + dw \tag{22}$$

and $dq = TdS$ and $dw = -PdV$ for reversible exchanges of energy by heat and pressure-volume work mechanisms for closed simple systems. Thus,

$$dU = TdS - PdV \tag{23}$$

for such changes. In other words, the internal energy of a closed, simple system, with or without chemical reactions, can be reversibly altered in two different kinds of interactions with the surroundings: those involving a force operating through a distance (work mechanisms, $dU = -PdV$ for reversible work exchanges of simple systems) and those that do not (heat mechanisms, $dU = TdS$ for reversible heat exchanges of simple systems). If, in addition, reversible matter exchange occurs, then

$$dU = TdS - PdV + \sum_{i=1}^{c} \mu_i dn_i \tag{24}$$

where c is the number of chemical substances (substances for which n_i, the number of moles, can be defined) reversibly exchanged with the surroundings, and

$$\mu_i = \frac{\partial U}{\partial n_i}\Big)_{s,v,n_j} \tag{25}$$

by definition. The fundamental equation for reversible changes in simple systems (Eq. 24) forms the basis for the discussion of heterogeneous equilibrium in Chapter 7.

1.4. Diffraction

Diffraction[3,4] can be analyzed in terms of the interactions of waves modeled by complex numbers, i.e., by $f \exp i\phi$ where f is the *magnitude* and ϕ is the *phase angle*. By Euler's theorem,

$$f \exp i\phi = f(\cos\phi + i \sin\phi) \tag{26}$$

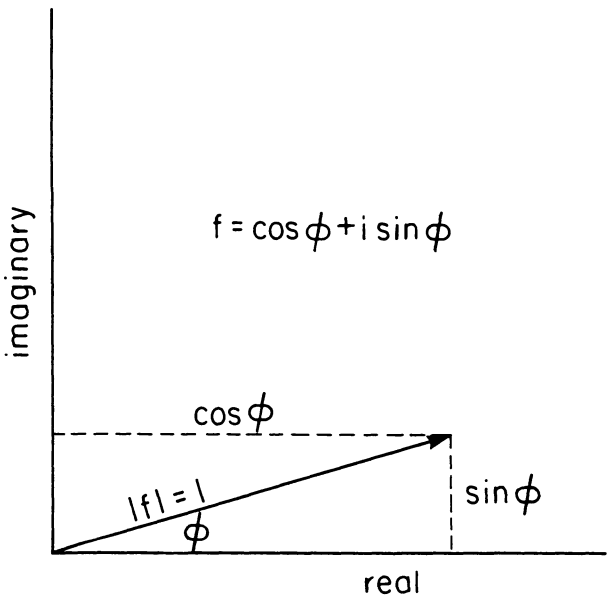

Fig. 1.2. Complex plane diagram illustrating that $\exp i\phi$ is an operator that rotates a vector by ϕ in this plane.

and thus

$$|f \exp i\theta| = \sqrt{f^2(\cos\phi + i\sin\phi)(\cos\phi - i\sin\phi)} = f\sqrt{\cos^2\phi + \sin^2\phi} = f\,. \tag{27}$$

In the complex plane exp $i\phi$ is a unit vector that makes the angle ϕ with the positive real axis (Fig. 1.2). X-rays, neutrons, electrons and other diffracting entities combine as do complex numbers, i.e., two waves f_i exp $i\phi_1$ and f_2 exp $i\phi_2$ combine as shown in Fig. 1.3.

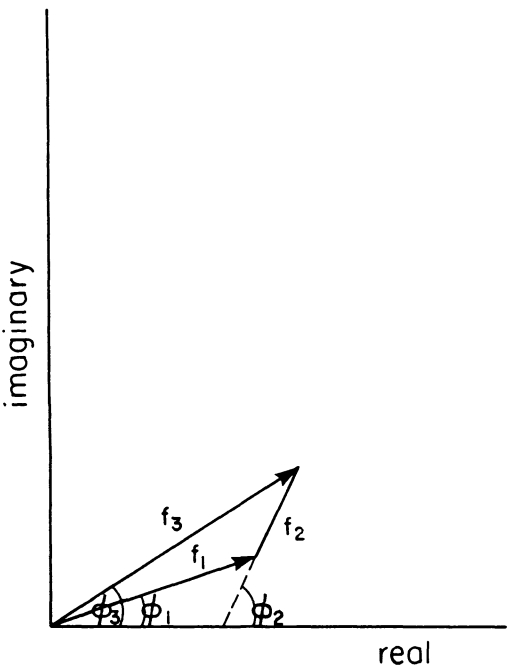

Fig. 1.3. Vector combination in the complex plane.

X-ray diffraction is an important tool of solid-state research and is the subject of Chapters 8 and 9. If an incoming ray is scattered at random by a variety of scatterers, the scattered waves will be out of phase, i.e., will point in a variety of directions in the complex plane. If there are sufficiently many random phases, then the vector sum (the resultant wave) will have negligible magnitude. If the scatterers are systematically out of phase,

then when summed over a sufficiently large number of scatterers the vector sum will also have negligible magnitude. This is the case of destructive interference. On the other hand, when subsets of the scatterers are in phase (line up along the real axis in the positive or negative direction), then the diffraction is constructive unless the subsets exactly cancel (which is the case of systematic absence), and this is the condition for observation of diffraction.

1.5. Quantum Mechanics

It is very helpful when applying quantum mechanics[5] to chemical systems to think in terms of operators that change functions in specified ways. For example, if a symmetry operator carries $\mathbf{r}$ into $T\mathbf{r}(x, y, z$ into $x', y', z')$ then it carries $f(\mathbf{r})$ into $f(T\mathbf{r})$ and we can write

$$\theta(T)f(\mathbf{r}) = f(T\mathbf{r}) \tag{28}$$

where $\theta(T)$ is the operator for the function f corresponding to T. If the operator yields the function itself multiplied by a real or complex number, then the function is an *eigenfunction* of the operator, and the number is its *eigenvalue*. Thus, the basis functions for one-dimensional representations of a symmetry group are eigenfunctions of the symmetry operators and the eigenvalues of these function are the characters of one-dimensional representations.

The Hamiltonian operator, $H(\mathbf{r})$, is the same at all symmetry equivalent points in the system and is thus invariant under symmetry operations of the group. Thus, it is the same whether $H(\mathbf{r})$ or $H(T\mathbf{r})$ operates upon $f(\mathbf{r})$, i.e.,

$$\theta(T)H(\mathbf{r})f(\mathbf{r}) = H(T\mathbf{r})f(T\mathbf{r}) \tag{29}$$

$$= H(T\mathbf{r})\theta(T)f(\mathbf{r}) \tag{30}$$

$$= H(\mathbf{r})\theta(T)f(\mathbf{r})\,, \tag{31}$$

and

$$\theta(T)H(\mathbf{r}) = H(\mathbf{r})\theta(T) \tag{32}$$

i.e., the Hamiltonian operator and symmetry operators for a given system commute. Thus, if $\{\phi_n(\mathbf{r})\}$ is a complete set of ℓ independent eigenfunctions

of $H(\mathbf{r})$ with eigenvalue E, then

$$H(\mathbf{r})\theta(T)\phi_n(\mathbf{r}) = \theta(T)H(\mathbf{r})\phi_n(\mathbf{r}) \tag{33}$$

$$= E\theta(T)\phi_n(\mathbf{r}) \tag{34}$$

and $\theta(T)\phi_n(\mathbf{r})$ is also an eigenfunction of $H(\mathbf{r})$ with eigenvalue E and therefore it must be a linear combination of $\phi_n(\mathbf{r})$ with $n = 1, 2 \ldots, \ell$ because these functions, by hypothesis, formed a complete set. Thus

$$\theta(T)\phi_n(\mathbf{r}) = \sum_{m=1}^{\ell} \Gamma_{mn}(T)\phi_m(\mathbf{r}) \tag{35}$$

for each n. Considering three symmetry operators, T_1, T_2 and T_1T_2,

$$\theta(T_1)\phi_n(\mathbf{r}) = \sum_{m=1}^{\ell} \Gamma_{mn}(T_1)\phi_m(\mathbf{r})\,, \tag{36}$$

$$\theta(T_2)\theta(T_1)\phi_n(\mathbf{r}) = \sum_{p=1}^{\ell} \Gamma_{pn}(T_1)\theta(T_2)\phi_p(\mathbf{r}) \tag{37}$$

$$= \sum_{p=1}^{\ell} \Gamma_{pn}(T_1) \sum_{m=1}^{\ell} \Gamma_{mp}(T_2)\phi_m(\mathbf{r}) \tag{38}$$

$$= \sum_{m=1}^{\ell} \sum_{p=1}^{\ell} \Gamma_{pn}(T_1)\Gamma_{mp}(T_2)\phi_m(\mathbf{r}) \tag{39}$$

and since

$$\theta(T_2T_1)\phi_n(\mathbf{r}) = \sum_{m=1}^{\ell} \Gamma_{mn}(T_2T_1)\phi_m(\mathbf{r}) \tag{40}$$

$$= \theta(T_2)\theta(T_1)\phi_n(\mathbf{r})\,, \tag{41}$$

therefore,

$$\sum_{m=1}^{\ell} \sum_{p=1}^{\ell} \Gamma_{pn}(T_1)\Gamma_{mp}(T_2)\phi_m(\mathbf{r}) = \sum_{m=1}^{\ell} \Gamma_{mn}(T_2T_1)\phi_m(\mathbf{r})\,. \tag{42}$$

The linear independence of the ϕ_n's implies the equality of the coefficients of the same ϕ_m on each side of the equality, and

$$\Gamma_{mn}(T_2T_1) = \sum_{p=1}^{\ell} \Gamma_{pn}(T_1)\Gamma_{mp}(T_2)\,. \tag{43}$$

These are the characteristics of basis functions of the group, i.e., by Eq. 42 linear combinations of the functions transform into linear combinations and Eq. 43 describes how the elements of representation matrices combine. In other words, a set of eigenfunctions that correspond to a single eigenvalue of the Hamiltonian operator are also basis functions for a representation of the symmetry group. Since functions with different symmetries will correspond to different energies (and thus different eigenvalues of the Hamiltonian) except by accident, the energy eigenvalues correspond to single irreducible representations, the dimensions of the representations are the degeneracies of the energy levels, and the energy levels can be labeled according to the irreducible representations to which they correspond. This is the basis for the assignment of labels to points and lines that appear on energy band diagrams. The irreducible representations of space groups are the subject of Chapter 5, and the elementary energy band concepts to which these irreducible representations correspond are the subject of Chapter 10.

Bibliography

1. F. A. Cotton, *Chemical Applications of Group Theory* (Wiley-Interscience, New York, 1990), 3rd ed.
2. M. Modell and R. C. Reid, *Thermodynamics and Its Applications* (Prentice-Hall, Englewood Cliffs, New Jersey, 1983), 2nd ed.
3. A. Guinier, *X-Ray Diffraction* (W.H. Freeman, San Francisco, 1963).
4. M. J. Buerger, *Crystal-Structure Analysis* (John Wiley and Sons, New York, 1960).
5. J. F. Cornwell, *Group Theory and Electronic Energy Bands in Solids* (North Holland, Amsterdam, 1969).

Problems

1. Find the irreducible representations of the point group C_3.
2. Decompose the vector representation of C_3 into irreducible representations (also of C_3).
3. Find the representation of C_4 for which $\sin \pi x$ and $\sin \pi y$ form a basis and decompose this representation into irreducible representations.
4. Show that $\Sigma \mu_i dn_i = 0$ for a reversible chemical reaction in a closed simple system.
5. Show that Cu(s), Cu_2O(s) and CuO(s) will coexist in equilibrium at a single fixed temperature if the pressure is fixed.
6. Show that $\sum_{n=1}^{\infty} \exp in\pi/10 = 0$.
7. Find $|F|$ if $F = 6 \exp i\pi/3 + 8 \exp i\pi/6$.
8. For diamond at 298 K and 1 bar, $C_p = 6.11$ JK^{-1} mol^{-1}, $\kappa = -\frac{1}{V}\left(\frac{\partial V}{\partial P}\right)_T = 1.87 \times 10^{-7}$ bar^{-1}, $\alpha = \frac{1}{V}\left(\frac{\partial V}{\partial T}\right)_P = 2.7 \times 10^{-6}$ K^{-1} and $\rho = 3.513$ g cm^{-3}. Taking C_p, κ and α to be constant, find $\Delta \overline{U}$ when P is increased from 1 bar to 1000 bar at 298 K, and when T is increased from 298 K to 1000 K at 1 bar.

CHAPTER 2

THE BRAVAIS LATTICES

2.1. The Space Lattice

Translationally periodic solids are described by the specification of atom positions within unit cells, i.e., within conceptual parallelopipeds that pack so as to fill space. The parallelopipeds are defined by three vectors, of which no two are collinear and which are not coplanar (Fig. 2.1). The vectors are labeled so that the projection of $\mathbf{b} \times \mathbf{c}$ upon $\mathbf{a}$ is positive, i.e., so that $\mathbf{a} \cdot \mathbf{b} \times \mathbf{c} > 0$. The quantity $\mathbf{a} \cdot \mathbf{b} \times \mathbf{c} = \mathbf{b} \cdot \mathbf{c} \times \mathbf{a} = \mathbf{c} \cdot \mathbf{a} \times \mathbf{b} = \mathbf{V}$ is the volume of the unit cell. The vectors $n_1\mathbf{a} + n_2\mathbf{b} + n_3\mathbf{c}$, with n_1, n_2, n_3 any triple of integers, terminate in environments that are symmetrically equivalent to the origin.

To achieve a compact notation, let $\mathbf{a}_1 = \mathbf{a}, \mathbf{a}_2 = \mathbf{b}, \mathbf{a}_3 = \mathbf{c}, |\mathbf{a}_i| = a_i$ and $r_{ij} = \mathbf{a}_i \cdot \mathbf{a}_j = a_i a_j \cos \alpha_{ij}$. The set of vectors $\{\mathbf{T}\}$ defined by $\mathbf{T} = \sum_{i=1}^{3} n_i \mathbf{a}_i$

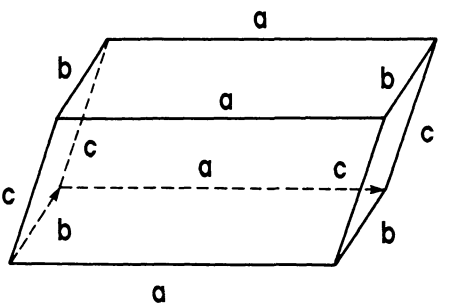

Fig. 2.1. A unit cell.

with n_1, n_2, n_3 running over all possible triples of integers and with the vectors originating from a common origin specifies an infinite array of end points. This array of end points is called a *space lattice.*

2.2. Symmetry of Lattices

A rotational symmetry of a lattice is a relationship which relates the coordinates of lattice points through a 3×3 matrix. For example, all sets of vectors $\{\mathbf{T}\}$ contain $-\mathbf{T}$ whenever they contain $\mathbf{T}$ and thus if $\mathbf{R} = X\mathbf{a}_1 + Y\mathbf{a}_2 + Z\mathbf{a}_3$ is the location of a lattice point, regardless of the axis system, then also is $-\mathbf{R} = -X\mathbf{a}_1 - Y\mathbf{a}_2 - Z\mathbf{a}_3$, and the corresponding 3 × 3 matrix is

$$\begin{pmatrix} \bar{1} & 0 & 0 \\ 0 & \bar{1} & 0 \\ 0 & 0 & \bar{1} \end{pmatrix} \begin{pmatrix} X \\ Y \\ Z \end{pmatrix} = \begin{pmatrix} \overline{X} \\ \overline{Y} \\ \overline{Z} \end{pmatrix} \tag{1}$$

All lattices have the symmetry of inversion through the origin.

If $\mathbf{a}_1$ is perpendicular to both $\mathbf{a}_2$ and $\mathbf{a}_3$ (i.e., is proportional to $\mathbf{a}_2 \times \mathbf{a}_3$), then a lattice point at $X\mathbf{a}_1 + Y\mathbf{a}_2 + Z\mathbf{a}_3$ implies one at $-X\mathbf{a}_1 + Y\mathbf{a}_2 + Z\mathbf{a}_3$ and the lattice is said to have reflection symmetry with the reflection plane perpendicular to $\mathbf{a}_1$ (Fig. 2.2). In this case the matrix operation is

$$\begin{pmatrix} \bar{1} & 0 & 0 \\ 0 & 1 & 0 \\ 0 & 0 & 1 \end{pmatrix} \begin{pmatrix} X \\ Y \\ Z \end{pmatrix} = \begin{pmatrix} \overline{X} \\ Y \\ Z \end{pmatrix} . \tag{2}$$

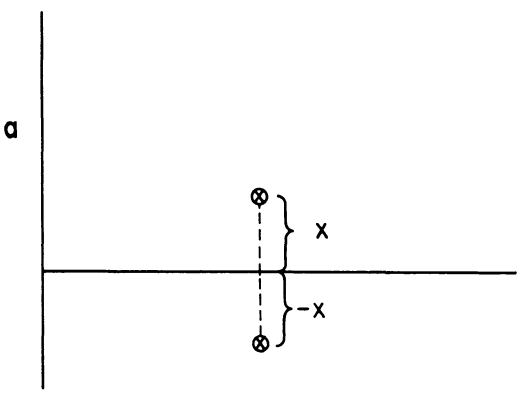

Fig. 2.2. The operation of reflection through a plane perpendicular to a.

If a lattice does exhibit reflection symmetry through a plane perpendicular to $\mathbf{a}_1$, then because all lattices exhibit inversion symmetry, it also has the symmetry implied by

$$\begin{pmatrix} \bar{1} & 0 & 0 \\ 0 & \bar{1} & 0 \\ 0 & 0 & \bar{1} \end{pmatrix} \begin{pmatrix} \bar{1} & 0 & 0 \\ 0 & 1 & 0 \\ 0 & 0 & 1 \end{pmatrix} = \begin{pmatrix} 1 & 0 & 0 \\ 0 & \bar{1} & 0 \\ 0 & 0 & \bar{1} \end{pmatrix} \tag{3}$$

which is a 180° rotation about the a_1 axis (Fig. 1.1).

2.3. Proper and Improper Rotation Symmetry

Two symmetry operations that are related as are the rotation and reflection discussed above, i.e., for which

$$\overline{C}_n = i \cdot C_n \,, \tag{4}$$

where C_n means rotation by $2\pi/n$, are called proper and improper rotations. For proper rotations, the determinant of the 3 × 3 matrix is positive; for improper rotations, it is negative. Since all lattices are centrosymmetric, they necessarily exhibit both proper and improper rotational symmetry if they exhibit either. The operations of inversion and reflection are both improper rotations: inversion is the operation of a $\bar{1}$ axis and reflection is the operation of a $\bar{2}$ axis. The combination of $C_2, \overline{C}_2 = \sigma_n$ and i is as shown in Fig. 1.1 and is given the symbols C_{2h} and $2/m$. Lattices with $2/m$ symmetry are called *monoclinic*.

2.4. Categories of Lattices

A general lattice can be described with the a_1 axis expressed as the sum of a component perpendicular to both $\mathbf{a}_2$ and $\mathbf{a}_3(\lambda_1 \mathbf{a}_2 \times \mathbf{a}_3)$ and components along $\mathbf{a}_2$ and $\mathbf{a}_3(\lambda_2 \mathbf{a}_2$ and $\lambda_3 \mathbf{a}_3$, with $\lambda_2 < 1$ and $\lambda_3 < 1)$ without loss of generality, i.e.,

$$\mathbf{a}_1 = \lambda_1 \mathbf{a}_2 \times \mathbf{a}_3 + \lambda_2 \mathbf{a}_2 + \lambda_3 \mathbf{a}_3 \,. \tag{5}$$

Thus, in general,

$$\begin{aligned} \mathbf{T} = n_1 \mathbf{a}_1 + n_2 \mathbf{a}_2 + n_3 \mathbf{a}_3 = n_1 \lambda_1 (\mathbf{a}_2 \times \mathbf{a}_3) \\ + (n_2 + \lambda_2 n_1) \mathbf{a}_2 + (n_3 + \lambda_3 n_1) \mathbf{a}_3 \,. \end{aligned} \tag{6}$$

2.4.1. *The Monoclinic Lattice*

Choosing the vector with $n_1 = 1, n_2 = n_3 = 0$ in Eq. 6 yields

$$\mathbf{T} = \lambda_1(\mathbf{a}_2 \times \mathbf{a}_3) + \lambda_2\mathbf{a}_2 + \lambda_3\mathbf{a}_3\,, \tag{7}$$

a translational symmetry vector. If a plane of lattice points perpendicular to $\mathbf{a}_2 \times \mathbf{a}_3$ is a reflection plane, then

$$\sigma\mathbf{T} = -\lambda_1(\mathbf{a}_2 \times \mathbf{a}_3) + \lambda_2\mathbf{a}_2 + \lambda_3\mathbf{a}_3 \tag{8}$$

is also a translational symmetry operation and therefore also is

$$\mathbf{T} - \sigma\mathbf{T} = 2\lambda_1(\mathbf{a}_2 \times \mathbf{a}_3)\,. \tag{9}$$

There are two possibilities — either the point midway along $\mathbf{T} - \sigma\mathbf{T}$ is a lattice point or it is not. If it is, then the shortest vector perpendicular to $\mathbf{a}_2 \times \mathbf{a}_3$ is $\lambda_1(\mathbf{a}_2 \times \mathbf{a}_3)$ and by convention (*b axis unique*) this is taken to be the *b* axis. The lattice vectors are $\mathbf{a}_2 = \mathbf{c}, \mathbf{a}_3 = \mathbf{a}, \lambda_1(\mathbf{a}_2 \times \mathbf{a}_3) = \mathbf{b}$ and the *lattice parameters* are $a = |\mathbf{a}|, b = |\mathbf{b}|, c = |\mathbf{c}|, \beta = \cos^{-1}(\mathbf{a} \cdot \mathbf{c}/ac)$. Using the vectors $\mathbf{a}, \mathbf{b}, \mathbf{c}$ to describe the lattice, the symmetry operations of the lattice can be described in matrix form as shown in Table 2.1.

Table 2.1. Matrices transforming X, Y, Z in $2/m$.

Symmetry operation	Matrix operating on $\begin{pmatrix} X \\ Y \\ Z \end{pmatrix}$
σ_y	$\begin{pmatrix} 1 & 0 & 0 \\ 0 & \bar{1} & 0 \\ 0 & 0 & 1 \end{pmatrix}$
C_{2y}	$\begin{pmatrix} \bar{1} & 0 & 1 \\ 0 & 1 & 0 \\ 0 & 0 & \bar{1} \end{pmatrix}$
i	$\begin{pmatrix} \bar{1} & 0 & 0 \\ 0 & \bar{1} & 0 \\ 0 & 0 & \bar{1} \end{pmatrix}$

2.4.2. *The Centered Monoclinic Lattice*

On the other hand, a *centered* monoclinic cell results when $\lambda_1(\mathbf{a}_2 \times \mathbf{a}_3)$ is not a lattice translation, and $\mathbf{b} = 2\lambda_1(\mathbf{a}_2 \times \mathbf{a}_3)$. To see this, first consider

$$\mathbf{T} + \sigma\mathbf{T} = 2\lambda_2\mathbf{a}_2 + 2\lambda_3\mathbf{a}_3 \tag{10}$$

which is necessarily a lattice translation. Since $\lambda_2 = \lambda_3 = 0$ is not possible (as $\lambda_1(\mathbf{a}_2 \times \mathbf{a}_3)$ is not a lattice translation), and since λ_2 and λ_3 are both less than one, the possible solutions are $\lambda_2 = 0, \lambda_3 = 1/2; \lambda_2 = 1/2, \lambda_3 = 1/2; \lambda_2 = 1/2, \lambda_3 = 0$ because the coefficients of $\mathbf{a}_2$ and $\mathbf{a}_3$ must be integral. Consider the first of these. Together with $\mathbf{a}_2 = \mathbf{c}, \mathbf{a}_3 = \mathbf{a}$ and $2\lambda_1(\mathbf{a}_2 \times \mathbf{a}_3) = \mathbf{b}$, this implies that $\mathbf{T}$ in Eq. 7,

$$\mathbf{T} = \frac{\mathbf{a} + \mathbf{b}}{2}, \tag{11}$$

is a lattice translation and in this case the monoclinic cell is centered on the C face. The case of $\lambda_2 = 1/2, \lambda_3 = 0$ centers the A face, and by relabeling the axes this can be transformed to C-centering, which is the conventional choice.

The case $\lambda_2 = \lambda_3 = 1/2$ remains. In this case

$$\mathbf{T} = \frac{\mathbf{a} + \mathbf{b} + \mathbf{c}}{2} \tag{12}$$

and the cell is body-centered. However, the axial transformation

$$\begin{pmatrix} 1 & 0 & 1 \\ 0 & 1 & 0 \\ 0 & 0 & 1 \end{pmatrix} \begin{pmatrix} \mathbf{a} \\ \mathbf{b} \\ \mathbf{c} \end{pmatrix}_{bcm} = \begin{pmatrix} \mathbf{a} \\ \mathbf{b} \\ \mathbf{c} \end{pmatrix}_{ecm} \tag{13}$$

converts the body-centered monoclinic (bcm) cell into an end-centered monoclinic (ecm) cell with C-centering. Hence, the three centered cells: A-centered, C-centered and I(body)-centered monoclinic are equivalent and the cell is usually described as C-centered with the b-axis unique.

In the preceding discussion it was assumed that the plane of lattice points was also a plane of reflection symmetry. If a lattice has reflection symmetry, then every parallel plane of lattice points is coincident with a reflection plane. To see that this is so (refer to Fig. 2.3), the occurrence of a lattice point (1), and a reflection plane (m) implies lattice point (2).

Lattice points (1) and (2) imply translation $\mathbf{T}_\perp$, which in turn implies lattice point (3). Thus, (1) and m together imply (3), which is related to (1) by reflection through the parallel plane containing (2). Since (1), (2) and (3) are all equivalent, there are parallel reflection planes through each of them. Thus, in general, lattices exhibiting reflection symmetry have parallel, equal-spaced reflection planes that coincide with lattice planes and additional reflection planes midway between them.

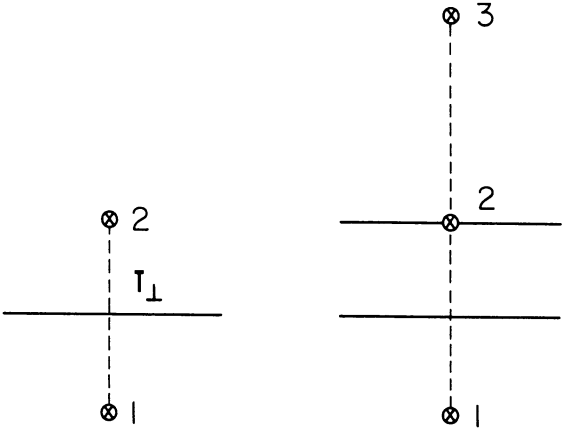

Fig. 2.3. Combination of reflection and translation symmetries.

2.4.3. *Orthorhombic Symmetry*

Consider what happens if a lattice symmetry includes two mirror planes that intersect at right angles. By the argument above we can consider the planes to intersect at a lattice point, which can be taken to be an origin. The intersection line is a two-fold axis since

$$\sigma_x \equiv \begin{pmatrix} \bar{1} & 0 & 0 \\ 0 & 1 & 0 \\ 0 & 0 & 1 \end{pmatrix}, \tag{14}$$

$$\sigma_y \equiv \begin{pmatrix} 1 & 0 & 0 \\ 0 & \bar{1} & 0 \\ 0 & 0 & 1 \end{pmatrix}, \tag{15}$$

and

$$\sigma_x \cdot \sigma_y \equiv \begin{pmatrix} \bar{1} & 0 & 0 \\ 0 & 1 & 0 \\ 0 & 0 & 1 \end{pmatrix} \begin{pmatrix} 1 & 0 & 0 \\ 0 & \bar{1} & 0 \\ 0 & 0 & 1 \end{pmatrix} = \begin{pmatrix} \bar{1} & 0 & 0 \\ 0 & \bar{1} & 0 \\ 0 & 0 & 1 \end{pmatrix} \equiv (C_{2z}) . \qquad (16)$$

Now C_{2z} and i (a symmetry of any lattice) combine to yield

$$\begin{pmatrix} \bar{1} & 0 & 0 \\ 0 & \bar{1} & 0 \\ 0 & 0 & 1 \end{pmatrix} \begin{pmatrix} \bar{1} & 0 & 0 \\ 0 & \bar{1} & 0 \\ 0 & 0 & \bar{1} \end{pmatrix} = \begin{pmatrix} 1 & 0 & 0 \\ 0 & 1 & 0 \\ 0 & 0 & \bar{1} \end{pmatrix} \equiv \sigma_z , \qquad (17)$$

the operation of a mirror plane perpendicular to the line of intersection of the other two mirror planes. It follows that a lattice with two mirror planes intersecting at right angles has three mirror planes perpendicular to each of the three orthogonal directions and intersecting at a lattice point. This lattice point is coincident with an inversion center, and a two-fold axis of symmetry lies along each of the intersection lines of the mirror planes. A symbol for this lattice symmetry is $2/m\ 2/m\ 2/m$, however this is usually shortened to *mmm* since the three mutually perpendicular mirror operations suffice to generate all other operations in the point group. An alternative symbol for this group is D_{2h}.

2.4.4. *The Orthorhombic Lattices*

The primitive orthorhombic lattice has the basic vectors **a**, **b** and **c** along the three mutually perpendicular directions of the two-fold axes. The lengths of the axes are unrelated, and the lattice parameters are $a = |\mathbf{a}|, b = |\mathbf{b}|$ and $c = |\mathbf{c}|$. As demonstrated in Section 2.4.2 the rectangular faces and the cell itself can each be centered. Centering leads to body-centered orthorhombic (*bco*), end-centered orthorhombic (*eco*) and faced-centered orthorhombic (*fco*), designated, respectively, as $I; A, B$ or C; and F centering. There is no orthorhombic lattice that centers two faces but not a third for A and B centering imply $(\mathbf{b}+\mathbf{c})/2 \in \{\mathbf{T}\}$ and $(\mathbf{a}+\mathbf{c})/2 \in \{\mathbf{T}\}$, which together imply $(\mathbf{a}+\mathbf{b})/2+\mathbf{c}$ and thus $(\mathbf{a}+\mathbf{b})/2 \in \{\mathbf{T}\}$, i.e., if two faces are centered so is the third and the lattice is face-centered orthorhombic.

2.4.5. *The Tetragonal Lattices*

The special case of a primitive lattice with *mmm* symmetry and $a = b$ exhibits 4-fold symmetry about an axis along **c** and thus $4/mmm$ (or D_{4h})

symmetry. The symbol $4/mmm$ can be dissected as follows: the 4 means 4-fold rotational symmetry along the unique, c axis. The $/m$ means a mirror plane perpendicular to this axis, the adjacent m means a mirror plane perpendicular to **a** (and one perpendicular to **b**) and the third m means a mirror plane perpendicular to $\mathbf{a}-\mathbf{b}$ (and perpendicular to $\mathbf{a}+\mathbf{b}$). These last, diagonal, reflection planes are implied by the preceding axial reflections and mirror planes as can be seen by

$$C_{4z} \equiv \begin{pmatrix} 0 & \bar{1} & 0 \\ 1 & 0 & 0 \\ 0 & 0 & 1 \end{pmatrix}, \tag{18}$$

$$\sigma_y \equiv \begin{pmatrix} 1 & 0 & 0 \\ 0 & \bar{1} & 0 \\ 0 & 0 & 1 \end{pmatrix}, \tag{19}$$

and (see Fig. 2.4)

$$C_{4z} \cdot \sigma_y \equiv \begin{pmatrix} 0 & \bar{1} & 0 \\ 1 & 0 & 0 \\ 0 & 0 & 1 \end{pmatrix} \begin{pmatrix} 1 & 0 & 0 \\ 0 & \bar{1} & 0 \\ 0 & 0 & 1 \end{pmatrix} = \begin{pmatrix} 0 & 1 & 0 \\ 1 & 0 & 0 \\ 0 & 0 & 1 \end{pmatrix} \equiv \sigma_{x+y} \,. \tag{20}$$

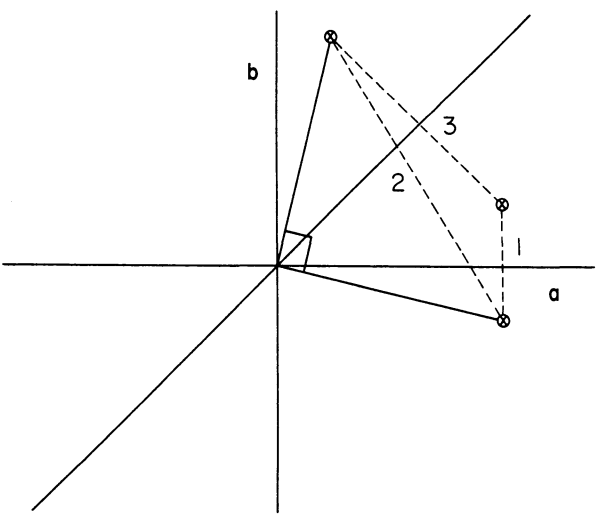

Fig. 2.4. Combination of C_{4z} and σ_y to yield σ_{x+y}.

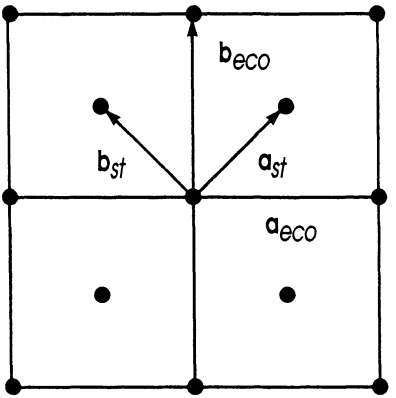

Fig. 2.5. Primitive cell for C-centered *eco* with $a = b$.

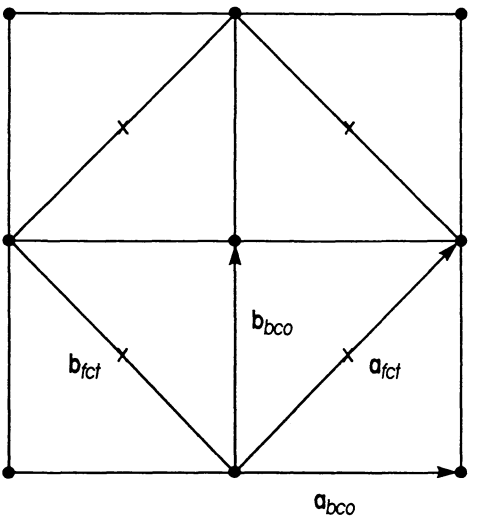

Fig. 2.6. Equivalence of *bct* and *fct*.

The eco cells, if centered on the A or B faces, do not exhibit 4-fold rotational symmetry even when $a = b$, and the C-centered eco cell with $a = b$ has $4/mmm$ symmetry but yields a smaller, primitive cell upon the transformation (see Fig. 2.5)

$$\begin{pmatrix} 1/2 & 1/2 & 0 \\ 1/2 & 1/2 & 0 \\ 0 & 0 & 1 \end{pmatrix} \begin{pmatrix} \mathbf{a} \\ \mathbf{b} \\ \mathbf{c} \end{pmatrix}_{eco} = \begin{pmatrix} \mathbf{a} \\ \mathbf{b} \\ \mathbf{c} \end{pmatrix}_{pt} \tag{21}$$

Thus, there is no end-centered tetragonal cell. Body-centered orthorhombic with $a = b$ yields body-centered tetragonal (*bct*) and face-centered orthorhombic yields face-centered tetragonal (*fct*), however *bct* and *fct* are equivalent (see Fig. 2.6) and this case is conventionally described as bct ($I4/mmm$ lattice symmetry).

2.4.6. *The Hexagonal Case*

A C-centered orthorhombic cell with $b = \sqrt{3}a$ exhibits $P6/mmm$ (or D_{6h}) symmetry (see Fig. 2.7). The hexagonal vectors, in terms of the orthorhombic ones, are

$$\begin{pmatrix} 1 & 0 & 0 \\ 1/2 & 1/2 & 0 \\ 0 & 0 & 1 \end{pmatrix} \begin{pmatrix} \mathbf{a} \\ \mathbf{b} \\ \mathbf{c} \end{pmatrix}_{eco} = \begin{pmatrix} \mathbf{a} \\ \mathbf{b} \\ \mathbf{c} \end{pmatrix}_{h}, \tag{22}$$

and thus $a_h = a_{eco}$,

$$b_h = \sqrt{\frac{a_{eco}^2}{4} + \frac{b_{eco}^2}{4}} \tag{23}$$

$$= \frac{1}{2}\sqrt{a_{eco}^2 + 3a_{eco}^2} \tag{24}$$

$$= a_{eco}, \tag{25}$$

$$\mathbf{a}_h \cdot \mathbf{b}_h = \mathbf{a}_{eco} \cdot (-\mathbf{a}_{eco} - \mathbf{b}_{eco})/2 \tag{26}$$

$$= a_h^2 \cos\gamma \tag{27}$$

and thus $\cos\gamma = -a_{eco}^2/2a_{eco}^2 = -\frac{1}{2}$, or $\gamma = 120°$.

Only C-centered and F-centered orthorhombic have the C face-centered and thus could yield hexagonal when $b = \sqrt{3}a$, however, the fco lattice does

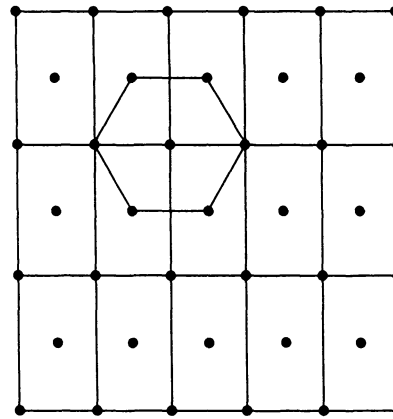

Fig. 2.7. Equivalence of hexagonal and C-centered *eco* with $b = \sqrt{3}a$.

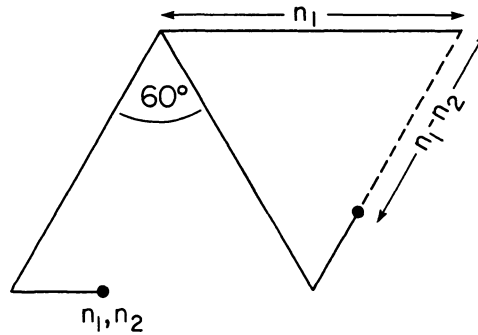

Fig. 2.8. Transformation of lattice points under C_{6z}.

not, in this case, exhibit 6-fold rotational symmetry in the plane at $\mathbf{c}/2$ (see Problem 3).

2.4.7. *Six-Fold Rotation*

The relationship between $\mathbf{T} = X\mathbf{a} + Y\mathbf{b}$ and $C_{6z}\mathbf{T} = X'\mathbf{a} + Y'\mathbf{b}$ can be discerned by consideration of Fig. 2.8. Thus,

$$\begin{pmatrix} 1 & \bar{1} & 0 \\ 1 & 0 & 0 \\ 0 & 0 & 1 \end{pmatrix} \begin{pmatrix} X \\ Y \\ Z \end{pmatrix} = \begin{pmatrix} X-Y \\ X \\ Z \end{pmatrix} . \tag{28}$$

By matrix multiplication according to $C_{6z}^2 = C_{3z}$, $C_{6z}^3 = C_{2z}$, $C_{6z}^4 = C_{3z}^{-1}$ and $C_{6z}^5 = C_{6z}^{-1}$ the matrices of Table 2.2 are produced.

Table 2.2. Matrices for transformation of X, Y, Z in hexagonal lattices.

Symmetry operation	Matrix
C_{6z}	$\begin{pmatrix} 1 & \bar{1} & 0 \\ 1 & 0 & 0 \\ 0 & 0 & 1 \end{pmatrix}$
C_{3z}	$\begin{pmatrix} 0 & \bar{1} & 0 \\ 1 & \bar{1} & 0 \\ 0 & 0 & 1 \end{pmatrix}$
C_{2z}	$\begin{pmatrix} \bar{1} & 0 & 0 \\ 0 & \bar{1} & 0 \\ 0 & 0 & 1 \end{pmatrix}$
C_{3z}^{-1}	$\begin{pmatrix} \bar{1} & 1 & 0 \\ \bar{1} & 0 & 0 \\ 0 & 0 & 1 \end{pmatrix}$
C_{6z}^{-1}	$\begin{pmatrix} 0 & 1 & 0 \\ \bar{1} & 1 & 0 \\ 0 & 0 & 1 \end{pmatrix}$

2.4.8. *The Cubic Lattices*

Additional symmetry can be found in tetragonal lattices for which special relationships between a and c occur. If $a = c$ in the pt cell, then the lattice has $m3m$ symmetry ($m3m$ means: mirror planes perpendicular to $\mathbf{a}, \mathbf{b}$, and $\mathbf{c}$; 3 fold axes along $\mathbf{a}+\mathbf{b}+\mathbf{c}$, $\mathbf{a}+\mathbf{b}-\mathbf{c}$, $\mathbf{a}-\mathbf{b}+\mathbf{c}$ and $-\mathbf{a}+\mathbf{b}+\mathbf{c}$ and mirror planes perpendicular to the face diagonals). The matrices for the proper rotational symmetry operations of $m3m$ (also called O_h) are given in Table 2.3. The complete set of 48 matrices is generated by multiplying each by the matrix corresponding to inversion and adding the product to

the set, i.e., by including all the improper rotations corresponding to the proper rotations. These 48 matrices yield the 48 signed permutations of x, y, z.

Additional symmetry is also possible for *bct* when $a = c$ (yielding *bcc*) and for *fct* when $a = c$ yielding *fcc*. Both *bcc* and *fcc* have $m3m$ symmetry, but they are not equivalent as are *bct* and *fct*.

2.4.9. *The Rhombohedral Lattice*

The symmetry $\bar{3}m$ (a 3-fold improper axis along the intersection of three mirror planes (see Fig. 2.9)) is produced when a cubic lattice is distorted to yield $a = b = c, \alpha = \beta = \gamma \neq 90°$. The lattice symmetry is rhombohedral. There is no centered rhombohedral lattice (see Problem 4).

Table 2.3. Matrices for the proper rotational operations of $m3m$.

$\varepsilon \begin{pmatrix} 1 & 0 & 0 \\ 0 & 1 & 0 \\ 0 & 0 & 1 \end{pmatrix}$	$C_{4x} \begin{pmatrix} 1 & 0 & 0 \\ 0 & 0 & \bar{1} \\ 0 & 1 & 0 \end{pmatrix}$
$C_{2x} \begin{pmatrix} 1 & 0 & 0 \\ 0 & \bar{1} & 0 \\ 0 & 0 & \bar{1} \end{pmatrix}$	$C_{4y} \begin{pmatrix} 0 & 0 & 1 \\ 0 & 1 & 0 \\ \bar{1} & 0 & 0 \end{pmatrix}$
$C_{2y} \begin{pmatrix} \bar{1} & 0 & 0 \\ 0 & 1 & 0 \\ 0 & 0 & \bar{1} \end{pmatrix}$	$C_{4z} \begin{pmatrix} 0 & \bar{1} & 0 \\ 1 & 0 & 0 \\ 0 & 0 & 1 \end{pmatrix}$
$C_{2z} \begin{pmatrix} \bar{1} & 0 & 0 \\ 0 & \bar{1} & 0 \\ 0 & 0 & 1 \end{pmatrix}$	$C_{4x}^3 \begin{pmatrix} 1 & 0 & 0 \\ 0 & 0 & 1 \\ 0 & \bar{1} & 0 \end{pmatrix}$
$C_{3(x+y+z)} \begin{pmatrix} 0 & 0 & 1 \\ 1 & 0 & 0 \\ 0 & 1 & 0 \end{pmatrix}$	$C_{4y}^3 \begin{pmatrix} 0 & 0 & \bar{1} \\ 0 & 1 & 0 \\ 1 & 0 & 0 \end{pmatrix}$
$C_{3(x+y-z)} \begin{pmatrix} 0 & 1 & 0 \\ 0 & 0 & \bar{1} \\ \bar{1} & 0 & 0 \end{pmatrix}$	$C_{4z}^3 \begin{pmatrix} 0 & 1 & 0 \\ \bar{1} & 0 & 0 \\ 0 & 0 & 1 \end{pmatrix}$

Table 2.3 (*Continued*)

$C_{3(x-y+z)} \begin{pmatrix} 0 & \bar{1} & 0 \\ 0 & 0 & \bar{1} \\ 1 & 0 & 0 \end{pmatrix}$	$C_{2(x+y)} \begin{pmatrix} 0 & 1 & 0 \\ 1 & 0 & 0 \\ 0 & 0 & \bar{1} \end{pmatrix}$
$C_{3(-x+y+z)} \begin{pmatrix} 0 & \bar{1} & 0 \\ 0 & 0 & 1 \\ \bar{1} & 0 & 0 \end{pmatrix}$	$C_{2(x+z)} \begin{pmatrix} 0 & 0 & 1 \\ 0 & \bar{1} & 0 \\ 1 & 0 & 0 \end{pmatrix}$
$C^2_{3(x+y+z)} \begin{pmatrix} 0 & 1 & 0 \\ 0 & 0 & 1 \\ 1 & 0 & 0 \end{pmatrix}$	$C_{2(y+z)} \begin{pmatrix} \bar{1} & 0 & 0 \\ 0 & 0 & 1 \\ 0 & 1 & 0 \end{pmatrix}$
$C^2_{3(x+y-z)} \begin{pmatrix} 0 & 0 & \bar{1} \\ 1 & 0 & 0 \\ 0 & \bar{1} & 0 \end{pmatrix}$	$C_{2(x-y)} \begin{pmatrix} 0 & \bar{1} & 0 \\ \bar{1} & 0 & 0 \\ 0 & 0 & \bar{1} \end{pmatrix}$
$C^2_{3(x-y+z)} \begin{pmatrix} 0 & 0 & 1 \\ \bar{1} & 0 & 0 \\ 0 & \bar{1} & 0 \end{pmatrix}$	$C_{2(x-z)} \begin{pmatrix} 0 & 0 & \bar{1} \\ 0 & \bar{1} & 0 \\ \bar{1} & 0 & 0 \end{pmatrix}$
$C^2_{3(-x+y+z)} \begin{pmatrix} 0 & 0 & \bar{1} \\ \bar{1} & 0 & 0 \\ 0 & 1 & 0 \end{pmatrix}$	$C_{2(y-z)} \begin{pmatrix} \bar{1} & 0 & 0 \\ 0 & 0 & \bar{1} \\ 0 & \bar{1} & 0 \end{pmatrix}$

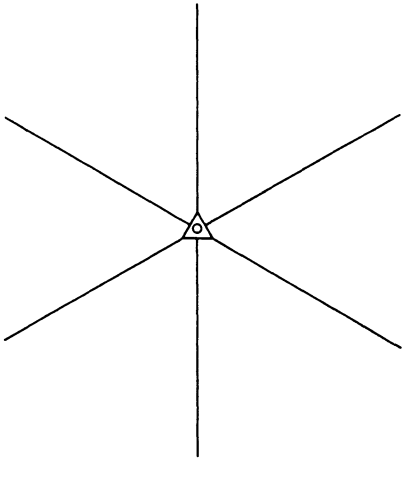

Fig. 2.9. The symmetry operations of $\bar{3}m$.

2.5. Plane Lattices

An alternative approach to the generation of lattices, and one that aids in the consideration of a number of crystallographic problems, is to consider the stacking of plane lattices. A plane lattice is defined by a set of vectors $\mathbf{T} = n_1\mathbf{a}_1 + n_2\mathbf{a}_2$ and a three-dimensional lattice is generated by a stacking vector $\mathbf{a}_3$. Symmetry elements (planes, axes) in the two-dimensional lattice may be preserved or not according to whether they are or are not aligned in the three-dimensional lattice, and new symmetry can be generated by appropriate stacking vectors. For example, a general plane lattice ($\mathbf{a}_1$ and $\mathbf{a}_2$ arbitrary) can be stacked with arbitrary $\mathbf{a}_3$ yielding a triclinic ($\bar{1}$) lattice or can be stacked according to $\mathbf{a}_3 = \lambda(\mathbf{a}_1 \times \mathbf{a}_2)$ preserving the C_2 symmetry of the plane lattice and creating σ symmetry (reflection planes parallel to the stacked planes lattices) and thus yield *pm* lattice symmetry in the three-dimensional lattice.

2.6. Symmetry Elements of Plane Lattices

To systematically discover all alternatives it is necessary to know the nature and location of symmetry axes and "planes" (lines, actually, but they become planes when appropriately stacked) in the plane lattice. All plane lattices exhibit 2-fold rotational symmetry about axes perpendicular to the plane and through each lattice point (since $\mathbf{T} \in \{\mathbf{T}\}$ implies $-\mathbf{T} \in \{\mathbf{T}\}$). It is of value to explore the question: in the general plane lattice are there other axes through other points?

In order to explore this question it is helpful to introduce the matrix:

$$\begin{pmatrix} S_{11} & S_{12} & S_{13} & t_1 \\ S_{21} & S_{22} & S_{23} & t_2 \\ S_{31} & S_{32} & S_{33} & t_3 \\ 0 & 0 & 0 & 1 \end{pmatrix}$$

which as shown will be appropriate to three-dimensional space, but which can be restricted to two-dimensional space by setting $S_{31} = S_{32} = t_3 = 0$ and $S_{33} = 1$. This matrix operates on the vector

$$\begin{pmatrix} X \\ Y \\ Z \\ 1 \end{pmatrix}$$

and transforms X, Y, Z according to:

$$\begin{pmatrix} S_{11} & S_{12} & S_{13} & t_1 \\ S_{21} & S_{22} & S_{23} & t_2 \\ S_{31} & S_{32} & S_{33} & t_3 \\ 0 & 0 & 0 & 1 \end{pmatrix} \begin{pmatrix} X \\ Y \\ Z \\ 1 \end{pmatrix} = \begin{pmatrix} S_{11}X+S_{12}Y+S_{13}Z+t_1 \\ S_{21}X+S_{22}Y+S_{23}Z+t_2 \\ S_{31}X+S_{32}Y+S_{33}Z+t_3 \\ 0 \quad 0 \quad 0 \quad 1 \end{pmatrix} . \tag{29}$$

For example, suppose the rotation to be C_{2z} and the translation $\mathbf{a}$, then (letting $x = X/a, y = Y/b, z = Z/c$)

$$\begin{pmatrix} \bar{1} & 0 & 0 & 1 \\ 0 & \bar{1} & 0 & 0 \\ 0 & 0 & 1 & 0 \\ 0 & 0 & 0 & 1 \end{pmatrix} \begin{pmatrix} x \\ y \\ z \\ 1 \end{pmatrix} = \begin{pmatrix} -x+1 \\ -y \\ z \\ 1 \end{pmatrix} \tag{30}$$

and we can write

$$C_{2z}|\mathbf{a} \equiv \begin{pmatrix} \bar{1} & 0 & 0 & 1 \\ 0 & \bar{1} & 0 & 0 \\ 0 & 0 & 1 & 0 \\ 0 & 0 & 0 & 1 \end{pmatrix} . \tag{31}$$

Since z is unchanged in this operation it is appropriate to a plane lattice.

This operation, the combination of a two-fold rotation and a translation, is necessarily an operation for all plane lattices. The combination is a rotation about an axis that does not pass through the origin. To see that this is so, and to find the location of the axis, note that rotation about an axis located relative to the origin by the vector $\mathbf{t}_\perp$ perpendicular to the axis is equivalent to translation by $-\mathbf{t}_\perp$, followed by rotation by the angle appropriate to the axis about the origin, followed by translation by $\mathbf{t}_\perp$, i.e., the operation is equivalent to

$$\begin{aligned} &\varepsilon|\mathbf{t}_\perp \cdot C_{2z}|0 \cdot \varepsilon| - \mathbf{t}_\perp \\ &\quad \equiv \begin{pmatrix} 1 & 0 & 0 & t_1 \\ 0 & 1 & 0 & t_2 \\ 0 & 0 & 1 & 0 \\ 0 & 0 & 0 & 1 \end{pmatrix} \begin{pmatrix} \bar{1} & 0 & 0 & 0 \\ 0 & \bar{1} & 0 & 0 \\ 0 & 0 & 1 & 0 \\ 0 & 0 & 0 & 1 \end{pmatrix} \begin{pmatrix} 1 & 0 & 0 & -t_1 \\ 0 & 1 & 0 & -t_2 \\ 0 & 0 & 1 & 0 \\ 0 & 0 & 0 & 1 \end{pmatrix} \qquad (32) \\ &\quad = \begin{pmatrix} \bar{1} & 0 & 0 & 2t_1 \\ 0 & \bar{1} & 0 & 2t_2 \\ 0 & 0 & 1 & 0 \\ 0 & 0 & 0 & 1 \end{pmatrix} \qquad (34) \end{aligned}$$

Equating this matrix with that corresponding to $C_{2z}|\mathbf{a}$:

$$\begin{pmatrix} \bar{1} & 0 & 0 & 2t_1 \\ 0 & \bar{1} & 0 & 2t_2 \\ 0 & 0 & 1 & 0 \\ 0 & 0 & 0 & 1 \end{pmatrix} = \begin{pmatrix} \bar{1} & 0 & 0 & 1 \\ 0 & \bar{1} & 0 & 0 \\ 0 & 0 & 1 & 0 \\ 0 & 0 & 0 & 1 \end{pmatrix} \tag{34}$$

from which it follows that $t_1 = 1/2$ and $t_2 = 0$, i.e., $C_{2z}|\mathbf{a}$ is equivalent to rotation by 180° about an axis at $\mathbf{a}/2$ (see Fig. 2.10). Since a similar result holds for C_{2z} followed by $\mathbf{b}$ and by $\mathbf{a} + \mathbf{b}$, it follows that all plane lattices have 2-fold axes of symmetry not only through all lattice points but also through points midway between them (see Fig. 2.11).

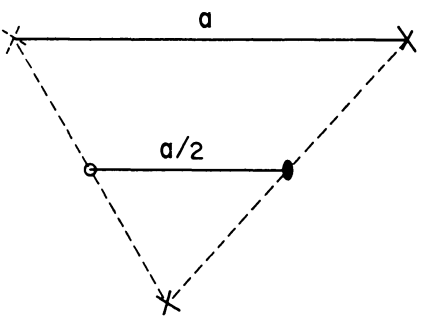

Fig. 2.10. The operation $C_{2z}|\mathbf{a}$ is equivalent to 180° rotation about $\mathbf{a}/2$.

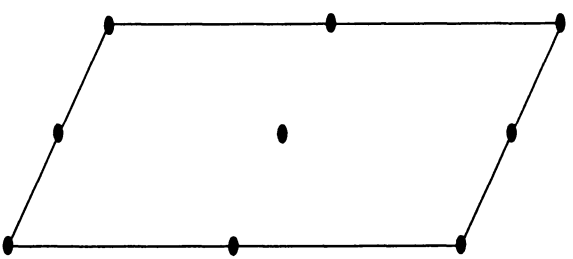

Fig. 2.11. Location of 2-fold axes in the general plane lattice.

In stacking plane parallelogram lattices so as to preserve 2-fold rotational symmetry (and therefore, because inversion is a symmetry of all lattices, to generate at least $2/m$ lattice symmetry in three dimensions), it is only necessary to stack the plane lattices so that two-fold axes superimpose. This stacking requirement is met by four different stacking vectors: $\lambda(\mathbf{a}_1 \times \mathbf{a}_2)$, $\lambda(\mathbf{a}_1 \times \mathbf{a}_2)+\mathbf{a}_1/2$, $\lambda(\mathbf{a}_1 \times \mathbf{a}_2)+\mathbf{a}_2/2$ and $\lambda(\mathbf{a}_1 \times \mathbf{a}_2)+(\mathbf{a}_1+\mathbf{a}_2)/2$, as shown in Fig. 2.12. As discussed in Section 2.4.2, the first choice yields a *pm* lattice and the latter three are all equivalent to *C*-centered monoclinic.

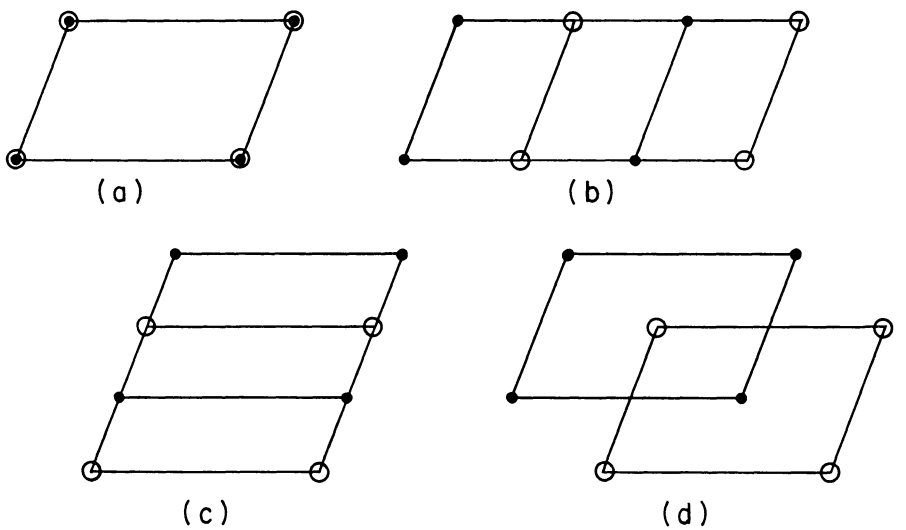

Fig. 2.12. Possible stacking of plane lattices to preserve 2-fold rotation symmetry.

2.7. The Allowed Rotational Symmetries of Plane Lattices

Translation symmetry places restrictions upon the rotational symmetry operations that can appear in plane lattices. However, as was shown in the preceding section, translational symmetry also implies that rotation axes need not go through the origin. Therefore, in order to consider the allowed rotational symmetries, it is helpful to have the following theorem: If rotation by ϕ about an axis perpendicular to a plane lattice and located anywhere within the unit cell is a rotational symmetry operation of the

plane lattice, then rotation by ϕ about a perpendicular axis through any lattice point is also. Consider Fig. 2.13. Let A be the location of the axis and 1 be any lattice point. Rotation by ϕ about A carries 1 into 2 and thus implies a lattice point at 2, as well as at 1, and thus the lattice translation, $\mathbf{T}$. Now consider rotating the plane lattice about A by ϕ and then translation $-\mathbf{T}$. This combined operation, which is necessarily a symmetry operation, is equivalent to rotation of the lattice about 1 by ϕ and the proof is complete.

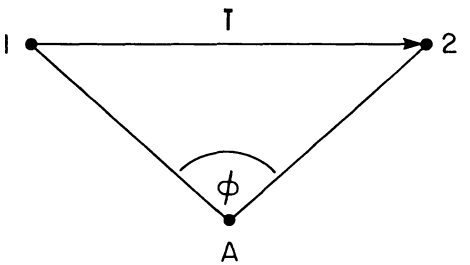

Fig. 2.13. If C_ϕ is a rotation operation of a plane lattice then C_ϕ through any lattice point is as well.

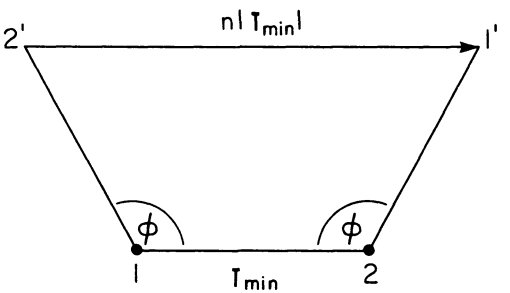

Fig. 2.14. Translational symmetry operations implied by rotational symmetry place restraints on the allowed rotational symmetries.

Next consider two lattice points labelled 1 and 2 in Fig. 2.14. These lattice points are chosen so that the vector between them is as short as any parallel lattice vector in the plane lattice. If the plane lattice exhibits

rotational symmetry such that rotation by ϕ about some axis is a symmetry operation, then rotation by ϕ about 1 and by $-\phi$ about 2 are symmetry operations as well, and lattice points 1′ and 2′ are implied. The vector between 1′ and 2′ must be an integral multiple of $\mathbf{T}_{min}$, i.e., $|\mathbf{T}| = n|\mathbf{T}_{min}|$. Possible values for n and ϕ are collected in Table 2.4. It follows that only $C_2(\phi = 180°), C_3(\phi = 120°, 240°), C_4(\phi = 90°, 180°, 270°)$ and $C_6(\phi = 60°, 120°, 180°, 240°, 300°)$ are allowed.

Furthermore, since all plane lattices have C_2 symmetry through each lattice point, and since C_3 symmetry if present implies a 3-fold axis through each lattice point, the plane lattice with 3-fold rotational symmetry also has 6-fold rotational symmetry. The unit cells for plane lattices with 2-fold, 4-fold and 6-fold symmetry are shown in Fig. 2.15 and the symmetries are discussed in the following sections.

Table 2.4. Allowed rotational symmetries of plane lattices.

n	ϕ
0	60°, 300°
1	90°, 270°
2	120°, 240°
3	180°

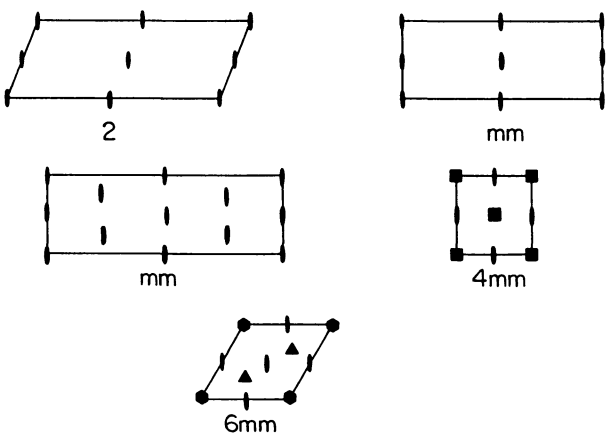

Fig. 2.15. Unit cells of the allowed plane lattices and their rotational symmetries.

2.8. Plane Lattices with *mm* Symmetry

The general plane lattice has 2-fold symmetry only. In the special case that **a** and **b** are orthogonal, additional symmetry enters in the form of reflection symmetry. Since a 2-fold axis and a vertical mirror imply a second mirror plane (see Fig. 2.16), the symmetry in this case is mm. Also when $|\mathbf{a}| = |\mathbf{b}|$ (Fig. 2.17), mm symmetry results and the cell is centered rectangular. Thus, there are two rectangular plane lattices: primitive and centered.

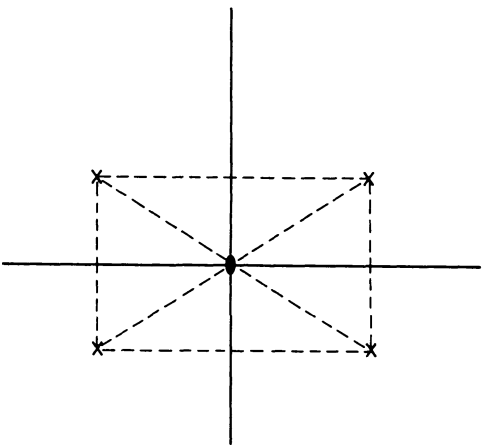

Fig. 2.16. A mirror plane containing an axis implies a second, orthogonal mirror plane.

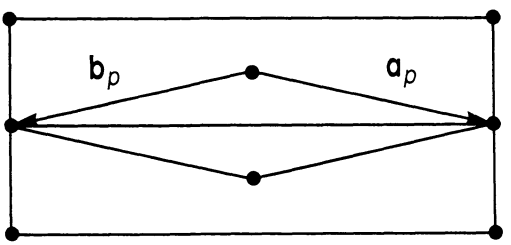

Fig. 2.17. When $|\mathbf{a}| = |\mathbf{b}|$ the lattice has *mm* symmetry.

2.9. Plane Lattices with 4-Fold Symmetry

The lattices with 4-fold rotational symmetry have 2-fold axes through the center of each edge and the cell center, in common with all other plane lattices. By the proof of Section 2.7 there is a 4-fold axis through every lattice point. The location of any other 4-fold axes (i.e., through the cell center, as is obvious by inspection) can be found using $\varepsilon|\mathbf{t}_\perp \cdot C_{4z}|0\cdot\varepsilon|-\mathbf{t}_\perp = C_{4z}|\mathbf{T}$ where $\mathbf{T}$ is any translation and $\mathbf{t}_\perp$ locates the axis relative to the origin.

Thus,

$$\begin{pmatrix} 1 & 0 & 0 & t_1 \\ 0 & 1 & 0 & t_2 \\ 0 & 0 & 1 & 0 \\ 0 & 0 & 0 & 1 \end{pmatrix} \begin{pmatrix} 0 & \bar{1} & 0 & 0 \\ 1 & 0 & 0 & 0 \\ 0 & 0 & 1 & 0 \\ 0 & 0 & 0 & 1 \end{pmatrix} \begin{pmatrix} 1 & 0 & 0 & -t_1 \\ 0 & 1 & 0 & -t_2 \\ 0 & 0 & 1 & 0 \\ 0 & 0 & 0 & 1 \end{pmatrix} = \begin{pmatrix} 0 & \bar{1} & 0 & n_1 \\ 1 & 0 & 0 & n_2 \\ 0 & 0 & 1 & 0 \\ 0 & 0 & 0 & 1 \end{pmatrix} \tag{35}$$

or

$$\begin{pmatrix} 0 & \bar{1} & 0 & t_1+t_2 \\ 1 & 0 & 0 & t_2-t_1 \\ 0 & 0 & 1 & 0 \\ 0 & 0 & 0 & 1 \end{pmatrix} = \begin{pmatrix} 0 & \bar{1} & 0 & n_1 \\ 1 & 0 & 0 & n_2 \\ 0 & 0 & 1 & 0 \\ 0 & 0 & 0 & 1 \end{pmatrix} \tag{36}$$

where n_1 and n_2 are any integers. For example, $n_1 = 1, n_2 = 0$ yields $t_1 = t_2 = 1/2$ and demonstrates that a 4-fold axis passes through the center of the plane square cell center.

2.10. Plane Lattices with Hexagonal Symmetry

The hexagonal plane lattice has a 3-fold axis through the point 1/3, 2/3 (and 2/3, 1/3) as can be seen by

$$\begin{pmatrix} 1 & 0 & 0 & t_1 \\ 0 & 1 & 0 & t_2 \\ 0 & 0 & 1 & 0 \\ 0 & 0 & 0 & 1 \end{pmatrix} \begin{pmatrix} 0 & \bar{1} & 0 & 0 \\ 1 & \bar{1} & 0 & 0 \\ 0 & 0 & 1 & 0 \\ 0 & 0 & 0 & 1 \end{pmatrix} \begin{pmatrix} 1 & 0 & 0 & -t_1 \\ 0 & 1 & 0 & -t_2 \\ 0 & 0 & 1 & 0 \\ 0 & 0 & 0 & 1 \end{pmatrix} = \begin{pmatrix} 0 & \bar{1} & 0 & n_1 \\ 1 & \bar{1} & 0 & n_2 \\ 0 & 0 & 1 & 0 \\ 0 & 0 & 0 & 1 \end{pmatrix} \tag{37}$$

or

$$\begin{pmatrix} 0 & \bar{1} & 0 & t_2+t_1 \\ 1 & \bar{1} & 0 & 2t_2-t_1 \\ 0 & 0 & 1 & 0 \\ 0 & 0 & 0 & 1 \end{pmatrix} = \begin{pmatrix} 0 & \bar{1} & 0 & n_1 \\ 1 & \bar{1} & 0 & n_2 \\ 0 & 0 & 1 & 0 \\ 0 & 0 & 0 & 1 \end{pmatrix} \tag{38}$$

and taking $n_1 = n_2 = 1$ yields $t_1 = 1/3, t_2 = 2/3$.

2.11. Stacking of Plane Lattices

The possible stackings that preserve and create symmetry are given in Table 2.4, which reproduces the findings of Section 2.4. The stacking vector is

$$\mathbf{a}_3 = \lambda_1(\mathbf{a}_1 \times \mathbf{a}_2) + \lambda_2\mathbf{a}_1 + \lambda_3\mathbf{a}_2 \tag{39}$$

and the chosen values for $\mathbf{t}_\perp = \lambda_2\mathbf{a}_1 + \lambda_3\mathbf{a}_2$ are those that preserve axial symmetry in the three-dimensional lattice. Special values for the stacking height (values for λ_1) were chosen to introduce additional symmetries into the three-dimensional lattice.

2.12. Cell Reduction

Any lattice can be described by triples of vectors other than the conventional set. If two sets describe the same lattice, then their primitive unit cells will have the same volumes. For example, the three plane lattice cells shown in Fig. 2.18 all have the same area, and any pair $\mathbf{a}_2, \mathbf{b}_2; \mathbf{a}_1, \mathbf{b}_1$ or $\mathbf{a}_0, \mathbf{b}_0$ (and an unlimited number of other pairs) equally describe the same lattice. The question posed by this fact is: is it possible to find the lattice symmetry given an arbitrary set of primitive vectors? The answer and the method were found by Niggli and the method is called cell reduction.

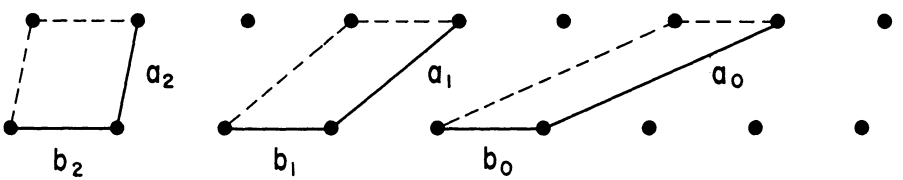

Fig. 2.18. Some alternative unit cells for a plane lattice.

Cells are reduced in one plane at a time, it therefore suffices to consider reduction in a plane. Consider the plane shown in Fig. 2.18. Suppose $\mathbf{a}_0$ and $\mathbf{b}_0$ are given. Reduction of a cell means finding a cell with the same area for which the angles are closer to 90°. Initially $r_{11} = a_0^2, r_{22} = b_0^2, r_{12} = \mathbf{a}_0 \cdot \mathbf{b}_0$,

and $\mathbf{b}_0$ is reducible by $\mathbf{a}_0$ if

$$\frac{|\mathbf{a}_0 \cdot \mathbf{b}_0|}{a_0} > \frac{1}{2}a_0 , \tag{40}$$

or

$$|r_{12}| > \frac{1}{2}r_{11} , \tag{41}$$

for in this case the length of the projection of $\mathbf{b}_0$ onto $\mathbf{a}_0$ is greater than one-half the length of $\mathbf{a}_0$. When this is the case, the angle between $\mathbf{a}_0$ and $\mathbf{b}_0$ can be changed in the direction of 90° by taking $\mathbf{b}_1 = \mathbf{b}_0 - n\mathbf{a}_0$ in place of $\mathbf{b}_0$. Thus, the first step in cell reduction is to determine whether $r_{12} > 1/2r_{11}$ and, if it is, replace $\mathbf{b}_0$ by $\mathbf{b}_0 - n\mathbf{a}_0$ where n (which may be positive or negative) has the value that makes $|(\mathbf{b}_0 - n\mathbf{a}_0) \cdot \mathbf{a}_0|$ closest to $1/2a_0$. This process can be repeated for other combinations of axes until $|r_{ij}| \leq r_{ii}/2$ for all i and j.

2.13. Example of a Cell Reduction

For example, suppose it is given that a lattice has a primitive cell with

$$\begin{aligned} a_0 &= 5.000 \text{ Å} , \\ b_0 &= 8.660 \text{ Å} , \\ c_0 &= 6.403 \text{ Å} , \\ \alpha &= 47.4° , \\ \beta &= 67.0° , \\ \gamma &= 30.0° , \end{aligned} \tag{42}$$

and the problem is to find the lattice symmetry and the conventional lattice parameters. From the definitions (Section 2.1):

$$\begin{aligned} r_{11} &= 25.0 \text{ Å}^2 , \\ r_{22} &= 75.0 \text{ Å}^2 , \\ r_{33} &= 41.0 \text{ Å}^2 , \\ r_{12} &= 37.5 \text{ Å}^2 , \\ r_{13} &= 12.5 \text{ Å}^2 , \\ r_{23} &= 37.5 \text{ Å}^2 . \end{aligned} \tag{43}$$

Since $r_{11}/2 = 12.5 < 37.5 = r_{12}$, it is possible to reduce $\mathbf{b}_0$ by $\mathbf{a}_0$. Thus, find n such that

$$|\mathbf{b}_1 \cdot \mathbf{a}_0| = |(\mathbf{b}_0 - n\mathbf{a}_0) \cdot \mathbf{a}_0| \leq a_0^2/2 \tag{44}$$

or

$$|r_{12} - nr_{11}| \leq r_{11}/2\,, \tag{45}$$

i.e.,

$$37.5 - 25.0n \leq 12.5\,. \tag{46}$$

The solution is $n = 1$ and the new vectors are

$$\begin{aligned} \mathbf{a}_1 &= \mathbf{a}_0\,, \\ \mathbf{b}_1 &= \mathbf{b}_0 - \mathbf{a}_0\,, \\ \mathbf{c}_1 &= \mathbf{c}_0\,. \end{aligned} \tag{47}$$

The $r'_{ij}s$ become

$$\begin{aligned} r_{11} &= 25.0\ \text{Å}^2\,, \\ r_{22} &= b_0^2 - 2\mathbf{b}_0\mathbf{a}_0 + a_0^2 = 75.0 - 2(37.5) + 25.0 = 25.0\ \text{Å}^2\,, \\ r_{33} &= 41.0\ \text{Å}^2\,, \\ r_{12} &= 37.5 - 25.0 = 12.5\ \text{Å}^2\,, \\ r_{13} &= 12.5\ \text{Å}^2\,, \\ r_{23} &= 37.5 - 12.5 = 25.0\ \text{Å}^2\,. \end{aligned} \tag{48}$$

Now $r_{33}/2 = 20.5 < r_{23} = 25.0$, so $\mathbf{c}_1$ is reducible by $\mathbf{b}_1$, i.e., find n such that

$$r_{23} - nr_{22} < r_{22}/2 \tag{49}$$

or

$$25.0 - 25.0n < 12.5 \tag{50}$$

and $n = 1$ (thus $\mathbf{c}_2 = \mathbf{c}_1 - \mathbf{b}_1$ and the new $r_{23} = 0$). Hence,

$$\begin{aligned} r_{11} &= 25.0\ \text{Å}^2\,, \\ r_{22} &= 25.0\ \text{Å}^2\,, \\ r_{33} &= 41.0 - 2(25.0) + 25.0 = 16.0\,, \\ r_{12} &= 12.5\,, \\ r_{13} &= 12.5 - 12.5 = 0\,, \\ r_{23} &= 0\,. \end{aligned} \tag{51}$$

At this point $r_{13} = r_{23} = 0$ and thus the reduction is complete so far as the a–c and b–c pairs are concerned; and $r_{12} = r_{11}/2 = r_{22}/2$ and thus a–b reduction is also complete. Thus, the reduced cell is given by

$$\begin{aligned} a &= \sqrt{r_{11}} = 5.00 \text{ Å}, \\ b &= \sqrt{r_{22}} = 5.00 \text{ Å}, \\ c &= \sqrt{r_{33}} = 4.00 \text{ Å}, \\ \alpha &= \beta = 90^\circ, \\ \gamma &= \cos^{-1}(12.5/25.0) = 60^\circ. \end{aligned} \tag{52}$$

The reduced cells for all fourteen conventional lattice descriptions (Table 2.5) are available and are tabulated in Appendix III. In order to use these tables the cell should be transformed so that: (1) it is right-handed, (2) $b \geq a \geq c$, and (3) at most one of the r_{ij}'s is nonzero and positive. The results given in Eqs. 51 are in this form. Under the subheading $r_{11} = r_{22} \neq r_{33}$ in Appendix III there appears $r_{12} = r_{11}/2, r_{13} = r_{23} = 0$, all of which are true for the problem under consideration. The entry in the table informs the user that the lattice is hexagonal. The matrix

$$\begin{pmatrix} 1 & 0 & 0 \\ \bar{1} & 1 & 0 \\ 0 & 0 & 1 \end{pmatrix}$$

converts the cell to a conventional hexagonal cell, thus

$$\begin{pmatrix} \mathbf{a} \\ \mathbf{b} \\ \mathbf{c} \end{pmatrix}_h = \begin{pmatrix} 1 & 0 & 0 \\ \bar{1} & 1 & 0 \\ 0 & 0 & 1 \end{pmatrix} \begin{pmatrix} \mathbf{a}_2 \\ \mathbf{b}_2 \\ \mathbf{c}_2 \end{pmatrix} = \begin{pmatrix} \mathbf{a}_2 \\ \mathbf{b}_2 - \mathbf{a}_2 \\ \mathbf{c}_2 \end{pmatrix} \tag{53}$$

and

$$\begin{aligned} a_h &= a_2 = 5.00 \text{ Å} \\ b_h &= \sqrt{b_2^2 - 2a_2b_2\cos 60^\circ + a_2^2} = 5.00 \text{ Å} \\ c_h &= c_2 = 4.00 \text{ Å} \\ \gamma_2 &= \cos^{-1}\left[\frac{(a_2b_2\cos 60^\circ - a_2^2)}{a_2b_2}\right] = 120^\circ. \end{aligned} \tag{54}$$

Table 2.5. Three-dimensional lattices from stacking of plane lattices.

Plane lattice	λ_1	λ_2	λ_3	Symmetry	Conventional lattice	Parameter	
p	–	–	–	i	tr	$a, b, c, \alpha, \beta, \gamma$	tr = triclinic p = parallelogram
p	–	0	0	$2/m$	pm	a, b, c, β	pm = primitive monoclinic
p	–	1/2	0	$2/m$	ecm	a, b, c, β	ecm = end-centered monoclinic
p	–	0	1/2	$2/m$	ecm	a, b, c, β	
p	–	1/2	1/2	$2/m$	$bcm = ecm$	a, b, c, β	bcm = body-centered monoclinic
sr	–	0	0	mmm	po	a, b, c	po = primitive orthorhombic sr = simple rectangular
sr	–	1/2	0	mmm	eco	a, b, c	eco = end-centered orthorhombic
sr	–	0	1/2	mmm	eco	a, b, c	
sr	–	1/2	1/2	mmm	bco	a, b, c	bco = body-centered orthorhombic
sr	a_1^{-1}	0	0	$4/mmm$	pt	a, c	pt = primitive tetragonal
sr	a_2^{-1}	0	0	$4/mmm$	pt	a, c	
sr	a_1^{-1}	1/2	1/2	$4/mmm$	bct	a, c	bct = body-centered tetragonal
sr	a_2^{-1}	1/2	1/2	$4/mmm$	bct	a, c	
sr	–	0	0	mmm	eco	a, b, c	

Table 2.5 (*Continued*)

cr	–	1/2	0	*mmm*	*fco*	a, b, c	*fco* = face-centered orthorhombic
cr	–	0	1/2	*mmm*	*fco*	a, b, c	*cr* = centered rectangular
cr	–	1/2	1/2	*mmm*	*eco*	a, b, c	
cr	$1/2a_1^{-1}$	1/2	0	$4/mmm$	$fct = bct$	a, c	*fct* = face-centered tetragonal
cr	$1/2a_2^{-1}$	1/2	0	$4/mmm$	$fct = bct$	a, c	
s	–	0	0	$4/mmm$	*pt*	a, c	*s* = square
s	–	1/2	1/2	$4/mmm$	*bct*	a, c	
s	a_2^{-1}	0	0	$m3m$	*pc*	a	*pc* = primitive cubic
s	$1/2a_2^{-1}$	1/2	1/2	$m3m$	*bcc*	a	*bcc* = body-centered cubic
s	$1/\sqrt{2}a_2^{-1}$	1/2	1/2	$m3m$	*fcc*	a	*fcc* = face-centered cubic
h	–	0	0	$6/mmm$	*h*	a, c	*h* = hexagonal
h	–	1/3	2/3	$\bar{3}$	*r*	a, α	*r* = rhombohedral
h	$\sqrt{2}/3a_1^{-1}$	1/3	2/3	$m3m$	*pc*	a	
h	$2\sqrt{2}/3a_1^{-1}$	1/3	2/3	$m3m$	*fcc*	a	
h	$\sqrt{2}/6a_1^{-1}$	1/3	2/3	$m3m$	*bcc*	a	

2.14. Transformation of Axes

If the cell is not in the standard form such that $b \geq a \geq c$ or if more than one of the asymmetric scalars were nonzero and positive, then the cell can be transformed and the handedness maintained by: (1) reversing two axes, (2) reversing one axis and interchanging two axes, (3) interchanging two pairs of axes, and these transformations are shown in Table 2.6.

Table 2.6. Axial transformations that maintain handedness.

1.	a b c	r_{12}	r_{13}	r_{23}
2.	−a − b c	r_{12}	$-r_{13}$	$-r_{23}$
3.	−a b − c	$-r_{12}$	r_{13}	$-r_{23}$
4.	a − b − c	$-r_{12}$	$-r_{13}$	r_{23}
5.	b c a	r_{23}	r_{12}	r_{13}
6.	c a b	r_{13}	r_{23}	r_{12}
7.	−b a c	$-r_{12}$	$-r_{23}$	r_{13}
8.	b − a c	$-r_{12}$	r_{23}	$-r_{13}$
9.	b a − c	r_{12}	$-r_{23}$	$-r_{13}$
10.	−a c b	$-r_{13}$	$-r_{12}$	r_{23}
11.	a − c b	$-r_{13}$	r_{12}	$-r_{23}$
12.	a c − b	r_{13}	$-r_{12}$	$-r_{23}$
13.	−c b a	$-r_{23}$	$-r_{13}$	r_{12}
14.	c − b a	$-r_{23}$	r_{13}	$-r_{12}$
15.	c b − a	r_{23}	$-r_{13}$	$-r_{12}$

For example, suppose a reduced cell is given by

$$\begin{aligned} r_{11} &= 25.00 \text{ Å}^2, \\ r_{22} &= r_{33} = 36.00 \text{ Å}^2, \\ r_{12} &= r_{13} = 12.5 \text{ Å}, \\ r_{23} &= 6.25 \text{ Å}. \end{aligned} \tag{55}$$

To bring this into the $b \geq a \geq c$ form with no more than one $r_{ij} > 0$, it is necessary to exchange a and c and to change the signs of two r_{ij}'s. Examination of Table 2.5 shows that transformation 5 followed by 2 yields

$$\begin{aligned} r_{11} &= r_{22} = 36.00\ \text{Å}^2, \\ r_{33} &= 25.00\ \text{Å}^2, \\ r_{13} &= r_{23} = -12.50\ \text{Å}^2, \\ r_{12} &= 6.25\ \text{Å} \end{aligned} \tag{56}$$

which is in the standard form, and comparison with Appendix III shows this to be a *bct* lattice.

2.15. Transformations of Positions within Cells

The positions within cells ($0 \leq x = X/a < 1, 0 \leq y = Y/b < 1, 0 \leq z = Z/c < 1$):

$$\mathbf{r} = x\mathbf{a} + y\mathbf{b} + z\mathbf{c} \tag{57}$$

must be transformed when axes are transformed. If the transformation

$$\begin{pmatrix} w_{11} & w_{12} & w_{13} \\ w_{21} & w_{22} & w_{23} \\ w_{31} & w_{32} & w_{33} \end{pmatrix} \begin{pmatrix} \mathbf{a}_0 \\ \mathbf{b}_0 \\ \mathbf{c}_0 \end{pmatrix} = \begin{pmatrix} \mathbf{a}_1 \\ \mathbf{b}_1 \\ \mathbf{c}_1 \end{pmatrix} \tag{58}$$

carries the old vectors $\mathbf{a}_0, \mathbf{b}_0, \mathbf{c}_0$ into the new, $\mathbf{a}_1, \mathbf{b}_1, \mathbf{c}_1$, then $\mathbf{r}$ in the final cell corresponds to

$$\mathbf{r} = x_1\mathbf{a}_1 + y_1\mathbf{b}_1 + z_1\mathbf{c}_1 \tag{59}$$

$$\begin{aligned} &= x_1(w_{11}\mathbf{a}_0 + w_{12}\mathbf{b}_0 + w_{13}\mathbf{c}_0) \\ &\quad + y_1(w_{21}\mathbf{a}_0 + w_{22}\mathbf{b}_0 + w_{23}\mathbf{c}_0) \\ &\quad + z_1(w_{31}\mathbf{a}_0 + w_{32}\mathbf{b}_0 + w_{33}\mathbf{c}_0) \end{aligned} \tag{60}$$

or

$$\begin{pmatrix} x_0 \\ y_0 \\ z_0 \end{pmatrix} = \begin{pmatrix} w_{11} & w_{21} & w_{31} \\ w_{12} & w_{22} & w_{32} \\ w_{13} & w_{23} & w_{33} \end{pmatrix} \begin{pmatrix} x_1 \\ y_1 \\ z_1 \end{pmatrix} \tag{61}$$

i.e., the positional parameters transform as the transpose of the inverse vector transformation.

For example, suppose an *fcc* lattice is slightly distorted to rhombohedral (Fig. 2.19). The vector transformation from *fcc* to *r* is

$$\begin{pmatrix} \mathbf{a} \\ \mathbf{b} \\ \mathbf{c} \end{pmatrix}_r = \begin{pmatrix} 1/2 & 0 & 1/2 \\ 1/2 & 1/2 & 0 \\ 0 & 1/2 & 1/2 \end{pmatrix} \begin{pmatrix} \mathbf{a} \\ \mathbf{b} \\ \mathbf{c} \end{pmatrix}_{fcc} \tag{62}$$

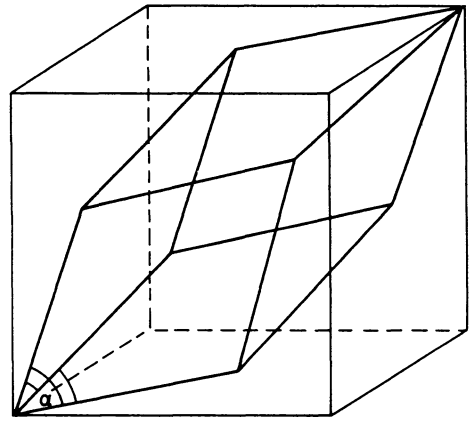

Fig. 2.19. Rhombohedral distortion of *fcc*.

and thus

$$\begin{pmatrix} x \\ y \\ z \end{pmatrix}_r = \begin{pmatrix} 1 & \bar{1} & 1 \\ 1 & 1 & \bar{1} \\ \bar{1} & 1 & 1 \end{pmatrix} \begin{pmatrix} x \\ y \\ z \end{pmatrix}_{fcc} . \tag{63}$$

2.16. Lattice Planes

The specification of 3 lattice points within a space lattice defines a plane lattice from which the lattice could be constructed by some appropriate stacking vector. It is necessary to name planes in a lattice, and the names given refer to the families of planes that are parallel to each other and equally spaced. Starting with the planes that contain lattice points (those related by a primitive stacking vector), it is possible to generalize to include planes with half the spacing (and thus alternate planes do not contain lattice points), with one-third the spacing (and thus only every third plane contains lattice points) and so forth. We start by dealing with families of planes all of which contain lattice points.

For any plane sublattice of a space lattice, it is always possible to find three lattice points in the plane each of which is an integral number of primitive translations removed from the same lattice point not in the plane (Fig. 2.20). Consider a set of four lattices points related in this way for which n_1, n_2 and n_3 have no common divisor (if they did have a common

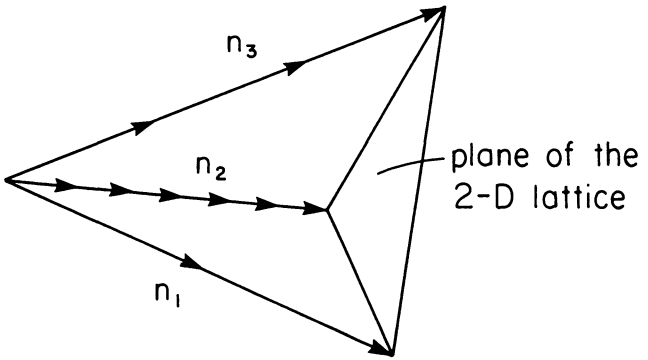

Fig. 2.20. The definition of a plane by three noncolinear lattice translations.

divisor a point closer to the plane for which there was none could be found). Three vectors:

$$\begin{aligned} \mathbf{T}_1 &= n_2\mathbf{b} - n_1\mathbf{a}\,, \\ \mathbf{T}_2 &= n_3\mathbf{c} - n_1\mathbf{a}\,, \\ \mathbf{T}_3 &= n_3\mathbf{c} - n_2\mathbf{b}\,, \end{aligned} \tag{64}$$

all lie within the plane. It follows that any cross product among these, e.g.,

$$\mathbf{T}_1 \times \mathbf{T}_2 = n_2n_3\ \mathbf{b}\times\mathbf{c} + n_1n_3\mathbf{c}\times\mathbf{a} + n_1n_2\mathbf{a}\times\mathbf{b} \tag{65}$$

is a vector perpendicular to the plane and is therefore suitable for use in naming the plane. It is convenient, for reasons that will later become apparent, to assign to such a perpendicular vector, $\mathbf{K}$, a length, $|\mathbf{K}| = 2\pi/d$, where d is the spacing between the planes. In order to do this, it is helpful to know the number of interplanar spacings that occur between the origin and the plane as in Fig. 2.20. If each pair n_1, n_2; n_1, n_3; and n_2, n_3 has no common divisor, then this number is $n_1n_2n_3$. On the other hand, if d_{ij} is the common divisor of n_i and n_j, then this number is $n_1n_2n_3/d_{12}d_{13}d_{23}$. The distance between the planes (the d spacing) is the vertical distance between the origin point and the defining plane, D, divided by the number of interplanar spacings:

$$d = \frac{Dd_{12}d_{13}d_{23}}{n_1n_2n_3} \tag{66}$$

where D is the projection of $n_1\mathbf{a}$ (or $n_2\mathbf{b}$, or $n_3\mathbf{c}$) onto the vertical to the plane, i.e.,

$$D = n_1\mathbf{a} \cdot \frac{\mathbf{T}_1 \times \mathbf{T}_2}{|\mathbf{T}_1 \times \mathbf{T}_2|}. \tag{67}$$

Thus,

$$\begin{aligned} D &= n_1\mathbf{a} \cdot \frac{[n_2n_3\mathbf{b} \times \mathbf{c} + n_1n_3\mathbf{c} \times \mathbf{a} + n_1n_2\mathbf{a} \times \mathbf{b}]}{|\mathbf{T}_1 \times \mathbf{T}_2|} \\ &= \frac{n_1n_2n_3\mathbf{a} \cdot \mathbf{b} \times \mathbf{c}}{|\mathbf{T}_1 \times \mathbf{T}_2|} \\ &= \frac{n_1n_2n_3\ V}{|\mathbf{T}_1 \times \mathbf{T}_2|} \end{aligned} \tag{68}$$

and

$$d = \frac{d_{12}d_{13}d_{23}\ V}{|\mathbf{T}_1 \times \mathbf{T}_2|}. \tag{69}$$

Now $\mathbf{K}$ is proportional to $\mathbf{T}_1 \times \mathbf{T}_2$, say

$$|\mathbf{K}| = S|\mathbf{T}_1 \times \mathbf{T}_2|, \tag{70}$$

and since by choice $|\mathbf{K}| = 2\pi/d$,

$$\frac{2\pi}{d} = S \cdot \frac{d_{12}d_{13}d_{23}\ V}{d} \tag{71}$$

or

$$S = \frac{2\pi}{d_{12}d_{13}d_{23}\ V}. \tag{72}$$

Using Eq. 65,

$$\mathbf{K} = 2\pi \left\{ \left[\frac{n_2n_3}{d_{12}d_{13}d_{23}}\right] \frac{\mathbf{b}\times\mathbf{c}}{V} + \left[\frac{n_1n_3}{d_{12}d_{13}d_{23}}\right] \frac{\mathbf{c}\times\mathbf{a}}{V} + \left[\frac{n_1n_2}{d_{12}d_{13}d_{23}}\right] \frac{\mathbf{a}\times\mathbf{b}}{V} \right\}. \tag{73}$$

2.17. Miller Indices and the Reciprocal Lattice

We therefore define

$$\begin{aligned} h &= n_2n_3/d_{12}d_{13}d_{23}, \\ k &= n_1n_3/d_{12}d_{13}d_{23}, \\ \ell &= n_1n_2/d_{12}d_{13}d_{23} \end{aligned} \tag{74}$$

and

$$\begin{aligned} \mathbf{a}^* &= 2\pi \mathbf{b} \times \mathbf{c}/V\,, \\ \mathbf{b}^* &= 2\pi \mathbf{c} \times \mathbf{a}/V\,, \\ \mathbf{c}^* &= 2\pi \mathbf{a} \times \mathbf{b}/V\,, \end{aligned} \tag{75}$$

and obtain

$$\mathbf{K} = h\mathbf{a}^* + k\mathbf{b}^* + \ell\mathbf{c}^*\,. \tag{76}$$

This is called a *reciprocal lattice vector*, and the basis vectors for the reciprocal lattice are $\mathbf{a}^*, \mathbf{b}^*$ and $\mathbf{c}^*$. The integers h, k and ℓ are called the Miller indices for the lattice planes and serve to name the planes. The Miller indices also include the generalized indices which have a common divisor, in this case the common divisor is called an order. If h, k and ℓ have no common divisor, then nh, nk, $n\ell$ are the nth order planes and only the fraction $1/n$ of the planes is occupied by lattice points if the lattice is primitive.

For example, consider the case (Fig. 2.20) $n_1 = 2, n_2 = 6$ and $n_3 = 3$. By definition $h = 18/6 = 3$, $k = 6/6 = 1$ and $\ell = 12/6 = 2$ and the parallel planes in the family are the 3, 1, 2 planes. The 6, 2, 4 planes are the planes parallel to the 3, 1, 2 planes with one-half the d spacing. If the cell defined by $\mathbf{a}, \mathbf{b}$ and $\mathbf{c}$ is primitive, then every alternate 6, 2, 4 plane is empty of lattice points. The reciprocal vector

$$\mathbf{K} = 3\mathbf{a}^* + \mathbf{b}^* + 2\mathbf{c}^* \tag{77}$$

is perpendicular to the 3, 1, 2 planes, and with $\mathbf{a}^*, \mathbf{b}^*$ and $\mathbf{c}^*$ defined as in Eq. 75,

$$|\mathbf{K}| = \frac{2\pi}{d_{312}}\,, \tag{78}$$

where d_{312} is the spacing between the 3, 1, 2 planes.

2.18. The Lattice Reciprocal to the *fcc* Lattice

A primitive unit cell for a *fcc* lattice is defined by the vectors

$$\begin{aligned} \mathbf{a}_p &= \frac{a_{fcc}}{2}(\mathbf{i} + \mathbf{k})\,, \\ \mathbf{b}_p &= \frac{a_{fcc}}{2}(\mathbf{i} + \mathbf{j})\,, \\ \mathbf{c}_p &= \frac{a_{fcc}}{2}(\mathbf{j} + \mathbf{k}) \end{aligned} \tag{79}$$

Table 2.7. The lattice reciprocal to *fcc*.

$hk\ell$	$h+k-\ell$	$-h+k+\ell$	$h-k+\ell$
100	1	$\bar{1}$	1
110	2	0	0
111	1	1	1
200	2	$\bar{2}$	2
210	3	$\bar{1}$	1
211	2	0	2
220	4	0	0

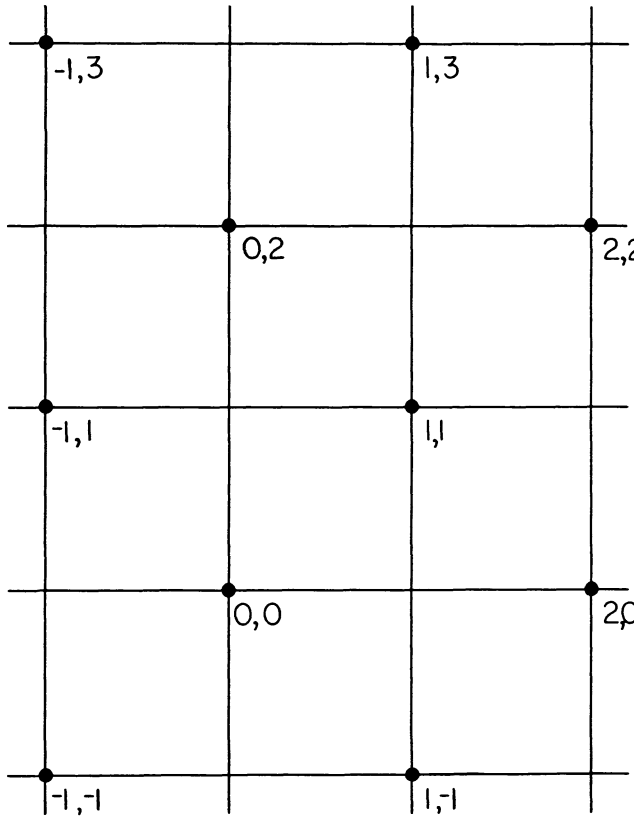

Fig. 2.21. The *bcc* lattice reciprocal to *fcc*.

and

$$V = \mathbf{a}_p \cdot \mathbf{b}_p \times \mathbf{c}_p = \frac{a_{fcc}^3}{8}(\mathbf{i}+\mathbf{k}) \cdot (\mathbf{i}+\mathbf{j}) \times (\mathbf{j}+\mathbf{k})$$

$$= \frac{a_{fcc}^3}{4} . \tag{80}$$

Thus,

$$\mathbf{a}^* = \frac{2\pi}{a_{fcc}}(\mathbf{i}+\mathbf{j}) \times (\mathbf{j}+\mathbf{k}) = \frac{2\pi}{a_{fcc}}(\mathbf{i}-\mathbf{j}+\mathbf{k}) ,$$

$$\mathbf{b}^* = \frac{2\pi}{a_{fcc}}(\mathbf{j}+\mathbf{k}) \times (\mathbf{i}+\mathbf{k}) = \frac{2\pi}{a_{fcc}}(\mathbf{i}+\mathbf{j}-\mathbf{k}) , \tag{81}$$

$$\mathbf{c}^* = \frac{2n}{a_{fcc}}(\mathbf{i}+\mathbf{k}) \times (\mathbf{i}+\mathbf{j}) = \frac{2\pi}{a_{fcc}}(-\mathbf{i}+\mathbf{j}+\mathbf{k}) ,$$

and

$$\mathbf{K} = \frac{2\pi}{a_{fcc}}[h(\mathbf{i}-\mathbf{j}+\mathbf{k}) + k(\mathbf{i}+\mathbf{j}-\mathbf{k}) + \ell(-\mathbf{i}+\mathbf{j}+\mathbf{k})] \tag{82}$$

with h, k and ℓ integers. Rearranging,

$$\mathbf{K} = \frac{2\pi}{a_{fcc}}[(h+k-\ell)\mathbf{i} + (-h+k+\ell)\mathbf{j} + (h-k+\ell)\mathbf{k}] . \tag{83}$$

Table 2.7 gives some values of the coefficients of $\mathbf{i}, \mathbf{j}$ and $\mathbf{k}$ corresponding to some h, k and ℓ values. Thus, expressed in terms of orthogonal vectors, only $\mathbf{K}$'s with all even or all odd coefficients appear in the table. The fact that the reciprocal lattice can be described in terms of orthogonal vectors of equal length means that it has cubic symmetry. The fact that the coefficients are either all even or all odd means that the reciprocal lattice is *bcc* (see Fig. 2.21).

2.19. The Scalar Products of Real and Reciprocal Lattice Vectors

Consider a real lattice translation

$$\mathbf{T} = m\mathbf{a} + n\mathbf{b} + p\mathbf{c} , \tag{84}$$

and a vector from the corresponding reciprocal lattice

$$\mathbf{K} = h\mathbf{a}^* + k\mathbf{b}^* + \ell\mathbf{c}^* . \tag{85}$$

By the definitions (Eq. 75),

$$\mathbf{a} \cdot \mathbf{a}^* = \mathbf{b} \cdot \mathbf{b}^* = \mathbf{c} \cdot \mathbf{c}^* = 2\pi \tag{86}$$

and

$$\mathbf{a}^* \cdot \mathbf{b} = \mathbf{a}^* \cdot \mathbf{c} = \mathbf{b}^* \cdot \mathbf{a} = \mathbf{b}^* \cdot \mathbf{c} = \mathbf{c}^* \cdot \mathbf{a} = \mathbf{c}^* \cdot \mathbf{b} = 0\,, \tag{87}$$

and thus

$$\mathbf{K} \cdot \mathbf{T} = 2\pi[mh + nk + p\ell] \tag{88}$$

i.e., the scalar product of a real lattice vector and a reciprocal lattice vector is an integer times 2π.

Bibliography

1. M. J. Buerger, *Elementary Crystallography* (John Wiley and Sons, New York, 1956).
2. Duncan McKie and Christine McKie, *Essentials of Crystallography* (Blackwell Scientific Publications, Boston, 1986).
3. Leonid K. Azaroff and Martin J. Buerger, *The Powder Method in X-Ray Crystallography* (McGraw Hill, New York, 1958).
4. Majorie Senechal, *Crystalline Symmetries* (Adam Hilger, New York, 1990).

Problems

1. Express the volume of the cell with **b** perpendicular to **a** and **c**, and the angle β between **a** and **c** in terms of a, b, c and β.
2. Show that if a lattice has C_{2v} symmetry, then it has D_{2h} symmetry.
3. Why is there no body-centered hexagonal lattice?
4. (a) Sketch a 110 plane of a triply primitive hexagonal cell of a rhombohedral lattice ($\lambda_2 = \lambda_3 = 0$).
   (b) Why is there no body-centered rhombodhedral lattice?
5. Find the lattice parameters of the conventional primitive cell of *bcc* in terms of a_{bcc}.
6. A *fct* lattice is distorted by changing only the γ angle away from $\pi/2$. What is the new lattice type and what are the lattice parameters in terms of a_{fct} and c_{fct}?
7. Generate the matrix for the proper C_{4z} rotation from those for C_{2x} and $C_{2(x+y)}$.
8. Find the stacking vector that creates a *bcc* cell from stacked plane hexagonal lattices and compare your answer with the vector of Table 2.4.
9. Find the reciprocal lattice vector for the $h = 2, k = 3$ and $\ell = 5$ planes of the reduced rhombohedral cell of Problem 8 in terms of $\mathbf{i}, \mathbf{j}, \mathbf{k}$ and a_{bcc}. Find the d spacing.
10. (a) What are h, k and ℓ in terms of the *bcc* lattice for the planes of Problem 9?
    (b) Find the matrix converting $(hk\ell)_r$ to $(hk\ell)_{bcc}$.
    (c) Multiply the matrix of c with that which takes $(\mathbf{a}, \mathbf{b}, \mathbf{c})_{bcc}$ to $(\mathbf{a}, \mathbf{b}, \mathbf{c})_r$ (given in the solution to Problem 8).
11. Find the coordinates of the site in the rhombohedral primitive cell that is equivalent to $x = 1/8$, $y = 3/8$, $z = 5/8$ in the *bcc* cell.
12. Use the reduced cell and Appendix III to find the conventional cell for the lattice defined by: $a = 3.905$ Å, $b = 5.000$ Å, $c = 4.717$ Å, $\alpha = 47.28°$, $\beta = 70.16°$ and $\gamma = 62.55°$.

CHAPTER 3

SPACE GROUP SYMMETRY

3.1. Space Group Symmetry Operations

A solid that is characterized by translational periodicity is in correspondence with a space lattice (Section 2.1) and is invariant under operations represented by

$$\epsilon|\mathbf{T} \equiv \begin{pmatrix} 1 & 0 & 0 & n_1 \\ 0 & 1 & 0 & n_2 \\ 0 & 0 & 1 & n_3 \\ 0 & 0 & 0 & 0 \end{pmatrix} \tag{1}$$

as described in Section 2.6. Such a solid is also characterized by a set of operations $\{\beta|\mathbf{t}\}$ that carry positions within or on the boundaries of a unit cell, $\mathbf{r} = x\mathbf{a} + y\mathbf{b} + z\mathbf{c}$ with $0 \leq x \leq 1$, $0 \leq y \leq 1$, $0 \leq z \leq 1$ to other positions within, or on, the boundaries of that cell. The operations $\{\beta|\mathbf{t}\}$ combined with the operations $\{\epsilon|\mathbf{T}\}$ form the *space group* of the crystalline solid. In $\beta|\mathbf{t}$, the β stands for the rotational (proper or improper) part of the operation that is specified by a 3×3 matrix as given in Tables 2.2 and 2.3. The $\mathbf{t}$ stands for the translational part, it is a vector by which the position is translated after rotation. One purpose of this chapter is to consider the consequences of the fact that the translations $\mathbf{t}$, although not arbitrary, are not restricted to the pure translational symmetry operations.

Multiplication of the 4×4 matrix corresponding to $\beta_1|\mathbf{t}_1$ by that corresponding to $\beta_2|\mathbf{t}_2$ yields a matrix corresponding to the product operation, and examination of the product matrix shows the operations combining according to

$$\beta_2|\mathbf{t}_2 \cdot \beta_1|\mathbf{t}_1 = \beta_2\beta_1|\beta_2\mathbf{t}_1 + \mathbf{t}_2\,. \tag{2}$$

3.2. Allowed Rotational Symmetries

In general, if $\beta|\mathbf{t}\epsilon g$ (where g is the space group), then $\beta^{-1}|-\beta^{-1}\mathbf{t}\epsilon g$ since

$$\beta|\mathbf{t}\cdot\beta^{-1}|-\beta^{-1}\mathbf{t}=\varepsilon|\mathbf{t}-\mathbf{t}=\varepsilon|0 \tag{3}$$

and the inverse of a symmetry operation is a symmetry operation. Furthermore, since this is so, and since $\varepsilon|\mathbf{T}\epsilon g$, it follows that

$$\begin{aligned}\beta|\mathbf{t}\cdot\varepsilon|\mathbf{T}\cdot\beta^{-1}|-\beta^{-1}t&=\beta|\mathbf{t}\cdot\beta^{-1}|-\beta^{-1}\mathbf{t}+\mathbf{T}\\&=\varepsilon|\beta\mathbf{T}\epsilon g\,.\end{aligned} \tag{4}$$

Thus, if $\beta(C_{2z},\sigma_z,i,$ etc.) is the rotational part of a space-group symmetry operation, then β is a symmetry operation of the lattice. Thus, only C_n with $n=1,2,3,4$ and 6 and $\overline{C}_n$ with the same n values (since $\overline{C}_n\cdot i=C_n$, and all space lattices have inversion symmetry) are allowed β parts of space-group operations.

Therefore, $\beta|\mathbf{t}$ can belong to g so long as β is one of the allowed rotations of the lattice, and so long as the operation permits closure. That is, for some n, $\beta^n=\varepsilon$ and it is then necessary that

$$(\beta|\mathbf{t})^n=\beta^n\Big|\sum_{m=1}^{n}\beta^{m-1}\mathbf{t}=\varepsilon\Big|\sum_{m=1}^{n}\beta^{m-1}\mathbf{t}\,, \tag{5}$$

and thus $\beta|\mathbf{t}\epsilon g$ is possible if and only if $\sum_{m=1}^{n}\beta^{m-1}\mathbf{t}$ is a pure translation for n given by $\beta^n=\varepsilon$.

3.3. Reflection Operations

Simple reflection through a plane containing the origin, for example $\sigma_z|0$, yields immediately

$$(\sigma_z|0)^2=\varepsilon|0 \tag{6}$$

and is allowed. However, $\sigma_z|\mathbf{c}/2$, which, as is shown in Fig. 3.1, is a reflection through a plane perpendicular to $\mathbf{c}$ at $z=1/4$ is also allowed since

$$(\sigma_z|\mathbf{c}/2)^2=\varepsilon|\mathbf{c}/2-\mathbf{c}/2=\varepsilon|0\,. \tag{7}$$

Furthermore, this possible space group operation can be combined with a pure translation to prove that if reflection through $z=1/4$ is an operation

for the space group, then reflection through $z = 0$ is a symmetry operation of the *lattice*:

$$\sigma_z|\mathbf{c}/2 \cdot \varepsilon|\mathbf{T} \cdot \sigma_z|\mathbf{c}/2 = \sigma_z|\mathbf{c}/2 \cdot \sigma_z|\mathbf{T} + \mathbf{c}/2$$
$$= \varepsilon|\sigma_z \mathbf{T}\,. \tag{8}$$

The location of a mirror plane at z (or x or y) $= 1/4$ is to some extent arbitrary since the origin could be placed in the mirror plane. However, there are conventional locations of the origin (e.g., at an inversion center) which locate the origin midway between mirror planes in some instances.

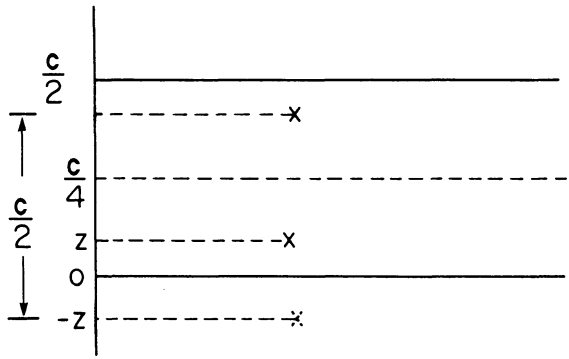

Fig. 3.1. $\sigma_z|\mathbf{c}/2$ is reflection through a horizontal plane at $z = 1/4$.

3.4. Glide Operations

In the cases discussed above, either $\mathbf{t}$ was perpendicular to the reflection plane or $\mathbf{t} = 0$. It is also possible for $\mathbf{t}$ to be parallel to the reflection plane and not a pure translation, as is the case for $\sigma_z|\mathbf{a}/2$, the operation of a *glide plane*. This meets the closure criterion because

$$\sigma_z|\mathbf{a}/2 \cdot \sigma_z|\mathbf{a}/2 = \varepsilon|\mathbf{a}\,. \tag{9}$$

This operation (see Fig. 3.2) takes x, y, z into $x + 1/2, y, \bar{z}$. The operation $\sigma_z|\mathbf{a}/2$ is not factorable, i.e., neither σ_z nor $\mathbf{a}/2$ is, by itself, a symmetry operation so long as $\mathbf{a}$ is a primitive translation. Unlike the case of translation perpendicular to a reflection plane, the translational component of this

operation is unaltered by a change in origin. Furthermore, when $\sigma_z|\mathbf{a}/2\epsilon g$, then σ_z is a symmetry operation of the space lattice. In other words, a three-dimensional structure with a single glide plane and no reflection symmetry has lattice symmetry m (and therefore the lattice symmetry is monoclinic).

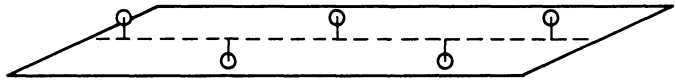

Fig. 3.2. A glide operation.

The limitation on all glide operations is that

$$\sigma|\mathbf{t} \cdot \sigma|\mathbf{t} = \varepsilon|2\mathbf{t}\,\varepsilon\{\mathbf{T}\} \tag{10}$$

i.e., glides are only allowed for $\mathbf{T} = 2\mathbf{t}$. Thus, glides can be axial glides ($2\mathbf{t} = \mathbf{a}$ or $\mathbf{b}$ or $\mathbf{c}$), diagonal glides ($2\mathbf{t} = \mathbf{a}+\mathbf{b}$ or $\mathbf{a}+\mathbf{c}$ or $\mathbf{b}+\mathbf{c}$) and diamond glides ($2\mathbf{t} = (\mathbf{a}+\mathbf{b}+\mathbf{c})/2$ in the case of body-centering and $2\mathbf{t} = (\mathbf{a}+\mathbf{b})/2$ or $(\mathbf{a}+\mathbf{c})/2$ or $(\mathbf{b}+\mathbf{c})/2$ in the cases of centered faces). Some examples are: $\sigma_x|\mathbf{c}/2$ (the operation of a c-glide perpendicular to a, carries x, y, z into $\bar{x}, y, z + 1/2$ if the origin is in the plane), $\sigma_x|(\mathbf{b}+\mathbf{c})/2$ (the operation of an n glide perpendicular to x, carries x, y, z into $\bar{x}, y + 1/2, z + 1/2$ if the origin is in the plane), $\sigma_{x+y}|(\mathbf{a}+\mathbf{b}+\mathbf{c})/4$ (the operation of a d glide perpendicular to $\mathbf{a}+\mathbf{b}$, carries x, y, z into $\bar{y}+1/4, \bar{x}+1/4, z+1/4$ if the origin is in the plane, and $\sigma_x|(\mathbf{b}+\mathbf{c})/4$ (the operation of a d glide perpendicular to $\mathbf{a}$, carries x, y, z into $\bar{x}, y + 1/4, z + 1/4$ if the origin is in the plane).

3.5. Rotation-Translation Operations

It is possible for nonintegral translations to also be coupled to proper rotations. A component of the translation perpendicular to the rotation axis means the axis operates through a point removed from the origin. Thus, $C_{2z}|\mathbf{a}/2$ is the operation of a 2-fold axis about an axis parallel to $\mathbf{c}$ and through $x = 1/4, y = 0$ (Fig. 3.3). On the other hand, a translational component parallel to an axis and not a pure translation implies an operation that differs from a pure rotation. For example, $C_{2z}|\mathbf{c}/2$ is allowed by closure since

$$(C_{2z}|\mathbf{c}/2)^2 = \varepsilon|\mathbf{c}\,, \tag{11}$$

and yet the existence of this operation implies neither that $C_{2z}|0$ nor that $\epsilon|c/2$ is a symmetry operation. This operation is one of a 2_1, *screw axis* (see Fig. 3.4). From the result of Section 3.2, it follows that if $\beta|t\epsilon g$ then β is a rotational symmetry operation of the lattice, and it in turn follows that screw axes must be 2-, 3-, 4-, or 6-fold. The allowed axes are summarized in Table 3.1.

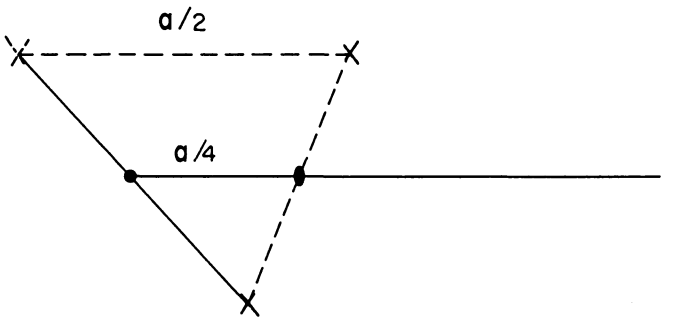

Fig. 3.3. $C_{2z}|a/2$ is a 180° rotation about $x = 1/4, y = 0$.

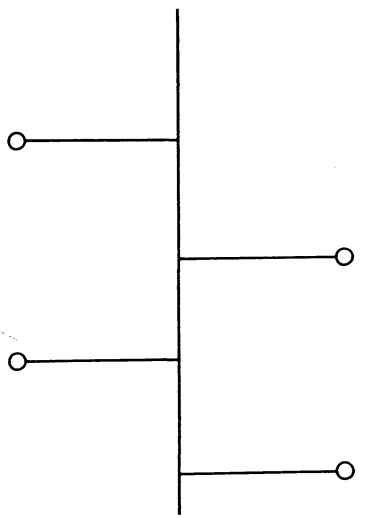

Fig. 3.4. The operations of a 2_1 axis.

Table 3.1. The allowed screw axes and their basic operations.

Axis	Basic operation	Lattice types
2_1	$C_{2z}\|\mathbf{c}/2$	m, o, r, h, t, c
3_1	$C_{3z}\|\mathbf{c}/3$	r, h, c
3_2	$C_{3z}\|2\mathbf{c}/3$	r, h, c
4_1	$C_{4z}\|\mathbf{c}/4$	t, c
4_2	$C_{4z}\|\mathbf{c}/2$	t, c
4_3	$C_{4z}\|3\mathbf{c}/4$	t, c
6_1	$C_{6z}\|\mathbf{c}/6$	h
6_2	$C_{6z}\|\mathbf{c}/3$	h
6_3	$C_{6z}\|\mathbf{c}/2$	h
6_4	$C_{6z}\|2\mathbf{c}/3$	h
6_5	$C_{6z}\|5\mathbf{c}/6$	h

3.6. Monoclinic Space Groups

Space groups can be considered from the point of view of combining operations. If the operations among the β parts include one σ and/or one C_2, then the lattice type must be monoclinic. The space groups consistent with a monoclinic lattice then include the cases of a single mirror or glide, of a single two-fold or two-fold screw axis and all allowed combinations of these for the two monoclinic lattice types. These space groups are collected in Table 3.2. The space group is the set of all symmetry operations and can be generated by combining the essential symmetry operations (column 1 of Table 3.2 for monoclinic groups) with all translations (including the null vector).

Care must be exercised in analyzing the $\beta|\mathbf{t}$ terms. If there exists a component of $\mathbf{t}$ that is perpendicular to a symmetry axis (e.g., $C_{2y}|\mathbf{c}/2$ or $C_{2y}|(\mathbf{b}+\mathbf{c})/2$), then the axis (a two-fold axis in the first case, and a 2_1 axis in the second) does not pass through the origin (in both cases it passes through $x = 0, z = 1/4$). If there exists a component of $\mathbf{t}$ that is perpendicular to a plane of symmetry (e.g., $\sigma_y|\mathbf{b}/2$ or $\sigma_y|(\mathbf{b}+\mathbf{c})/2$), then the plane (a mirror in the first case and a c-glide in the second) does not pass through the origin but is displaced relative to it (by $y = 1/4$ in these cases).

Table 3.2. The monoclinic space groups.

Essential symmetry operations	Space group symbol	Translations beyond $n_1\mathbf{a}+n_2\mathbf{b}+n_3\mathbf{c}$
$\varepsilon\|0, C_{2y}\|0$	$P2(C_2^1)$	
$\varepsilon\|, C_{2y}\|\mathbf{b}/2$	$P2_1(C_2^2)$	
$\varepsilon\|0, C_{2y}\|0$	$C2(C_2^3)$	$(\mathbf{a}+\mathbf{b})/2$
$\varepsilon\|0, \sigma_y\|0$	$Pm(C_s^1)$	
$\varepsilon\|0, \sigma_y\|\mathbf{c}/2$	$Pc(C_s^2)$	
$\varepsilon\|0, \sigma_y\|0$	$Cm(C_s^3)$	$(\mathbf{a}+\mathbf{b})/2$
$\varepsilon\|0, \sigma_y\|\mathbf{c}/2$	$Cc(C_s^4)$	$(\mathbf{a}+\mathbf{b})/2$
$\varepsilon\|0, \sigma_y\|0, C_{2y}\|0, i\|0$	$P2/m(C_{2h}^1)$	
$\varepsilon\|0, \sigma_y\|\mathbf{b}/2, C_{2y}\|\mathbf{b}/2, i\|0$	$P2_1/m(C_{2h}^2)$	
$\varepsilon\|0, \sigma_y\|0, C_{2y}\|0, i\|0$	$C2/m(C_{2h}^3)$	$(\mathbf{a}+\mathbf{b})/2$
$\varepsilon\|0, \sigma_y\|\mathbf{c}/2, C_{2y}\|\mathbf{c}/2, i\|0$	$P2/c(C_{2h}^4)$	
$\varepsilon\|0, \sigma_y\|(\mathbf{b}+\mathbf{c})/2, C_{2y}\|(\mathbf{b}+\mathbf{c})/2, i\|0$	$P2_1/c(C_{2h}^5)$	
$\varepsilon\|0, \sigma_y\|\mathbf{c}/2, C_{2y}\|\mathbf{c}/2, i\|0$	$C2/c(C_{2h}^6)$	$(\mathbf{a}+\mathbf{b})/2$

3.7. Essential Symmetry Operations

The *essential* symmetry operations are a set of operations which when combined with the pure translations yield the space group. The essential symmetry operations by themselves are not necessarily closed and thus do not necessarily form a group. For example, in the case of $P2_1/m$:

$$(C_{2y}|\mathbf{c}/2)^2 = \varepsilon|\mathbf{c} \tag{12}$$

and since $\varepsilon|\mathbf{c}$ is not an essential symmetry operation while $C_{2y}|\mathbf{c}/2$ is, the set is not closed. In some special cases the sets of essential symmetry operations are closed and in this case they are isomorphic to point groups. The monoclinic cases and the corresponding point groups are listed in Table 3.3.

Table 3.3. The symmorphic monoclinic space groups.

Space groups	Point groups
$P2, C2$	C_2
Pm, Cm	C_s
$P2m, C2/m$	C_{2h}

3.8. Symmorphic and Nonsymmorphic Space Groups

Table 3.3 lists the symmorphic monoclinic space groups, i.e., those monoclinic space groups for which the essential symmetry operations are isomorphic with a point group. Note that although $C2$ and $C2/m$ are symmorphic there are, nonetheless, screw axis operations in the space groups because

$$\varepsilon|(\mathbf{a}+\mathbf{b})/2 \cdot C_{2y}|0 = C_{2y}|(\mathbf{a}+\mathbf{b})/2 \tag{13}$$

which is the operation of a 2_1 axis along $\mathbf{b}$ at $x = 0$ and $z = 1/4$ (see Fig. 3.5). Thus, the space group $C2_1$ is equivalent to $C2$ (and $C2_1/m$ is equivalent to $C2/m$). In general, when there are, because of centering operations, screw and glide operations that would not be screw or glide operations if a primitive cell had been chosen, then the essential symmetry operations are those appropriate to the primitive cell (i.e., not including the introduced screw and glide operations). This statement removes any ambiguity introduced by centering. For example, without this restriction one could choose $\{\varepsilon, C_{2y}|0\}$ or $\{\varepsilon, C_{2y}|(\mathbf{a}+\mathbf{b})/2\}$ to generate the group,

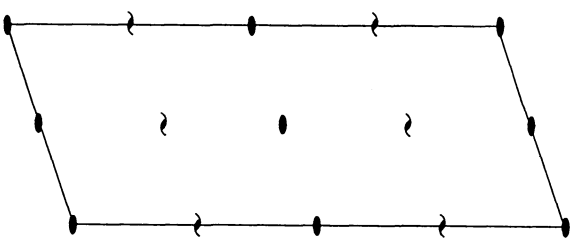

Fig. 3.5. The axes of the space group $C2$.

however this restriction limits the choice to $\{\varepsilon, C_{2y}|0\}$ and clearly places $C2$ among the symmorphic groups.

3.9. Crystal Class

Space groups can be categorized according to the β parts of their essential symmetry operations. Thus, for $P2, P2_1$, and $C2$ these are ε and C_{2y}, and for $P2/m$, $P2_1/m$, $C2/m$, $P2/c$, $P2_1/c$, and $C2/c$ they are $\varepsilon, \sigma_y, C_{2y}$ and i. These sets of β operations are isomorphic with the point groups C_2 and C_{2h}, and the point-group symbol forms the basis for the Schoenfliess symbol for the space group (in parentheses in column 2 of Table 3.2). Those space groups, the β parts of which are the same, form a *crystal class*. There are two triclinic classes (1 and $\bar{1}$), three monoclinic classes (2, m and $2/m$), three orthorhombic classes (222, $mm2$ and mmm) and etc. (see Table 3.4). The classes are subgroups of the lattice symmetries, and the space groups can be generated by systematically replacing mirror planes and rotation axes of the classes by glide planes and screw axes. Thus, $P4_2/nbc$ is in

Table 3.4. The 32 crystal classes.

Lattice type	Crystal classes
tr	$C_i(1), C_i(\bar{1})$
m	$C_2(2), C_s(m), C_{2h}(2/m)$
o	$D_2(222), C_{2v}(mm2), D_{2h}(mmm)$
t	$C_4(4), S_4(\bar{4}), C_{4h}(4/m), D_4(422)$ $C_{4v}(4mm), D_{2d}(\bar{4}2m, \bar{4}m2), D_{4h}(4/mmm)$
$h \neq r$	$C_3(3), C_{3i}(\bar{3}), D_3(312, 321, 32)$ $C_{3v}(31m, 3m1, 3m), D_{3d}(\bar{3}1m, \bar{3}m1, \bar{3}m)$
h	$C_6(6), C_{3h}(\bar{6}), C_{6h}(6/m), D_6(622),$ $C_{6v}(6mm), D_{3h}(\bar{6}m2, \bar{6}2m), D_{6h}(6/mmm)$
c	$T(23), Th(m3), O(432), Td(\bar{4}3m),$ $O_h(m3m)$

the same crystal class as $P4/mmm$, which in turn is the symmorphic space group with the same symmetry as the lattice. The space-group symmetry elements in the nonsymmorphic cases are generally not in the same relative positions as are those in the symmorphic groups. The locations of the planes and axes can be worked out in a fashion that is exemplified by the solution in the next section.

3.10. An Orthorhombic Example: *Pmna*

The symmorphic space groups in the mmm crystal class are: *Pmmm*, *Cmmm*, *Fmmm* and *Immm*. In this class there are 24 different nonsymmorphic variants that arise from interactions of glide planes of different types. For example, consider *Pmna*. This symbol means: there is a mirror perpendicular to **a**, a diagonal glide perpendicular to **b** and an *a*-glide perpendicular to **c**. Thus, leaving open with $\mathbf{t}_1 \perp \mathbf{a}$, $\mathbf{t}_2 \perp \mathbf{b}$ and $\mathbf{t}_3 \perp \mathbf{c}$, the locations of the three planes relative to the origin, the inversion operation $i|\mathbf{t}$ is the product $\sigma_x|\mathbf{t}_1 \cdot \sigma_y|(\mathbf{a}+\mathbf{c})/2 + \mathbf{t}_2 \cdot \sigma_z|\mathbf{a}/2 + \mathbf{t}_3$, i.e.,

$$\begin{pmatrix} \bar{1} & 0 & 0 & t_1 \\ 0 & 1 & 0 & 0 \\ 0 & 0 & 1 & 0 \\ 0 & 0 & 0 & 1 \end{pmatrix} \begin{pmatrix} 1 & 0 & 0 & 1/2 \\ 0 & \bar{1} & 0 & t_2 \\ 0 & 0 & 1 & 1/2 \\ 0 & 0 & 0 & 1 \end{pmatrix} \begin{pmatrix} 1 & 0 & 0 & 1/2 \\ 0 & 1 & 0 & 0 \\ 0 & 0 & \bar{1} & t_3 \\ 0 & 0 & 0 & 1 \end{pmatrix}$$

$$= \begin{pmatrix} \bar{1} & 0 & 0 & -t_1 \\ 0 & \bar{1} & 0 & t_2 \\ 0 & 0 & \bar{1} & 1/2 - t_3 \\ 0 & 0 & 0 & 1 \end{pmatrix} \tag{14}$$

and the inversion operation is through the point $-t_1\mathbf{a}/2 + t_2\mathbf{b}/2 + (1/2 - t_3)\mathbf{c}/2$ relative to the as yet unpositioned origin. In order to place the origin at the inversion center, which is a generally accepted location, the inversion operation is set to be $i|0$, i.e., $t_1 = 0$, $t_2 = 0$ and $t_3 = 1/2$. Then the operations of the mirror and the glides are $\sigma_x|0$ (reflection through the yz plane at $x = 0$), $\sigma_y|(\mathbf{a}+\mathbf{c})/2$ (diagonal glide through the xz plane at $y = 0$), and $\sigma_z|(\mathbf{a}+\mathbf{c})/2$ (an *a*-glide through the xy plane at $z = 1/4$). Combining the above:

$$\begin{aligned} i|0 \cdot \sigma_x|0 &= C_{2x}|0 \\ \sigma_y|(\mathbf{a}+\mathbf{c})/2 \cdot i|0 &= C_{2y}|(\mathbf{a}+\mathbf{c})/2 \\ \sigma_z|(\mathbf{a}+\mathbf{c})/2 \cdot i|0 &= C_{2z}|(\mathbf{a}+\mathbf{c})/2 . \end{aligned} \tag{15}$$

The $C_{2x}|0$ is a two-fold rotation about an axis through the origin, the $C_{2y}|(\mathbf{a}+\mathbf{c})/2$ is a two-fold rotation about an axis through $x = z = 1/4$, and the $C_{2z}|(\mathbf{a}+\mathbf{c})/2$ is the operation of a 2_1 axis along c and through $x = 1/4, y = 0$ (see Fig. 3.6). The resultant space-group is shown in Fig. 3.7.

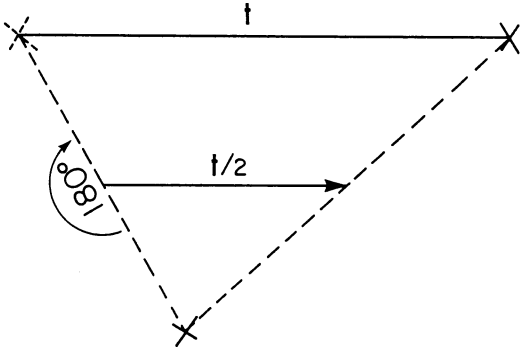

Fig. 3.6. The operation of a 2_1 axis along z through $x = 1/4, y = 0$.

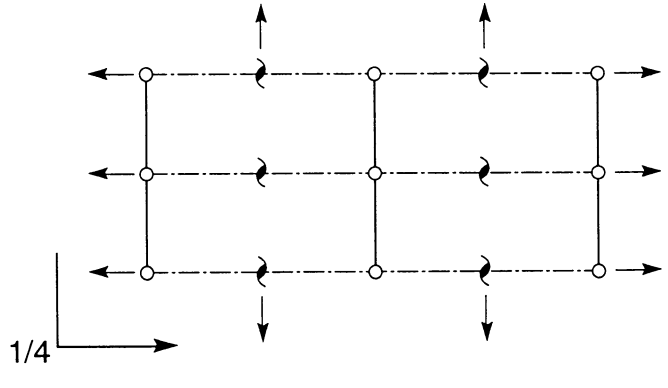

Fig. 3.7. The space group *Pmna*.

3.11. Group-Subgroup Relations Among the Crystal Classes

The allowed crystal classes are all subgroups of either $P6/mmm(D_{6n})$ or $m3m(O_h)$. In terms of their effect upon positions, the operations of O_h take

x, y, z into the 48 signed permutations of x, y, z (Table 3.5). The operations of D_{6h} are expressed in terms of hexagonal axes (see Section 2.4.7) and take the forms shown in Table 3.6. With the help of the operations listed in Tables 3.5 and 3.6, the group-subgroup relations among the crystal classes can be worked out. The results are given in Table 3.7.

Table 3.5. The symmetry operations of O_h.

Position	Symmetry operation	Position	Symmetry operation
x, y, z	ε	$\bar{x}, \bar{y}, \bar{z}$	i
$x, \bar{y}, \bar{z}$	C_{2x}	$\bar{x}, y, z$	σ_x
$\bar{x}, y, \bar{z}$	C_{2y}	$x, \bar{y}, z$	σ_y
$\bar{x}, \bar{y}, z$	C_{2z}	$x, y, \bar{z}$	σ_z
y, z, x	$C^2_{3(x+y+z)}$	$\bar{y}, \bar{z}, \bar{y}$	$\overline{C}^5_{3(x+y+z)}$
$y, \bar{z}, \bar{x}$	$C_{3(x+y-z)}$	$\bar{y}, z, x$	$\overline{C}_{3(x+y+z)}$
$\bar{y}, z, \bar{x}$	$C_{3(-x+y+z)}$	$y, \bar{z}, x$	$\overline{C}_{3(-x+y+z)}$
$\bar{y}, \bar{z}, x$	$C_{3(x-y+z)}$	$y, z, \bar{x}$	$\overline{C}_{3(x-y+z)}$
z, x, y	$C_{3(x+y+z)}$	$\bar{z}, \bar{x}, \bar{y}$	$\overline{C}_{3(x+y+z)}$
$z, \bar{x}, \bar{y}$	$C^2_{3(x-y+z)}$	$\bar{z}, x, y$	$\overline{C}^5_{3(x-y+z)}$
$\bar{z}, x, \bar{y}$	$C^2_{3(x+y-z)}$	$z, \bar{x}, y$	$\overline{C}^5_{3(x+y-z)}$
$\bar{z}, \bar{x}, y$	$C^2_{3(-x+y+z)}$	$z, x, \bar{y}$	$\overline{C}^5_{3(-x+y+z)}$
$\bar{y}, \bar{x}, \bar{z}$	$C_{2(y-x)}$	y, x, z	σ_{y-x}
$\bar{y}, x, z$	C_{4z}	$y, \bar{x}, \bar{z}$	$\overline{C}^3_{4z}$
$y, \bar{x}, z$	C^3_{4z}	$\bar{y}, x, \bar{z}$	$\overline{C}_{4z}$
$y, x, \bar{z}$	$C_{2(x+y)}$	$\bar{y}, \bar{x}, z$	σ_{x+y}
$\bar{x}, \bar{z}, \bar{y}$	$C_{2(z-y)}$	x, z, y	σ_{z-y}
$\bar{x}, z, y$	$C_{2(z+y)}$	$x, \bar{z}, \bar{y}$	σ_{z+y}
$x, \bar{z}, y$	C_{4x}	$\bar{x}, z, \bar{y}$	$\overline{C}^3_{4x}$
$x, z, \bar{y}$	C^3_{4x}	$\bar{x}, \bar{z}, y$	$\overline{C}_{4x}$
$\bar{z}, \bar{y}, \bar{x}$	$C_{2(z-x)}$	z, y, x	σ_{z-x}
$\bar{z}, y, x$	C^3_{4y}	$z, \bar{y}, \bar{x}$	$\overline{C}_{4y}$
$z, \bar{y}, x$	$C_{2(x+z)}$	$\bar{z}, y, \bar{x}$	σ_{x+y}
$z, y, \bar{x}$	C_{4y}	$\bar{z}, \bar{y}, x$	$\overline{C}^3_{4y}$

Table 3.6. The 24 operations of $6/mmm(D_{6h})$.

Position	Symmetry operation	Position	Symmetry operation
x, y, z	e	$\bar{x}, \bar{y}, \bar{z}$	i
$x-y, x, z$	C_{6z}	$y-x, \bar{x}, \bar{z}$	$\overline{C}_{6z}$
$\bar{y}, x-y, z$	C_{3z}	$y, y-x, \bar{z}$	$\overline{C}_{3z}$
$\bar{x}, \bar{y}, z$	C_{2z}	$x, y, \bar{z}$	σ_z
$y-x, \bar{x}, z$	C_{3z}^2	$x-y, x, \bar{z}$	$\overline{C}_{3z}^5$
$y, y-x, z$	C_{6z}^5	$\bar{y}, x-y, \bar{z}$	$\overline{C}_{6z}^5$
$\bar{x}, y-x, \bar{z}$	C_{2y}	$x, x-y, z$	σ_y
$\bar{y}, \bar{x}, \bar{z}$	$C_{2(x-y)}$	y, x, z	σ_{x-y}
$x-y, \bar{y}, \bar{z}$	C_{2x}	$y-x, y, z$	σ_x
$x, x-y, \bar{z}$	$C_{2(2x+y)}$	$\bar{x}, y-x, z$	σ_{2x+y}
$y, x, \bar{z}$	$C_{2(x+y)}$	$\bar{y}, \bar{x}, z$	σ_{x+y}
$y-x, y, \bar{z}$	$C_{2(x+2y)}$	$x-y, \bar{y}, z$	σ_{x+2y}

Table 3.7. The group-subgroup relations among the crystal classes.

Group	Maximal subgroups	Group	Maximal subgroups
O_h	$O, T_h, T_d, D_{4h}, D_{3d}$	D_{6h}	$C_6, C_{3h}, C_{3i}, D_{2h}$
O	T, D_4, D_3	D_{3h}	$C_{3h}, C_{3v}, D_3, C_{2v}$
T_h	T, D_{2h}, C_{3i}	C_{6v}	C_6, C_{3v}, C_{2v}
T_d	T, D_{2d}, D_{3d}	D_6	C_6, D_3, D_2
T	D_2, C_3	C_6	C_3, C_2
D_{4h}	$D_{2d}, C_{4h}, C_{4v} D_4, D_{2h}$	C_{3v}	C_3, C_s
D_{2d}	S_4, D_2	D_3	C_3, C_2
D_{2h}	S_4, D_2	C_{3i}	C_3, C_i
S_4	C_2		
C_{4h}	C_4, C_{2h}		
C_{4v}	C_4, C_{2v}		
D_4	C_4, D_2		
C_4	C_2		
D_{2h}	D_2, C_{2h}, C_{2v}		
C_{2v}	C_s		
D_2	C_2		

3.12. The Equivalent Positions in $I4_1/amd$

In this section the various aspects of space-groups presented in the preceding sections are brought to bear on the problem: starting with the space group symbol, $I4_1/amd$, generate the general equivalent positions in a unit cell. The location of the origin is arbitrary, and there are two different origins given in the International Tables, Volume I, one on the $\bar{4}$ axis and the other at an inversion center. The former location is chosen here, and this exercise then illustrates how the "generator" symmetry operations (those given by the international space-group symbol) and the space-group operation combination rules can be used to provide a detailed understanding of the symmetry.

From the space group symbol it is immediately known that the crystal class is $4/mmm(D_{4h})$ and that the lattice type is *bct*. The crystal class is inferred from the β parts implied by $4_1, a, m$ and d, namely $C_{4z}, \sigma_z, \sigma_x$, and σ_{x-y}. Since the symmetry is tetragonal there is also a b-glide perpendicular to $\mathbf{c}$, and two space group operations are:

$$\sigma_z|\mathbf{b}/2 + t_3\mathbf{c} = \begin{pmatrix} 1 & 0 & 0 & 0 \\ 0 & 1 & 0 & 1/2 \\ 0 & 0 & \bar{1} & t_3 \\ 0 & 0 & 0 & 1 \end{pmatrix} \tag{16}$$

and

$$\sigma_{x-y}|(\mathbf{a}+\mathbf{b}+\mathbf{c})/4 + t_1(\mathbf{a}-\mathbf{b}) = \begin{pmatrix} 0 & \bar{1} & 0 & 1/4+t_1 \\ 1 & 0 & 0 & 1/4-t_1 \\ 0 & 0 & 1 & 1/4 \\ 0 & 0 & 0 & 1 \end{pmatrix} \tag{17}$$

where the b-glide perpendicular to $\mathbf{c}$ is located at $t_3\mathbf{c}/2$ relative to the origin (Section 3.3) and the d-glide perpendicular to $\mathbf{a}-\mathbf{b}$ is located at $t_1(\mathbf{a}-\mathbf{b})/2$ relative to the origin. Combining:

$$\begin{pmatrix} 1 & 0 & 0 & 0 \\ 0 & 1 & 0 & 1/2 \\ 0 & 0 & \bar{1} & t_3 \\ 0 & 0 & 0 & 1 \end{pmatrix} \cdot \begin{pmatrix} 0 & \bar{1} & 0 & 1/4+t_1 \\ 1 & 0 & 0 & 1/4-t_1 \\ 0 & 0 & \bar{1} & 1/4 \\ 0 & 0 & 0 & 1 \end{pmatrix} = \begin{pmatrix} 0 & \bar{1} & 0 & 1/4+t_1 \\ 1 & 0 & 0 & 3/4-t_1 \\ 0 & 0 & \bar{1} & t_3-1/4 \\ 0 & 0 & 0 & 1 \end{pmatrix} \tag{18}$$

which, if the origin is at the $\overline{C}_4$ axis, yields $t_1 = -1/4$ and $t_3 = 1/4$. Thus, we have $\sigma_z|\mathbf{b}/2 + \mathbf{c}/4$, $\sigma_{x-y}|\mathbf{b}/2 + \mathbf{c}/4$ and $\overline{C}_{4z}|0$, and these operations suffice to generate the space group $I4_1/a$ (see Table 3.8).

Table 3.8. The symmetry operations of $I4_1/a$ and $I4_1/amd$ ($\tau = \mathbf{b}/2 + \mathbf{c}/4$).

Operation	x, y, z
$\varepsilon\|0$	x, y, z
$\overline{C}_{4z}\|0$	$\bar{y}, x, \bar{z}$
$C_{2z}\|0 = C_{4z}\|0 \cdot C_{4z}\|0$	$\bar{x}, \bar{y}, z$
$\overline{C}^3_{4z}\|0 = C_{4z}\|0 \cdot C_{2z}\|0$	$y, \bar{x}, \bar{z}$
$\sigma_z\|\tau$	$x, 1/2 + y, 1/4 - z$
$i\|\tau = \sigma_z\|\tau \cdot C_{2z}\|0$	$\bar{x}, 1/2 - y, 1/4 - z$
$C^3_{4z}\|\tau = i\|\tau \cdot \overline{C}_{4z}\|0$	$\bar{y}, 1/2 + x, 1/4 + z$
$C_{4z}\|\tau = i\|\tau \cdot \overline{C}^3_{4z}\|0$	$y, 1/2 - x, 1/4 + z$
$\sigma_x\|0$	$\bar{x}, y, z$
$\sigma_y\|0$	$x, \bar{y}, z$
$C_2(x-y)\|0 = \sigma_x\|0 \cdot C_{4z}\|0$	$\bar{y}, \bar{x}, \bar{z}$
$C_2(x+y)\|0 = \sigma_y\|0 \cdot \overline{C}_{4z}\|0$	$y, x, \bar{z}$
$C_{2x}\|\tau = i\|\tau \cdot \sigma_x\|0$	$x, 1/2 - y, 1/4 - z$
$C_{2y}\|\tau = i\|\tau \cdot \sigma_y\|0$	$\bar{x}, 1/2 + y, 1/4 - z$
$\sigma_{x-y}\|\tau = i\|\tau \cdot C_{2(x-y)}\|0$	$y, 1/2 + x, 1/4 + z$
$\sigma_{x+y}\|\tau = i\|\tau \cdot C_{2(x+y)}\|0$	$\bar{y}, 1/2 - x, 1/4 + z$

The addition of mirror planes perpendicular to **a** and **b** to $I4_1/a$ generates $I4_1/amd$. To locate these planes relative to the origin note that

$$\begin{pmatrix} \bar{1} & 0 & 0 & t_1 \\ 0 & 1 & 0 & 0 \\ 0 & 0 & 1 & 0 \\ 0 & 0 & 0 & 1 \end{pmatrix} \begin{pmatrix} 1 & 0 & 0 & 0 \\ 0 & \bar{1} & 0 & t_2 \\ 0 & 0 & 1 & 0 \\ 0 & 0 & 0 & 1 \end{pmatrix} = \begin{pmatrix} \bar{1} & 0 & 0 & t_1 \\ 0 & \bar{1} & 0 & t_2 \\ 0 & 0 & 1 & 0 \\ 0 & 0 & 0 & 1 \end{pmatrix} \tag{19}$$

and since $C_{2z}|0$ is a symmetry operation of the group, $t_1 = t_2 = 0$ and the operations are $\sigma_x|0$ and $\sigma_y|0$. The bottom half of Table 3.8 completes the exercise.

The general position of $I4_1/amd$ is a 32-fold position, i.e., each of the positions of Table 3.8 plus each coupled with $\varepsilon|(\mathbf{a} + \mathbf{b} + \mathbf{c})/2$. Those atom positions that fall on rotation axes and mirror planes (but not if a screw or glide translation separates them) have reduced numbers of equivalent positions. For example, in $I4_1/amd$ if a position is on a mirror plane (e.g.,

0, y, z) then all positions related by that mirror coincide and the position is a 16-fold position. Similarly, the multiplicities of positions are reduced even more at the intersections of mirror planes, of axes or mirror planes and axes. Thus, *special positions* are positions of special symmetry with reduced multiplicity.

3.13. Group-Subgroup Relations Among Space Groups

There are two different ways in which subgroups can be related to supergroups, namely with no loss of translations (the translational subgroups are the same in the superspace-group and the subspace-group), and with loss of translations (the translational subgroup of the subspace-group is a subgroup of that of the superspace-group). In the first case, called 'zellengleich' in German, the lattices can have the same symmetry (e.g., both lattices could be face-centered cubic) or the lattice can be distorted in the subgroup (e.g., cubic to tetragonal or rhombohedral). In either zellengleich case some symmetry elements from among the essential symmetry operations of the supergroup are missing in the subgroup. In cases of differing translational subgroups some pure translational symmetry operations and perhaps some essential symmetry operations are found in the supergroup but not in the subgroup.

3.14. Some Subgroups of $I4_1/amd$

The subgroups of a space group can be found by considering the possible classes to which subgroups might belong. For example, consider the 16 essential symmetry operations of $I4_1/amd$ (Table 3.8). The crystal class is $4/mmm$ and the subclasses include all tetragonal, orthorhombic, monoclinic and triclinic classes (Table 3.4). Some more or less obvious zellengleich tetragonal subgroups are: $I4_1/a, I4_122, I4_1md, I\bar{4}m2$ and $I\bar{4}2d$. Subgroups of these are, in turn, subgroups of $I4_1/amd$ (but not maximal subgroups).

If we are interested, for example, in the subgroups in the crystal class $2/m(C_{2h})$, we would seek all 2-fold and 2-fold screw rotation axes perpendicular to mirror and glide planes. Considering the operations of the 4_1 axis, these include those of a 2_1 axis, thus $I2_1/a$ (with the same c axis as $I4_1/amd$) is a monoclinic subgroup of $I4_1/amd$. However,

$$\varepsilon|(\mathbf{a}+\mathbf{b}+\mathbf{c})/2 \cdot C_{2z}|\mathbf{c}/2 = C_{2z}(\mathbf{a}+\mathbf{b})/2\,, \tag{20}$$

thus $I2_1/a$ and $I2/a$ are the same space group. To place the origin on the 2-fold axis, the origin must be shifted by 1/4, 1/4, 0 relative to the 2_1 axis, and to place the space group in its conventional setting the axes must be transformed (see Fig. 3.8):

$$\begin{pmatrix} 1 & \bar{1} & 0 \\ 0 & 0 & \bar{1} \\ 1 & 0 & 0 \end{pmatrix} \begin{pmatrix} \mathbf{a} \\ \mathbf{b} \\ \mathbf{c} \end{pmatrix}_{bcm} = \begin{pmatrix} \mathbf{a} \\ \mathbf{b} \\ \mathbf{c} \end{pmatrix}_{ecm} . \tag{21}$$

With this transformation and the origin shift, the conventional setting of $C2/c$ is achieved. The positions in $C2/c$ are related to those in $I2_1/a$ by the inverse transpose of the axial transformation (Section 2.15) with a shift of 1/4, 1/4, 0 to allow for the origin shift, i.e.,

$$\begin{pmatrix} 0 & \bar{1} & 0 & 0 \\ 0 & 0 & 1 & 0 \\ \bar{1} & \bar{1} & 0 & 0 \\ 0 & 0 & 0 & 1 \end{pmatrix} \begin{pmatrix} 1 & 0 & 0 & -1/4 \\ 0 & 1 & 0 & -1/4 \\ 0 & 0 & 1 & 0 \\ 0 & 0 & 0 & 1 \end{pmatrix} \begin{pmatrix} x \\ y \\ z \end{pmatrix}_{bcm} = \begin{pmatrix} x \\ y \\ z \end{pmatrix}_{ecm} . \tag{22}$$

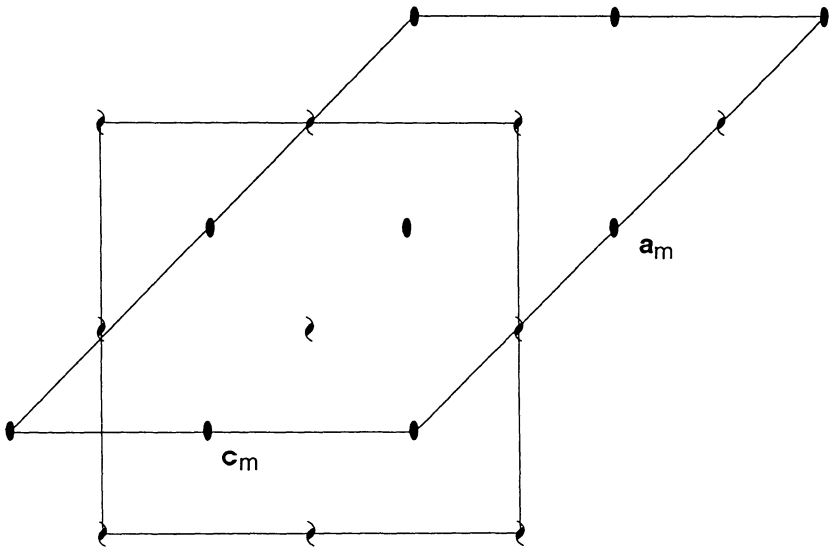

Fig. 3.8. Transformation to *ecm*.

Two additional monoclinic subgroups in the class $2/m$ can be found, namely $C2/m$ with

$$\begin{pmatrix} 1 & 0 & 1 \\ 0 & 1 & 0 \\ 0 & 0 & 1 \end{pmatrix} \begin{pmatrix} \mathbf{a} \\ \mathbf{b} \\ \mathbf{c} \end{pmatrix}_{bcm} = \begin{pmatrix} \mathbf{a} \\ \mathbf{b} \\ \mathbf{c} \end{pmatrix}_{ecm} \tag{23}$$

and $P2/c$ with

$$\begin{pmatrix} 0 & 0 & 1 \\ 1 & 1 & 0 \\ 1/2 & 1/2 & 1/2 \end{pmatrix} \begin{pmatrix} \mathbf{a} \\ \mathbf{b} \\ \mathbf{c} \end{pmatrix}_{bcm} = \begin{pmatrix} \mathbf{a} \\ \mathbf{b} \\ \mathbf{c} \end{pmatrix}_{sm} . \tag{24}$$

3.15. Superstructure

If some translational symmetry operations are missing in a subgroup relative to a supergroup, then the new structure is called a *superstructure* (note that the superstructure lattice (sometimes called the superlattice!) corresponds to a translational subgroup (there are fewer translational symmetry operations corresponding to the superlattice). In the case of a superstructure the primitive translations of the substructure $(\mathbf{a}_0, \mathbf{b}_0, \mathbf{c}_0)$ and those of the superstructure $(\mathbf{a}_s, \mathbf{b}_s, \mathbf{c}_s)$ are related by

$$\begin{pmatrix} a_{11} & a_{12} & a_{13} \\ a_{21} & a_{22} & a_{23} \\ a_{31} & a_{32} & a_{33} \end{pmatrix} \begin{pmatrix} \mathbf{a}_0 \\ \mathbf{a}_0 \\ \mathbf{c}_0 \end{pmatrix} = \begin{pmatrix} \mathbf{a}_s \\ \mathbf{b}_s \\ \mathbf{c}_s \end{pmatrix} , \tag{25}$$

where

$$\begin{bmatrix} a_{11} & a_{12} & a_{13} \\ a_{21} & a_{22} & a_{23} \\ a_{31} & a_{32} & a_{33} \end{bmatrix} = \frac{\mathbf{a}_s \cdot \mathbf{b}_s \times \mathbf{c}_s}{\mathbf{a}_0 \cdot \mathbf{b}_0 \times \mathbf{c}_0} > 1 . \tag{26}$$

The value of this determinant is called the *order* of the superstructure.

3.16. Symmetry Operations in Subgroups

The operations $C_{2y}|\mathbf{t}, \sigma_x|\mathbf{t}$ and $i|\mathbf{t}$ when combined with $n\mathbf{a}$ (a pure translation in the $\mathbf{a}$ direction) all generate symmetry elements (axes, planes or points) that are displaced by $n\mathbf{a}/2$ relative to the original operation. Thus, 2-fold axes perpendicular to $\mathbf{a}$, planes perpendicular to $\mathbf{a}$ and inversion centers all appear at intervals of $\mathbf{a}/2$ (and similarly in other directions). If the translational symmetry is broken such that a period is doubled, then one

half of these elements remain in the superstructure. For example, if along a given direction perpendicular mirror planes two-fold axes and inversion centers occur (see Fig. 3.9a) and the period along that direction is doubled, then the symmetry that remains in the superstructure is as shown in Figs. 3.9b, 3.9c, 3.9d and 3.9e.

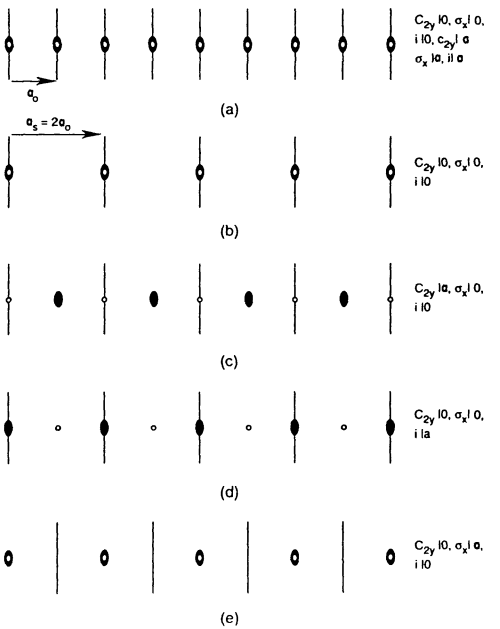

Fig. 3.9. Symmetry operations consistent with a doubled period.

In each case the effect upon other symmetry elements must also be considered. For example, $C_{2y}|0$ and $\sigma_x|0$ imply $\sigma_z|0$ and if $C_{2y}|0$ and $\sigma_x|0$ remain in the superstructure then so too does $\sigma_z|0$, whereas if $C_{2y}|\mathbf{a}_0 = C_{2y}|\mathbf{a}_s/2$ and $\sigma_x|0$ remain, then

$$C_{2y}|\mathbf{a}_s/2 \cdot \sigma_x|0 = \sigma_z|\mathbf{a}/2\,, \tag{27}$$

the operation of an a-glide perpendicular to $\mathbf{c}$, remains. Next consider the operation $\sigma_y|0$. If $C_{2y}|\mathbf{a}_0$ and $i|0$, or $C_{2y}|0$ and $i|\mathbf{a}_0$ remain, then since

$$i|\mathbf{a}_0 \cdot C_{2y}|0 = C_{2y}|\mathbf{a}_0 \cdot i|0 = \sigma_y|\mathbf{a}_s/2 \tag{28}$$

and the remaining plane perpendicular to **b** is an *a*-glide. Thus, for the supergroup *Pmmm* the case of Fig. 3.9b yields *Pmmm* (with $a = 2a_0$), the case of Fig. 3.9c yields *Pmaa*, Fig. 3.9d yields *Pmam* and Fig. 3.9e yields *Pmma*. The groups *Pmam* and *Pmma* are equivalent by exchange of **b** and **c** (and reversal of one axis to maintain a right-handed system), and thus three space-group types can result when a superstructure is formed from *Pmmm* by doubling of an axis.

3.17. The Subgroups of $P6_3/mmc$ in the Crystal Class D_{2h} Arising from Doubling of a

The doubling of a hexagonal *a*-axis while the *b*-axis is unchanged results in a primitive orthorhombic cell (Fig. 3.10). The essential symmetry operations of $P6_3/mmc$, for example, are given in Table 3.9. Those relevant to the orthorhombic subgroups under consideration are: $\varepsilon|0$, $\sigma_{2x+y}|\mathbf{c}/2$, $\sigma_y|0$, $\sigma_z|\mathbf{c}/2$ and $i|0$. Transforming to the orthorhombic axes (Fig. 3.10) converts $\sigma_{2x+y}|\mathbf{c}/2$ into $\sigma_x|\mathbf{c}/2$. Therefore, the possible space groups in D_{2h}, in accordance with the discussion in the preceding section, are the distinct combinations of $\sigma_x|\mathbf{c}/2$, $\sigma_x|\mathbf{c}/2 + \mathbf{a}_{hex} = \sigma_x|(\mathbf{a} + \mathbf{b} + \mathbf{c})/2$, $\sigma_y|0$, $\sigma_y|\mathbf{a}_{hex} = \sigma_y|(\mathbf{a} + \mathbf{b})/2$, $\sigma_z|\mathbf{c}/2$ and $\sigma_z|\mathbf{a}_{hex} + \mathbf{c}/2 = \sigma_z|(\mathbf{a} + \mathbf{b} + \mathbf{c})/2$.

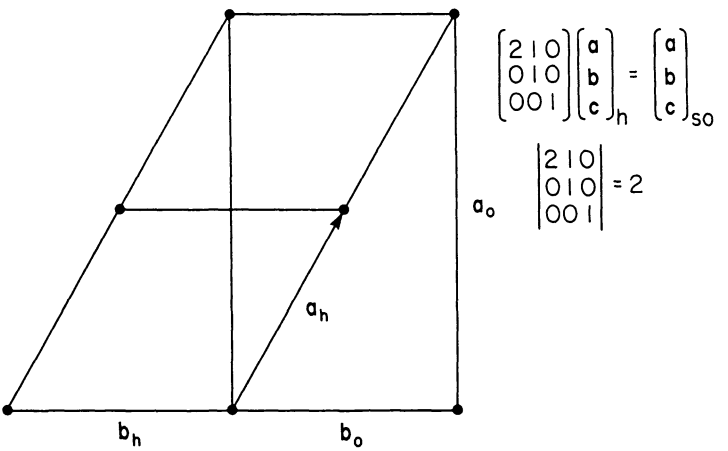

Fig. 3.10. The orthorhombic lattice that results from doubling a hexagonal basal plane axis.

These are the operations of, respectively, a c-glide perpendicular to **a**, an n-glide perpendicular to **a**, a mirror perpendicular to **b**, an a-glide perpendicular to **b** (and at $y = 1/4$), a mirror perpendicular to **c** (and at $z = 1/4$) and an n-glide perpendicular to **c** (and at $z = 1/4$). Thus, the possible space groups in D_{2h} from doubling **a** in $P6_3/mmc$ are those listed in Table 3.10.

Table 3.9. The essential symmetry operations of $P6_3/mmc$.

$\varepsilon\|0$	$i\|0$
$C_{6z}\|\mathbf{c}/2$	$\overline{C}_{6z}\|\mathbf{c}/2$
$C_{6z}^2\|0$	$\overline{C}_{3z}\|0$
$C_{2z}\|\mathbf{c}/2$	$\sigma_z\|\mathbf{c}/2$
$C_{6z}^4\|0$	$\overline{C}_{3z}^2\|0$
$C_{6z}^5\|\mathbf{c}/2$	$\overline{C}_{6z}^5\|\mathbf{c}/2$
$C_{2y}\|0$	$\sigma_y\|0$
$C_{2(x-y)}\|\mathbf{c}/2$	$\sigma_{x-y}\|\mathbf{c}/2$
$C_{2x}\|0$	$\sigma_x\|0$
$C_{2(2x+y)}\|\mathbf{c}/2$	$\sigma_{2x+y}\|\mathbf{c}/2$
$C_{2(x+y)}\|0$	$\sigma_{x+y}\|0$
$C_{2(x+2y)}\|\mathbf{c}/2$	$\sigma_{x+2y}\|\mathbf{c}/2$

Table 3.10. Space groups in D_{2h} for superstructures doubling **a** in $P6_3/mmc$.

$Pcmm$	$Pcmn$
$Pnmm$	$Pnmn$
$Pcam$	$Pcan$
$Pnam$	$Pnan$

Bibliography

1. Theo Hahn, Ed., *International Tables for Crystallography, Vol. A, Space-Group Symmetry* (Int. Union of Crystallography, Kluwer Academic Publishers, Boston, 1989).

2. Gerald Burns and A. M. Glazer, *Space Groups for Solid State Scientists* (Academic Press, New York, 1990).
3. Duncan McKie and Christine McKie, *Essentials of Crystallography* (Blackwell Scientific Publications, Boston, 1986).
4. M. J. Buerger, *Elementary Crystallography* (John Wiley and Sons, New York, 1956).
5. O. V. Kovalev, *Irreducible Representations of the Space Groups*, translated by A. Murray Gross (Gordon and Breach, New York, 1961).
6. Marjorie Senechal, *Crystalline Symmetries* (Adam Hilger, New York, 1990).

Problems

1. Apply all of the relevant proofs to the specific case of $C_{5z}|\mathbf{c}/5 + \mathbf{t}_\perp$, where $\mathbf{t}_\perp$ is some translation perpendicular to $\mathbf{c}$, to show that this is not a possible symmetry operation of a space group.
2. Using the result of Section 3.2, find the translation of a *d*-glide in a body-centered cell.
3. Show that if a space group includes body-centering and a mirror plane, then it also contains glide planes parallel to the mirror planes and midway between them.
4. Find the essential symmetry operations of *Pbcn*; list the corresponding symmetry elements and their locations.
5. Give the crystal class for $C2/c$, $Pna2_1$, $Cmcm$, $I4$, $P4cc$, $P4_2/mcm$, $P6_322$, $I2_13$, $P\bar{4}3n$.
6. Find the same cell(Zellengleich) subgroups of $I4_1/amd$ in the class $2/m$.
7. Find a subgroup of $P6_3/mmc$ in the crystal class C_{3h}.
8. Find the atomic positions of *Pbcn*.
9. A superstructure forms by the ordering of vacancies in every other plane perpendicular to $\mathbf{a} + \mathbf{b} + \mathbf{c}$ in the NaCl-type structure (M in 0, 0, 0 and X in 1/2, 1/2, 1/2 of $Fm3m$). Find the cell parameters (in terms of a_{fcc}) of the superstructure and the order of the superstructure.
10. Find the orthorhombic subgroups of $P6_3/mcm$ in the class D_{2h} arising from doubling of $\mathbf{a}_{\text{hex}}$.
11. What is the order of the superstructures in Problem 10?
12. Show that $I4_1/amd$ is a subgroup of $Fd3m$.

CHAPTER 4

RECIPROCAL SPACE

4.1. Rotational Symmetry of Reciprocal Space

In Section 3.2 it was shown that if $\beta|\mathbf{t}\epsilon g$ and $T\epsilon\{\mathbf{T}\}$ then $\beta\mathbf{T}\epsilon\{\mathbf{T}\}$. The essential feature of a reciprocal lattice vector is that $\mathbf{K}\cdot\mathbf{T}$ equals an integer times 2π, therefore,

$$\mathbf{K}\cdot\beta\mathbf{T} = 2\pi x \text{ integer} \tag{1}$$

for all $\mathbf{T}\epsilon\{\mathbf{T}\}$ and $\beta|\mathbf{t}\epsilon g$. Furthermore, since the scalar product (1) is the same whether $\mathbf{T}$ is rotated by β or $\mathbf{K}$ is rotated by β^{-1},

$$\beta^{-1}\mathbf{K}\cdot\mathbf{T} = 2\pi x \text{ integer} \tag{2}$$

for all $\mathbf{T}\epsilon\{\mathbf{T}\}, \mathbf{K}\epsilon\{\mathbf{K}\}$ and $\beta|\mathbf{t}\epsilon g$. Thus, the inverses of the β parts of all space-group operations, and thus the β parts themselves, are rotational symmetry operations of reciprocal space. It follows that the β operations of the crystal class are also symmetry operations of the reciprocal lattice.

4.2. Lattice Periodicity

One use of the vectors $\{\mathbf{K}\}$ is in generating functions which are periodic with the periodicity of the lattice. Since if $\mathbf{T} = m\mathbf{a}+n\mathbf{b}+p\mathbf{c}$ it follows that $\mathbf{K}\cdot\mathbf{T} = 2\pi(mh+nk+p\ell)$, and therefore $\cos\mathbf{K}\cdot\mathbf{r}, \sin\mathbf{K}\cdot\mathbf{r}$ and $\exp i\mathbf{K}\cdot\mathbf{r}$ all have the periodicity of the lattice, since in each case:

$$f(\mathbf{r}+\mathbf{T}) = f(\mathbf{r}+(mh+nk+p\ell)\cdot 2\cdot\pi) = f(\mathbf{r})\,. \tag{3}$$

The translational symmetry operations form a group [1. they include the null vector and $\mathbf{T}+\mathbf{O}=\mathbf{T}$; 2. if $\mathbf{T}\epsilon\{\mathbf{T}\}$, then$-\mathbf{T}\epsilon\{\mathbf{T}\}$; 3. $\mathbf{T}_1+(\mathbf{T}_2+$

$\mathbf{T}_3) = (\mathbf{T}_1 + \mathbf{T}_2) + \mathbf{T}_3$; 4. if $\mathbf{T}_1 \epsilon \{\mathbf{T}\}$ and $\mathbf{T}_2 \epsilon \{\mathbf{T}\}$, then $(\mathbf{T}_1 + \mathbf{T}_2) \epsilon \{\mathbf{T}\})]$. The functions $\cos \mathbf{K} \cdot \mathbf{r}, \sin \mathbf{K} \cdot \mathbf{r}$ and $\exp i\mathbf{K} \cdot \mathbf{r}$ are three different basis functions for the totally symmetric representation of this translational subgroup. In other words, these functions are eigenfunctions of the translational symmetry operators, and their eigenvalues are unity.

4.3. Nonintegral Periods

It is frequently of use to be able to write down periodic functions with periods that are some multiple of the lattice translations. This task is made easy by defining $\mathbf{k} = \lambda \mathbf{K}$ where $0 < \lambda < 1$. The functions $\cos \mathbf{k} \cdot \mathbf{r}, \sin \mathbf{k} \cdot \mathbf{r}$ and $\exp i\mathbf{k} \cdot \mathbf{r}$ have periods that differ from those of the lattice in the desired way. For example, letting $\mathbf{K} = \mathbf{a}^*$ and $\lambda = 1/2$ yields $\mathbf{k} \cdot \mathbf{r} = 1/2\mathbf{a}^* \cdot x\mathbf{a} = \pi x$, and the functions $\cos \pi x, \sin \pi x$ and $\exp i\pi x$ all have periods twice that of the lattice in the $\mathbf{a}$ direction. In this case all translations with an even number of $\mathbf{a}$ components carry these functions into themselves (have character $+1$) and all translations with an odd number of $\mathbf{a}$ components carry these functions into their negatives (have character -1). An infinite variety of periodicities is allowed mathematically, i.e., $\mathbf{k} = \mu\mathbf{a}^* + \nu\mathbf{b}^* + \omega\mathbf{c}^*$ with all values of μ, ν and ω between 0 and 1 allowed, however physically, as discussed in Section 10.2, a finite but very large number is allowed for a finite lattice.

The vectors $\mathbf{k} = \mu\mathbf{a}^* + \nu\mathbf{b}^* + \omega\mathbf{c}^*$ with $0 \leq \mu \leq 1, 0 \leq \nu \leq 1$ and $0 \leq \omega \leq 1$ define a unit cell volume in a reciprocal space based upon a primitive lattice. The significance of this unit cell can be understood by comparing $\exp i\mathbf{k} \cdot \mathbf{r}$ with $\exp i(\mathbf{k} + \mathbf{K}) \cdot \mathbf{r}$($\mathbf{k}$ is inside the unit cell, $\mathbf{k} + \mathbf{K}$ is outside the unit cell except for special points on the boundary). Now

$$\exp i(\mathbf{k} + \mathbf{K}) \cdot \mathbf{r} = (\exp i\mathbf{k} \cdot \mathbf{r})(\exp i\mathbf{K} \cdot \mathbf{r}) \tag{4}$$

and thus $\exp i(\mathbf{k} + \mathbf{K}) \cdot \mathbf{r}$ is the product of $\exp i\mathbf{k} \cdot \mathbf{r}$ and a totally symmetric basis function of the translations, i.e., $\exp i(\mathbf{k} + \mathbf{K}) \cdot \mathbf{r}$ has the same periodicity, and is a basis function for the same irreducible representation of the translations, as $\exp i\mathbf{k} \cdot \mathbf{r}$. For example, consider $\mathbf{k} = (\mathbf{a}^* + \mathbf{b}^*)/2$ and $\mathbf{K} = \mathbf{a}^* + \mathbf{b}^* + \mathbf{c}^*$. Then

$$\exp i\mathbf{k} \cdot \mathbf{r} = \exp i\pi(x + y) \tag{5}$$

and

$$\exp i(\mathbf{k} + \mathbf{K}) \cdot \mathbf{r} = (\exp i\pi(x + y))(\exp i2\pi(x + y + z)) \,. \tag{6}$$

Since any translational symmetry operation carries $\exp i2\pi(x+y+z)$ into itself, $\exp i\mathbf{k}\cdot\mathbf{r}$ and $\exp i(\mathbf{k}+\mathbf{K})\cdot\mathbf{r}$ are bases for the same representation. Hence, if one wishes to consider all possible symmetries, one need consider only the points within the reciprocal unit cell since points outside are related to those within by $\mathbf{K}$, a reciprocal lattice vector. Thus, each point outside of the cell can be related to one within the cell which corresponds to the same representation.

4.4. The Brillouin Zone

The conventional unit cell in reciprocal space is not that described above, but is that defined by $-1/2 \leq \mu \leq 1/2, -1/2 \leq \nu \leq 1/2$ and $-1/2 \leq \omega \leq 1/2$ in the case of a reciprocal lattice based upon a primitive lattice. In general, the conventional reciprocal unit cells are the volumes enclosed by the perpendicular bisecting planes of the $\mathbf{K}$ vectors to the nearest neighbors. These conventional unit cells are called the first *Brillouin zones* (BZ). A two-dimensional example is shown in Fig. 4.1.

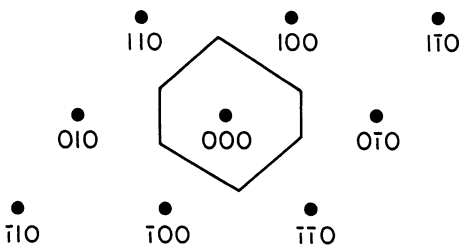

Fig. 4.1. A two-dimensional Brillouin zone.

In three dimensions a useful example is the BZ reciprocal to the *fcc* real cell. In this case the reciprocal cell is *bcc* (Section 2.18). The zone has square faces bisecting $\pm 2\pi\mathbf{i}/a, \pm 2\pi\mathbf{j}/a, \pm 2\pi\mathbf{k}/a$ since there are no lattice points at these $\mathbf{k}'s$, but there are lattice points at $\pm 4\pi\mathbf{i}/a$, etc. The zone has hexagonal faces bisecting the reciprocal lattice vectors along the eight $\mathbf{a}^* + \mathbf{b}^* + \mathbf{c}^*$ type vectors (at $\pm\pi\mathbf{i}/a \pm \pi\mathbf{j}/a \pm \pi\mathbf{k}/a$) as shown in Fig. 4.2. The centers of the square faces (e.g., $2\pi\mathbf{i}/a$) are labeled X, the centers of the hexagonal faces (e.g., $\pi/a[\mathbf{i}+\mathbf{j}+\mathbf{k}]$) are labeled L and the zone center (0, 0, 0) is labeled Γ. The points where two hexagonal faces and a square face share a corner (e.g., $\pi/a(2\mathbf{i}+\mathbf{j})$) are called W.

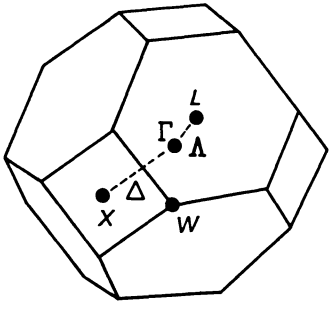

Fig. 4.2. The BZ of an *fcc* lattice.

4.5. The Symmetry of Reciprocal Space

The BZ contains all wave vectors, $\mathbf{k}$, required to describe all periodicities in terms of multiples (integral, rational, irrational) of periods of the lattice. Some of these periodicities are related by rotational symmetry, e.g., in the cubic classes $\pm\lambda\mathbf{a}^*, \pm\lambda\mathbf{b}^*$ and $\pm\lambda\mathbf{c}^*$ are so related, in the tetragonal classes $\pm\lambda\mathbf{a}^*$ and $\pm\lambda\mathbf{b}^*$ are related and in all classes with i, C_{2z} or σ_x symmetry $-\lambda\mathbf{a}^*$ and $\lambda\mathbf{a}^*$ are so related. However, when $\lambda = 1/2, \mathbf{a}^*/2$ and $-\mathbf{a}^*/2$ differ by $\mathbf{a}^*$ and if $\mathbf{a}^* \epsilon \{\mathbf{K}\}$, then $\mathbf{a}^*/2$ and $-\mathbf{a}^*/2$ correspond to the same periodicity. Thus, in this case we can say that $\mathbf{a}^*/2$ and $-\mathbf{a}^*/2$ are equal so far as symmetry is concerned. Two wave vectors, $\mathbf{k}$, that differ by a reciprocal lattice vector $\mathbf{K}$ are equal modulo $\mathbf{K}$. Two wave vectors that are related by rotational symmetry but are not equal modulo $\mathbf{K}$ belong to a *star*. Thus, in the primitive cubic case there are six vectors in the star of $\lambda\mathbf{a}^*$ for $0 < \lambda < 1/2$. When $\lambda = 1/2, \pm\mathbf{a}^*/2$ are equal modulo $\mathbf{a}^* \epsilon \{\mathbf{K}\}$ and similarly $\pm\mathbf{b}^*/2$ and $\pm\mathbf{c}^*/2$ are equal modulo $\mathbf{b}^*$ and $\mathbf{c}^*$, respectively, and there are three vectors in the star of $\mathbf{a}^*/2$. In the monoclinic case

$$\mathbf{a}^*/2 = -\mathbf{a}^*/2 \bmod \mathbf{a}^* \tag{7}$$

and there is one vector in the star of $\mathbf{a}^*/2$.

4.6. The Group of the Wave Vector

Thus, a rotational symmetry operation of reciprocal space (or of the crystal class) *either* carries a wave vector into itself modulo $\mathbf{K}$ or into a distinct $\mathbf{k}$

that is then in the same star with the original wave vector. Those operations of the crystal class that carry $\mathbf{k}$ into $\mathbf{k}$ mod $\mathbf{K}$ form the *point group of the wave vector*, $g^0(\mathbf{k})$. That it is indeed a group can be seen as follows:

1. $\epsilon\mathbf{k} = \mathbf{k} + 0$ and $0\epsilon\{\mathbf{K}\}$, thus $\epsilon\epsilon g^0(\mathbf{K})$.
2. If $\beta\mathbf{k} = \mathbf{k} + \mathbf{K}$, then $\beta^{-1}\beta\mathbf{k} = \mathbf{k} = \beta^{-1}\mathbf{k} + \beta^{-1}\mathbf{K}$, and since $\beta^{-1}\mathbf{K}\epsilon\{\mathbf{K}\}$, $\beta^{-1}\epsilon g^0(\mathbf{K})$.
3. If $\beta_1\mathbf{k} = \mathbf{k} + \mathbf{K}_1$ and $\beta_2\mathbf{k} = \mathbf{k} + \mathbf{K}_2$, then $\beta_2\beta_1\mathbf{k} = \beta_2(\mathbf{k} + \mathbf{K}_1) = \mathbf{k}+\mathbf{K}_2+\beta_2\mathbf{K}_1$; and since $(\mathbf{K}_2+\beta_1\mathbf{K}_1)\epsilon\{\mathbf{K}\}$, it follows that if $\beta_1\epsilon g^0(\boldsymbol{k})$ and $\beta_2\epsilon g^0(\boldsymbol{k})$, then $\beta_1\beta_2\epsilon g^0(\boldsymbol{k})$.
4. Combination of symmetry elements is associative.

The point group of the wave vector, $g^0(\mathbf{k})$, is related to the *group of the wave vector*, $g(\mathbf{k})$ as the crystal class is related to the space group, i.e., $g(\mathbf{k})$ is generated from $g^0(\mathbf{k})$ by associating the appropriate translations (lattice and nonlattice) with the β parts of $g^0(\mathbf{k})$. The essential operations of $g(\mathbf{k})$ can be found by selecting from the essential operations of the complete group those that have β parts in $g^0(\mathbf{k})$.

4.7. The Group of the Wave Vector $\mathbf{k} = \mathbf{a}^*/2$ in $P6_3/mmc$

As an example of a group of a wave vector consider the case of $\mathbf{a}^*/2$ for $P6_3/mmc$ (see Fig. 4.3). In this zone this point is called M. The vectors $\mathbf{a}^*/2, \mathbf{b}^*/2$ and $(\mathbf{a}^* - \mathbf{b}^*)/2$ form a star. The symmetry operations in the point group of the wave vector are those of D_{2h}, i.e.,

$$\begin{aligned}
\sigma_y \cdot \mathbf{a}^*/2 &= \mathbf{a}^*/2 \\
\sigma_{2x+y} \cdot \mathbf{a}^*/2 &= \mathbf{a}^*/2 \\
\sigma_z \cdot \mathbf{a}^*/2 &= \mathbf{a}^*/2 \\
i \cdot \mathbf{a}^*/2 &= -\mathbf{a}^*/2 \\
C_{2y} \cdot \mathbf{a}^*/2 &= -\mathbf{a}^*/2 \\
C_{2x+y} \cdot \mathbf{a}/2 &= \mathbf{a}^*/2 \\
C_{2z} \cdot \mathbf{a}^*/2 &= -\mathbf{a}^*/2
\end{aligned} \tag{8}$$

and since $-\mathbf{a}^*/2 = \mathbf{a}^*/2$ mod $\mathbf{a}^*$, these operations all belong to $g^0(\mathbf{a}^*/2)$. The corresponding group of the wave vector can be found using Table 3.9 of Chapter 3: $\epsilon|0$, $\sigma_y|0$, $C_{2x+y}|\mathbf{c}/2$, $\sigma_z|\mathbf{c}/2$, $i|0$, $C_{2y}|0$, $C_{2(2x+y)}|\mathbf{c}/2$, $C_{2z}|\mathbf{c}/2$. Taking $\mathbf{a}_0 = 2\mathbf{a}_h + \mathbf{b}_h, \mathbf{b}_0 = \mathbf{b}_n$ and $\mathbf{c}_0 = \mathbf{c}_n$ defines an orthorhombic unit

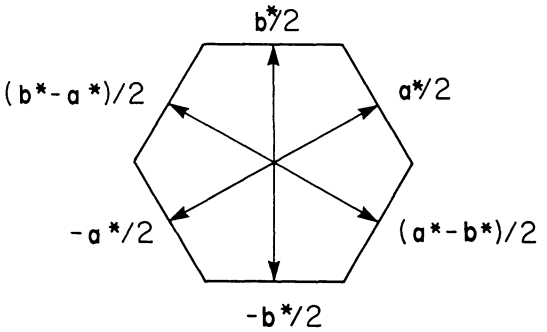

Fig. 4.3. The star of $\mathbf{a}^*/2$ in a hexagonal BZ.

cell. The group of the wave vector is then *Pcmm* which, in its conventional setting, is *Pmma*.

4.8. Group-Subgroup Relations

By taking the group of the wave vector $\mathbf{a}^*/2$ for $P6_3/mmc$ a space-group for a superstructure that doubles $\mathbf{a}$, namely *Pmma*, is thus found. However, other possibilities exist because the operations that remain can be either the operations *per se*, or those operations coupled with a lost translation (Section 3.17). This point will be explored further in Section 5.4.

4.9. Special Points

The points Γ, X, L and W (Fig. 4.2) for the BZ of *fcc* are the points of high symmetry. That is, $g^0(\mathbf{k}=0) = O_h$, $g^0(\mathbf{a}^*/2) = D_{4h}$, $g^0((\mathbf{a}^*+\mathbf{b}^*+\mathbf{c}^*)/2) = D_{3h}$ and $g^0(\mathbf{a}^*+\mathbf{b}^*/2) = D_{2d}$, and points in the neighborhood of these points have lower symmetry. The high symmetry points of BZ's are distinguished by point groups of the wave vector that are proper supergroups of those of all wave vectors terminating in the neighborhood of the special points. As an example consider $\mathbf{k} = \lambda\mathbf{a}^*$ for the cases in the crystal class $C_{2h}(\varepsilon, C_{2y}, \sigma_y, i)$. We have

$$\begin{aligned} C_{2y}\lambda\mathbf{a}^* &= -\lambda\mathbf{a}^* \\ \sigma_y\lambda\mathbf{a}^* &= \lambda\mathbf{a}^* \\ i\cdot\lambda\mathbf{a}^* &= -\lambda\mathbf{a}^* \end{aligned} \tag{9}$$

and for $0 < \lambda < 1/2$, $g^\circ(\lambda \mathbf{a}^*) = C_s$, whereas for $\lambda = 0$, $g^\circ(\mathbf{k} = 0) = C_{2h}$, and for $\lambda = 1/2$, $g^\circ(\mathbf{k} = \mathbf{a}^*/2) = C_{2h}$, and $\lambda = 0$ and $\lambda = 1/2$ correspond to special points. Special points correspond to special periodicities, e.g., $\lambda = 1/2$ in the above corresponds to doubling of the period along $\mathbf{a}$, whereas $\lambda - \delta$ corresponds to a very large, generally incommensurate period.

Wave vectors along lines can also have additional symmetry relative to neighboring wave vectors not on the line. For example, $g^\circ(\lambda \mathbf{b}) = C_2$ in C_{2h} (b axis unique), whereas $g^\circ(\lambda \mathbf{b} + \mu \mathbf{a}^*) = \varepsilon$. Such lines of special symmetry are designated by captial letters of the Greek alphabet (see Fig. 4.2).

Bibliography

1. G. F. Koster, *Space Groups and their Representations* (Academic Press, New York, 1957).
2. O. V. Kovalev, *Irreducible Representations of the Space Groups* (Gordon and Breach, New York, 1961).

Problems

1. Find $g^{\circ}(\mathbf{a}^*/2)$ and $g(\mathbf{a}^*/2)$ for $P6_3/mcm$.
2. Find the vectors in the star with $\mathbf{a}^* + \mathbf{b}^*/2$ in $Fm3m$.
3. Find $g(\mathbf{a}^* + \mathbf{b}^*/2)$ for $Fm3m$.
4. Find $g((\mathbf{a}^* + \mathbf{b}^* + \mathbf{c}^*)/2)$ for $Fm3m$.
5. Find the subgroups of $P6_3/mcm$ that double $\mathbf{a}$ using $g(\mathbf{k})$ as a starting point.
6. Show that $\exp -i\mathbf{K}\cdot\mathbf{r}$ has the period of the lattice for $\mathbf{K} = \mathbf{a}^* + 2\mathbf{b}^* + 3\mathbf{c}^*$.
7. Show that $\cos \mathbf{k} \cdot \mathbf{r}$ has three times the period of the lattice in the $\mathbf{a}$ direction if $\mathbf{k} = \mathbf{a}^*/3$.
8. What is the point-group symmetry of the BZ for $I4_1/amd$?
9. Find $g^{\circ}(\mathbf{a}^*/2)$ and $g(\mathbf{a}^*/2)$ for $I4_1/amd$.
10. Find the special points in $Pnma$.
11. Find the volume of the BZ in terms of $\mathbf{a} \cdot \mathbf{b} \times \mathbf{c}$.
12. Sketch the ab plane of the BZ for a C-centered cell with $a = 8.00$ Å and $b = 6.00$ Å.

CHAPTER 5

IRREDUCIBLE REPRESENTATIONS OF SPACE GROUPS

5.1. Representations of the Translational Group

A representation of a symmetry group is a set of matrices, $\{\Gamma_i\}$, one, not necessarily distinct, $\Gamma(\beta|\mathbf{t})$, associated with each element, $\beta|\mathbf{t}$, such that if

$$\beta_2|\mathbf{t}_2 \cdot \beta_1|\mathbf{t}_1 = \beta_3|\mathbf{t}_3\,, \tag{1}$$

then

$$\Gamma(\beta_2|\mathbf{t}_2)\Gamma(\beta_1|\mathbf{t}_1) = \Gamma(\beta_3|\mathbf{t}_3)\,. \tag{2}$$

The simplest cases are those for which the Γ's are real or complex numbers (one-dimensional representations). A representation is irreducible when no similarity transformation places all of the Γ's in the same block-diagonal form. For example, a two-dimensional representation can be reduced to two one-dimensional representations if there exists a Γ_r such that the

$$\Gamma_{ri} = \Gamma_r^{-1}\Gamma_i\Gamma_r \tag{3}$$

are all diagonalized. If no such Γ_r exists, then the two-dimensional representation is irreducible.

A one-dimensional representation is necessarily irreducible. If all the elements of a group commute the group is called *Abelian*, and Abelian groups have only one-dimensional irreducible representations. Since vector addition commutes, the translational subgroup of a space group is Abelian and the irreducible representations of the translational symmetry operations are one-dimensional.

The eigenfunctions of the translational symmetry operations, i.e., those functions for which

$$\phi(\mathbf{r}+\mathbf{T}) = \lambda\phi(\mathbf{r}), \tag{4}$$

where λ is a real or complex number, are basis functions for an irreducible representation of a translational subgroup. This can be seen by

$$\begin{aligned}\phi(\mathbf{r}+\mathbf{T}_1) &= \lambda_1\phi(\mathbf{r}),\\ \phi(\mathbf{r}+\mathbf{T}_2) &= \lambda_2\phi(\mathbf{r}),\end{aligned} \tag{4}$$

and

$$\phi(\mathbf{r}+\mathbf{T}_1+\mathbf{T}_2) = \lambda_1\phi(\mathbf{r}+\mathbf{T}_2) = \lambda_1\lambda_2\phi(\mathbf{r}). \tag{6}$$

If

$$\mathbf{T}_1+\mathbf{T}_2 = \mathbf{T}_3, \tag{7}$$

then

$$\phi(\mathbf{r}+\mathbf{T}_3) = \lambda_3\phi(\mathbf{r}) \tag{8}$$

and thus $\mathbf{T}_1+\mathbf{T}_2 = \mathbf{T}_3$ implies $\lambda_1\lambda_2 = \lambda_3$, i.e., the eigenvalues combine multiplicatively as the symmetry operations combine by consecutive operation.

The function $\exp i\mathbf{k}\cdot\mathbf{r}$ has the property

$$\exp i\mathbf{k}(\mathbf{r}+\mathbf{T}) = (\exp i\mathbf{k}\mathbf{T})\cdot(\exp i\mathbf{k}\cdot\mathbf{r}) \tag{9}$$

and thus is an eigenfunction of the translational symmetry operator with eigenvalue $\exp i\mathbf{k}\cdot\mathbf{T}$. If $\mathbf{k} = \mu\mathbf{a}^* + \nu\mathbf{b}^* + \omega\mathbf{c}^*$ and $\mathbf{T} = m\mathbf{a} + n\mathbf{b} + p\mathbf{c}$, then $\lambda = \exp 2\pi i[\mu m + \nu n + \omega p]$. The irreducible representations of the translations are readily found, there is one for each point in the Brillouin zone, and an equivalent one for all points outside of the zone and related to the point within the zone by a reciprocal lattice vector. The representations are complex except when $\sin 2\pi(\mu m+\nu n+\omega p) = 0$ and $\exp 2\pi i(\mu m+\nu n+\omega p) = \cos 2\pi(\mu m+\nu n+\omega p)$. If, for example, $\mu = 1/2$ and $\nu = \omega = 0$, then $\sin m\pi = 0$ and $\exp 2\pi i(\mu m+\nu n+\omega p) = \exp m\pi i = \pm 1$ for m even or odd, respectively. Thus, the eigenvalues of an irreducible representation of the translational subgroup at $\mathbf{k} = \mathbf{a}^*/2$ are $+1$ for even $\mathbf{a}$ translations and -1 for odd $\mathbf{a}$ translations. This illustrates one of the ways in which

special points are special, i.e., the irreducible representations may be real in contrast to the complex irreducible representations at neighboring points.

5.2. Irreducible Representations of Symmorphic Space Groups

The symmorphic space groups (Section 3.8) can each be factored into two groups: the rotations of the crystal class and the translations. Therefore, an irreducible representation of a symmorphic space group at $\mathbf{k}$ is the product of the one-dimensional representation of the translations at $\mathbf{k}$ and an irreducible representation of the point group isomorphic to the group of the wave vector. Thus, for a symmorphic space group

$$\beta|\mathbf{T} = \beta|0 \cdot \varepsilon|\mathbf{T} \tag{10}$$

and

$$\Gamma(\beta|\mathbf{t}) = \Gamma(\beta)\Gamma(\mathbf{T}), \tag{11}$$

where $\Gamma(\beta)$ is the irreducible representation of β in $g^0(\mathbf{k})$ for all β and $\mathbf{T}$.

5.3. Loaded Representations

In the general (symmorphic or nonsymmorphic) case $\hat{\Gamma}(\beta)$ is defined as

$$\hat{\Gamma}(\beta) = e^{i\mathbf{k}\cdot\mathbf{t}}\Gamma(\beta|\mathbf{t}), \tag{12}$$

where $\beta|\mathbf{t}$ is a matrix representing $\beta|\mathbf{t}\epsilon g(\mathbf{k})$, and $\hat{\Gamma}(\beta)$ is called the *loaded representation* of the β part of $\beta|\mathbf{t}$ at point $\mathbf{k}$ in the BZ. Using this definition and considering $\beta_2|\mathbf{t}_2$ and $\beta_1|\mathbf{t}_1$:

$$\begin{aligned}\hat{\Gamma}(\beta_2)\hat{\Gamma}(\beta_1) &= \exp i\mathbf{k}\cdot(\mathbf{t}_2+\mathbf{t}_1)\Gamma(\beta_2|\mathbf{t}_2)\Gamma(\beta_1|\mathbf{t}_1)\\ &= \exp i\mathbf{k}\cdot(\mathbf{t}_2+\mathbf{t}_1)\Gamma(\beta_2\beta_1|\beta_2\mathbf{t}_1+\mathbf{t}_2)\\ &= \exp -i\mathbf{k}\cdot(\beta_2\mathbf{t}_1-\mathbf{t}_1)\hat{\Gamma}(\beta_2\beta_1).\end{aligned} \tag{13}$$

Thus, if $\mathbf{k}\cdot(\beta_2\mathbf{t}_1-\mathbf{t}_1) = (2\pi x \text{ integer})$ for all $\beta|\mathbf{t}\epsilon g(\mathbf{k})$, then $\exp -i\mathbf{k}\cdot(\beta_2\mathbf{t}_1-\mathbf{t}_1) = 1$. Thus, the $\hat{\Gamma}$'s form a representation of $g^0(\mathbf{k})$ at $\mathbf{k}$, i.e., in this case.

$$\hat{\Gamma}(\beta) = \Gamma(\beta). \tag{14}$$

For example, in the case of symmorphic space groups the only allowed $\mathbf{t}$'s are translational symmetry operations and

$$\hat{\Gamma}(\beta|\mathbf{T}) = \exp -i\mathbf{k}\cdot\mathbf{T}\hat{\Gamma}(\beta) = \Gamma(\mathbf{T})\hat{\Gamma}(\beta). \tag{15}$$

And $\hat{\Gamma}(\beta) = \Gamma(\beta)$, i.e., the loaded representation is an irreducible representation of $g^0(\mathbf{k})$.

For nonsymmorphic cases it is possible to find a variety of $\mathbf{k}$ points for which $\Gamma(\beta) = \hat{\Gamma}(\beta)$ because $\mathbf{k} \cdot \mathbf{t}_1 = \mathbf{k} \cdot \beta\mathbf{t}_1 = \beta^{-1}\mathbf{k} \cdot \mathbf{t}$. This is true:

1. when $\mathbf{k} = 0$ in all space groups,
2. at a general point in the BZ, where $g(\mathbf{k}) = \varepsilon|0$ and thus β can be only ε,
3. at any point in the BZ at which $\mathbf{t}$ and $\beta\mathbf{t}$ are perpendicular to $\mathbf{k}$ for all $\beta|t\epsilon g(\mathbf{k})$ — in this case $\mathbf{k} \cdot \mathbf{t}$ and $\beta^{-1}\mathbf{k} \cdot \mathbf{t}$ are both zero,
4. at a point in the BZ at which $\mathbf{k}$ is parallel to the axis at β (so that $\beta\mathbf{k} = \mathbf{k}$) or in the plane of β (again so that $\beta\mathbf{k} = \mathbf{k}$) for all β.

These cases cover most of the volume of most BZ's. However, there are some cases for which $\mathbf{k} \cdot \mathbf{t} \neq \beta^{-1}\mathbf{k} \cdot \mathbf{t}$. Consider the nonsymmorphic case of an even-fold axis with a perpendicular plane (e.g., $2_1/m, 2/c$, or $2_1/c$). Without loss of generality, consider the b-axis to be collinear with the evenfold axis. Using the definition of Eq. (12), the $\hat{\Gamma}$'s for $\mathbf{k} = \mathbf{b}^*/2$ and $\mathbf{k} = \mathbf{c}^*/2$ are given in Tables 5.1 and 5.2.

Table 5.1. Loaded representation products for nonsymmorphic primitive groups in the class $2/m$ at $\mathbf{k} = \mathbf{b}^*/2$.

	$\hat{\Gamma}(C_{2y})\hat{\Gamma}(i)$	$\hat{\Gamma}(i)\hat{\Gamma}(C_{2y})$
$P2_1/m$	$\hat{\Gamma}(C_{2y} \cdot i)$	$-\hat{\Gamma}(i \cdot C_{2y})$
$P2/c$	$\hat{\Gamma}(C_{2y} \cdot i)$	$\hat{\Gamma}(i \cdot C_{2y})$
$P2_1/c$	$\hat{\Gamma}(C_{2y} \cdot i)$	$-\hat{\Gamma}(i \cdot C_{2y})$

Table 5.2. Loaded representation products for nonsymmorphic primitive groups in the class $2/m$ at $\mathbf{k} = \mathbf{c}^*/2$.

	$\hat{\Gamma}(\sigma_y)\hat{\Gamma}(i)$	$\hat{\Gamma}(i)\hat{\Gamma}(C_{2y})$
$P2_1/m$	$\hat{\Gamma}(\sigma_y \cdot i)$	$\hat{\Gamma}(i \cdot C_{2y})$
$P2/c$	$\hat{\Gamma}(\sigma_y \cdot i)$	$-\hat{\Gamma}(i \cdot C_{2y})$
$P2_1c$	$\hat{\Gamma}(\sigma_y \cdot i)$	$-\hat{\Gamma}(i \cdot C_{2y})$

Thus, for $P2_1/m$ and $P2_1/c$ at $\mathbf{b}^*/2$ and for $P2/c$ and $P2_1/c$ at $\mathbf{c}^*/2$ there are elements among the loaded representations that do not commute, and thus it is not possible that these are irreducible representations of the C_{2h} point group (Table 1.4). In fact, one-dimensional representations always commute, and thus it follows for the nonsymmorphic space groups given above (and their supergroups) that the irreducible representations at $\mathbf{k} = \mathbf{b}^*/2$ (for $P2_1/m$ and $P2_1/c$) and at $\mathbf{k} = \mathbf{c}^*/2$ (for $P2/c$ and $P2_1/c$) are at least two-dimensional.

In cases of $P2_1/m$, $P2/c$ and $P2_1/c$ these irreducible representations can be no more than two dimensional since $2^2 = 4$ (see Section 1.2). In order to determine a set of $\hat{\Gamma}$'s, the so-called "*loaded small representation*", it is helpful to work out a full multiplication table such as shown in Table 5.3 for $P2_1/m$ at $\mathbf{k} = \mathbf{b}^*/2$. It is a relatively simple matter to find a set of 2×2 matrices that multiply as do these representations, and a set is given in Table 5.4. From this loaded small representation (which is not a true representation since it is not closed) the definition of Eq. (12) can be used to produce an irreducible representation of $P2_1/m$ at $\mathbf{b}^*/2$. First the loaded representation must be unloaded:

$$\Gamma(\varepsilon|0) = \hat{\Gamma}(\varepsilon) = \begin{pmatrix} 1 & 0 \\ 0 & 1 \end{pmatrix} \tag{16}$$

$$\Gamma(C_{2y}|\mathbf{b}/2) = e^{(\mathbf{b}^*/2\cdot\mathbf{b}/2)i}\Gamma(C_{2y}) = \begin{pmatrix} i & 0 \\ 0 & -i \end{pmatrix}$$

$$\Gamma(\sigma_y|\mathbf{b}/2) = i \cdot \Gamma(\sigma_y) = \begin{pmatrix} 0 & i \\ -i & 0 \end{pmatrix} \tag{17}$$

$$\Gamma(i|0) = \hat{\Gamma}(i) = \begin{pmatrix} 0 & 1 \\ 1 & 0 \end{pmatrix}$$

Next note that the matrix representing any one of the implied symmetry operations

$$\varepsilon|\mathbf{T}\cdot\beta|\mathbf{t} = \beta|\mathbf{T}+\mathbf{t} \tag{18}$$

is given by

$$\Gamma(\beta|\mathbf{T}+\mathbf{t}) = (\exp -i\mathbf{b}^*\cdot\mathbf{T}/2)\Gamma(\beta|\mathbf{t}) \tag{19}$$

and the irreducible representation is completed.

Thus, an irreducible representation for a space group is given by the irreducible matrices representing the essential operations and the $\mathbf{k}$ vector

Table 5.3. Loaded representation multiplication table for $P2_1/m$ at $\mathbf{k} = \mathbf{b}^*/2$.

$\beta/2$ \ $\beta 1$	$\hat{\Gamma}(\varepsilon)$	$\hat{\Gamma}(C_{2y})$	$\hat{\Gamma}(i)$	$\hat{\Gamma}(\sigma_y)$
$\hat{\Gamma}(\varepsilon)$	$\hat{\Gamma}(\varepsilon)$	$\hat{\Gamma}(C_{2y})$	$\hat{\Gamma}(i)$	$\hat{\Gamma}(\sigma_y)$
$\hat{\Gamma}(C_{2y})$	$\hat{\Gamma}(C_{2y})$	$\hat{\Gamma}(\varepsilon)$	$\hat{\Gamma}(\sigma_y)$	$\hat{\Gamma}(i)$
$\hat{\Gamma}(i)$	$\hat{\Gamma}(i)$	$-\hat{\Gamma}(\sigma_y)$	$\hat{\Gamma}(\varepsilon)$	$-\hat{\Gamma}(C_{2y})$
$\hat{\Gamma}(\sigma_y)$	$\hat{\Gamma}(\sigma_y)$	$-\hat{\Gamma}(i)$	$\hat{\Gamma}(C_{2y})$	$-\hat{\Gamma}(\varepsilon)$

Table 5.4. Loaded small representation of $P2_1/m$ at $\mathbf{k} = \mathbf{b}^*/2$.

β	$\hat{\Gamma}(\beta)$
ε	$\begin{pmatrix} 1 & 0 \\ 0 & 1 \end{pmatrix}$
C_{2y}	$\begin{pmatrix} 1 & 0 \\ 0 & -1 \end{pmatrix}$
i	$\begin{pmatrix} 0 & 1 \\ 1 & 0 \end{pmatrix}$
σ_y	$\begin{pmatrix} 0 & 1 \\ -1 & 0 \end{pmatrix}$

which yields the representations of the translations. In the event that there is more than one vector in the star, the process must include consideration of the symmetry operations that interconvert wave vectors in the star. An example is considered in the next section. It is sometimes useful to have in hand basis functions for an irreducible representation. These can frequently be discerned by comparing the action of the operation upon x, y, z with its action upon the matrices in the irreducible representation. This comparison for $P2_1/m$ at $\mathbf{b}^*/2$ is shown in Table 5.5. A pair of functions that transform as column 3 of Table 5.5 is: $\exp i\pi y$ and $\exp -i\pi y$ and thus, these functions form a basis for the two-dimensional irreducible representation of $P2_1/m$ at $\mathbf{b}^*/2$.

Table 5.5. Symmetry operations, behavior of x, y, z and irreducible representation of $P2_1/m$ at $\mathbf{b}^*/2$.

Symmetry operation	x, y, z	Matrix
$\varepsilon\|0$	x, y, z	$\begin{pmatrix} 1 & 0 \\ 0 & 1 \end{pmatrix}$
$C_{2y}\|\mathbf{b}/2$	$\bar{x}, y+1/2, \bar{z}$	$\begin{pmatrix} i & 0 \\ 0 & -i \end{pmatrix}$
$\sigma_y\|\mathbf{b}/2$	$x, 1/2-y, z$	$\begin{pmatrix} 0 & i \\ -i & 0 \end{pmatrix}$
$i\|0$	$\bar{x}, \bar{y}, \bar{z}$	$\begin{pmatrix} 0 & 1 \\ 1 & 0 \end{pmatrix}$
$\varepsilon\|\mathbf{b}$	$x, y+1, z$	$\begin{pmatrix} \bar{1} & 0 \\ 0 & \bar{1} \end{pmatrix}$

5.4. Some Irreducible Representations of $P6_3/mmc$ at $\mathbf{k} = \mathbf{a}^*/2$

At the $\mathbf{k} = \mathbf{a}^*/2$ point of $P6_3/mmc$ (D_{6h}^4) there are three vectors in the star (Fig. 4.3) and the eight operations of D_{2h} form the point group of the wave vector (Section 4.7). The nonlattice translation ($\mathbf{c}^*/2$, Table 3.9 of Chapter 3) is perpendicular to $\mathbf{a}^*/2$ and other wave vectors in the star, and thus this case meets condition 3 of Section 5.3. The $\hat{\Gamma}$'s and the $\Gamma(\beta|\mathbf{t})$'s of $g(\mathbf{a}^*/2)$ are the same as the irreducible representations of $g^0(\mathbf{a}^*/2) = D_{2h}$. These irreducible representations are collected, together with some basis functions for the point group operations relative to the orthorhombic axes, in Table 5.6. The relevant space-group operations of $P6_3/mmc$ are given in terms of the orthorhombic axes in Table 5.7.

Some of the functions listed on the bottom of Table 5.6 contain the factor $\sin 2\pi z$ and some do not. Those that do not are basis functions for the *space group* $P6_3/mmc$ at $\mathbf{k} = \mathbf{a}^*/2$, while those that do must include an additional factor. Each of the functions with a factor $\sin 2\pi z$ is transformed into its negative by translation by $\mathbf{c}/2$. Multiplication of those functions by $\cos 2\pi z$, which will also change sign under this translation but is otherwise uneffected by transformations, will result in basis functions for the space-group operations. Thus, basis functions for $g(\mathbf{a}^*/2)$ for $P6_3/mmc$ in terms of the orthorhombic superstructure axes are given in Table 5.8. The functions of Table 5.8 can be transformed into hexagonal coordinates.

Table 5.6. Character table for D_{2h}.

		R_1	R_2	R_3	R_4	R_5	R_6	R_7	R_8
ε	x,y,z	1	1	1	1	1	1	1	1
C_{2x}	$x,\bar{y},\bar{z}$	1	−1	1	−1	1	−1	1	−1
C_{2y}	$\bar{x},y,\bar{z}$	1	1	−1	−1	1	1	−1	−1
C_{2z}	$\bar{x},\bar{y},z$	1	−1	−1	1	1	−1	−1	1
i	$\bar{x},\bar{y},\bar{z}$	1	1	1	1	−1	−1	−1	−1
σ_x	$\bar{x},y,z$	1	−1	1	−1	−1	1	−1	1
σ_y	$x,\bar{y},z$	1	1	−1	−1	−1	−1	1	1
σ_z	$x,y,\bar{z}$	1	−1	−1	1	−1	1	1	−1
		$\cos 2\pi x$	$\sin 2\pi x$	$\cos 2\pi x$	$\sin 2\pi x$	$\sin 2\pi x$	$\cos 2\pi x$	$\sin 2\pi x$	$\cos 2\pi x$
			×	×	×	×	×		×
			$\sin 2\pi z$	$\sin 2\pi y$	$\sin 2\pi y$	$\sin 2\pi y$	$\sin 2\pi y$		$\sin 2\pi z$
				×		×			
				$\sin 2\pi z$		$\sin 2\pi z$			

Table 5.7. Operations of elements in $g(\mathbf{a}^*/2)$ of $P6_3/mmc$ in terms of orthorhombic axes.

Symmetry operation	x,y,z
$\varepsilon\|0$	x,y,z
$C_{2x}\|\mathrm{c}/2$	$x,\bar{y},1/2-z$
$C_{2y}/0$	$\bar{x},y,\bar{z}$
$C_{2z}\|\mathrm{c}/2$	$\bar{x},\bar{y},1/2+z$
$i\|0$	$\bar{x},\bar{y},\bar{z}$
$\sigma_x\|\mathrm{c}/2$	$\bar{x},y,1/2+z$
$\sigma_y\|0$	$x,\bar{y},z$
$\sigma_z\|\mathrm{c}/2$	$x,y,1/2-z$

Table 5.8. Basis functions for $g(\mathbf{a}^*/2)$ of $P6_3/mmc$ in terms of the orthorhombic superstructure axes.

Irreducible representation	Basis function
R_1	$\cos 2\pi x$
R_2	$\sin 2\pi x \sin 2\pi z \cos 2\pi z$
R_3	$\cos 2\pi x \sin 2\pi y \sin 2\pi z \cos 2\pi z$
R_4	$\sin 2\pi x \sin 2\pi y$
R_5	$\sin 2\pi x \sin 2\pi y \sin 2\pi z \cos 2\pi z$
R_6	$\cos 2\pi x \sin 2\pi y$
R_7	$\sin 2\pi x$
R_8	$\cos 2\pi x \sin 2\pi z \cos 2\pi z$

To see how this goes, consider one of the irreducible representations, namely R_8, and transforming according to the inverse transpose of the lattice transformation matrix:

$$\begin{pmatrix} 1/2 & 0 & 0 \\ -1/2 & 1 & 0 \\ 0 & 0 & 1 \end{pmatrix} \begin{pmatrix} x \\ y \\ z \end{pmatrix}_h = \begin{pmatrix} x_h/2 \\ y_h - x_h/2 \\ z_h \end{pmatrix} = \begin{pmatrix} x \\ y \\ z \end{pmatrix}_0 \tag{20}$$

which upon substitution into the basis function for R_8 in Table 5.8 yields

$$\phi_1 = \cos \pi x \sin 2\pi z \cos 2\pi z \tag{21}$$

as the basis function expressed in terms of the hexagonal axes. The operations

$$C_{3z} \equiv \begin{pmatrix} 0 & \bar{1} & 0 \\ 1 & \bar{1} & 0 \\ 0 & 0 & 1 \end{pmatrix} \tag{22}$$

and

$$c_{3z}^2 \equiv \begin{pmatrix} \bar{1} & 1 & 0 \\ \bar{1} & 0 & 0 \\ 0 & 0 & 1 \end{pmatrix} \tag{23}$$

carry $\mathbf{a}^*/2$ into $\mathbf{b}^*/2$ and $(\mathbf{a}^* - \mathbf{b}^*)/2$, the other vectors in the star, and yield for

$$\begin{aligned} \phi_2 = C_3\phi_1 &= \cos \pi\bar{y} \sin 2\pi z \cos 2\pi z \\ &= \cos \pi y \sin 2\pi z \cos 2\pi z \end{aligned} \tag{24}$$

and

$$\phi_3 = C_3^2\phi_1 = \cos\pi(y-x)\sin 2\pi z\cos 2\pi z\,. \tag{25}$$

The three functions, ϕ_1, ϕ_2 and ϕ_3, form a basis for a three-dimensional irreducible representation of $P6_3/mmc$ at $\mathbf{a}^*/2$. The coordinates given are relative to the hexagonal axes. In order to find the matrix representing a given $\beta|\mathbf{t}\varepsilon g$, it is only necessary to investigate how these functions transform under $\beta|\mathbf{t}$. For example, $C_{6z}^5|\mathbf{c}/2$ takes ϕ_1 into ϕ_2, ϕ_2 into ϕ_3 and ϕ_3 into ϕ_1 and thus, $C_{6z}^5|\mathbf{c}/2$ is represented by

$$\begin{pmatrix} 0 & 1 & 0 \\ 0 & 0 & 1 \\ 1 & 0 & 0 \end{pmatrix} \begin{pmatrix} \phi_1 \\ \phi_2 \\ \phi_3 \end{pmatrix} = \begin{pmatrix} \phi_2 \\ \phi_3 \\ \phi_1 \end{pmatrix}. \tag{26}$$

5.5. Relationships Between Irreducible Representations and Subgroups: $P6_3/mmc$ at $\mathbf{a}^*/2$

The subgroups of $P6_3/mmc$ that double $\mathbf{a}$ correspond to the different irreducible representations of $P6_3/mmc$ at $\mathbf{a}^*/2$. If the eigenvalue of a given symmetry operation is -1, that operation is lost and if it is $+1$, the operation remains. That is, referring to Table 5.6, $\Gamma(\beta|\mathbf{t}) = -1$ means that $\beta|\mathbf{t}$ is not a symmetry operation of the subgroup, whereas $\Gamma(\beta|\mathbf{t}) = 1$ means that it is. Since $\Gamma(\varepsilon|\mathbf{a}_h) = -1$, it follows that if $\Gamma(\beta|\mathbf{t}) = -1$, then

$$\Gamma(\varepsilon|\mathbf{a}_h)\Gamma(\beta|\mathbf{t}) = \Gamma(\beta|\mathbf{t}+\mathbf{a}_h) = +1\,. \tag{27}$$

If an operation is lost at $\mathbf{k} = \mathbf{a}^*/2$, then that operation followed by translation by $\mathbf{a}_h$ remains in the subgroup. Recall that

$$\mathbf{a}_h = (\mathbf{a}_0 + \mathbf{b}_0)/2\,, \tag{28}$$

thus, using just the $\sigma_x, \sigma_y, \sigma_z$ portion of Table 5.6 and finding the operations that remain in the subgroup ($\beta|\mathbf{t}$ or $\beta|\mathbf{t}+\mathbf{a}_h$ depending upon whether the operation has character plus or minus one) yields the results of Table 5.9.

Table 5.9. The subgroups of $P6_3/mmc$ at $\mathbf{a}^*/2$.

R_1	R_2	R_3	R_4
$\sigma_x\|\mathbf{c}/2$	$\sigma_x\|(\mathbf{a}+\mathbf{b}+\mathbf{c})/2$	$\sigma_x\|\mathbf{c}/2$	$\sigma_x\|(\mathbf{a}+\mathbf{b}+\mathbf{c})/2$
$\sigma_y\|0$	$\sigma_y\|0$	$\sigma_y\|(\mathbf{a}+\mathbf{b})/2$	$\sigma_y\|(\mathbf{a}+\mathbf{b})/2$
$\sigma_z\|\mathbf{c}/2$	$\sigma_z\|(\mathbf{a}+\mathbf{b}+\mathbf{c})/2$	$\sigma_z\|(\mathbf{a}+\mathbf{b}+\mathbf{c})/2$	$\sigma_z\|\mathbf{c}/2$
$Pcmm$	$Pnmn$	$Pcan$	$Pnam$
R_5	R_6	R_7	R_7
$\sigma_x\|(\mathbf{a}+\mathbf{b}+\mathbf{c})/2$	$\sigma_x\|\mathbf{c}/2$	$\sigma_x\|(\mathbf{a}+\mathbf{b}+\mathbf{c})/2$	$\sigma_x\|\mathbf{c}/2$
$\sigma_y\|(\mathbf{a}+\mathbf{b})/2$	$\sigma_y\|(\mathbf{a}+\mathbf{b})/2$	$\sigma_y\|0$	$\sigma_y\|0$
$\sigma_z\|(\mathbf{a}+\mathbf{b}+\mathbf{c})/2$	$\sigma_z\|\mathbf{c}/2$	$\sigma_z\|\mathbf{c}/2$	$\sigma_z\|(\mathbf{a}+\mathbf{b}+\mathbf{c})/2$
$Pnan$	$Pcam$	$Pnmm$	$Pcmn$

Bibliography

1. O. V. Kovalev, *Irreducible Representations of the Space Groups* (Gordon and Breach, New York, 1961).
2. G. F. Koster, *Space Groups and Their Representations* (Academic Press, New York, 1957).

Problems

1. Show that $\cos \pi x$ and $\sin \pi x$ are both antisymmetric with respect to translation by $m\mathbf{a}$ where m is odd.
2. Find the irreducible representations of $P2/m$ at $\mathbf{k} = \mathbf{c}^*/2$.
3. Create a multiplication table for the loaded small representation of $P2_1/c$ at $\mathbf{k} = \mathbf{c}^*/2$.
4. Find the loaded small representation of $P2_1/c$ at $\mathbf{k} = \mathbf{c}^*/2$.
5. Find the small representation of $P2_1/c$ at $\mathbf{k} = \mathbf{c}^*/2$.
6. Using Table 3.5 show that the matrices of the 2-D irreducible representation of $P4/mmm$ at $\mathbf{k} = 0$ multiply as do the symmetry operations. Use $\overline{C}_{4z}|0$ times $C_{2(x+y)}|0$ and $\sigma_y|0$ times $\overline{C}_{4z}^3|0$ as examples.

CHAPTER 6

LANDAU THEORY

6.1. The Order Parameter

Landau theory deals with symmetry-breaking changes in solids that can be conceptualized as occurring continuously. It is then possible to express the particle density of the distorted structure, ρ, in terms of the undistorted particle density, ρ°, a distortion function, ϕ, and an order parameter, η:

$$\rho = \rho^\circ + \eta\phi\,, \tag{1}$$

and as $\eta \to 0, \rho \to \rho^\circ$.

6.2. The Variation of η with Thermodynamic State

The distortion function, ϕ, has thermodynamic consequences, i.e., changing ρ° by an amount of $\eta\phi$ changes the energy and entropy of a solid. At some temperature (at a given pressure and chemical composition) η can change continuously away from zero with decreasing T (see Fig. 6.1), and the symmetry changes at the temperature at which η starts to change. For example, suppose that in some solid with space-group symmetry $P2/m$ with atoms located on the two-fold axis, the atoms move in a concerted fashion so that the linear chain becomes increasingly zig-zag in character (Fig. 6.2). If the behavior is as shown in Fig. 6.1, the amount of distortion (the magnitude of the horizontal distance of the atoms from the vertical line) increases from zero at T_t to increasing values with decreasing T. The translational symmetry along the axis (say the $\mathbf{b}$ direction) is altered ($\mathbf{b}_n = 2\mathbf{b}_0$) and the new (superstructure) space group is $P2_1/m$.

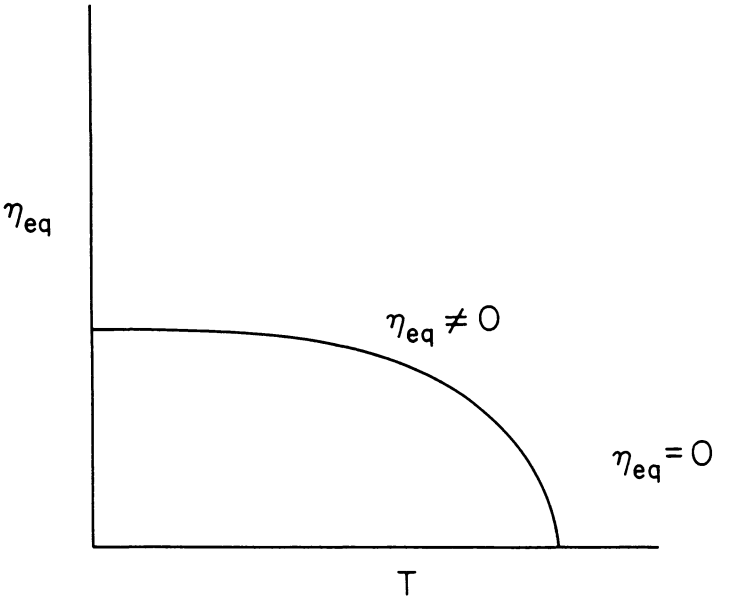

Fig. 6.1

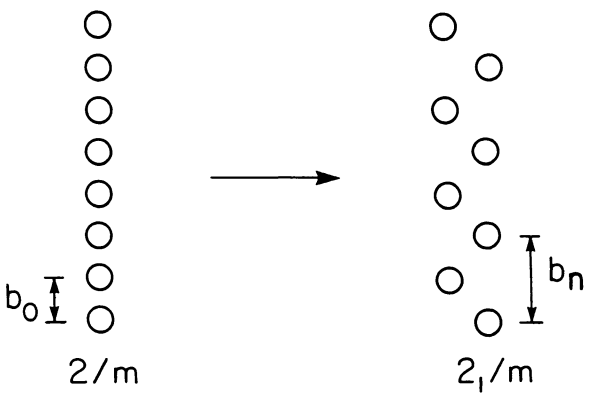

Fig. 6.2

6.3. Single Irreducible Representation Condition

In general, any distortion ϕ can be projected onto a complete set of basis functions for the irreducible representations of the space group of the high symmetry structure. Those functions which form a basis for a single irreducible representation would, by symmetry, have similar thermodynamic consequences. Thus, if ϕ_1 and ϕ_2 were basis functions for a single irreducible representation (either corresponding to two arms of a single star and a singly degenerate small representation, or corresponding to a doubly degenerate small representation and a single function in a star), then $\rho = \rho^0 + \eta\phi_1$ and $\rho = \rho^0 + \eta\phi_2$ would have the same thermodynamic consequences, i.e., would correspond to the same transition temperature, pressure or mole fraction. On the other hand, a distinct function that is a basis function of a different irreducible representation will have a different set of thermodynamic consequences and, in general, a different transition temperature, pressure or mole fraction.

In other words, if at equilibrium

$$\rho = \rho^0 + \eta\phi \tag{2}$$

and η changes away from zero at some T_t, then this occurs in general with ϕ a basis function for a single irreducible representation, or a combination of basis functions for a single irreducible representation. In this case G, the Gibbs free energy of the solid, can be expanded in η about G^0 to obtain, at a particular thermodynamic state, the Gibbs free energy of a distorted solid relative to the undistorted solid:

$$G = G^0 + \alpha\eta + A\eta^2 + B\eta^3 + C\eta^4 + \dots, \tag{3}$$

where $\alpha, A, B, C, \dots$ are coefficients that depend upon thermodynamic state and are specific to a particular irreducible representation.

6.4. The ρ Expansion

A set of ϕ_i's forming a basis for a single irreducible representation yield the generalized distortion function

$$\rho - \rho^0 = \sum c_i\phi_i \tag{4}$$

and setting $\eta^2 = \Sigma c_i^2$ and defining $\gamma_i = c_i/\eta$ so that

$$\sum \gamma_i^2 = \left(\sum c_i^2\right) \Big/ \eta^2 = 1, \tag{5}$$

the generalized distortion function is

$$\sum c_i\phi_i = \eta \sum \gamma_i\phi_i \,. \tag{6}$$

Letting $\phi = \Sigma\gamma_i\phi_i$ yields

$$\rho = \rho^0 + \eta\phi \,. \tag{7}$$

as in (2) above.

6.5. Symmetry Transformation of the γ_i's

A symmetry transformation carries $\Sigma\gamma_i\phi_i$ into $\Sigma\gamma_i'\phi_i$, and thus can be looked upon as transforming γ_i into γ_i'. For example, using the R_8 irreducible representation of $P6_2/mmc$ at $\mathbf{a}^*/2$ (Section 5.4) as an example, and taking the operation in question to be $c_{6z}^5|\mathbf{c}/2$ which, by Eq. 26 of Chapter 5, carries ϕ_1, ϕ_2, ϕ_3 into ϕ_2, ϕ_3, ϕ_1, we find that for this case $\gamma_2 \rightarrow \gamma_1$, $\gamma_3 \rightarrow \gamma_2$ and $\gamma_1 \rightarrow \gamma_3$. In general, the γ_i transformations can be similarly found from the irreducible representation of the space group to which the distortion corresponds. The terms in the G expansion contain polynomials in γ_i, and these polynomials are of the same order as the term. For example, the third-order term in the Taylor's series for G arises from third-order derivatives of G, multiplying terms like $c_i^3, c_i^2c_j$ and $c_ic_jc_k$, i.e., terms such as $\gamma_i^3\eta^3, \gamma_i^2\gamma_j\eta^3$ and $\gamma_i\gamma_j\gamma_k\eta^3$. Since symmetrically equivalent distortions have the same G, combinations of the γ's transformed by symmetry must multiply the same expansion coefficient, and the terms in G will be grouped according to invariant combinations. For example, if symmetry operations permute three basis functions without change of sign, then they carry $\gamma_i^3 + \gamma_2^3 + \gamma_3^3$ into itself, $\gamma_1\gamma_2^2 + \gamma_2\gamma_1^2 + \gamma_1\gamma_3^2 + \gamma_3\gamma_1^2\gamma_2\gamma_3^2 + \gamma_3\gamma_2^2$ into itself and $\gamma_1\gamma_2\gamma_3$ into itself. In this case, there are three different third-order invariants and three distinct third-order terms in G:

$$G = G^0 + \alpha\eta + A\eta^2 + \left[B_1 \sum_{i=1}^{3} \gamma_1^3 + B_2 \sum_{i\neq j}^{3} \gamma_i\gamma_i^2 + B_3\gamma_1\gamma_2\gamma_3 \right] \eta^3 + \ldots . \tag{8}$$

On the other hand, if one symmetry operation changed the signs, of all three γ_i (with or without permutation), there would be no third-order invariant, and in fact no odd-order invariants, and thus, by symmetry, no odd-order terms in the G expansion.

In general, the terms of any order that remain in the G expansion are those that are invariant under all operations of the space group (including translations), and symmetrically distinct invariant combinations yield symmetrically distinct terms.

6.6. Lack of First-Order Invariants

There are some general features of polynomials of the type under consideration that are well known from group theory. One is that a first-order invariant occurs only in the case of the totally symmetric representation. Consider the representations of Table 1.3 of Chapter 1, for example. For representations other than the totally symmetric some operations in each case take γ into $-\gamma$. This means that

$$G = G^0 + \alpha\eta + \ldots = G^0 - \alpha\eta + \ldots \tag{9}$$

and thus $\alpha = -\alpha$, or $\alpha \equiv 0$. Thus, the only irreducible representation for which $\alpha \not\equiv 0$ is the totally symmetric, and this irreducible representation corresponds to no loss in symmetry and is therefore not relevant to a symmetry-breaking transition. Thus, the first order term can be dropped from the G expansion in the case of one dimensional symmetry breaking representations.

That this conclusion is generally true follows from a thermodynamic argument. If the ρ^0 structure is stable at the transition temperature, T_t, then G must be at a minimum with respect to η at T_t and $\eta = 0$. Thus,

$$\alpha = \left.\frac{\partial G}{\partial \eta}\right|_{\substack{T=T_t \\ \eta=0}} = 0\,. \tag{10}$$

6.7. Second-Order Invariants

In the case of real basis functions it is always possible to find a set of axes so that the only second-order invariant polynomial is

$$\eta^2 = \sum c_i^2\,. \tag{11}$$

If the basis functions are not real, it is nonetheless necessary that $\Sigma c_i\phi_i$ be real (because $\Sigma c_i\phi_i = \rho - \rho^0$, a particle density). For the two-dimensional

small representation of $P2_1/m$ at $\mathbf{b}^*/2$ (Table 5.5 of Chapter 5 provides an example involving complex basis functions), we have

$$\phi_1 = \exp i\pi y \tag{12}$$

and

$$\phi_2 = \exp -i\pi y = \phi_1^* . \tag{13}$$

Thus

$$\rho = \rho^0 + (\gamma_1\phi_1 + \gamma_1^*\phi_1^*) \cdot \eta , \tag{14}$$

which is real. In this case $C_{2y}|\mathbf{b}/2$ takes

$$\begin{pmatrix} \gamma_1 \\ \gamma_1^* \end{pmatrix} \rightarrow \begin{pmatrix} -i\gamma_1^* \\ i\gamma_1 \end{pmatrix}, \tag{15}$$

$\sigma_y|\mathbf{b}/2$ takes

$$\begin{pmatrix} \gamma_1 \\ \gamma_1^* \end{pmatrix} \rightarrow \begin{pmatrix} -i\gamma_1^* \\ i\gamma_1 \end{pmatrix} \tag{16}$$

and $i|0$ takes

$$\begin{pmatrix} \gamma_1 \\ \gamma_1^* \end{pmatrix} \rightarrow \begin{pmatrix} -\gamma_1 \\ -\gamma_1^* \end{pmatrix}. \tag{17}$$

In each case $\gamma_1\gamma_1^*$ is carried into itself, and thus it is a second-order invariant and $\eta^2 = c_1c_1^*$ is a real order parameter.

6.8. Even-Order Terms

In the event that there are no third-order invariant polynomials, and thus no third-order terms in the G expansion, G can be expressed (to fourth order) as

$$\begin{aligned} G &= G^0 + A\eta^2 + \eta^4 \left[\sum_j C_j f_j^{(4)}(\gamma_1) \right] \\ &= G^0 + A\eta^2 + C\eta^4 , \end{aligned} \tag{18}$$

where $f_j^{(4)}(\gamma_i)$ is the jth fourth-order invariant polynomial of the γ_i's and $C = \sum_j C_j f_j^{(4)}(\gamma_i)$.

There is always at least one fourth-order invariant polynomial, i.e., either $(\sum \gamma_i \gamma_i^*)^2$ or $(\sum \gamma_i^2)^2$. When Eq. 18 is appropriate $G - G^\circ$ vs. η is concave up provided $A > 0$ and $C > 0$ (Fig. 6.3), and concave down at the origin if $A < 0$ and $C > 0$ (Fig. 6.4). If $C < 0$, there is no stable solution to fourth order, but there may be when the sixth-order term is included. If $A > 0$ and $C > 0$, then the equilibrium value of η is zero and only the symmetrical form is stable. If $A < 0$, then the only stable form is for $\eta \neq 0$ which corresponds to the broken symmetry. Thus, when the second-order expansion coefficient of G changes sign as a function of thermodynamics state, i.e., when

$$A = A(T, P, X) = 0 \tag{19}$$

a continuous symmetry-breaking phase transition occurs so long as $B \equiv 0$ and $C > 0$.

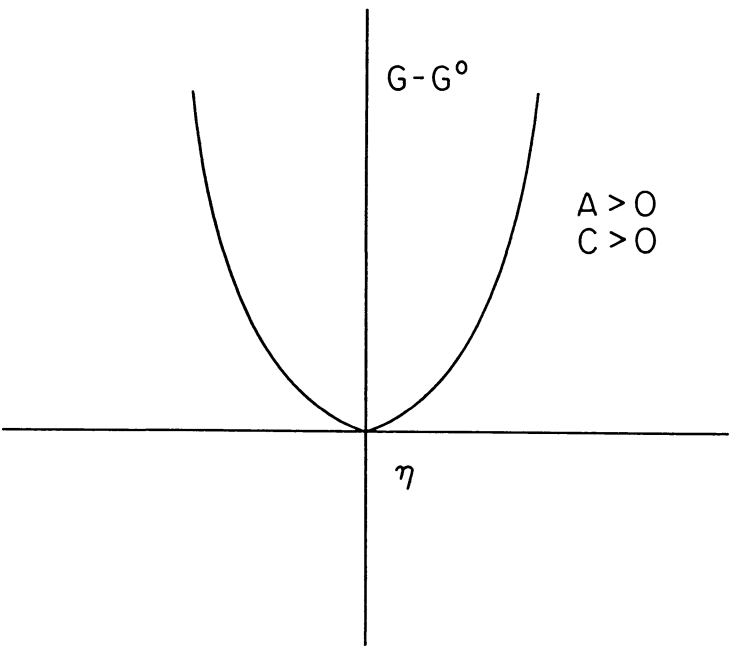

Fig. 6.3

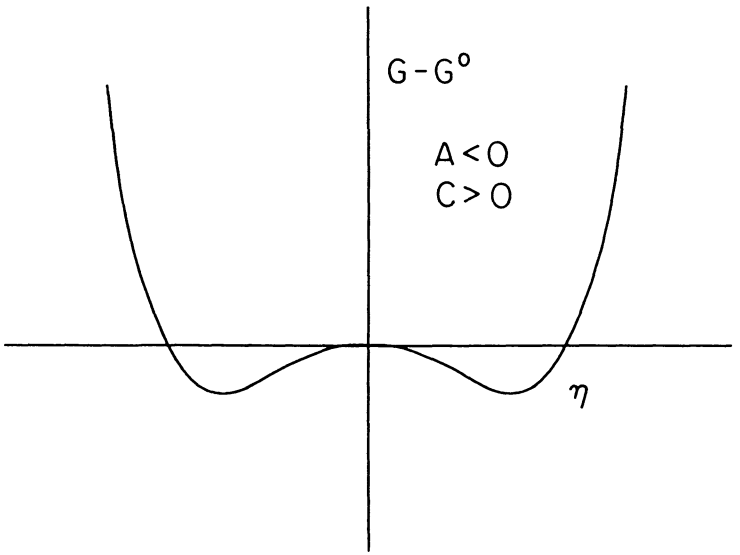

Fig. 6.4

6.9. The Third-Order Term

On the other hand, if there exists one third-order invariant polynomial, then

$$G = G^{\circ} + A\eta^2 + B\eta^3 + C\eta^4 \tag{20}$$

and, to fourth-order, $G - G^{\circ}$ vs. η has the form shown in Fig. 6.5 for $A > 0, B > 0$ and $C > 0$ (and it's reflection through the vertical axis for $A > 0, B < 0$ and $C > 0$). As A approaches zero, the minimum at $\eta \neq 0$ approaches the horizontal axis and when it touches $\eta = 0$ *and* $\eta \neq 0$ at equilibrium (Fig. 6.5). That is, as the temperature decreases a temperature is reached at which the symmetrical and distorted forms coexist in equilibrium, and a first-order phase transition occurs.

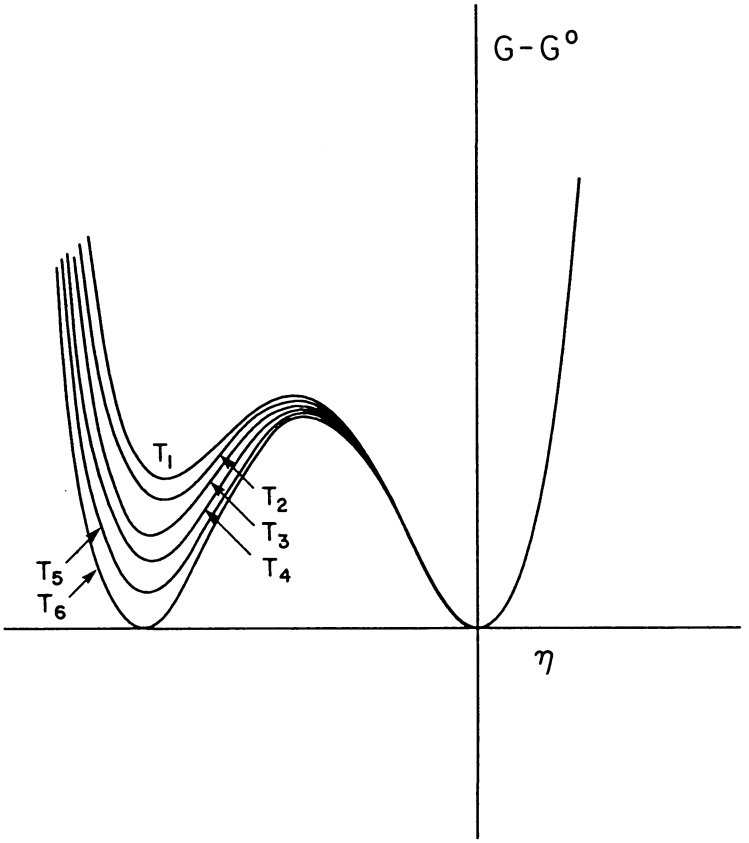

Fig. 6.5

6.10. Summary

A continuous structural change can result in a broken symmetry (a second-order phase transition can occur) when (1) the broken symmetry corresponds to a single irreducible representation and (2) there are no third-order invariant polynomials corresponding to this representation. The point about a single irreducible representation is that the A term in the G expansion will differ from one irreducible representation to another, and thus will vanish at some succession of states (e.g., T vs. X, see Fig. 6.6) for

one irreducible representation but not for others. It could happen that two such curves cross, and thus at some isolated point a second-order transition might correspond to two irreducible representations. However, the occurrence of a $T - X$ (or $T - P$ or $P - X$) line of second-order transition is an indication that the transition corresponds to a single irreducible representation. Furthermore, the occurrence of such a crossing is a rare event, so if a transition occurs with a continuous structure change the probability is very high that the transition corresponds to a single irreducible representation.

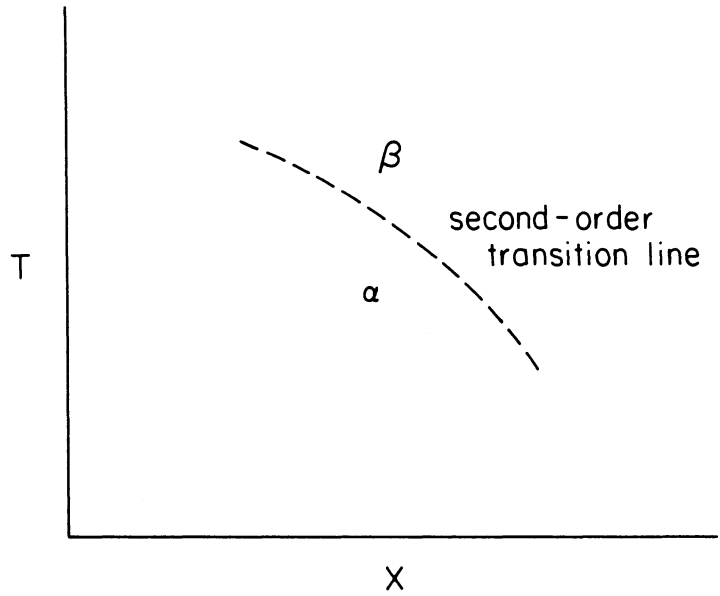

Fig. 6.6

6.11. Invariants of Third and Fourth Order

The polynomial terms in G are important in determining which distortions can correspond to minima in G. In the absence of a third-order term a continuous symmetry breaking can occur to yield a structure corresponding to a minimum in the fourth-order invariants (and thus a minimum in G). It is therefore worthwhile to have a method for determining polynomials

of third and fourth order. The invariant polynomials of any order can be found as follows:

1. write down every possible term of order n and provide each with a constant coefficient,
2. transform these terms according to a set of irreducible representation matrices corresponding to a set of generator operations (e.g., $\sigma_x, C_{3(x+y+z)}, \sigma_{x+y}$ for $m3m$),
3. equate coefficients of like terms and factor.

As an example the invariants corresponding to a particular irreducible representation are worked out in the next section.

6.12. The Totally Symmetric Small Representation of $Fm3m$ at the L Point

In this section the invariant polynomials corresponding to the totally symmetric small representation at the L point in the case of space-group $m3m$ are worked out using the ideas of the preceding sections. There are four wave vectors in the star, e.g.,

$$\begin{aligned} \boldsymbol{k}_1 &= (\mathbf{a}^* + \mathbf{b}^* + \mathbf{c}^*)/2 \\ \boldsymbol{k}_2 &= (\mathbf{a}^* + \mathbf{b}^* - \mathbf{c}^*)/2 \\ \boldsymbol{k}_3 &= (\mathbf{a}^* - \mathbf{b}^* + \mathbf{c}^*)/2 \\ \boldsymbol{k}_4 &= (-\mathbf{a}^* + \mathbf{b}^* + \mathbf{c}^*)/2 \end{aligned} \tag{21}$$

so the representation will be four dimensional. A sufficient set of symmetry operations to generate the space group is: $\varepsilon|(\mathbf{a}+\mathbf{b})/2$, $\sigma_x|0$, $C_{3(x+y+z)}|0$, $\sigma_{x-y}|0$ and $\mathbf{T} = n\mathbf{a} + m\mathbf{b} + p\mathbf{c}$. A set of basis functions that transform into themselves under the appropriate $m\bar{3}m$ subgroups, and thus form bases for the totally symmetric *small* representation at L is

$$\begin{aligned} \phi_1 &= \cos \pi(x + y + z) \\ \phi_2 &= \cos \pi(x + y - z) \\ \phi_3 &= \cos \pi(x - y + z) \\ \phi_4 &= \cos \pi(-x + y + z) \end{aligned} \tag{22}$$

These functions form a basis for a four dimensional representation which can be figured out by considering the behavior of the ϕ_i's under the generating operations of the group ($m3m$):

$$1.\quad \sigma_x|0(\bar{x},y,z): \begin{bmatrix} 0 & 0 & 0 & 1 \\ 0 & 0 & 1 & 0 \\ 0 & 1 & 0 & 0 \\ 1 & 0 & 0 & 0 \end{bmatrix} \tag{23}$$

$$2.\quad C_{3(x+y+z)}|0(z,x,y): \begin{bmatrix} 1 & 0 & 0 & 0 \\ 0 & 0 & 1 & 0 \\ 0 & 0 & 0 & 1 \\ 0 & 1 & 0 & 0 \end{bmatrix} \tag{24}$$

$$3.\quad \sigma_{x-y}|0(y,x,z): \begin{bmatrix} 1 & 0 & 0 & 0 \\ 0 & 1 & 0 & 0 \\ 0 & 0 & 0 & 1 \\ 0 & 0 & 1 & 0 \end{bmatrix} \tag{25}$$

$$4.\quad \varepsilon|(\mathbf{a}+\mathbf{b})/2(x+1/2,y+1/2,z): \begin{bmatrix} \bar{1} & 0 & 0 & 0 \\ 0 & 1 & 0 & 0 \\ 0 & 0 & 1 & 0 \\ 0 & 0 & 0 & \bar{1} \end{bmatrix}. \tag{26}$$

All possible third order terms are included in

$$\begin{aligned} &c_1\gamma_1^3 + c_2\gamma_2^3 + c_3\gamma_3^3 + c_4\gamma_4^3 + c_5\gamma_1\gamma_2^2 + c_6\gamma_2\gamma_1^2 + c_7\gamma_1\gamma_3^2 \\ &\quad + c_8\gamma_3\gamma_1^2 + c_9\gamma_1\gamma_4^2 + c_{10}\gamma_4\gamma_1^2 + c_{11}\gamma_2\gamma_3^2 + c_{12}\gamma_3\gamma_2^2 \\ &\quad + c_{13}\gamma_2\gamma_4^2 + c_{14}\gamma_4\gamma_2^2 + c_{15}\gamma_3\gamma_4^2 + c_{16}\gamma_4\gamma_3^2 + c_{17}\gamma_1\gamma_2\gamma_3 \\ &\quad + c_{18}\gamma_1\gamma_2\gamma_4 + c_{19}\gamma_2\gamma_3\gamma_4 + c_{20}\gamma_1\gamma_3\gamma_4 \end{aligned} \tag{27}$$

Under $\varepsilon|\mathbf{a}$ all $\phi_i \to -\phi_i$ and thus $\gamma_i \to -\gamma_i$. It follows that each coefficient C_i must vanish. The possible fourth-order polynominals are

$$\begin{aligned} &c_1\gamma_1^4 + c_2\gamma_2^4 + c_3\gamma_3^4 + c_4\gamma_4^4 + c_5\gamma_1\gamma_2^3 + c_6\gamma_1\gamma_3^3 + c_7\gamma_1\gamma_4^3 \\ &\quad + c_8\gamma_2\gamma_3^3 + c_9\gamma_2\gamma_4^3 + c_{10}\gamma_4\gamma_4^3 + c_{11}\gamma_2\gamma_1^3 + c_{12}\gamma_3\gamma_1^3 \\ &\quad + c_{13}\gamma_4\gamma_1^3 + c_{14}\gamma_3\gamma_2^3 + c_{15}\gamma_4\gamma_2^3 + c_{16}\gamma_4\gamma_3^3 + c_{17}\gamma_1^2\gamma_2^2 \\ &\quad + c_{18}\gamma_1^2\gamma_3^2 + c_{19}\gamma_1^2\gamma_4^2 + c_{20}\gamma_2^2\gamma_3^2 + c_{21}\gamma_2^2\gamma_4^2 \\ &\quad + c_{22}\gamma_3^2\gamma_4^2 + c_{23}\gamma_1\gamma_2\gamma_3\gamma_4 \end{aligned} \tag{28}$$

The following result from the respective transformations:

1. $\varepsilon|(\mathbf{a}+\mathbf{b})/2: \; c_6 = c_7 = c_8 = c_9 = c_{12} = c_{13} = c_{14} = c_{15} = 0,$
2. $\varepsilon|(\mathbf{a}+\mathbf{c})/2: \; c_5 = c_7 = c_8 = c_{10} = c_{11} = c_{13} = c_{14} = c_{16} = 0.$

At this point we are left with

$$c_1\gamma_1^4 + c_2\gamma_2^4 + c_3\gamma_3^4 + c_4\gamma_4^4 + c_{17}\gamma_1^2\gamma_2^2 + c_{18}\gamma_1^2\gamma_3^2 + c_{19}\gamma_1^2\gamma_4^2 + c_{20}\gamma_2^2\gamma_3^2 + c_{21}\gamma_2^2\gamma_4^2 + c_{22}\gamma_3^2\gamma_4^2 + c_{23}\gamma_1\gamma_2\gamma_3\gamma_4 . \quad (29)$$

Using the rotational operations:

1. $\sigma_x|0$: $c_1 = c_4$, $c_2 = c_3$, $c_{18} = c_{21}$, $c_{19} = c_{20}$,
2. $c_{3(x+y+z)}|0$: $c_1 = c_3$, $c_2 = c_4$, $c_{17} = c_{18}$, $c_{18} = c_{19}$, $c_{20} = c_{22}$, $c_{20} = c_{21}$, $c_{21} = c_{22}$.

Thus, $c_1 = c_2 = c_3 = c_4$ and $\gamma_1^2 + \gamma_2^2 + \gamma_3^2 + \gamma_4^2$ is an independent fourth-order invariant, also $c_{17} = c_{18} = c_{19} = c_{20} = c_{21} = c_{22}$ and $\gamma_1^2\gamma_2^2 + \gamma_1^2\gamma_3^2 + \gamma_2^2\gamma_3^2 + \gamma_2^2\gamma_4^2 + \gamma_3^2\gamma_4^2$ is also an independent fourth-order invariant. The term $\gamma_1\gamma_2\gamma_3\gamma_4$ goes into itself under all symmetry operations of the group, and thus is a third fourth-order invariant. Thus, for the totally symmetric small representation of $Fm3m$ at the L point:

$$G = G^\circ + A\eta^2 + [C_1(\gamma_1^4 + \gamma_2^4 + \gamma_3^4 + \gamma_4^4) + C_2(\gamma_1^2\gamma_2^2 + \gamma_1^2\gamma_3^2 + \gamma_1^2\gamma_4^2 + \gamma_2^2\gamma_3^2 + \gamma_2^2\gamma_4^2 + \gamma_1^2\gamma_4^2) + C_3\gamma_1\gamma_2\gamma_3\gamma_4]\eta^4 . \quad (30)$$

6.13. Possible Minima in G

To find the possible stable structures corresponding to an irreducible representation, the G expansion is minimized with respect to the γ_i's subject to the restraint $\Sigma\gamma_i^2 = 1$. For example, consider minimizing G in Eq. 30. First note that

$$\left(\sum\gamma_1^2\right)^2 = 1 = \gamma_1^4 + \gamma_2^4 + \gamma_3^4 + \gamma_4^4 + 2(\gamma_1^2\gamma_2^2 + \gamma_1^2\gamma_3^2 + \gamma_1^2\gamma_4^2 + \gamma_2^2\gamma_3^2 + \gamma_2^2\gamma_4^2 + \gamma_3^2\gamma_4^2) \quad (31)$$

and thus one of the polynomials in Eq. 30 can be eliminated in favor of a constant:

$$G = G^\circ + A\eta^2 + [C_2/2 + (C_1 - C_2/2)(\gamma_1^4 + \gamma_2^4 + \gamma_3^4 + \gamma_4^4) + C_3\gamma_1\gamma_2\gamma_3\gamma_4]\eta^4 . \quad (32)$$

The extrema and saddle points in G (Eq. 32) relative to the γ_i's subject to $\Sigma\gamma_i^2 = 1$ can be found using Lagranges method of undetermined multipliers (λ = the undetermined multiplier). Letting $C_1 - C_2/2 = C_2'$,

$$\frac{\partial\left[C_2'\sum_{i=1}^{3}\gamma_i^4 + C_3\gamma_1\gamma_2\gamma_3\gamma_4 + \lambda\sum_{i=1}^{3}\gamma_i^2\right]}{\partial\gamma_i}$$

$$= 4C_2'\gamma_i^3 + \frac{C_3\gamma_1\gamma_2\gamma_3\gamma_4}{\gamma_i} + 2\lambda_i\gamma_i = 0\,, \tag{33}$$

or

$$4C_2'\gamma_i^4 + 2\lambda\gamma_i^2 = -C_3\gamma_1\gamma_2\gamma_3\gamma_4 \tag{34}$$

for $i = 1$ to 4. It follows that

$$\gamma_1^4 + \frac{\lambda}{2C_2'}\gamma_1^2 = \gamma_2^4 + \frac{\lambda}{2C_2'}\gamma_2^2 \tag{35}$$

or

$$\gamma_1^4 - \gamma_2^4 = (\gamma_1^2 + \gamma_2^2)(\gamma_1^2 - \gamma_2^2) = \frac{\lambda}{2C_2'}(\gamma_2^2 - \gamma_1^2)\,. \tag{36}$$

First, we seek the solutions for which $\gamma_i \neq 0$ for $i = 1$ to 4. In this case,

$$\gamma_1^2 + \gamma_2^2 = -\lambda/2C_2' \tag{37}$$

and similarly

$$\gamma_1^2 + \gamma_3^2 = \gamma_1^2 + \gamma_4^2 = \gamma_2^2 + \gamma_3^2 = \gamma_2^2 + \gamma_4^2 = \gamma_1^2 + \gamma_4^2 = -\lambda/2C_2'\,, \tag{38}$$

i.e., $\gamma_1^2 = \gamma_2^2 = \gamma_3^2 = \gamma_4^2$, and since $\sum\gamma_i^2 = 1$, $\gamma_i = \pm 1/2$ for $i = 1$ to 4. Thus, provided these solutions are not saddle points, extrema occur at points for which $|\gamma_i| = 1/2$. Looking at Eq. 32 two values result for G, one for an even number of negative γ_i's (letting $C_1' = C_2/2$ and $C_2' = C_1 - C_2/2$):

$$G = G^\circ + A\eta^2 + [C_1' + C_2'/4 + C_3/16]\eta \tag{39}$$

and a second:

$$G = G^\circ + A\eta^2 + [C_1' + C_2'/4 - C_3/16]\eta \tag{40}$$

for an odd number of negative values. Thus, if these are not necessarily saddle points, there are in this case two possible stable structures, one given

by $\gamma_1 = \gamma_2 = \gamma_3 = \gamma_4 = 1/2$ and the other by $\gamma_1 = \gamma_2 = \gamma_3 = -\gamma_4 = 1/2$. That these solutions are extrema and not saddle points follows from the fact that C_3 could be large in magnitude relative to C_1' and C_2' and either positive (in which case the $\gamma_1 = \gamma_2 = \gamma_3 = -\gamma_4$ type solution would minimize G) or negative (in which case the $\gamma_1 = \gamma_2 = \gamma_3 = \gamma_4$ type solution would minimize G).

Returning to Eq. 34, if at least one of the γ_i's is zero, then

$$4C_2'\gamma_i^4 + 2\lambda\gamma_i^2 = 0 \tag{41}$$

for $i = 1$ to 4. There are three distinct types of solutions for the case of at least one $\gamma_i = 0$:

1. $|\gamma_1| = 1, \gamma_2 = \gamma_3 = \gamma_4 = 0$ and $G = G^0 + A\eta^2 + (C_1' + C_2')\eta^4$, (42)
2. $|\gamma_1| = |\gamma_2| = 1/\sqrt{2}, \gamma_3 = \gamma_4 = 0$ and $G = G^0 + A\eta^2 + [C_1' + C_2'/2]\eta^4$, (43)
3. $|\gamma_1| = |\gamma_2| = |\gamma_3| = 1/\sqrt{3}, \gamma_4 = 0$ and $G = G^0 + A\eta^2 + [C_1' + C_2'/3]\eta^4$. (44)

Adding the two solutions found above,

4. $\gamma_1 = \gamma_2 = \gamma_3 = \gamma_4$ and $G = G^0 + A\eta^2 + [C_1' + C_2'/4 + C_3/16]\eta^4$, (45)
5. $\gamma_1 = \gamma_2 = \gamma_3 = -\gamma_4$ and $G = G^0 + A\eta^2 + [C_1' + C_2'/4 - C_3/16]\eta^4$. (46)

yields a complete set of five solutions (extrema and saddle points) to Eq. 34.

As will be shown in the next section, solutions 4 and 5 correspond to two different cubic superstructures, so these will be called the cubic solutions. As mentioned above, the cubic solutions are stable if C_3 is sufficiently large.

Consider the circumstance that C_3 is so small as to be negligible relative to C_1' and/or C_2'. Then if C_2' is positive, one of the cubic cases has the lowest Gibbs free energy, and if C_2' is negative, case 1 has the lowest Gibbs free energy. Cases 2 and 3 never have the lowest Gibbs free energies. Thus, cases 2 and 3 are saddle point solutions and do not correspond to stable phases in the system.

In order to determine the condition that case 1 coexists with one of the cubic phases set

$$C_2' = C_2'/4 - |C_3|/16 \tag{47}$$

and find that case 1 and one of the cubic phases coexist when

$$12C_2' = -|C_3|. \tag{48}$$

Thus, for the transition from case 1 to cubic (Eq. 45 or 46 minus 42):

$$\Delta G = -3C_2'/4 - |C_3|/16 \tag{49}$$

and when

$$-|C_3|/12 < C_2', \tag{50}$$

then

$$\Delta G < 0 \tag{51}$$

and one of the cubic forms is stable. The symmetries of the three stable distorted structures are considered in the next section.

6.14. The Symmetries of the Allowed Solutions Corresponding to the Totally Symmetric Small Representation of $Fm3m$ at the L Point

A question that is generally of interest is, what are the symmetry and lattice of the structures of the stable solutions such as those found in Section 6.13. For case 1

$$\rho = \rho^\circ + \eta \cos \pi(x + y + z) \tag{52}$$

yields the correct *symmetry* for the low-symmetry structure, although the distortion function is not a proper difference particle density function. The symmetry of this function follows immediately from the fact that $\cos \pi(x + y + z)$ is a basis function for the totally symmetric small representation at $\mathbf{k} = (\mathbf{a}^* + \mathbf{b}^* + \mathbf{c}^*)/2$ and the group of this wave vector is $R\bar{3}m$. The lattice of the superstructure can be found by noting that

$$\mathbf{k} \cdot (\mathbf{a} + \mathbf{b})/2 = \pi, \tag{53}$$

and similarly for the other face-centering translations, and thus the face-centering lattice points are lost. Also $\mathbf{a} \cdot \mathbf{k} = \pi$ (and similarly for the other basis vectors of $Fm3m$) and thus 1, 0, 0; 0, 1, 0 and 0, 0, 1 are lost. On the other hand,

$$\begin{aligned} \mathbf{k} \cdot (\mathbf{a} + (\mathbf{b} + \mathbf{c})/2) &= \mathbf{k} \cdot (\mathbf{b} + (\mathbf{a} + \mathbf{c})/2) \\ &= \mathbf{k} \cdot (\mathbf{c} + (\mathbf{a} + \mathbf{c})/2) = 2\pi \end{aligned} \tag{54}$$

and these translations remain. Thus,

$$\begin{pmatrix} 1 & 1/2 & 1/2 \\ 1/2 & 1 & 1/2 \\ 1/2 & 1/2 & 1 \end{pmatrix} \begin{pmatrix} \mathbf{a} \\ \mathbf{b} \\ \mathbf{c} \end{pmatrix}_{fcc} = \begin{pmatrix} \mathbf{a} \\ \mathbf{b} \\ \mathbf{c} \end{pmatrix}_r \tag{55}$$

and the new basis vectors are as shown in Fig. 6.7

The symmetries of the cubic solution can also be determined. For example, the symmetry of the $\gamma_1 = \gamma_2 = \gamma_3 = -\gamma_4 = 1/2$ solution can be found by inspection of the schematic particle density function

$$\rho = \rho^0 + \frac{1}{2}[\cos\pi(x+y+z) + \cos\pi(x+y-z) + \cos\pi(x-y+z) - \cos\pi(-x+y+z)]\eta \tag{56}$$

First, it is helpful to note that this function is carried into itself by:

1. translation by $2\mathbf{a}^0, 2\mathbf{b}^0, 2\mathbf{c}^0$ but not $\mathbf{a}^0, \mathbf{b}^0$ or $\mathbf{c}^0$,
2. by $\mathbf{a}^0+\mathbf{b}^0, \mathbf{b}^0+\mathbf{c}^0, \mathbf{a}^0+\mathbf{c}^0$ but not $(\mathbf{a}^0+\mathbf{b}^0)/2, (\mathbf{b}^0+\mathbf{c}^0)/2$, or $(\mathbf{a}^0+\mathbf{c}^0)/2$,

and in general $\mathbf{T} = m\mathbf{a}^0 + n\mathbf{b}^0 + p\mathbf{c}^0$ remains if $m+n+p$ is even and is lost if the sum is odd. The lattice that remains is fcc with $\mathbf{a} = 2\mathbf{a}^0$. Thus, this is established to be a "cubic solution". Furthermore, $\rho(\bar{x}, \bar{y}, \bar{z}) = \rho(x, y, z)$,

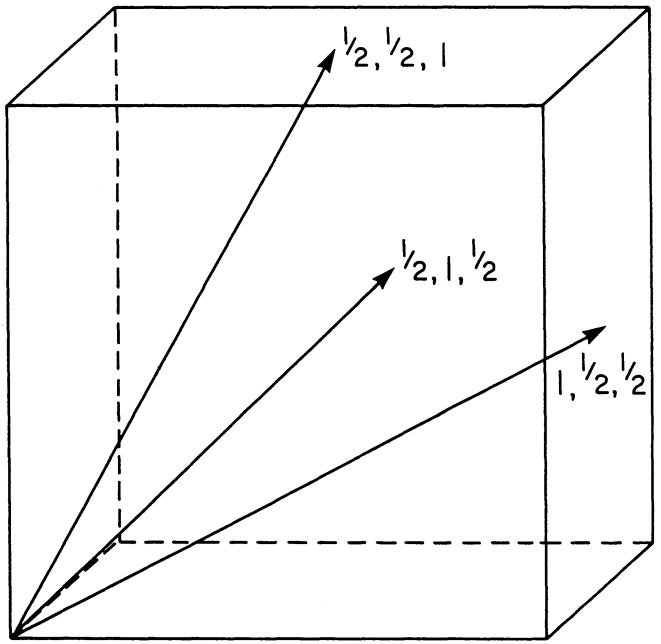

Fig. 6.7

thus the new space group is centrosymmetric, and we look initially for a solution in the crystal class $m3m$.

The symmetry operation $\sigma_x|0$ takes x, y, z into $\bar{x}, y, z$ and thus $\cos\pi(x+y+z)+\cos\pi(x+y-z)+\cos\pi(x-y+z)-\cos\pi(-x+y+z)$ into $\cos\pi(-x+y+z)+\cos\pi(x-y+z)+\cos\pi(x+y-z)-\cos\pi(x+y+z)$ and thus ρ is not invariant under $\sigma_x|0$. However, $\sigma_x|(\mathbf{b}+\mathbf{c})/2$ takes ρ into itself because the translation $(\mathbf{b}+\mathbf{c})/2$ changes the signs of the first and fourth terms but leaves the second and third unaltered. Hence, in the new, superstructure symmetry the plane perpendicular to $\mathbf{a}$ is a d-glide (recall that $(\mathbf{b}+\mathbf{c})/2$ in the substructure is $(\mathbf{b}+\mathbf{c})/4$ in the superstructure).

The operation $\overline{C}_3(x+y+z)|0$ takes x, y, z into $\bar{z}, \bar{x}, \bar{y}$ and thus takes $\cos\pi(x+y+z)+\cos\pi(x+y-z)+\cos\pi(x-y+z)-\cos\pi(-x+y+z)$ into $\cos\pi(x+y+z)+\cos\pi(x-y+z)+\cos\pi(-x+y+z)-\cos\pi(x+y-z)$ and this symmetry operation is lost. However, $\overline{C}_{3(x+y+z)}|(\mathbf{a}-\mathbf{c})/2$ does remain since translation by $(\mathbf{a}-\mathbf{c})/2$ changes the signs of the last two terms by leaves the first two unaltered. Since $(\mathbf{a}-\mathbf{c})/2$ is perpendicular to the axis of the operation $\overline{C}_{3(x+y+z)}$, the combined operation that remains, $\overline{C}_{3(x+y+z)}|(\mathbf{a}-\mathbf{c})/2$ is the operation of a $\overline{C}_3$ axis parallel to the 1,1,1 diagonal but displaced away from the origin. The operation $\sigma_{x+y}|(\mathbf{a}-\mathbf{b})/2$ takes x, y, z into $\bar{x}+1/2, \bar{y}-1/2, z$, and thus ρ into itself, and the operation $\sigma_{x+y}|(\mathbf{a}-\mathbf{b})/2$, the operation of a diagonal mirror, remains in the superstructure. The operations and the lattice found above suffice to show that the space-group symmetry of the $\gamma_1=\gamma_2=\gamma_3=-\gamma_4=1/2$ solution is $Fd3m$ with $a=2a^\circ$.

The case of $\gamma_1=\gamma_2=\gamma_3=\gamma_4=1/2$ shows invariance of ρ under $\sigma_x|0, \overline{C}_{3(x+y+z)}|0$ and $\sigma_{x+y}|0$ and all of the lattice translations found for the $Fd3m$ solution. Thus, this second cubic solution with $a=2a^\circ$ has $Fm3m$ symmetry.

The superlattices corresponding to the $R\bar{3}m$ and $Fd3m$ solutions can form in a variety of different ways, e.g., 1,0,0,0; 0,1,0,0; 0,0,1,0; 0,0,0,1 for the $R\bar{3}m$ solution and $-1/2$, $1/2$, $1/2$, $1/2$; $1/2$, $-1/2$, $1/2$, $1/2$; $1/2$, $1/2$, $-1/2$, $1/2$; $1/2$, $1/2$, $1/2$, $-1/2$ for the $Fd3m$ solution. Thus, there are in these cases many possibilities for superlattice twinning of the underlying sublattice, i.e., for the development of domains with different orientations and for the interpretation of these domains.

6.15. The Lifshitz Condition

In order that $\mathbf{k}$ correspond to a phase transition (i.e., that an irreducible representation at $\mathbf{k}$ correspond to a transition), it is necessary that $G(\mathbf{k})$

correspond to a minimum, for otherwise the structure will be unstable with respect to continuous change in periodicity and development of incommensurate structure (one mechanism for such an occurrence is presented in Section 11.3). A minimum in G in reciprocal space can occur at two different kinds of points: those which fix the $\mathbf{k}$ point by symmetry and those that do not. To examine this point the case of a one-dimensional small representation is considered first. If G is expanded about $\mathbf{k}$,

$$G(\mathbf{k}+\delta\mathbf{k}) = G(\mathbf{k}) + \boldsymbol{\alpha}\cdot\delta\mathbf{k} + \dots . \tag{57}$$

Unless the first-order coefficient, $\boldsymbol{\alpha}$, vanishes by symmetry it will always be possible to find a $\delta\mathbf{k}$ that lowers G relative to $G(\mathbf{k})$ and thus $G(\mathbf{k})$ will not be at a possible minimum. But $\delta\mathbf{k}$ is in general carried into $\beta\delta\mathbf{k}$ by $\beta\epsilon g^0(\mathbf{k})$. Thus,

$$G(\mathbf{k}+\beta\delta\mathbf{k}) = G(\mathbf{k}) + \boldsymbol{\alpha}\cdot\beta\delta\mathbf{k} + \dots \tag{58}$$

and since, by symmetry, $G(\mathbf{k}+\delta\mathbf{k}) = G(\mathbf{k}+\beta\delta\mathbf{k})$,

$$\boldsymbol{\alpha}\cdot\beta\delta\mathbf{k} = \boldsymbol{\alpha}\cdot\delta\mathbf{k}\,. \tag{59}$$

It follows that

$$\beta^{-1}\boldsymbol{\alpha}\cdot\delta\mathbf{k} = \boldsymbol{\alpha}\cdot\delta\mathbf{k} \tag{60}$$

or

$$\beta^{-1}\boldsymbol{\alpha} = \boldsymbol{\alpha}\,. \tag{61}$$

There are point groups of the wave vector for which this is possible only if $\boldsymbol{\alpha} \equiv 0$. For example, if $i\epsilon g^0(\mathbf{k})$, then

$$i\boldsymbol{\alpha} = -\boldsymbol{\alpha} = \boldsymbol{\alpha} \tag{62}$$

and $\boldsymbol{\alpha} \equiv 0$. Similarly, if $g^0(\mathbf{k})$ contains C_{3h} or S_4, then $\boldsymbol{\alpha} \equiv 0$. However, if $g^0(\mathbf{k})$ contains σ_h or C_{2v}, but not both, then $\boldsymbol{\alpha}$ can line up in the plane in the first case and along the axis in the second, and thus $\boldsymbol{\alpha} \not\equiv 0$ in these cases. Thus, $\boldsymbol{\alpha} \equiv 0$ and a stable superstructure can occur at $\mathbf{k}$ if $g^0(\mathbf{k})$ contains operations that eliminate the possibility of an invariant vector.

However, it might also be the case that $\boldsymbol{\alpha}(T, P, X) = 0$ at some arbitrary point for which $\boldsymbol{\alpha} \not\equiv 0$. In this case $\mathbf{k}$ is not fixed by symmetry and the

location of a minimum in G can vary with state. This is the case of an incommensurate structure, for $\mathbf{k}$ will vary with state.

The condition that a minimum in G be allowed at some fixed $\mathbf{k}$ point is called the Lifshitz condition. In the case of a multidimensional small representation this condition takes the following form: a stable solution can occur at a $\mathbf{k}$ point and for a small representation for which the product of the antisymmetric square representation and the vector representation does not contain the totally symmetric representation. The character of the antisymmetric square representation of $\beta|\mathbf{t}$

$$[\chi^2](\beta|\mathbf{t}) = \frac{1}{2}[-\chi(\beta^2|\beta\mathbf{t}+\mathbf{t}) + \chi^2(\beta|\mathbf{t})], \tag{63}$$

where $\chi(\beta^2|\beta\mathbf{t}+\mathbf{t})$ and $\chi(\beta|\mathbf{t})$ are, respectively, the traces of the matrices representing $\beta^2|\beta\mathbf{t}+\mathbf{t}$ and $\beta|\mathbf{t}$ at $\mathbf{k}$. The vector representation has character $\chi_v(\beta)$ which is the trace of the matrix that transforms x, y, z corresponding to β. The use of such characters in applying the Lifshitz condition is illustrated in the next section.

6.16. Transitions at the Γ Point of *m3m*

It is possible to examine the possible second-order phase transitions with no loss in translational symmetry (no superstructure) by examining the small representations at the Γ point. These representations are isomorphous with those of the point group of the crystal class for both symmorphic and nonsymmorphic space groups. Thus, the entire crystal class can be considered simultaneously.

The small representations of $m3m$ at the Γ point are the same as those of O_h. Since all representations at Γ are symmetric with respect to all translations, if a function is antisymmetric with respect to a β operation then the operation is lost in the new crystal class (i.e., it does not remain in combination with a translation). Thus, for the one-dimensional representations (except the totally symmetric which corresponds to no symmetry change and thus no transition), one-half of all the symmetry operations are lost. In these cases there is only one polynomial of each order $(\gamma^2, \gamma^3, \gamma^4, \ldots)$ and since $\gamma \rightarrow -\gamma$ under some symmetry operations there is no third-order invariant. Since $g^0(\mathbf{k}=0)$ of the $m3m$ contains $i|0$, these irreducible representations meet the Lifshitz condition, and the second-order transitions corresponding to these irreducible representations are all allowed. The resulting crystal classes are the three subgroups of O_h with half (24) of the

48 symmetry operations, namely O, T_{2d} and T_{2h}, each corresponding to one of the three nontotally symmetric small representations.

The remaining irreducible representations are two-dimensional (e_g and e_u) and three-dimensional ($t_{1g}, t_{1u}, t_{2g}, t_{2u}$). The irreducible representation for the e_g case is given in Table 6.1. Table 6.2 is set up to check the products of $[\chi^2]$ with χ_v. Since the sum across the bottom row is zero, the product of the antisymmetric square representation and the vector representation is orthogonal to the identity representation, and the e_g representation is found to meet the Lifshitz condition. However, an examination of Table 6.1 shows that, since $\varepsilon^3 = \varepsilon^6 = 1$, $\phi_1^3 + \phi_2^3$ is invariant and thus also is $\gamma_1^3 + \gamma_2^3$ and a third-order invariant exists for the e_g representation. The space groups that would result consist of those operations that carry ϕ_1 into itself (the $\gamma_1 = 1, \gamma_2 = 0$ solution) and that carry $\phi_1 + \phi_2$ into itself (the $\gamma_1 = \gamma_2 = 1/\sqrt{2}$ solution). An examination of Table 6.1 shows these to be: $D_{2h}(\varepsilon,\ C_{2x},\ C_{2y},\ C_{2z},\ i,\ \sigma_x,\ \sigma_y,\ \sigma_z)$ and $D_{4h}(\varepsilon,\ C_{2x},\ C_{2y},\ C_{2z},\ C_{2(y-x)},\ C_{4z}^3,\ C_{2(x+y)},\ i,\ \sigma_x,\ \sigma_y,\ \sigma_z,\ \sigma_{y-x},\ S_{4z},\ S_{4z}^3$ and $\sigma_{x+y})$, respectively. That is, the transitions from $m3m$ to mmm and $4/mmm$ at $\mathbf{k} = 0$ must be first order.

Table 6.1. An e_g irreducible representation of $O_h(\varepsilon = \exp(2\pi i/3))$.

ε $\begin{pmatrix} 1 & 0 \\ 0 & 1 \end{pmatrix}$	C_{2x} $\begin{pmatrix} 1 & 0 \\ 0 & 1 \end{pmatrix}$	C_{2y} $\begin{pmatrix} 1 & 0 \\ 0 & 1 \end{pmatrix}$	C_{2z} $\begin{pmatrix} 1 & 0 \\ 0 & 1 \end{pmatrix}$	$C_{3(x+y+z)}^2$ $\begin{pmatrix} \varepsilon & 0 \\ 0 & \varepsilon^2 \end{pmatrix}$
$C_{3(x+y-z)}$ $\begin{pmatrix} \varepsilon & 0 \\ 0 & \varepsilon^2 \end{pmatrix}$	$C_{3(-x+y+z)}$ $\begin{pmatrix} \varepsilon & 0 \\ 0 & \varepsilon^2 \end{pmatrix}$	$C_{3(x-y+z)}$ $\begin{pmatrix} \varepsilon & 0 \\ 0 & \varepsilon^2 \end{pmatrix}$	$C_{3(x+y+z)}$ $\begin{pmatrix} \varepsilon^2 & 0 \\ 0 & \varepsilon \end{pmatrix}$	$C_{3(x-y+z)}^2$ $\begin{pmatrix} \varepsilon^2 & 0 \\ 0 & \varepsilon \end{pmatrix}$
$C_{3(x+y-z)}^2$ $\begin{pmatrix} \varepsilon^2 & 0 \\ 0 & \varepsilon \end{pmatrix}$	$C_{3(-x+y+z)}^2$ $\begin{pmatrix} \varepsilon^2 & 0 \\ 0 & \varepsilon \end{pmatrix}$	$C_{2(y-x)}$ $\begin{pmatrix} 0 & 1 \\ 1 & 0 \end{pmatrix}$	C_{4z} $\begin{pmatrix} 0 & 1 \\ 1 & 0 \end{pmatrix}$	C_{4z}^3 $\begin{pmatrix} 0 & 1 \\ 1 & 0 \end{pmatrix}$
$C_{2(x+y)}$ $\begin{pmatrix} 0 & 1 \\ 1 & 0 \end{pmatrix}$	$C_{2(z-y)}$ $\begin{pmatrix} 0 & \varepsilon \\ \varepsilon^2 & 0 \end{pmatrix}$	$C_{2(z+x)}$ $\begin{pmatrix} 0 & \varepsilon \\ \varepsilon^2 & 0 \end{pmatrix}$	C_{4z} $\begin{pmatrix} 0 & \varepsilon \\ \varepsilon^2 & 0 \end{pmatrix}$	C_{4z}^3 $\begin{pmatrix} 0 & \varepsilon \\ \varepsilon^2 & 0 \end{pmatrix}$
$C_{2(z-x)}$ $\begin{pmatrix} 0 & \varepsilon^2 \\ \varepsilon & 0 \end{pmatrix}$	C_{4y}^3 $\begin{pmatrix} 0 & \varepsilon^2 \\ \varepsilon & 0 \end{pmatrix}$	$C_{2(x+y)}$ $\begin{pmatrix} 0 & \varepsilon^2 \\ \varepsilon & 0 \end{pmatrix}$	C_{4y} $\begin{pmatrix} 0 & \varepsilon^2 \\ \varepsilon & 0 \end{pmatrix}$	i $\begin{pmatrix} 1 & 0 \\ 0 & 1 \end{pmatrix}$

Table 6.2. Table of characters to determine $[\chi^2]\chi_v$ for $_u$.

n	1	3	6	3	6	6	6	8	8	1
g	ε	C_2	C_2	σ	σ	C_4	S_4	C_3	$\overline{C}_3$	i
g^2	ε	ε	ε	ε	ε	C_2	C_2	C_3	C_3	ε
$\chi(g)$	2	2	0	2	0	0	0	−1	−1	2
$\chi(g^2)$	2	2	2	2	2	2	2	−1	−1	2
χ_v	3	−1	−1	1	1	1	−1	0	0	−3
$\frac{n}{2}\chi_v[\chi^2]$	3	−1	1	1	−1	−1	1	0	0	−3

The e_u representation, on the other hand, has no corresponding third-order invariant since $\phi_1^3 + \phi_2^3$ is carried into $-\phi_1^3 - \phi_2^3$ by inversion in this case. We can again use Table 6.2 because $\chi^2(g)$ is the same in ε_u and ε_g except for $\overline{C}_3$, and this exception does not effect the sum along the bottom row since $\chi_v = 0$ for this operation. Thus, ε_u at Γ meets both the third-order invariant and the Lifshitz condition, and transitions corresponding to this irreversible representation can occur as second-order processes.

A pair of real basis functions (ρ must be real!) that transform as ε_u are

$$\phi_1 = (2\cos 4\pi z - \cos 4\pi x - \cos 4\pi y)(\sin 4\pi x - \sin 4\pi y) \times (\sin 4\pi y - \sin 4\pi z)(\sin 4\pi z - \sin 4\pi x)\,, \tag{64}$$

$$\phi_2 = \sqrt{3}(\cos 4\pi y - \cos 4\pi x)(\sin 4\pi x - \sin 4\pi y)(\sin 4\pi y - \sin 4\pi z) \times (\sin 4\pi z - \sin 4\pi x)\,. \tag{65}$$

These functions individually have 422 symmetry and when summed have 222 symmetry. Thus, $O_h \rightarrow D_{4d}$ and $O_h \rightarrow D_{2d}$ can occur as second order transitions at the Γ point.

All of the triply degenerate representations at Γ have the $\chi^2(g), \chi(g^2)$ and $[\chi^2(g)]\chi_v/2$ values given in Table 6.3. Thus, since summing across the bottom row yields zero, all three-dimensional irreducible representations at Γ of $m3m$ meet the Lifshitz condition. In the case of T_{1g} the representation matrices are those of the vector representation for the elements in the O subgroup, and these matrices are repeated by the identity matrix, which represents i, in T_{1g}. These matrices permute ϕ_1, ϕ_2 and ϕ_3 and change

the signs of an even number of the functions. Thus, $\phi_1\phi_2\phi_3$ (and $\gamma_1\gamma_2\gamma_3$) are third-order invariants, and T_{1g} cannot correspond to a second-order transition of $m3m$ at Γ. The T_{2g}, T_{1u} and T_{2u} representations do not yield third-order invariants, and two stable solutions (minima in G) occur for each. The symmetries are summarized in Table 6.4.

Table 6.3. Table of characters to determine $[\chi^2]\chi_v$ for the Triply Degenerate Irr. Reps. of O_h.

	1	3	6	3	6	6	6	8	8	1
g	ε	C_2	C_2	σ	σ	C_4	S_4	C_3	$\overline{C}_3$	i
g^2	ε	ε	ε	ε	ε	C_2	C_2	C_3	C_3	ε
$\chi^2(g)$	9	1	1	1	1	1	1	0	0	9
$\chi(g^2)$	3	3	3	3	3	−1	−1	0	0	3
χ_v	3	−1	−1	1	1	1	−1	0	0	−3
$\frac{1}{2}\chi_v[\chi^2]$	9	1	1	−1	−1	1	−1	0	0	−9

Table 6.4. Stable solutions from the T_{2g}, T_{1u} and T_{2u} Irr. Reps. of O_h.

	$\gamma_1 = 1, \gamma_2 = \gamma_3 = 0$	$\gamma_1 = \gamma_2 = \gamma_3 = 1/\sqrt{3}$
$\mathbf{T_{2g}}$	$4/m$	$\bar{3}$
$\mathbf{T_{1u}}$	$\bar{4}m2$	32
$\mathbf{T_{2u}}$	$4mm$	$3m$

Bibliography

1. L. D. Landau and E. M. Lifshitz, *Statistical Physics* (Pergamon Press, London, 1958) Vol. **5**.
2. Jean-Claude Tolédano and Pierre Toledano, *The Landau Theory of Phase Transitions* (World Scientific, New Jersey, 1987).
3. Yu. A. Izyumov and V. N. Syromyatnikov, *Phase Transitions and Crystal Symmetry* (Kluwer Academic Publishers, Boston, 1990).

4. G. Y. Lyubarski, *Application of Group Theory in Physics* (Pergamon, London, 1980).
5. Hugo F. Franzen, Landau Theory of Symmetry-Breaking Transitions: A Basis for Clarification of Diffraction Studies of Phase Behavior, *Chem. of Materials* **2**, 485–491 (1990).

Problems

1. Show that $P6_3/mmc \rightarrow Pcmn$ at $\mathbf{a}^*/2$ is allowed to occur as a second-order transition (small representation from Table 5.6 of Chapter 5).
2. Show that $Fm3m \rightarrow R\bar{3}m$ at Γ is not allowed by Landau theory.
3. A simple cubic structure with Ru at 0,0,0 and Ta at 1/2, 1/2, 1/2 distorts to form a tetragonal structure with $c/a \cong 1$. Show that this distortion must occur as a first-order transition.
4. A tetragonal structure with Ru at 0,0,0 and Ta at 1/2, 1/2, 1/2 distorts via a change in γ away from 90°. Show that this transition can occur as a second-order transition.
5. Show that the ordering of Problem 3.9 can occur as a second-order transition.
6. Find an alternative ordered superstructure corresponding to the irreducible representation of Problem 5.

CHAPTER 7

THERMODYNAMICS OF CONDENSED SYSTEMS

7.1. Introduction

This chapter treats the application of thermodynamics to chemical processes. The importance of this topic in solid-state chemistry derives from the role that heterogeneous equilibria play in solid-state synthesis and in nonstoichiometry in solids. In particular, these equilibria must be thoroughly understood (i.e., the number of independent chemical reactions among the species of a system must be enumerated) if the phase rule is to be properly applied. Thus, an important aspect is determining the number of independent intensive variables, a knowledge of which is important to experimental design, is a rigorous method for finding the number of independent net reactions. A method for this determination and its underlying thermodynamic basis are the subject of this chapter.

7.2. Simple Systems

The number of variables required to fix the state of a system depends upon the ways in which external forces can act upon the system, and upon the presence of any arbitrary barriers to equilibration. For this reason a simple system is defined as in Section 1.3 such that there are no arbitrary barriers to flow of heat or matter and such that the only macroscopic mechanical energy exchange between the system and the surroundings is via $P-V$ work. A fundamental postulate of thermodynamics then takes the form that $c+2$ macroscopic variables (at least one of which is extensive) fix the macroscopic state of a system at rest. The number c is the number of variables required to fix the chemical contents of the system. For example, a system under

consideration might be H_2 (g), O_2 (g) and H_2O(g) at equilibrium in a system and the temperature and volume are two variables and the quantities of H_2 and O_2 from which the system is formed would be $c = 2$ chemical content variables. Thus, the temperature, T, volume V, moles of O_2, $n^c_{O_2}$, and moles of H_2, $n^c_{H_2}$, constitute $c + 2$ variables that fix the macroscopic state.

7.3. Species and Components

In the example given above, H_2 and O_2 enter in two capacities: as species in the system at equilibrium and as components the quantities of which are specified in the description of the formulation of the system. This distinction is important. As components the numbers of moles are variables which are specified to provide, along with the other two variables, a preparation that will lead to a unique result. As species the numbers of moles are the quantities of the chemical substances present in the resulting system. The numbers of moles of chemical substances from which a system is synthesized can be very different from the numbers of moles of those substances present at equilibrium, for example in the system under consideration the conditions might be such that the vast majority of O_2 and H_2 placed into the system react so that at equilibrium H_2O is far and away the predominant species and O_2 and H_2 would be present in very small amounts. In any case, for the system, $c + 2 = 2 + 2 = 4$ and the moles of species ($n^S_{H_2}$, $n^S_{O_2}$ and $n^S_{H_2O}$) are determined in the equilibrium state by four macroscopic variables, e.g., $T, V, n^c_{O_2}, n^c_{H_2}$.

7.4. Arbitrary Restraints

Barriers were eliminated in defining the simple system in order to eliminate one kind of arbitrary restraint. However, it sometimes occurs that a simple system is formed in such a fashion that arbitrary restraints are placed on the system by virtue of the method of preparation. For example, a system containing, as the one discussed above, the species H_2 (g), O_2 (g) and H_2O(g) at equilibrium could be prepared from H_2O alone, placed in a given volume at a given temperature. The states accessible to this system are only a subset of those accessible to the system prepared from H_2 and O_2, i.e., a restraint, namely $n_{O_2} = 1/2 n_{H_2}$ is implied in the latter whereas no restraint is implied in the former. In this way the method of preparation can place restraints upon the states accessible to a system and thus imply a

relationship among the variables that describe the system in its equilibrium state.

7.5. Determination of c

A general method for the determination of c can be described as follows: (1) determine which chemical species are important in the equilibrium state, (2) determine the number of natural restraints limiting independent variation of the number of moles of species at equilibrium, (3) determine the number of externally imposed restraints upon *intensive* variables and (4) subtract from the number of species the number of restraints of both kinds. With regard to (1) the decision of what species are or are not important is to some extent arbitrary, e.g., in a gaseous system it is possible to say that $P_i/\Sigma P_i$ is a measure of importance and set the lower limit at 10^{-2} or 10^{-10}, or at some other value. It is impossible to consider too many species, e.g., for the systems considered above the species list could have been taken to be: H (g), O (g), OH (g), H_2O_2 (g), H_2O (g), O_2 (g) and H_2 (g) and no problems would arise in determining the number of independent variables from considering species that make an insignificant contribution to the equilibrium state. Of course, if very high temperatures and/or low pressures are considered, some species which contribute negligibly at room temperature and atmospheric pressure will predominate and an accurate description of the system will require their inclusion.

The natural restraints, mentioned under (2), occur in the form of balanced net reactions that are equilibrated. These restraints are found by applying the equation for a reversible internal energy change to a closed, simple system undergoing reversible chemical reaction:

$$dU = TdS - PdV\,, \tag{1}$$

(where $dn_i^c = 0$ because the system is closed), and to an open, simple system in which the chemical reactions are frozen

$$dU = TdS - PdV + \sum \mu_i dn_i\,. \tag{2}$$

If the two systems are carried over the same states (if the open system is made to mimic the chemical reactions by the reversible addition and removal of chemical substances), then dU, dS, dV, P and T are the same in both systems and

$$\sum \mu_i dn_i = 0\,. \tag{3}$$

7.6. Chemical Reaction Thermodynamics

The condition that the open, nonreacting system is carried over the same states as the closed, reacting one imposes:

$$dn_i = \sum_j v_{ij} d\xi_j \,, \tag{4}$$

where v_{ij} is the stoichiometric coefficient of the ith species in the jth *independent net* reaction and ξ_j is the extend of progress of the jth reaction. Thus,

$$\sum \mu_i dn_i = \sum_i \sum_j v_{ij} \mu_i d\xi_j = 0 \,. \tag{5}$$

Several important concepts entered into the above. One is the concept of reactions as processes involving identifiable species in the system. Such a process is called a *net* reaction, and because thermodynamics depends only upon changes between states of rest, it is not at all relevant whether or not the net reactions have any resemblance to the mechanistic processes whereby the reactions proceed. "Identifiable" has a special meaning in this context. As discussed above, the species O(g) could be included as an identifiable species in the H_2–O_2 system in which it is present at negligible levels. This is because it is a known and important species at high temperatures and low pressures and thus its presence can be extrapolated to less extreme conditions. This kind of extrapolation is generally possible in chemical systems, but is not always necessary.

7.7. Independent Net Reactions

Another point about the reactions discussed above is that they should be independent. In practice this means that the ratios of the stoichiometric coefficients in a single independent reaction are fixed by the species involved in the reaction (i.e., there is only one way to balance the reaction up to a multiplicative factor), and that there exists no linear relationship among the coefficients of the independent reactions. These conditions insure that the ξ_j's are independent variables and that the complete set of reactions serves to describe all changes in moles of species via equations such as 5.

If there are two or more net reactions there are alternative ways to choose the set of net reactions. Having found one set, other sets can be found by adding and subtracting net reactions in such a fashion that at

least one species is cancelled because it is consumed in one reaction and produced in a second in the same stoichiometric quantity.

7.8. Number of Independent Net Reactions

In order to find the number of independent net reactions, it is helpful to create a species-by-element matrix and determine its rank. The number of species minus the rank is the number of independent net reactions. It is then necessary to decide independently, based upon chemical knowledge, whether or not the system is equilibrated with respect to each independent reaction, i.e., whether some path whereby the reactants are converted to products is available under the conditions of the equilibrium.

For example, suppose the system under consideration is a system containing $H_2(g)$, $O_2(g)$, $H_2O(g)$ and $H_2O(\ell)$. The species-by-element matrix is

	$H_2(g)$	$O_2(g)$	$H_2O(g)$	$H_2O(\ell)$
H	2	0	2	2
O	0	2	1	1

Noting that there is a nonzero minor determinant

$$\begin{vmatrix} 2 & 0 \\ 0 & 2 \end{vmatrix} = 4 \tag{6}$$

or using row reduction to yield

	$H_2(g)$	$O_2(g)$	$H_2O(g)$	$H_2O(\ell)$
H	1	0	1	1
O	0	1	1/2	1/2

both demonstrate that the rank of the matrix is 2. The number of independent net reactions is, then, $4 - 2 = 2$. These can be taken to be

$$H_2(g) + 1/2\,O_2(g) = H_2O(g) \tag{7}$$

and

$$H_2(g) + 1/2\,O_2(g) = H_2O(\ell), \tag{8}$$

or

$$H_2(g) + 1/2\,O_2(g) = H_2O(g) \tag{9}$$

and

$$H_2O(\ell) = H_2O(g). \tag{10}$$

7.9. Examples Involving Solids

Two examples will be cited to demonstrate how these concepts relate to reactions involving solids. The first is in the case of the system containing: $FeSO_4$ (s), Fe_2O_3 (s), SO_2 (g), SO_3 (g) and O_2 (g), synthesized by decomposition of $FeSO_4$. The species-by-element matrix is

	$FeSO_4$ (s)	Fe_2O_3 (s)	SO_2 (g)	SO_3 (g)	O_2 (g)
S	1	0	1	1	0
Fe	1	2	0	0	0
O	4	3	2	3	2

Row reduction yields

	$FeSO_4$ (s)	Fe_2O_3 (s)	SO_2 (g)	SO_3 (g)	O_2 (g)
S	1	0	0	2	4
Fe	0	1	0	−1	−2
O	0	0	1	−1	−4

and thus the rank of this matrix is 3, and there are $5 - 3 = 2$ independent net reactions. Using the row reduced matrix

$$\begin{aligned} \Delta n_{FeSO_4} &= -2\Delta n_{SO_3} \\ \Delta n_{Fe_2O_3} &= \Delta n_{SO_3} \\ \Delta n_{SO_2} &= \Delta n_{SO_3} \end{aligned} \tag{11}$$

for one reaction, i.e.,

$$2FeSO_4(s) = Fe_2O_3(s) + SO_2(g) + SO_3(g), \tag{12}$$

and

$$\begin{aligned} \Delta n_{FeSO_4} &= -4\Delta n_{O_2} \\ \Delta n_{Fe_2O_3} &= 2\Delta n_{O_2} \\ \Delta n_{SO_2} &= 4\Delta n_{O_2} \end{aligned} \tag{13}$$

for another, i.e.,

$$4FeSO_4\,(s) = 2Fe_2O_3\,(s) + 4SO_2\,(g) + O_2\,(g)\,, \tag{14}$$

Each equilibrated independent net reaction implies a natural restraint upon the system, $\Sigma v_i \mu_i = 0$. Thus, in the absence of imposed restraints, c would be equal to the number of species minus the number of independent net reactions, and in this case c would be $5-2 = 3$. However, since the system is specified as formed from $FeSO_4$ there is a restraint upon intensive variables. This can be seen as follows (taking $n^{\circ}_{FeSO_4}$ to be the initial number of moles of $FeSO_4$):

1. sulfur balance: $n^{\circ}_{FeSO_4} = n_{FeSO_4} + n_{SO_2} + n_{SO_3}$,
2. oxygen balance: $4n^{\circ}_{FeSO_4} = 4n_{FeSO_4} + 3n_{Fe_2O_3} + 3n_{SO_3} + 2n_{SO_2} + 2n_{O_2}$,
3. iron balance: $n^{\circ}_{FeSO_4} = n_{FeSO_4} + 2n_{Fe_2O_3}$.

Eliminating $n^{\circ}_{FeSO_4}$, n_{FeSO_4} and $n_{Fe_2O_3}$ yields

$$n_{SO_2} = n_{SO_3} + 4n_{O_2} \tag{15}$$

which implies that in the gas phase

$$X_{SO_2} = X_{SO_3} + 4X_{O_2} \tag{16}$$

a relationship among intensive variables. The restraint results from the fact that the system was prepared in a certain way, i.e., from $FeSO_4$ rather than from $FeSO_4$, SO_2 and O_2, for example. Nonetheless, it means that the number of variables attributable to chemical content variation is reduced by 1, and for the system as synthesized, $c = 2$.

A second example is the system containing $Ti_4O_{7-x}\,(s)$, $Ti_3O_{5+y}\,(s)$, $O_2\,(g)$, $O\,(g)$, $TiO\,(g)$ and $Ti\,(g)$ prepared by removal of O_2 from TiO_2 at high temperature. This problem will be solved in two separate ways. The first is to recognize that nonstoichiometry can (in fact must) occur in solids, i.e., to recognize that the x and y used in the description of Ti_4O_{7-x} and Ti_3O_{5+y} may be significant. Labeling $Ti_3O_{5+y} = \alpha$ and $Ti_4O_{7-x} = \beta$,

$$\begin{aligned} X^{\alpha}_{O} &= \frac{5+y}{8+y}\,, \\ X^{\alpha}_{Ti} &= \frac{3}{8+y}\,, \\ X^{\beta}_{O} &= \frac{7-x}{11-x}\,, \end{aligned} \tag{17}$$

and

$$X_{\mathrm{Ti}}^{\beta} = \frac{4}{11 - x} . \tag{18}$$

The element-by-species matrix in this case is

	$Ti(g)$	$O(g)$	$O_2(g)$	$TiO(g)$	$Ti_3O_{5+y}(s)$
Ti	1	0	0	1	3
O	0	1	2	1	$5+y$
	$Ti_4O_{7-x}(s)$	$Ti(\alpha)$	$O(\alpha)$	$Ti(\beta)$	$O(\beta)$
Ti	4	1	0	1	0
O	$7-y$	0	1	0	1

which is row reduced and is of rank 2. There are thus eight independent net reactions. A useful set is

$$O(\alpha) = O(\beta) \tag{19}$$

$$Ti(\alpha) = Ti(\beta) \tag{20}$$

$$Ti(\alpha) = Ti(g) \tag{21}$$

$$O(\beta) = 1/2\, O_2(g) \tag{22}$$

$$1/2\, O_2(g) = O(g) \tag{23}$$

$$TiO(g) = Ti(g) + O(g) \tag{24}$$

$$Ti_3O_{5+y}(s) = 3Ti(\alpha) + (5+y)O(\alpha) \tag{25}$$

$$Ti_4O_{7-x}(s) = 4Ti(\beta) + (7-x)O(\beta) . \tag{26}$$

Each of these reactions indicates something important about the system. The first two indicate that the solids are solid solutions and they can be equilibrated with respect to distribution of the elements between the two solids, i.e., at equilibrium

$$\mu_{\mathrm{O}}^{\alpha} = \mu_{\mathrm{O}}^{\beta} \tag{27}$$

and

$$\mu_{\mathrm{Ti}}^{\alpha} = \mu_{\mathrm{Ti}}^{\beta} . \tag{28}$$

Equations 21 and 22 indicate that the elemental species can equilibrate between the solids and the vapor. These equilibrations mean that

$$\mu_{\mathrm{Ti}}^{\alpha} = \mu_{\mathrm{Ti}}^{g} = \mu_{\mathrm{Ti}}^{\mathrm{O},g} + RT \ln P_{\mathrm{Ti}} \tag{29}$$

and

$$\mu_O^\beta = 1/2\mu_{O_2}^g = 1/2\mu_{O_2}^{O,g} + RT \ln P_{O_2}^{1/2} . \tag{30}$$

In other words, the partial pressures of the elemental species in the gas phase provide concrete measures of the otherwise abstract ideas of chemical potentials of the elemental species in the solids.

Reaction 23 provides a way to think about O (g) if it is present at very low partial pressure, namely

$$K(T) = P_O / P_{O_2}^{1/2} \tag{31}$$

and thus P_O is a calculable quantity even when it is immeasurably small. The gas phase reaction involving TiO (g) serves to provide a more complete picture of the gas phase since TiO (g) is an important species in the vapor of the Ti–O system at high temperature.

The reactions 25 and 26 are analogous to solvent dissociation reactions. The variables x and y are fixed at fixed temperature ($f = 1$), i.e., Ti_4O_7 is saturated with Ti and Ti_3O_5 is saturated with O.

A simpler description of the same system is possible. The small x and y could be ignored, the formal possibility of discussing O (α), O (β), Ti (α) and Ti (β) could be passed up, and the small partial pressure of Ti (g) in the vapor could be ignored. In this case the species-by-element matrix is

	O (g)	TiO (g)	O_2 (g)	Ti_4O_7 (s)	Ti_3O_5 (s)
O	1	1	2	7	5
Ti	0	1	0	4	3

and again the rank is 2, and in this case there are three independent net reactions, e.g.

$$1/2\,O_2\,(g) = O\,(g) \tag{32}$$

$$Ti_4O_7\,(g) = 4TiO\,(g) + 3\,O\,(g) \tag{33}$$

$$Ti_3O_5\,(s) = 3TiO\,(g) + 2\,O\,(g) . \tag{34}$$

Thus, $c = 5 - 3 = 2$ and $f = 2 - 3 + 2 = 1$, as before. However, this view of this system is much simpler, taking the solids to be strictly stoichiometric and ignoring a very minor vapor phase species. So far as the overall macroscopic behavior is concerned, the conclusion that $f = 1$ is the same. So

far as a detailed understanding of a variety of equilibria that may have an impact upon the properties of the solids is concerned, the prior description has significantly more power.

7.10. Reactions Involving Only Condensed Phases

A feature of condensed phase reactions that differentiates them from reactions involving species in the vapor or in solution is that it is possible, in fact is true for more often than not, that condensed phase reactions occur to completion totally depleting the system of a reactant species. In the vapor and solution phases species that are observable under some circumstances (e.g., O (g) at high temperatures and low pressures) will be present under all conditions, although at negligible levels in some circumstances. For vapor or solution species there is a continuous change in the quantity of a species present at equilibrium (e.g., for O (g) in an O–O_2 mixture the partial pressure of O (g) at 298 K and 1 bar total pressure if 1.25×10^{-41} bar, whereas at 2 500 K and 10^{-5} bar its partial pressure is 0.92 bar). At no point is it possible to say, other than arbitrarily, that O (g) is not a species in the system.

On the other hand, the species present in an all solid system can change discontinuously with state. For a reaction such as

$$MX_a\,(\mathrm{s}) = \left(\frac{a-c}{b-c}\right) MX_b(\mathrm{s}) + \left(\frac{b-a}{b-c}\right) MX_c(\mathrm{s}) \qquad (35)$$

at a given T, P each of the solids is present in a given state with a fixed molar Gibbs free energy. If the reaction is shifted to the left or right, there is no change in the molar Gibbs free energies of any of the solids. Thus, if $\Delta G < 0$, the reaction will proceed until all of the MX_a(s) is consumed, and if $\Delta G > 0$, it will proceed to the left until all of the MX_b or MX_c, depending upon which is limiting, is consumed. Only if $\Delta G = \Delta H - T\Delta S = 0$, i.e., if $T = \Delta H/\Delta S$, will the three phases coexist. This coexistence, unlike the equilibria involving gaseous or solution species, will not determine the quantities of reactants and products. The equilibrium establishes only the presence of the three condensed phases at a temperature that depends only upon the applied pressure (since $f = 2 - 3 + 2 = 1$).

For example, consider the Cu–O system. If the applied pressure is sufficiently high that there is no vapor phase, then the possible relevant

species are: CuO (s), Cu_2O (s) and Cu (s). The element-by-species matrix is row reduced form is:

	Cu	Cu_2O	CuO
Cu	1	0	−1
O	0	1	1

and its rank is 2, and

$$Cu_2O\,(s) = CuO\,(s) + Cu\,(s)$$

is the only net reaction. For this reaction at all relevant temperatures $\Delta G > 0$ (Table 7.1), and thus Cu_2O (s), CuO (s) and Cu (s) cannot coexist in equilibrium. However, either Cu_2O (s) and Cu (s) or Cu_2O (s) and CuO (s) can coexist (see Fig. 7.1).

Table 7.1. $\Delta G/R$ values for Cu_2O (s) = CuO (s) + Cu (s).

T/K	$\Delta G/R$
300	2 000
500	2 400
700	2 750
900	3 100

7.11. Nonstoichiometry

Nonstoichiometry can effect the chemical consideration of solids in different ways depending upon whether the deviations from stoichiometry are very small (the case of a *line compound*) or are large enough that order-disorder processes can yield observable (e.g., by X-rays) structural effects. For example, $Zr_{1-x}S$ with $x \cong 0.25$ falls in the second category. In this material the vacancies are distributed at random (to X-rays) on NaCl-type sites at high temperature and thus at high temperatures it is a nonstoichiometric NaCl-type material, and not a compound Zr_3Z_4. When this solid is cooled, the vacancies order in alternate 1,1,1 planes and break the symmetry from $Fm3m$ to $R\bar{3}m$. This *order-disorder* transition is discussed further in Section 11.2.

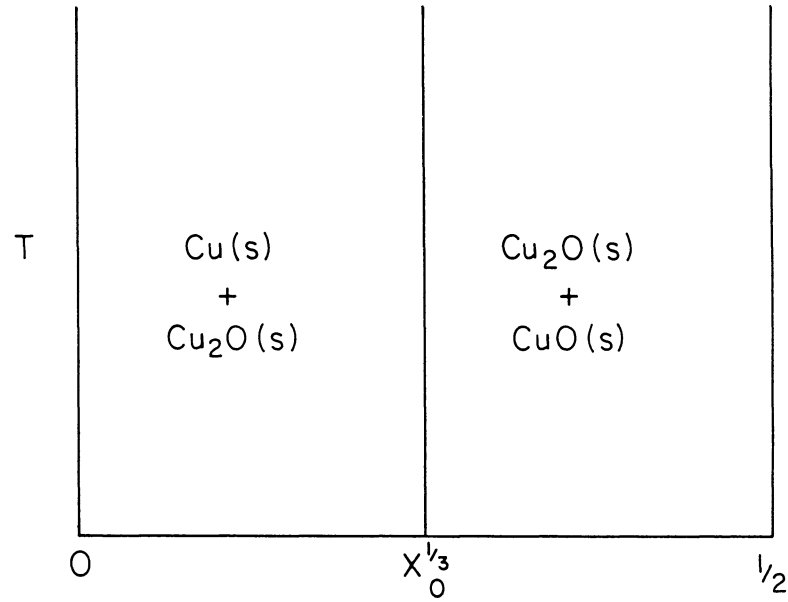

Fig. 7.1. The Cu–O phase diagram.

In principle the materials in the first category include all compounds not in the second, i.e., all compounds are inherently nonstoichiometric although perhaps at very low levels. For example, consider the classic line compound CaO (s). When CaO (s) co-exists with Ca (s or ℓ) it will certainly have a Ca chemical potential that is very different from that in CaO (s) in equilibrium with O_2 (g) at $P = 1$ bar. This very large variation in μ_{Ca} occurs as the result of a variation in the chemical content of CaO (s), i.e., Ca/O is not exactly 1 in all cases even though the deviations in Ca/O from 1 are so small that they cannot be determined by chemical analyses. However, exceedingly small deviations of Ca/O will have a large effect upon such important quantities as the numbers of free electrons or holes in the valence band of the solid.

Similarly, Cu_2O (s) has a slightly different Cu/O ratio when it coexists with Cu (s) and when it coexists with CuO (s), Ti_4O_7 (s) has a different Ti/O ratio when it coexists with Ti_3O_5 (s) and when it coexists with Ti_5O_9 (s), and ZrS (s) has a different Zr/S ratio when it coexists with

Zr_2S (s) and when it coexists with sulfur gas at $P = 1$ bar. The chemical potentials of the metal and nonmental in a binary compound are fixed when two condensed phases coexist with the vapor phase at a given temperature ($f = 2 - 3 + 2 = 1$) or when they coexist at a given temperature and applied pressure ($f = 2 - 2 + 2 = 2$). Furthermore, the chemical potential of metal (M) decreases as nonmetal (X) dissolves in the solid metal, and does so until a new M–X phase starts to form, and the chemical potential (or partial pressure, since $\mu_M^s = \mu_M^g = \mu_M^{\circ,g} + RT \ln P_M$ if the gas is ideal) of metal decreases while the chemical potential of X increases, as required by the Gibbs-Duhem equation

$$X_M d\mu_M + X_X d\mu_X = 0 . \tag{36}$$

Figure 7.2 shows a schematic representation of P_M and P_X for a hypothetical M–X system based upon these conclusions.

Proceeding from left to right in Fig. 7.2, the regions are: (1) a range of solid solution of X in M, (2) a two phase region of the most metal-rich compound, saturated with metal, together with metal saturated with X, (3) a range of solid solution of the metal-rich compound, (4) a two-phase region of coexistence of the more M-rich compound, saturated with X, and the more X-rich compound, saturated with M, and (5) a region in which the more X-rich compound coexists with vapor.

7.12. Nonstoichiometry and the Gibbs Free Energy

Behavior such as described above can also be represented on a $\overline{G}$ vs. X (= mole fraction) plot. A brief derivation is helpful. From basic thermodynamics,

$$\frac{G}{n_X + n_M} = \overline{G} = X_M \mu_M + X_X \mu_X . \tag{37}$$

Taking the derivative with respect to X_X at constant T, P,

$$\left.\frac{\partial \overline{G}}{\partial X_X}\right\}_{T,P} = \mu_X + \mu_M \frac{dX_M}{dX_X} + X_M \left.\frac{\partial \mu_M}{\partial X_X}\right\}_{T,P} + X_X \left.\frac{\partial \mu_X}{\partial X_X}\right\}_{T,P} . \tag{38}$$

By the Gibbs-Duhem equation the last two terms sum to zero, and since $X_X + X_M = 1$,

$$\frac{dX_M}{dX_X} = -1 \tag{39}$$

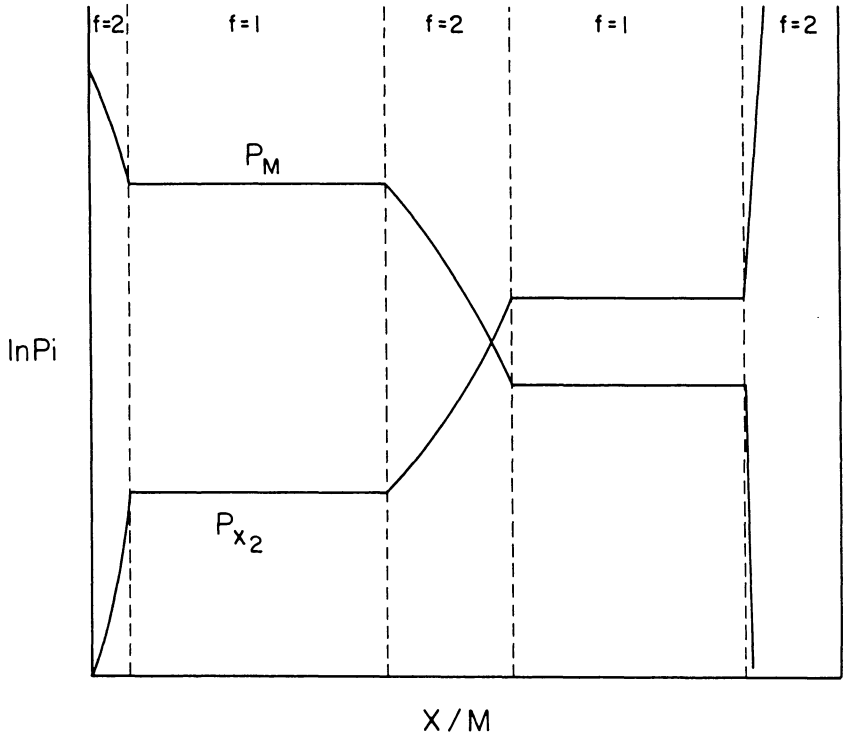

Fig. 7.2. Schematic representation of P_M and P_{X_2} for a hypothetical M–X system.

and thus

$$\left.\frac{\partial \overline{G}}{\partial X_X}\right\}_{T,P} = \mu_X - \mu_M \,. \tag{40}$$

Since at equilibrium between two phases (α and β) in the M–X system, $\mu_X^\alpha = \mu_X^\beta$ and $\mu_M^\alpha = \mu_M^\beta$, it follows from Eq. 40 that at equilibrium between α and β

$$\left.\frac{\partial \overline{G}^\alpha}{\partial X_X^\alpha}\right\}_{T,P} = \left.\frac{\partial \overline{G}^\beta}{\partial X_X^\beta}\right\}_{T,P} \tag{41}$$

i.e., the slopes of the G bar vs. X curves are equal. Thus, the $\overline{G}$ vs. X representation of the phase diagram of Fig. 2 is as given in Fig. 7.3.

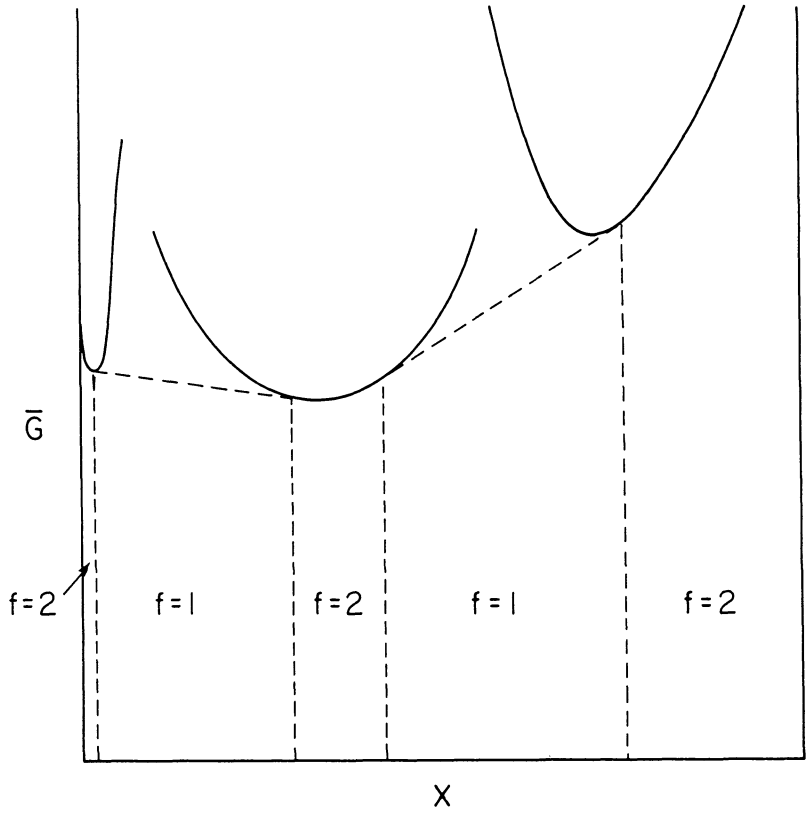

Fig. 7.3. $\overline{G}$ vs. X corresponding to Fig. 7.2.

7.13. Configurational Entropy

An important source of stabilization of nonstoichiometric solids is configurational entropy. If there are N_t sites of which N_0 are occupied and N_v vacant, then the number of different arrangements of atoms on the sites is

$$\Omega = N_t!/(N_0!N_v!) \tag{42}$$

and, using Stirling's approximation ($\ln N! \cong N\ell\text{n}N - N$)

$$S/k = -\ell\text{n}\,\Omega = -[N_V \ell\text{n}\,X_v + N_0 \ell\text{n}\,X_0] \tag{43}$$

where $X_v = N_v/N_t$ and $X_0 = N_0/N_t$, and

$$S/N_t k = S/nR = -[X_v \ell\text{n}\,X_v + X_0 \ell\text{n}\,X_0] \tag{44}$$

where n is the number of moles of sites. For example, $Ti_{1-x}\ O_{1-x}$, which has 15% of both Ti and O sites vacant on the NaCl-type structure, has configurational entropy,

$$\overline{S} = 0.845R = 7.02\ \text{J K}^{-1}\ \text{mol}^{-1} \tag{45}$$

per mole of pairs of Ti and O sites, or

$$\overline{S} = 7.02/0.85 = 8.26\ \text{J K}^{-1}\ \text{mol}^{-1} \tag{46}$$

per mole of TiO. The change in configurational entropy for the hypothetical process

$$Ti_{1.00}O_{1.00\,(s)} = 1.18Ti_{0.85}O_{0.85\,(s)} \tag{47}$$

is 8.26 J K^{-1} mol^{-1} and the contribution to ΔG at 1 500 K is 12.4 kJ mol^{-1}.

7.14. Energetics of Vacancy Creation

Reaction 47 is spontaneous at 1 500 K since TiO exists with the vacancies on the Ti and O sites. Presumably the creation of vacancies is endothermic and the configurational entropy obtained above puts an upper limit on the value of ΔH. This value (12.4 kJ mol^{-1}) is much smaller than would be predicted on the basis of an ionic model and gives an indication that factors other than ionic enter into the energetics of grossly nonstoichiometric solids. In the case of TiO (s), which exhibits metallic properties, intermetallic d interactions provide a significant stabilizing factor. In contrast to TiO (s), which is metallic in appearance and properties, CaO (s) is chalk white and insulating, and in CaO (s) there are no significant metal–metal bonding interactions.

7.15. Distribution Equilibria

In a variety of circumstances two phases (liquid-liquid, solid-liquid, solid-solid) coexist and each component distributes between the two phases.

There are two cases of particular interest in solid-state research: (1) distribution of a second component between two phases which when pure are a single component system, e.g., O (in solid solution) between Ti (hcp) and Ti (bcc), and (2) distribution between two phases which inherently contain two components (e.g., O and Ti between TiO (NaCl-type) and TiO (monoclinic).

The first case is one in which solvent can be meaningfully referred to the pure solvent standard state, i.e., can be considered relative to the Raoult's law standard state, and

$$\mu_M^{\alpha} = \mu^{\text{pure } \alpha} + RT \ln \gamma_M^{\alpha} X_M^{\alpha} \tag{48}$$

and

$$\mu_M^{\beta} = \mu^{\text{pure } \beta} + RT \ln \gamma_M^{\beta} X_M^{\beta} , \tag{49}$$

and $\sum v_i \mu_i = \mu_M^{\alpha} - \mu_M^{\beta} = 0$ yields

$$-RT \ln \frac{\gamma_M^{\beta} X_M^{\beta}}{\gamma_M^{\alpha} X_M^{\alpha}} = \mu^{\text{pure } \beta} - \mu^{\text{pure } \alpha} = \Delta G^{\circ}_{\text{transition}} . \tag{50}$$

Letting $\Delta H^{\circ}(T_{\text{tr}})$ be the standard enthalpy change for the transition at the normal transition temperature, and similarly for $\Delta S^{\circ}(T_{\text{tr}})$, and letting

$$\Delta G^{\circ}_{\text{transition}} = \Delta H^{\circ}(T_{\text{tr}}) - T\Delta S^{\circ}(T_{\text{tr}}) , \tag{51}$$

i.e., neglecting terms of the order of

$$\Delta C_p^{\circ}[(T - T_{\text{tr}}) - T\ell\text{n}(T_{\text{tr}}/T)] \tag{52}$$

and higher,

$$\ell\text{n} \frac{\gamma_M^{\beta} X_M^{\beta}}{\gamma_M^{\alpha} X_M^{\alpha}} = -\frac{\Delta H^{\circ}(T_{\text{tr}})}{R} \left[\frac{1}{T} - \frac{1}{T_{\text{tr}}}\right] . \tag{53}$$

In the case of dilute solutions, $\gamma_{\text{Ti}}^{\alpha} = \gamma_{\text{Ti}}^{\beta} = 1$ and

$$\ell\text{n} \frac{X_M^{\beta}}{X_M^{\alpha}} = -\frac{\Delta H^{\circ}(T_{\text{tr}})}{R} \left[\frac{1}{T} - \frac{1}{T_{\text{tr}}}\right] . \tag{54}$$

Taking $\Delta H^{\circ}(\text{Tr}) > \text{O}$, there are four possible cases:

1. $X_M^{\alpha} \cong 1, \ell\text{n} X_M^{\beta} = \dfrac{-\Delta H^{\circ}(T_{\text{tr}})}{R} \left[\dfrac{1}{T} - \dfrac{1}{T_{\text{tr}}}\right]$,

2. $X_M^\beta > X_M^\alpha$, but X_M^β is not approximately 1,
3. $X_M^\alpha > X_M^\beta$, but X_M^α is not approximately 1,
4. $X_M^\beta \cong 1$ and $\ell n X_M^\alpha = \dfrac{\Delta H^\circ(T_{tr})}{R}\left[\dfrac{1}{T} - \dfrac{1}{T_{tr}}\right]$.

Case 1 is the case of negligible solubility of solute in the high-temperature phase and is analogous to freezing point depression. In case 2 the solubility of solute in the low-temperature phase is less than that in the high-temperature phase and the transition point is depressed and becomes a two-phase region (Fig. 7.4). In case 3 the solubility of solute in the low-temperature phase is greater than in the high-temperature phase and the transition point is elevated (Fig. 7.5). Case 4 is the case of negligible solubility in the high-temperature form and is the transition-point elevation analog of the freezing-point depression law.

The distribution equilibrium of the second kind could result, for example, from the equilibrium established between two nonstoichiometric compounds, i.e., two solid solutions. At some composition and transition temperature the transition might occur congruently, and at other states a two-phase region will separate the two forms. Since in principle all binary compounds are nonstoichiometric, this behavior, shown in Fig. 7.6,

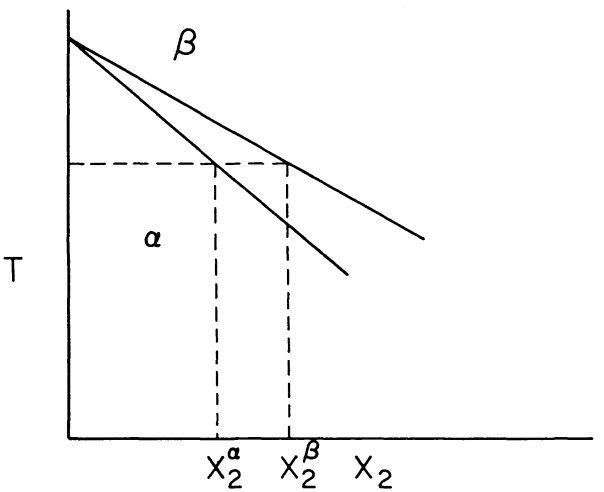

Fig. 7.4. Depression of transition temperature by solute.

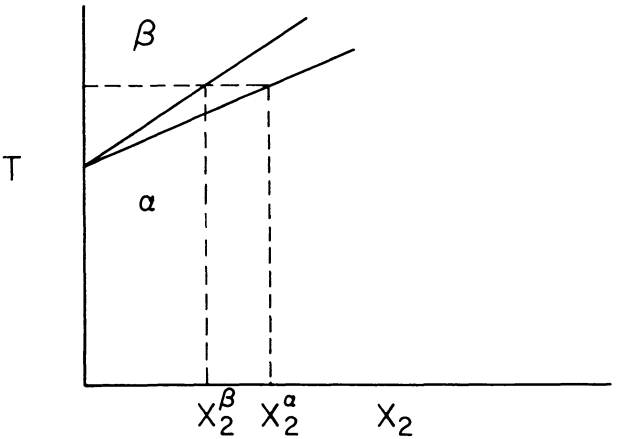

Fig. 7.5. Elevation of transition temperature by solute.

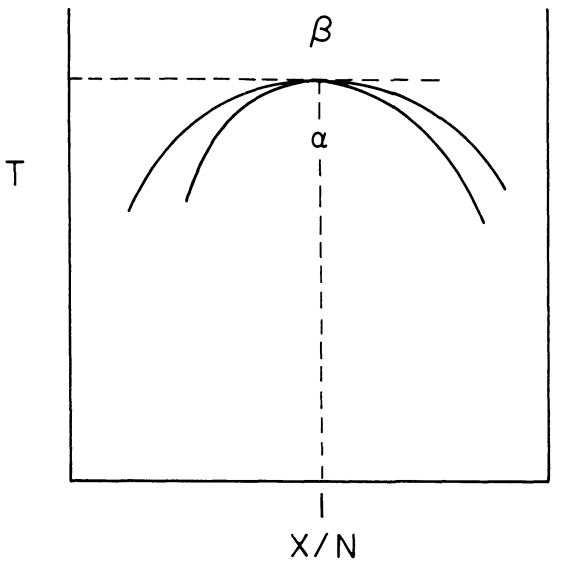

Fig. 7.6. A congruent phase change in a two component system.

will characterize all congruent phase transitions in binary compounds. However, for "line" compounds the width of the homogeneity range and of the two-phase regions will be negligible. On the other hand, it should be remembered that subtle structural consequences can result from very small differences in composition such as can result from incongruent processes in very nearly stoichiometric solids.

7.16. The Gibbs-Konovalow Equation

A congruent phase change, such as shown in Fig. 7.6, must occur at an extremum in T vs. X for both the α and the β curves. This follows directly from the Gibbs-Konovalow equation appropriate to T vs. X at constant P. The Gibbs-Konovalow equations are generalizations of the Clapeyron equation (which is appropriate to $c = 1$ systems) to $c = 2$ systems. The Gibbs-Konovalow equations are derived by applying the Gibbs-Duhem equation to the coexistence of two phases, and the T–X equation is

$$\left.\frac{\partial T}{\partial X_A^\alpha}\right\}_P = -\frac{\left\{\left.\frac{\partial \mu_A^\alpha}{\partial X_A^\alpha}\right\}_{T,P} + \left.\frac{\partial \mu_B^\alpha}{\partial X_B^\alpha}\right\}_{T,P}\right\} \Delta X}{\Delta \overline{S} + \left(\overline{S}_A^\alpha - \overline{S}_B^\alpha\right) \Delta X}, \tag{55}$$

where ΔX is the difference between mole fractions of component A in α and β. It follows that if $\Delta X = 0$ (i.e., if α and β have the same composition at equilibrium), then the T vs. X curve is at an extremum unless $\Delta \overline{S} = 0$. For a first-order transition $\Delta \overline{S} = \Delta \overline{H}/T \neq 0$.

7.17. Second-Order Phase Transitions

If the phases α and β have different symmetries but are separated by a line and not a two-phase region, as shown in Fig. 6.6, then according to Eq. 55, since $\Delta X = 0$ and the T–X curve is not at an extremum, $\Delta S = 0$, and the right-hand side of the equation can be nonzero. For a first-order transition that occurs congruently two G vs. T lines (at constant X, P) intersect, as shown in Fig. 7.7. At $T = 0$ K, the lower curve corresponding to symmetry α corresponds to the stable phase. As T increases towards T_t, the upper curve corresponding to metastable β approaches the lower curve because the slope of the upper curve is more negative than that of the lower curve. This will occur when the phase that is less stable

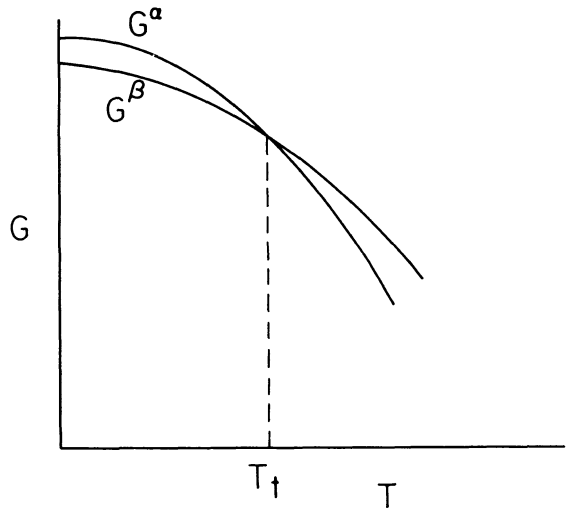

Fig. 7.7. G vs. T for two structures with a first-order transition.

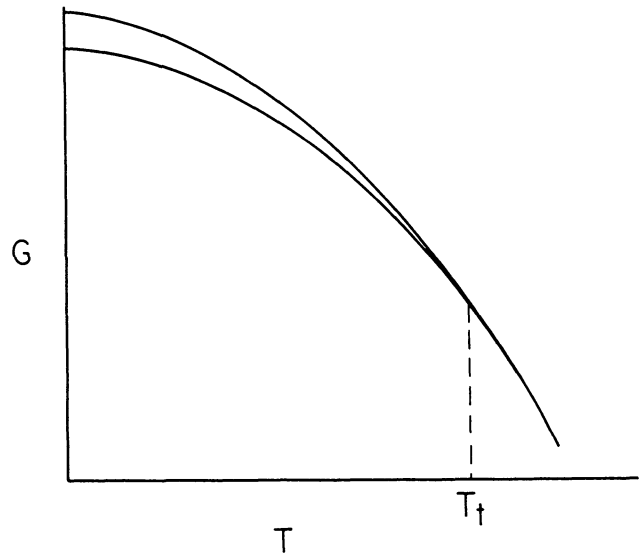

Fig. 7.8. G vs. T for two structures with a second-order transition.

at lower temperatures has the greater entropy. When the curves intersect, $\Delta G = 0$ and the transition occurs reversibly. The equilibrium transition is from the low-entropy phase to the high-entropy phase as T increases through T_t, and $\Delta S \neq 0$ for such a transition.

If the change is to occur with $\Delta S = 0$, it must be that G vs. T at constant X and P does not change slope discontinuously at T_t. This can occur if the slopes of the upper and lower curves approach the same value as T approaches T_t (see Fig. 7.8), i.e., if $\Delta S(T_t) = 0$.

7.18. Displacive Transitions

Transitions that occur as the result of displacements in the equilibrium positions of atoms in such a way as to break symmetry (Fig. 6.2) are called *displacive transitions*. When such a transition occurs continuously, Fig. 7.8 applies. The lower curve is the equilibrium curve, i.e., the point on the lower curve at T represents G for the equilibrium value of an order parameter η (Chapter 6). On the other hand, as η is conceptually decreased below η^{eq} at a given T, the system progresses through a continuum of metastable states with continuously increasing G until the upper-most curve, corresponding to $\eta = 0$, is reached. This curve corresponds to a phase (metastable below T_t) with unbroken symmetry. Increasing T along the lower curve corresponds to $\eta = \eta^{eq}$ and $\eta^{eq} \rightarrow 0$ as $T \rightarrow T_t$.

7.19. Order-Disorder Transition

A distinct way in which transitions can occur is through ordering of atoms and/or vacancies. Consider, for example, the grossly nonstoichiometric solids $Sc_{1-x}S$ and $Zr_{1-x}S$ (x values as large as 0.3). At high temperatures (above 500–1 200° C depending upon x and the compound) these solids in long range average exhibit the NaCl-type structure ($Fm3m$ space-group symmetry). Diffraction experiments show that at high temperatures the metal-atom sites are randomly occupied by vacancies and metal atoms. At lower temperatures these solids order such that the cubic cell with primitive parameters: $\mathbf{a}_p = (\mathbf{a}_c + \mathbf{b}_c)/2$, $\mathbf{b}_p = (\mathbf{a}_c + \mathbf{c}_c)/2$, $\mathbf{c}_p = (\mathbf{b}_c + \mathbf{c}_c)/2$, is lost and the new supercell has $\mathbf{a}_s = \mathbf{a}_c + (\mathbf{b}_c + \mathbf{c}_c)/2$, $\mathbf{b}_s = \mathbf{b}_c + (\mathbf{a}_c + \mathbf{c}_c)/2$, $\mathbf{c}_s = \mathbf{c}_c + (\mathbf{a}_c + \mathbf{c}_c)/2$ (as shown in Fig. 7.9). The volume of the supercell ($\mathbf{a}_s \cdot \mathbf{b}_s \times \mathbf{c}_s = a_c^3/2$) is twice that of the primitive cell. The primitive cell contains one metal atom position at 0,0,0 (and this position is fractionally occupied) and the supercell contains two, at 0,0,0 and 1/2,1/2,1/2 (and their occupancies

differ). Above T_t, then, the supercell positions are equivalent (and the true cell is the subcell) whereas below T_t the fractional occupancies differ and the $Fm\bar{3}m$ symmetry is broken to yield the $R\bar{3}m$ symmetry. This case is discussed from the point of view of Landau theory in Sections 6.12 through 6.14.

The occupancies of the 0,0,0 and 1/2,1/2,1/2 sites in the supercell are the occupancies of the alternating metal containing planes along one of the cube body-diagonals. Above T_t these planes are equally occupied and below T_t the symmetry is broken by differential occupation of alternating planes. The equilibrium amount of disorder corresponds to the bottom curve in Fig. 7.8 and as $T \rightarrow T_t$, $\eta^{eq} \rightarrow 0$, where $\eta^{eq} = 0$ corresponds to random distribution of vacancies in long range.

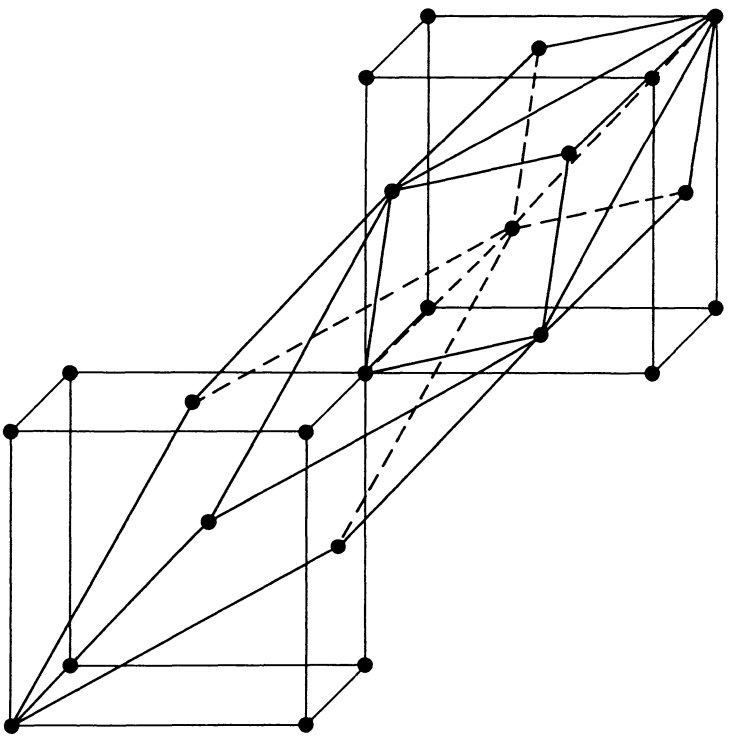

Fig. 7.9. Rhombohedral supercell for $Sc_{1-x}S$ and $Zr_{1-x}S$.

7.20. Behavior of C_p in the Case of Second-Order Transitions

As T_t is approached from below, ΔG for a transition from order→disorder or from distorted→undistorted decreases, and also, by virtue of the increasing temperature, more thermal energy becomes available. It is always true that more than one equivalent low-symmetry structure is possible, e.g., $\pm\eta$ in the simplest case, or various equivalent γ sets (1,0,0,0, or 0,1,0,0, etc.) in more complicated cases such as $Fm3m \rightarrow R\bar{3}m$ (Section 6.14). Thus, as the temperature increases and the barrier between the equivalent structures diminishes, and the available thermal energy increases as well, the systems tend to more and more readily, initially in short range, but with the range increasing with temperature, pass through the $\eta = 0$ state. As a result there is an increased rate of increase in entropy with increasing T. This

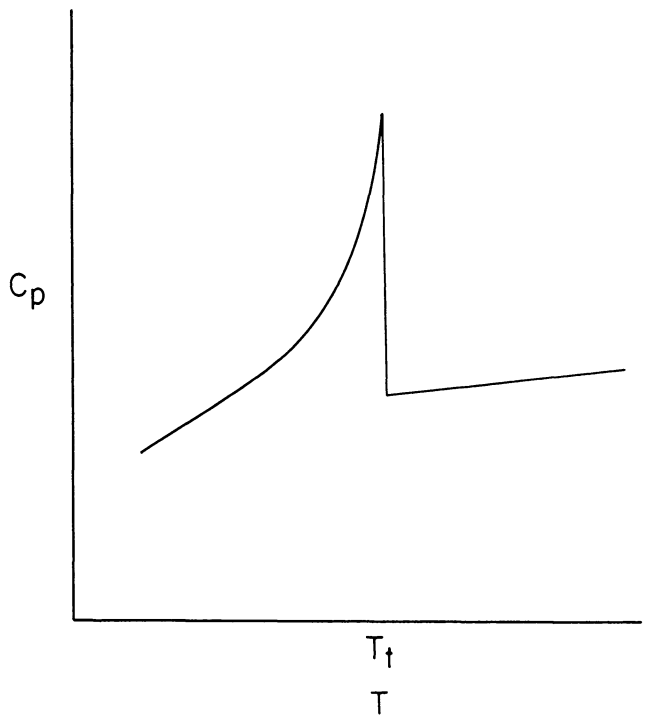

Fig. 7.10. Schematic C_p vs. T for a continuous symmetry breaking transition.

increase in heat capacity gives rise to a λ-type behavior in the heat capacity, as shown in Fig. 7.10. This behavior is characteristic of many second-order transitions. The behavior of C_p in the neighborhood of T_t is not predicted by Landau theory, because of the mean-field character of the theory. In fact, the Landau theory predicts a simple discontinuity in C_p. One of the successes of renormalization theory has been the account taken of increasing average domain size with T and thus a rationalization for the lambda-type behavior.

Bibliography

1. M. Modell and R. C. Reid, *Thermodynamics and Its Applications*, Second Ed. (Prentice Hall, Englewood Cliffs, NJ, 1983).
2. J. G. Kirkwood and I. Oppenheim, *Chemical Thermodynamics* (McGraw-Hill Book Co., New York, 1961).
3. H. F. Franzen and B. C. Gerstein, Application of the Gibbs-Konovalow Equations to Binary Phase Equilibria, *A. I. Ch. E. Journal* **12**, 364 (1966).
4. H. F. Franzen, The True Meaning of Component in the Gibbs Phase Rule, *J. Chem. Ed.* **63**, 948 (1986).
5. H. F. Franzen, An Instructive Problem in Heterogeneous Equilibrium, *J. Chem. Ed.* **65**, 146 (1988).
6. H. F. Franzen, The Freezing Point Depression Law in Physical Chemistry, *J. Chem. Ed.* **65**, 1077 (1988).

Problems

1. Provide a set of independent net reactions for the system containing the species: La_2O_3 (s), La_2S_3 (s), La_2O_2S (s), SO (g), SO_2 (g), O_2 (g).
2. Provide a set of independent net reactions for TiO_xC_{1-x} (s) in equilibrium with O_2 (g), CO (g), TiO (g) and Ti (g). Include solid solution species.
3. If the system of Problem 1 is synthesized by decomposition of La_2O_2S (s), how many independent intensive variables are there? What restraint is placed on the system?
4. At 2 000 K, ΔG_f^0 for Th_3N_4 (s) is −630.0 kJ/mol and for ThN (s) is −206.4 kJ/mol. Determine what phases are present and their quantities at equilibrium if 16 g. of Th and 1 g of N_2 react in an inert 0.500 liter container at 2 000 K.
5. Using the data given below determine the phases and their quantities at equilibrium if 1.00 g of a Zr–Al mixture with overall $X_{Zr} = 0.550$ is heated at 1 500 K in an inert 1.00 liter container.

	$\Delta H^\circ_{1\,500}$	$\Delta S^\circ_{1\,500}$
Zr_2Al_3 (s)=2 ZrAl (s) + Al (g)	372.8 kJ mol^{-1}	118.4 J K^{-1} mol^{-1}
5/7 Zr_2Al_3 (s)=2/7 Zr_5 Al_4 (s) + Al (g)	369.7 kJ mol^{-1}	115.5 J K^{-1} mol^{-1}

6. The simplest binary solution (liquid or solid) model beyond the ideal solution is the regular solution for which

$$\mu_A = \mu_A^0 + RT\ell n\, X_A + wX_B^2 .$$

   (a) Use the Gibbs-Duhem equation to show that $\mu_B = \mu_B^0 + RT\ell n\, X_B + wX_A^2$.

   (b) Show that $\overline{G}$ vs. X for a regular solution can exhibit a single minimum for some temperatures and a double minimum for others.

   (c) Show that for $w > 0$ this means that a regular solution spontaneously disproportionates into two solutions below some temperatures, and find that temperature in terms of w and R.

CHAPTER 8

X-RAY DIFFRACTION

8.1. X-Ray Diffraction by a Crystal

Diffraction of X-rays occurs as the result of scattering of rays by the electrons present in a crystalline solid. If the solid is periodic in three-dimensions, then the electron density in the solid, $\rho_E(\mathbf{r})$, obeys

$$\rho_E(\mathbf{r}+\mathbf{T}) = \rho_E(\mathbf{r})\,. \tag{1}$$

If an incoming wave travels in the direction $\mathbf{k}_{\text{in}}$ (where $|\mathbf{k}_{\text{in}}| = 2\pi$) and the detector is in the direction $\mathbf{k}_{\text{out}}$ (where, again, $|\mathbf{k}_{\text{out}}| = 2\pi$), then the difference in path length, ΔL, for the ray scattered at $\mathbf{r}+\mathbf{T}_\ell$ relative to that scattered at the origin is

$$\Delta L = (\mathbf{k}_{\text{out}} - \mathbf{k}_{\text{in}}) \cdot (\mathbf{r}+\mathbf{T}_\ell)/2\pi \tag{2}$$

as can be seen in Fig. 8.1, and the phase difference between the two scattered rays is

$$\Delta\phi = 2\pi\Delta L/\lambda = (\mathbf{k}_{\text{out}} - \mathbf{k}_{\text{in}}) \cdot (\mathbf{r}+\mathbf{T}_\ell)/\lambda\,. \tag{3}$$

Integration of $\rho(\mathbf{r}+\mathbf{T}_\ell)$ over a unit cell and summation over all translations to yield the total scattering by all electrons in the crystal (for the moment assumed to be infinite):

$$\sum_\ell \int_{\text{cell}} \rho(\mathbf{r}+\mathbf{T}\ell) \exp i[(\mathbf{k}_{\text{out}} - \mathbf{k}_{\text{in}}) \cdot (\mathbf{r}+\mathbf{T}\ell)/\lambda] d\mathbf{r}\,, \tag{4}$$

which equals

$$\sum_\ell \left[\int_{\text{cell}} \rho(\mathbf{r}) \exp i[(\mathbf{k}_{\text{out}} - \mathbf{k}_{\text{in}}) \cdot \mathbf{r}/\lambda] d\mathbf{r} \exp i(\mathbf{k}_{\text{out}} - \mathbf{k}_{\text{in}})\mathbf{T}_\ell/\lambda\right]\,. \tag{5}$$

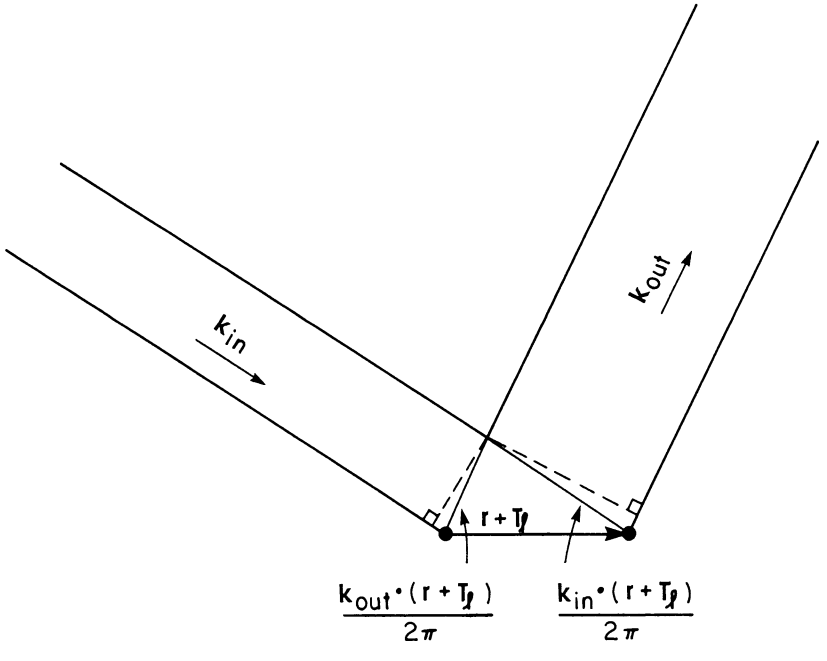

Fig. 8.1. Scattering from atoms related by $\mathbf{r} + \mathbf{T}_\ell$.

The integral over the cell volume is given the symbol F and is called the *structure factor*,

$$F = \int_{\text{cell}} \rho(\mathbf{r}) \exp i[(\mathbf{k}_{\text{out}} - \mathbf{k}_{\text{in}}) \cdot \mathbf{k}/\lambda] d\mathbf{r}\,, \tag{6}$$

and thus the scattered wave for a given $\mathbf{k}_{\text{in}} - \mathbf{k}_{\text{out}}$ pair is given by

$$F \sum_{\ell} \exp i(\mathbf{k}_{\text{out}} - \mathbf{k}_{\text{in}}) \cdot \mathbf{T}_\ell/\lambda \tag{7}$$

and the sum is over all translations. The translations are given by

$$\mathbf{T}_\ell = n_1\mathbf{a} + n_2\mathbf{b} + n_3\mathbf{c} \tag{8}$$

and thus

$$\sum_{\ell} \exp i(\mathbf{k}_{\text{out}} - \mathbf{k}_{\text{in}}) \cdot \mathbf{T}_{\ell}/\lambda$$

$$= \sum_{n_1} \exp in_1(\mathbf{k}_{\text{out}} - \mathbf{k}_{\text{in}}) \cdot \mathbf{a}/\lambda \sum_{n_2} \exp in_2(\mathbf{k}_{\text{out}} - \mathbf{k}_{\text{in}})$$

$$\cdot \mathbf{b}/\lambda \sum_{n_3} \exp in_3(\mathbf{k}_{\text{out}} - \mathbf{k}_{\text{in}}) \cdot \mathbf{c}/\lambda \,. \tag{9}$$

Each of the terms in the product on the right is a sum over vectors in the complex plane each with unit length, i.e.,

$$|\exp in_i(\mathbf{k}_{\text{out}} - \mathbf{k}_{\text{in}}) \cdot \mathbf{a}/\lambda| = 1 \,, \tag{10}$$

and with phase angles $n_1(\mathbf{k}_{\text{out}} - \mathbf{k}_{\text{in}})\mathbf{a}/\lambda$, and etc. Suppose that $(\mathbf{k}_{\text{out}} - \mathbf{k}_{\text{in}}) \cdot \mathbf{a}/\lambda \neq 2\pi$ times an integer. Then as n_1 runs over all integers the angles $n_1(\mathbf{k}_{\text{out}} - \mathbf{k}_{\text{in}}) \cdot \mathbf{a}/\lambda 2$ modulo 2π will run over all angles between 0 and 2π, and for each unit vector in the sum there will be one exactly out of phase with it. Thus, the product of the sums in Eq. 9 vanishes unless

$$(\mathbf{k}_{\text{out}} - \mathbf{k}_{\text{in}}) \cdot \mathbf{a}/\lambda = 2\pi \times \text{an integer} \,, \tag{11}$$

$$(\mathbf{k}_{\text{out}} - \mathbf{k}_{\text{in}}) \cdot \mathbf{b}/\lambda = 2\pi \times \text{an integer} \tag{12}$$

and

$$(\mathbf{k}_{\text{out}} - \mathbf{k}_{\text{in}}) \cdot \mathbf{c}/\lambda = 2\pi \times \text{an integer} \,, \tag{13}$$

in which case each of the sums will be equal to the number of cells in the crystal. This number was taken to be infinite in order that there would be complete destructive interference when the constructive interference condition of Eqs. 11–13 is not met. The effect of finite but large crystal size is to broaden the reflection, as will be considered in the next section.

In Section 2.19 it was found that a vector that yields a scalar product of 2π times an integer with $m\mathbf{a} + n\mathbf{b} + p\mathbf{c}$ is of the form $\mathbf{K} = h\mathbf{a}^* + k\mathbf{b}^* + \ell\mathbf{c}^*$, and thus the condition for constructive interference (see Fig. 8.2) is

$$(\mathbf{k}_{\text{out}} - \mathbf{k}_{\text{in}})/\lambda = \mathbf{K} \,, \tag{14}$$

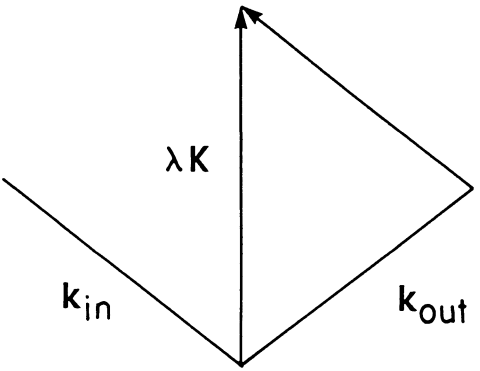

Fig. 8.2. K is proportional to $\mathbf{k}_{out} - \mathbf{k}_{in}$.

a reciprocal lattice vector. From the figure it follows that **K** is a bisector of the angle made by $\mathbf{k}_{in}$ and $\mathbf{k}_{out}$, and since $\mathbf{K} = h\mathbf{a}^* + k\mathbf{b}^* + \ell\mathbf{c}^*$ is perpendicular to the h, k, ℓ plane (Section 2.16), one condition for diffraction (constructive interference) is that the incoming and outgoing rays make the same angle (θ, see Fig. 8.3) with a plane of lattice points. Furthermore, according to Fig. 8.3,

$$\lambda|\mathbf{K}|/2|\mathbf{k}_{in}| = \sin\theta \tag{15}$$

and since $|\mathbf{K}| = 2\pi/d$, and $|\mathbf{k}_{in}| = 2\pi$,

$$\lambda = 2d\sin\theta\,, \tag{16}$$

the Bragg relation. Using $(\mathbf{k}_{out} - \mathbf{k}_{in})/\lambda = \mathbf{K}$ in Eq. 6 yields,

$$F = \int_{cell} \rho(\mathbf{r}) \exp i\mathbf{K}\cdot\mathbf{r}\, dr\,. \tag{17}$$

The integral is almost always evaluated by integrating over the individual atoms and then summing over the atoms:

$$F = \sum_j \left[\int_{\substack{\text{atom} \\ \text{at } \mathbf{r}_j}} \rho(\mathbf{r}) \exp i\mathbf{K}\cdot\mathbf{r}\, dr \right] \exp i\mathbf{K}\cdot\mathbf{r}_j \tag{18}$$

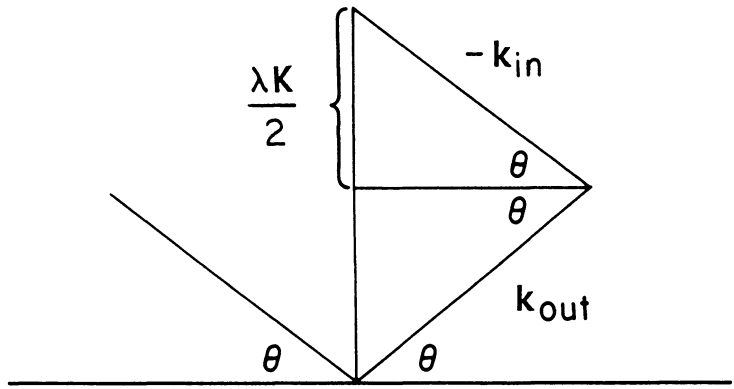

Fig. 8.3. Derivation of the Bragg relation.

where the $\mathbf{r}_j$'s are the atom positions within the cell and the integrals are over the corresponding free atom with $\mathbf{r}$ in the integral relative to the center of the nucleus. The integral over the atom is called the atomic scattering factor, f_j, and thus

$$F = \sum_j f_j \exp i\mathbf{K} \cdot \mathbf{r}_j \,. \tag{19}$$

The interatomic interference is usually calculated by the integral of Eq. 18 over a free atom, although in some refined calculations dealing with chemical bonding interpretation, attempts are made to express the atomic electron density distribution appropriate to the bound configuration of the atom. The intra-atomic interference is usually dealt with as a sum over the cell, as in Eq. 19, and a sum over the cells as discussed above and in the next section. The sum over the cells, in the treatment given above, yields only a yes or no answer: yes there is diffraction when $(\mathbf{k}_{\text{out}} - \mathbf{k}_{\text{in}})/\lambda = \mathbf{K}$, no there is not when $(\mathbf{k}_{\text{out}} - \mathbf{k}_{\text{in}})/\lambda \neq \mathbf{K}$. The diffraction is labelled by the particular h, k and ℓ values (the particular $\mathbf{K}$), for when $(\mathbf{k}_{\text{out}} - \mathbf{k}_{\text{in}})/\lambda = \mathbf{K} = h\mathbf{a}^* + k\mathbf{b}^* + \ell\mathbf{c}^*$, then

$$F_{hk\ell} = \sum_j f_j \exp 2\pi i(hx + ky + \ell z) \tag{20}$$

by Eq. 19, and diffraction occurs when the incoming beam and the detected beam each make the Bragg angle θ with the h, k, ℓ plane, by Eq. 16.

The f_j's are usually obtained from standard tables such as are found in the International Tables for Crystallography. They are generally given as functions of $\lambda^{-1} \sin\theta$, and they are observed to decay from the value of the number of electrons in the atom rather rapidly toward zero, but in a fashion that is quite consistent from atom to atom.

8.2. Finite Summation and Peak Widths (The Fresnel Construction)

In real cases crystals are not infinite, and thus the sums

$$\sum_{n=0}^{N} \exp i\mathbf{K} \cdot n\mathbf{a} \tag{21}$$

are finite and this fact leads to a finite peak width for the diffraction labelled by $\mathbf{K}$. In other words, because crystals are finite the diffractions do not occur as delta functions corresponding to reciprocal state points labelled by h, k and ℓ, but as peaks with finite width. In order to explore this width let $\alpha = \mathbf{K} \cdot \mathbf{a}$ and represent the sum above schematically by the resultant vector in Fig. 8.4. The intensity of the diffraction beam is the square of the magnitude of this vector. The base angles are $90 - \alpha/2$, and the apical angles are, therefore, α, as shown in the figure. Thus (see Fig. 8.5), letting Σ be the resultant magnitude:

$$\left(\sum/2\right) \cdot 2 \cdot \sin(\alpha/2) = \sin[(n+1)\alpha/2] \tag{22}$$

or

$$\sum = (\sin[(n+1) \cdot \alpha/2])/\sin(\alpha/2)\,. \tag{23}$$

Since $\alpha = \mathbf{K} \cdot \mathbf{a}$ we can set $\alpha = 2\pi h$, if h is now allowed to be nonintegral. That is, h is exactly an integer and all diffraction magnitudes resulting from the scattering are exactly in phase only when an infinite lattice is assumed, and for a finite lattice there results a peak with finite width and diffraction intensity corresponding to nonintegral h values according to

$$\sum = (\sin[(N+1) \cdot h \cdot \pi])/\sin(h\pi)\,. \tag{24}$$

We can take $h = I + \Delta h$ where I is an integer and obtain

$$\sum = (\sin[(N+1) \cdot \Delta h \cdot \pi])/\sin(\Delta h \cdot \pi)\,. \tag{25}$$

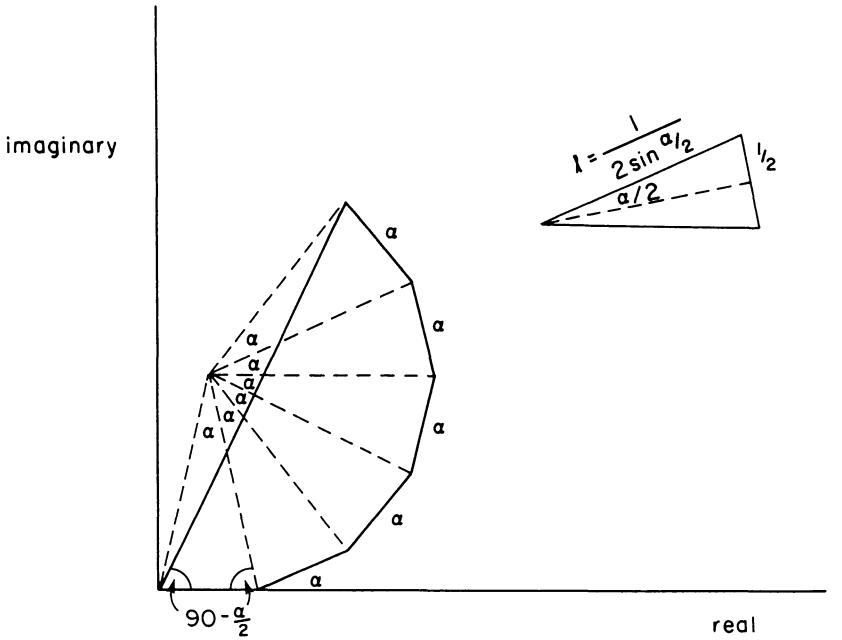

Fig. 8.4. Fresnel construction.

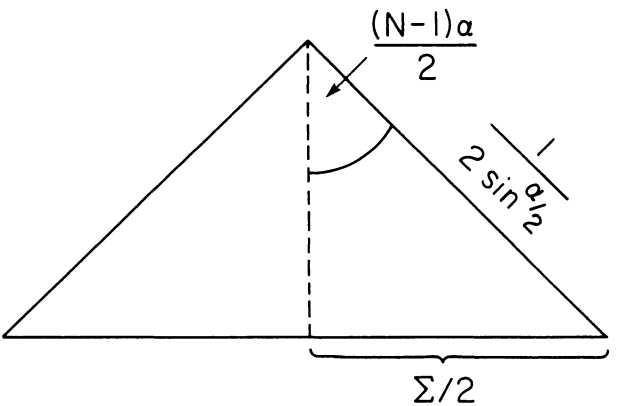

Fig. 8.5. Relation between α and diffraction magnitude.

Some values of $(\Sigma/\Sigma(\Delta h = 0))^2$ vs. Δh for various values of N are given in Table 8.1.

Table 8.1. Intensity $(\Sigma^2/\Sigma^2(\Delta h = 0))$ vs. Δh for various N values, $\Sigma = (\sin[(N+1)\cdot \Delta h \cdot \pi]/\sin(\Delta h \cdot \pi)$.

N	10	100	1 000	10 000
$10^5 \Delta h$				
1				0.968
2			0.999	0.875
4			0.995	0.573
8			0.979	0.055
16		0.999	0.918	
32		0.997	0.705	
64		0.986	0.202	
128	0.999	0.946	0.004	
256	0.997	0.799		
512	0.990	0.378		
1 024	0.959	0.001		
2 048	0.845			
4 096	0.490			
8 192	0.012			

What these values show, for example, is that for crystal size $N = 10\,000$ on an edge a diffraction peak that is broadened only by crystal size has dropped to one half maximum intensity when $(\Sigma/\Sigma(\Delta h = 0))^2 = \sqrt[3]{0.5}$, i.e., when $\Delta h \cong 3 \times 10^{-5}$. Assuming a cubic lattice for simplicity,

$$|\mathbf{K}| = \sqrt{\mathbf{K} \cdot \mathbf{K}} = \left(\sqrt{h^2 + k^2 + \ell^2}\right)/a \tag{26}$$

and

$$\begin{aligned} \delta|\mathbf{K}| &= \delta d^{-1} = (2/\lambda)\delta \sin\theta = (2/\lambda)\cos\theta\delta\theta \\ &= a^{-1}\delta(h^2 + k^2 + \ell^2)^{1/2} \\ &= (h + k + \ell)(\delta h + \delta k + \delta\ell)/(a \cdot (h^2 + k^2 + \ell^2)^{1/2}) \end{aligned} \tag{27}$$

or

$$\delta\theta = \frac{\lambda(h + k + \ell)(\delta h + \delta k + \delta\ell)}{2 \cdot a \cdot \cos\theta \cdot (h^2 + k^2\ell^2)^{1/2}} \cdot \tag{28}$$

For example, if $\lambda = 1.54$ Å (Cu Kα), $a = 5.5$ Å and the 1,1,1 reflection is considered, then for $N = 10^4$ in each dimension, $\delta h = \delta k = \delta \ell$ and the full width at half maximum is $(0.79)^3 = 0.50$ when $\Delta h \cong 3.0 \times 10^{-5}$ and

$$\delta\theta = \frac{(1.54) \cdot 3 \cdot 3 \cdot (3.0 \times 10^{-5})}{2 \cdot (5.5) \cdot \sqrt{3} \cdot \cos(24.83°)} = 2.4 \times 10^{-5} \text{ radians}$$

$$= 1.4 \times 10^{-3} \text{ degrees}. \tag{29}$$

Thus, a domain size of 10^4 unit translations on an edge has negligible effect upon peak width, and significant domain size broadening is indicative of domains smaller than 10^4 unit translations.

8.3. Powder Diffraction

Powder diffraction experiments, especially Guinier film and powder diffractometer techniques, play an important role is solid-state studies. A powder, provided there is no preferred orientation, orients crystallites at random and the only geometric condition on diffraction from a powder is that the diffraction angle meet the Bragg condition, i.e., a powder diffracts along the surface of a cone with apical angle equal to $4\theta = 4\sin^{-1}(\lambda/2d)$, where d is one of the interplanar spacings of the lattice (Fig. 8.6).

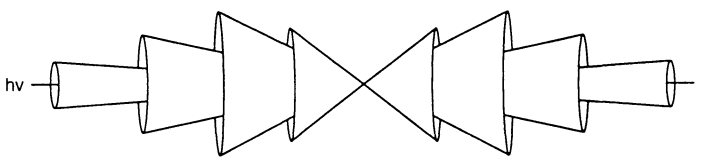

Fig. 8.6. Powder diffraction.

It is advantageous to have small particles for powder diffraction in order that the orientations be randomized insofar as possible. In the previous section it was found that particles could be reduced to about 5μ on an edge (at least for the conditions assumed in the calculation) without significantly broadening the diffraction peaks because of size effects. Thus, in the absence of strain broadening (a substantial problem with ductile materials),

it is advantageous to reduce samples to a very fine powder for diffraction studies.

8.4. Interplanar Spacing

In general, $d^{-2} = \mathbf{K} \cdot \mathbf{K}/4\pi^2$ and thus d^{-2} is relatively easily calculated for the various crystal systems in terms of h, k and ℓ and lattice parameters (see Table 8.2).

Table 8.2. d^{-2} for the 7 crystal systems.

c:	$(h^2 + h^2 + \ell^2)/a^2$
t:	$(h^2 + k^2)/a^2 + \ell^2/c^2$
h:	$4(h^2 + hk + k^2)/(3a^2) + \ell^2/c^2$
o:	$h^2/a^2 + k^2/b^2 + \ell^2/c^2$
r:	$\dfrac{\sin^2\alpha[(h^2 + k^2 + \ell^2) + 2(k\ell + h\ell + hk)(\cos^2\alpha - \cos\alpha)/\sin^2\alpha]}{a^2(1 - 3\cos^2\alpha + 2\cos^3\alpha)}$
m:	$\dfrac{h^2}{a^2\sin^2\beta} + \dfrac{k^2}{b^2} + \dfrac{\ell^2}{c^2\sin^2\beta} + \dfrac{2h\ell\cos(180 - \beta)}{ac\sin^2\beta}$
tr:	$h^2a^{*2} + k^2b^{*2} + \ell^2c^{*2} + 2[k\ell a^*c^*\cos\alpha^* + h\ell a^*c^*\cos\beta^* + hka^*\cos\gamma^*]$,
	$a^* = \dfrac{bc\sin\alpha}{V}$, $b^* = \dfrac{ac\sin\beta}{V}$, $c^* = \dfrac{ab\sin\gamma}{V}$
	$\cos\alpha^* = \dfrac{\cos\beta\cos\gamma - \cos\alpha}{\sin\beta\sin\gamma}$, $\cos\beta^* = \dfrac{\cos\alpha\cos\gamma - \cos\beta}{\sin\alpha\sin\gamma}$
	$\cos\gamma^* = \dfrac{\cos\alpha\cos\beta - \cos\gamma}{\sin\alpha\sin\beta}$ $V = abc\sqrt{1 - \cos^2\alpha - \cos^2\beta - \cos^2\gamma + 2\cos\alpha\cos\beta\cos\gamma}$

8.5. Coincident Reflections

In general, in a powder diffraction pattern more than one diffraction occurs at a given diffraction angle. All of the d^{-2} expressions of Table 8.2 are unchanged by replacing h, k, ℓ by $\bar{h}, \bar{k}, \bar{\ell}$, and furthermore, $|F_{hk\ell}| = |F_{\bar{h}\bar{k}\bar{\ell}}|$ in all cases, therefore, the multiplicity of all powder diffraction lines is at least two. In the cubic case all signed permutations of h, k, ℓ occur at the same diffraction angle. Also for some higher index combinations different sets of integers (e.g., 300 and 221) yield the same value of $h^2+k^2+\ell^2$. Counting the signed permutations (but not the coincidences of equal $h^2 + k^2 + \ell^2$ with different triples of integers) gives the number of diffractions contributing to a powder line of a cubic sample collected in Table 8.3. Consideration of the effect of symmetry upon the structure factor shows that all of the diffractions for the signed permutations of h, k and ℓ are equivalent in the crystal classes $m3m, \bar{4}3m$ and 432, and in $m3$ and 23 the diffractions h, k, ℓ and k, h, ℓ are not equivalent ($|F_{hk\ell}| \neq |F_{kh\ell}|$), although they occur at the same diffraction angle. Thus, in the cubic classes $m3$ and 23 there are two sets of 12 equivalent reflections for $h, k, 0$ and $k, h, 0$, and two sets of 24 equivalent reflections for h, k, ℓ and k, h, ℓ.

Table 8.3. Multiplicities of cubic powder patterns for the $m3m, \bar{4}3m$ and 432 crystal classes.

$hk\ell$	Multiplicity
$h\ 0\ 0$	6
$h\ k\ 0$	24
$h\ h\ 0$	12
$h\ h\ \ell$	24
$h\ h\ h$	8
$h\ k\ \ell$	48

8.6. Hexagonal Indexing

In the general hexagonal case, h, k, ℓ triples with the same value of h^2+hk+k^2 correspond to the same diffraction angle. In this case there is a trick for finding these values. This trick derives from the fact (Fig. 8.7) that $\mathbf{a}, \mathbf{b}$ and $-(\mathbf{a}+\mathbf{b})$ are all equally good axes for the description of the lattice, and thus the index $i = -(h + k)$ appropriate to this axis is frequently added to the

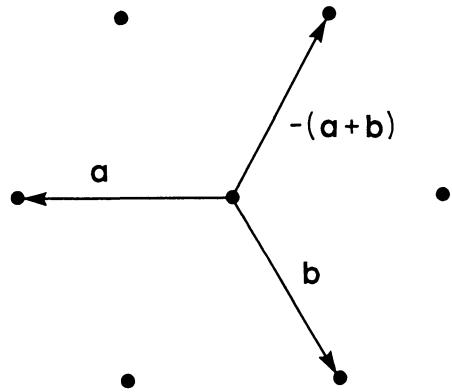

Fig. 8.7. Equivalent basis vectors for the hexagonal case.

Table 8.4. Multiplicities of powder patterns in hexagonal classes.

	Multiplicities			
hkℓ	**$6/mmm$, $6mm$ $\bar{6}m2$, 622**	**$6/m$, $\bar{6}$, 6**	**$\bar{3}m1$, $3m1$, 321**	**$\bar{3}1m$, $31m$, 312**
$0\,0\,\ell$	2	2	2	2
$h\,0\,0$	6	6	6	6
$h\,h\,0$	6	6	6	6
$h\,k\,0$	12	6 + 6	12	12
$h\,0\,\ell$	12	12	12	6 + 6
$h\,h\,\ell$	12	12	6 + 6	12
$h\,k\,\ell$	24	12 + 12	12 + 12	12 + 12

index set. Thus, hexagonal indices are often given as h, k, i, ℓ, e.g., 2, 1, $\bar{3}$, ℓ, etc. It is possible to cyclically permute h, k, i to obtain indices for planes with the same d spacing, e.g., 2, 1, $\bar{3}$, ℓ; 1, $\bar{3}$, 2, ℓ; $\bar{3}$, 2, 1, ℓ all correspond to $h^2 + hk + k^2 = 7$. Thus, there are, for h, k, ℓ, 24 diffractions at the same Bragg angle: (the permutations h, k, i, ℓ; k, i, h, ℓ; and i, h, k, ℓ yield three, times two for exchanging h and k, times two for changing the sign of ℓ, times two for changing the signs of h and k together). The planes with equal d spacing found in this way all have the same $|F_{hk\ell}|$ values only for the crystal classes $6/mmm$, $6mm$, $\bar{6}m2$ and 622. In the other classes some

planes with the same d spacing have different intensities. This information is summarized in Table 8.4.

8.7. Rhombohedral Indexed as Hexagonal

The rhombohedral lattice can be described as a hexagonal lattice with centering at 1/3, 2/3, 1/3 and 2/3, 1/3, 2/3 (or 1/3, 2/3, 2/3 and 2/3, 1/3, 1/3) (Fig. AI.3). The axial transformation from rhombohedral to hexagonal corresponding with Fig. AI.3 is

$$\begin{pmatrix} \mathbf{a} \\ \mathbf{b} \\ \mathbf{c} \end{pmatrix}_h = \begin{pmatrix} 0 & 1 & \bar{1} \\ \bar{1} & 0 & 1 \\ 1 & 1 & 1 \end{pmatrix} \begin{pmatrix} \mathbf{a} \\ \mathbf{b} \\ \mathbf{c} \end{pmatrix}_r , \tag{30}$$

In Appendix III it is shown that h, k, ℓ transforms as $\mathbf{a}, \mathbf{b}, \mathbf{c}$, i.e.,

$$\begin{pmatrix} h \\ k \\ \ell \end{pmatrix}_h = \begin{pmatrix} 0 & 1 & \bar{1} \\ \bar{1} & 0 & 1 \\ 1 & 1 & 1 \end{pmatrix} \begin{pmatrix} h \\ k \\ \ell \end{pmatrix}_r . \tag{31}$$

The number of diffractions contributing to a general h, k, ℓ (rhombohedral indexing) power line is 12, a factor of 6 from the permutation of h, k and ℓ and a factor of 2 from the sign change in all three indices at the same time. The multiplicity in the crystal classes $\bar{3}m$, $3m$ and 32 is 12 whereas in the classes $\bar{3}$ and 3 these are split into 6 and 6 (only the cyclicly permuted h, k, ℓ sets are equivalent).

The fact that a general plane in rhombohedral has half the multiplicity of the same plane in hexagonal is a result of the fact that there are systematic absences in the diffraction from a rhombohedral lattice when it is indexed on a hexagonal basis. The inverse of the transformation of Eq. 31

$$\begin{pmatrix} h \\ k \\ \ell \end{pmatrix}_r = \begin{pmatrix} -1/3 & -2/3 & 1/3 \\ 2/3 & 1/3 & 1/3 \\ -1/3 & 1/3 & 1/3 \end{pmatrix} \begin{pmatrix} h \\ k \\ \ell \end{pmatrix}_h \tag{32}$$

shows that $1/3(-h - 2k + \ell)$, $1/3(2h + k + \ell)$ and $1/3(-h + k + \ell)$ must all be integers. All of these are integers if $-h + k + \ell = 3n$, and this is the condition that is met by hexagonal Miller indices when there exists a primitive rhombohedral cell.

In summary, it is always possible to index a rhombohedral lattice using hexagonal basis vectors. This may be done intentionally, or it may be that

a diffraction pattern is indexed as hexagonal without first recognizing that it is also rhombohedral. When this is the case the primitive rhombohedral lattice can be discovered by noting that the planes obey the condition $-h+k+\ell = 3n$. When a rhombohedral lattice is indexed as hexagonal,

$$|\mathbf{c}_h| = |\mathbf{a}_r + \mathbf{b}_r + \mathbf{c}_r| \tag{33}$$

and

$$|\mathbf{a}_h| = |\mathbf{a}_r - \mathbf{b}_{rh}| \tag{34}$$

which yield

$$a_h = a_r\sqrt{2 - 2\cos\alpha} \tag{35}$$

and

$$c_h = a_r\sqrt{3 + 6\cos\alpha}\,. \tag{36}$$

8.8. Indexing of Power Patterns

The geometry of the diffraction experiment (shown in Fig. 8.8 for the Guinier powder diffraction experiment) can be analyzed to yield θ angles which, using the Bragg relation, can be converted into d^{-2} values. The usual problem is to interpret the pattern in terms of h, k, ℓ values (called indexing). An initial approach to this problem is to compare the values with sets of values calculated for known structures that might be expected. A useful calculated result in this regard is a line diagram for which the positions are those appropriate to the experiment and the lengths of the lines are proportional to the calculated intensities (Fig. 8.9). The intensities are calculated using $I\alpha|F_{hk\ell}|^2$ where $F = \Sigma f_j \exp 2\pi i(hx_j + ky_j + \ell z_j)$, the multiplicities appropriate to the system, and Lorentz and polarization corrections appropriate to the system, an absorption correction if it varies with θ and estimated or calculated thermal factors. The details of the corrections are treated in texts on crystallography several of which are listed in the bibliography at the end of this chapter.

A close fit between calculated and observed d spacings may indicate a satisfactory solution to the indexing problem. However, in some cases it may remain somewhat uncertain as to whether a satisfactory solution has been found. Typically nonstoichiometry results in changes in lattice

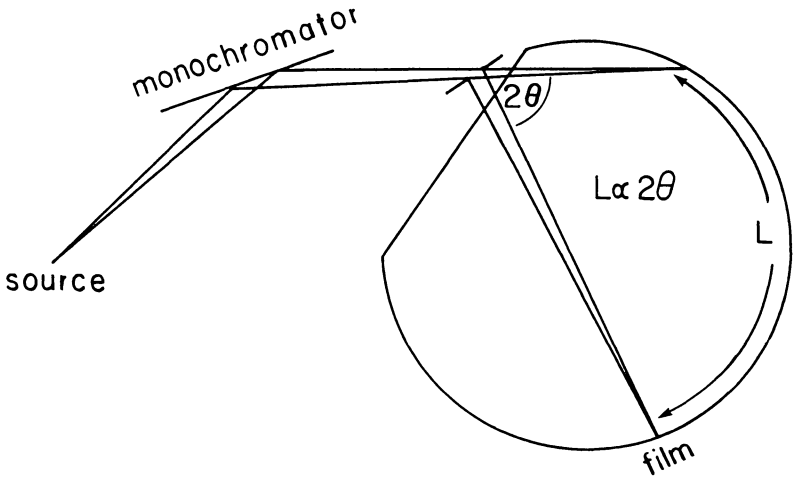

Fig. 8.8. The Guinier powder diffraction experiment.

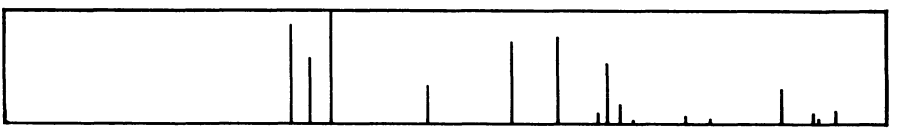

Fig. 8.9. Schematic Guinier pattern.

parameters and intensities and a fit may have been attempted using lattice parameters and structure factors appropriate to a sample somewhat different from the experimental sample.

One procedure to follow when this may have occurred is to use the fit obtained to assign Miller indices to the observed d^{-2} values. Using these values and the appropriate d^{-2} expression (Table 8.2), perform a least squares calculation (an example is shown in the next section) to obtain new lattice parameters and repeat the process until there is no change in the parameters obtained. One necessary ingredient in this process is a means for deciding when a calculated d^{-2} value is or is not sufficiently close to a measured value to be considered satisfactorily indexed. This ingredient is provided by the *law of propagation of errors*:

$$R_X^2 = \sum_j \left(\frac{\partial X}{\partial x_j}\right)^2 r_{x_j}^2 \tag{37}$$

which relates the uncertainty, R_x, in a derived quantity, X, to the uncertainties, r_{x_j}, in the measured quantities, x_j, upon which X depends. For example, if θ is proportional to the measured length, L, on a film (see Fig. 8.8) and that measurement results in a $\pm 0.02°$ uncertainty in θ, then, using Bragg's relation and the law of propagation of errors,

$$R_d = \frac{\lambda}{2} \left| \partial \frac{\left(\frac{1}{\sin\theta}\right)}{\partial\theta} \right| r_\theta \tag{38}$$

or

$$R_d/d = r_\theta \cdot \text{cotan}\theta\,. \tag{39}$$

It is necessary that r_θ be expressed in radians, i.e., $r_\theta = 3.5 \times 10^{-4}$ radians in the case under consideration, and $Rd/d = 3.5 \times 10^{-4}$ cotan θ. It is important that r_θ be fairly accurately estimated. It may be that some line broadening or other factors increase the uncertainty in the measurement of some or all θ values. When it has been determined that $|d_{\text{calc}} - d_{\text{obs}}| \lesssim R_d$ for all diffraction lines, the powder pattern can be said to be indexed. It sometimes happens that most diffraction lines fit this criterion, but a pair of close-spaced adjacent maxima do not. This occurrence suggests that the indices of the two closed-spaced lines should be interchanged and a new refinement carried out.

8.9. Least Squares Refinement of Lattice Parameters

The least-squares method is straightforward only when there are no cross terms between parameters. This is the case for cubic, tetragonal, hexagonal and orthorhombic lattices. Since rhombohedral can be indexed and refined as hexagonal (and then transformed to rhombohedral if it is of interest to do so), there are left only the monoclinic and triclinic cases that require some additional effort. This effort involves expanding the variable (d^{-2}) in a Taylor's series and retaining only the lowest order terms with no cross products. This approximate expression for d^{-2} is used in the least-squares refinement and the process is repeated until the changes in the parameters are all smaller than the standard deviations.

The hexagonal case can be used to illustrate the least-squares method. A residual is defined as

$$r_j = d_j^{-2} - (4/3)(h_j^2 + h_j k_j + k_j^2)/a^2 - \ell_j^2/c^2 \tag{40}$$

and the derivatives of the sum of the squares of the residuals with respect to a and c are set equal to zero. Letting $\lambda_j = h_j^2 + h_j k_j + k_j^2$, this yields

$$\sum_j \lambda_j d_j^{-2} = \left[4/3 \sum \lambda_j^2\right] a^{-2} + \left[\sum \lambda_j \ell_j^2\right] c^{-2} \tag{41}$$

and

$$\sum_j \ell_j^2 d_j^{-2} = \left[4/3 \sum \lambda_j \ell_j^2\right] a^{-2} + \left[\sum \ell_j^4\right] c^{-2} \tag{42}$$

which can be solved as two linear equations in a^{-2} and c^{-2}. The equations are of the form

$$\alpha_{11} a^{-2} + \alpha_{21} c^{-2} = \beta_1 \tag{43}$$

and

$$\alpha_{12} a^{-2} + \alpha_{22} c^{-2} = \beta_2 \tag{44}$$

or

$$\begin{pmatrix} \alpha_{11} & \alpha_{21} \\ \alpha_{12} & \alpha_{22} \end{pmatrix} \begin{pmatrix} a^{-2} \\ c^{-2} \end{pmatrix} = \begin{pmatrix} \beta_1 \\ \beta_2 \end{pmatrix} . \tag{45}$$

Solution involves finding the inverse matrix, i.e., (letting $\gamma = \alpha_{11}\alpha_{22} - \alpha_{12}\alpha_{21}$),

$$\begin{pmatrix} \alpha_{22}/\gamma & -\alpha_{21}/\gamma \\ -\alpha_{12}/\gamma & \alpha_{11}/\gamma \end{pmatrix} \begin{pmatrix} \beta_1 \\ \beta_2 \end{pmatrix} = \begin{pmatrix} a^{-2} \\ c^{-2} \end{pmatrix} . \tag{46}$$

The standard deviations of a^{-2} and c^{-2} are

$$\sigma_{a^{-2}} = \sqrt{\frac{\alpha_{22}}{\gamma} \frac{\sum r_j^2}{(m-2)}} \tag{47}$$

and

$$\sigma_{c^{-2}} = \sqrt{\frac{\alpha_{11}}{\gamma} \frac{\sum r_j^2}{(m-2)}} \tag{48}$$

where m is the number of independent observations (diffraction lines) and 2 is the number of parameters. The standard deviations in a^{-2} and c^{-2} can be converted to standard deviations in a and c using the law of propagation of errors

$$\sigma_a = \left|\frac{\partial a}{\partial a^{-2}}\right| \sigma_{a^{-2}} = \frac{a^3}{2}\sigma_{a^{-2}} \tag{49}$$

or

$$\sigma_c = \frac{c^3}{2}\sigma_{c^{-2}} . \tag{50}$$

8.10. Indexing of Powder Patterns with No Initial Model

If a powder pattern is not closely approximated by a calculated pattern, the indexing problem is significantly more complicated, and many such problems have resisted solution. The most powerful methods for determining the lattice type are single crystal methods that are discussed in the next chapter. However, it is not always possible to find a suitable single crystal. Thus, a method such as the one described below, or some alternative method involving trial and error, may be the only route to obtaining additional information about lattice symmetry. The problem is complicated by the fact that in many cases only a small subset of all possible reflections have intensities of sufficient magnitude that they are apparent in a powder diffraction pattern, and there is no way short of knowing the structure to determine which diffraction maxima will be observable.

The problem is also complicated by the fact that the observed d^{-2} values are to some extent uncertain, and this results in an uncertainty in the indexing process. This problem is maximally reduced by choosing the experimental method that yields the lowest uncertainty in d^{-2} and for this reason the Guinier method is a good choice.

8.11. A Hexagonal Example

The data used in this example were obtained from $Ni_2Ta_9S_6$ using a Guinier powder diffraction camera and Cu $K\alpha_2$ radiation. The d^{-2} data are given in the left-hand column of Table 8.5, and the remaining columns contain differences in the d^{-2} values. What is sought in a table of this type is a repeating number of integral products of a number, since it is hoped the pairs of diffractions with the same ℓ value (tetragonal or hexagonal) or the

Table 8.5. Difference d^{-2} values for $Ni_2Ta_9S_6$.

$10^5 d^2$	$-d_1^{-2}$	$-d_2^{-2}$	$-d_3^{-2}$	$-d_4^{-2}$	$-d_5^{-2}$	$-d_6^{-2}$	$-d_7^{-2}$	$-d_8^{-2}$	$-d_9^{-2}$	$-d_{10}^{-2}$
1 309										
3 893	2 584									
8 778	7 469	4 886								
9 069	7 759	5 176	290							
11 654	10 344	7 761	2 875	2 585						
12 677	11 367	8 784	3 898	3 608	1 023					
13 988	12 679	10 095	5 209	4 919	2 334	1 311				
15 538	14 229	11 645	6 760	6 470	3 885	2 862	1 550			
16 853	15 544	12 960	8 074	7 784	5 199	4 176	2 865	1 315		
17 873	16 563	13 980	9 094	8 804	6 219	5 196	3 885	2 334	1 020	
20 744	19 434	16 851	11 965	11 676	9 091	8 068	6 756	5 206	3 891	2 872

same h and ℓ value (orthorhombic or monoclinic) will occur and subtraction will leave an integral multiple of a single inverse square parameter.

For example, columns 1, 7 and 8 Table 8.5 are headed by 0.01309, 0.01311 and 0.01315, suggesting that 0.0131 is an integer times the inverse square of a lattice parameter. The simplest initial assumption would be that the integer is 1, and this yields a 10.08 Å axis. This is not an unreasonable value (1.5 Å would certainly be too small to be possible, and 20 Å would be too large to offer much hope).

Looking for multiples of 0.0131 provides the values of Table 8.6. The multiple 2 can arise from the difference between $1,1,\ell$ and $1,0,\ell$ reflection in the hexagonal case. Thus, a plausible working assumption at this stage is to index the first line as 1,0,0 and the second as 1,1,0. Dividing all d^{-2} values by 0.0130 yields the values of column 2 of Table 8.7. Possible h, k, ℓ values are given in column 3. Taking the average value (0.01298) gives

$$a = (3/4 \cdot 0.01298)^{1/2} = 10.136 \text{ Å}, \tag{51}$$

a value that satisfactorily indexes seven of the eleven lines. If the interpretation up to this point is correct the remaining four lines have $\ell \neq 0$. To continue, possible integral values of $h^2 + hk + k^2(0, 1, 3, 4, 7, \ldots)$ times 0.01298 are subtracted from the unindexed d^{-2} values to yield the quantities in Table 8.8. Since the number 8786 ± 4 appears once in each row a possible solution is $c = (0.08786)^{-1/2} = 3.37$ Å and the four lines are indexed 0,0,1; 1,1,1; 2,0,1; and 2,1,1, respectively. The least squares values, using the results of Section 8.1, are $a = 10.14 \pm 0.03$ Å and $c = 3.372 \pm 0.002$ Å. The corresponding observed and calculated d^{-2} values are given in Table 8.9.

Table 8.6. Multiples of 0.0130 from Table 8.5.

0.025 84/2	0.012 92
0.025 85/2	0.012 93
0.051 76/4	0.012 94
0.051 99/4	0.012 99
0.051 96/4	0.012 99

Table 8.7. d^{-2} values of $Ni_2Ta_9S_6$ divided by 0.0130.

1 309/130	1.007	100
3 893/130	2.995	110
8 778/130	6.75	—
9 069/130	6.976	210
11 654/130	8.965	300
12 677/130	9.75	—
13 988/130	10.76	—
15 538/130	11.95	220
16 853/130	12.96	310
17 873/130	13.74	—
20 744/130	15.69	400

Table 8.8. d^{-2} values reduced by multiples of 0.01298 for $Ni_2Ta_9S_6$.

$10^5 d^{-2}$	−1 298	−3 × 1 298	−4 × 1 298	−7 × 1 298	−9 × 1 298
8 778	7 480	4 884	3 580	—	—
12 677	11 379	8 783	7 485	3 591	995
13 988	12 690	10 094	8 796	4 902	2 306
17 873	16 575	13 979	12 681	8 787	6 191

Table 8.9. Observed and calculated d^{-2} values for hexagonal $Ni_2Ta_9S_6$.

d^{-2}(obs.)	d^{-2}(calc.)	$hk\ell$
0.013 09	0.012 96	100
0.038 93	0.038 88	110
0.087 78	0.087 94	001
0.090 69	0.090 72	210
0.116 54	0.116 64	300
0.126 77	0.126 83	111
0.139 88	0.139 79	201
0.155 38	0.155 52	220
0.168 53	20.168 48	310
0.178 73	0.178 67	211
0.207 44	0.207 36	400

Bibliography

1. H. P. Klug and L. E. Alexander, *X-Ray Diffraction Procedures* (Wiley, New York, 1974).
2. A. Guiner, *X-Ray Diffraction* (W. H. Freeman, San Francisco, 1963).
3. B. Harbrecht and H. F. Franzen, $M_2Ta_9S_6$ (M ≡ Fe, Co, Ni): A Metal-Rich Channel Structure with Condensed Tetrakaidecahedral Tantalum Cluster, *J. Less-Common Met.* **113**, 349 (1985).
4. B. D. Cullity, *Elements of X-Ray Diffraction* (Addition-Wesley Publishing, Menlo Park, California, 1956).

Problems

1. Ignoring physical factors such as thermal motion, absorption, and Lorentz and polarization factors, and taking the atomic scattering factors to be just the total number of electrons in an atom, calculate the diffraction peaks (Bragg angle and intensity) for $\theta \leq 40°$ and using Cu Kα radiation ($\lambda = 1.54$ Å) for:
   (a) $Fm3m$ with Zr in 0,0,0 and S in 0,0,1/2 ($a = 5.163$ Å).
   (b) same as (a) but with 0.75Zr in 0,0,0.
   (c) same as (b) but ordered as in problem 3.9 ($\alpha = 33.377°, a = 6.3194$ Å).
   (d) $Pm3m$ with Rh in 0,0,0, and Ti in 1/2, 1/2, 1/2 ($a = 3.126$ Å).
   (e) same as (d) but distorted to tetragonal ($a = 4.226$ Å, $c = 3.350$ Å),
   (f) same as (e) but distorted such that $\gamma = 90.89°$ with a, b, c unchanged.
   (g) $P6_3/mmc$ with V in 0,0,0 and S in 1/3, 2/3,1/4, $a = 3.340$ Å, $c = 5.840$ Å.
   (h) same as (g) but distorted as in problem 6.1, $a = 5.825$ Å, $b = 3.300$ Å, $c = 5.868$ Å(ignore the shifts of V, S within the unit cell).
2. Estimate the width (FWHM) of the strongest line in 1(a) if the width is determined only by domain size and there are cubic domains 511 Å on an edge.
3. Given the following 2θ values for a tetragonal substance index the powder pattern: 21.04, 26.54, 29.93, 34.13, 40.42, 42.83, 48.15, 51.10, 54.76, 55.80, 59.30. $\lambda = 1.540$ Å.
4. Refine the lattice parameters of problem 3 by least squares.
5. Find hexagonal indexing and lattice parameters for 1(c).
6. If in problem 2 the 2θ angle is uncertain by $\pm 1/2$ the line width, by how much is $\sin\theta$ uncertain?

CHAPTER 9

SINGLE CRYSTAL DIFFRACTION

9.1. Introduction

When a suitable single crystal can be found, which is very often the case, information about the lattice type and space-group symmetry can be inferred directly from a single-crystal diffraction pattern. The Ewald construction is a powerful tool of use in the indexing of single-crystal patterns and in the consideration of diffraction geometry.

9.2. The Ewald Sphere

Place a crystal at the center of a sphere with a radius $2\pi/\lambda$ (an Ewald sphere) and consider an X-ray beam along a diameter of the sphere (Fig. 9.1). At the point where the beam exists the sphere place the origin of a reciprocal lattice. When the crystal rotates the reciprocal lattice rotates along with it, thus the crystal can be rotated until a reciprocal lattice vector, $\mathbf{K}_{hk\ell}$, intersects the sphere. Figure 9.1 shows the plane containing $\mathbf{K}_{hk\ell}$ and the X-ray beam. The line from the crystal to the middle of $\mathbf{K}_{khl}$ is parallel to the h, k, ℓ planes (since $\mathbf{K}_{hk\ell}$ is perpendicular to those planes) and bisects the apical angle of the isosceles triangle formed by the origin of the reciprocal lattice, the crystal and the end point of $\mathbf{K}_{hk\ell}$. The sine of the half apical angle is thus

$$\frac{\lambda|\mathbf{K}_{hk\ell}|}{2\pi \cdot 2} = \frac{\lambda}{2d} \tag{1}$$

and this angle, which by Bragg's law is θ, is the angle between both the incoming rays and the C–T vector and the h, k, ℓ planes. Thus, diffraction occurs along C to T, where C is the center of an Ewald sphere and T is

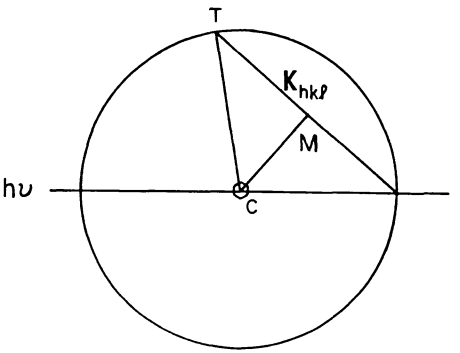

Fig. 9.1. The Ewald sphere.

the intersection between a reciprocal lattice vector with origin defined as above and the Ewald sphere.

9.3. Rotation with a Cylindrical Film

For example, consider a rotating single crystal with the rotation axis along the center line of a film cylinder. When the crystal is "aligned", a real axis of the crystal lies along the rotation axis, and thus a set of reciprocal lattice planes are perpendicular to the axis of the cylinder. Whether or not this axis is the conventional c-axis for the crystal system is a matter that remains to be determined (e.g., by cell reduction, see Section 2.12) at a later stage. Nonetheless, it is possible at this point to designate this as the c-axis and thus label the reciprocal lattice planes perpendicular to the axis as $h, k, 0; h, k, \pm\ell$, etc. As the crystal is rotated about the c-axis, these reciprocal lattice planes will rotate and the intersections of the lattice points with the Ewald sphere will define cones along which diffractions occur (Fig. 9.2). These cones in turn define circles on the film cylinder which, when a developed film is laid out flat, appear as *layers lines* on the film. The spacing between these layer lines can be related to the length of the c-axis in question by means of the Ewald construction (Fig. 9.3).

The reciprocal layer line spacing, ℓ_R, is the length of the projection of $\mathbf{c}^*$ onto $\mathbf{c}$, i.e.,

$$\ell_R = \left| \frac{\mathbf{c}^* \cdot \mathbf{c}}{c} \right| = \frac{2\pi \mathbf{c} \cdot \mathbf{a} \times \mathbf{b}}{c \cdot V_{\text{cell}}} = \frac{2\pi}{c} . \tag{2}$$

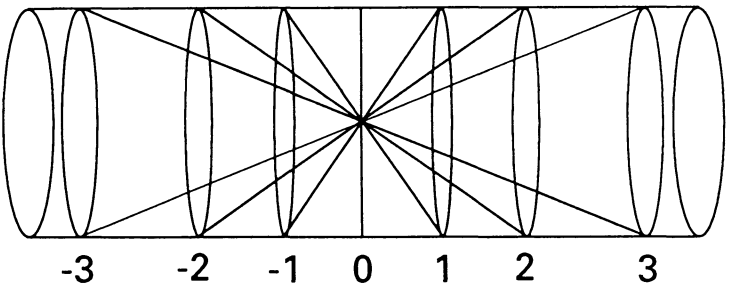

Fig. 9.2. Layer lines in the rotation experiment.

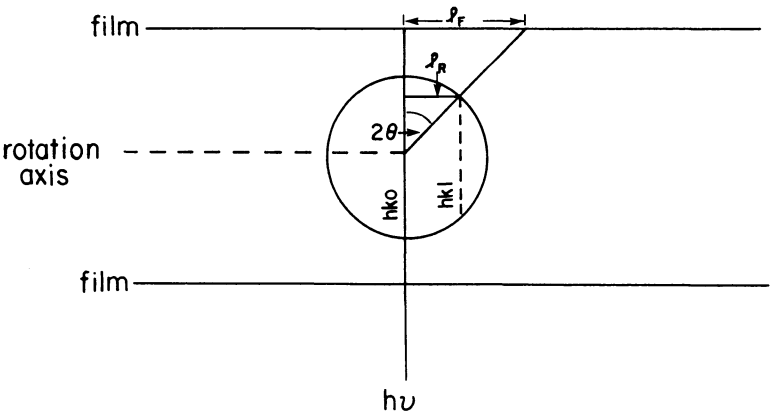

Fig. 9.3. Single crystal diffraction with a cylindrical film.

Since $\sin 2\theta$ is ℓ_R divided by the radius of the Ewald sphere (Fig. 9.3),

$$\sin 2\theta = \frac{\lambda}{2\pi} \cdot \frac{2\pi}{c} = \frac{\lambda}{c} \tag{3}$$

and as can be seen from the figure

$$\tan 2\theta = \ell_F / R, \tag{4}$$

where R is the cylinder radius, thus

$$\frac{\ell_F}{\sqrt{R^2 + \ell_F^2}} = \frac{\lambda}{c}. \tag{5}$$

9.4. Weissenberg Patterns

Once a crystal has been aligned for a rotation experiment (Fig. 9.2), it is also aligned for a Weissenberg experiment. This experiment is accomplished by placing a cylindrical screen (a layer-line screen) with a slit such that it allows diffracted radiation from only one layer (taken here to be the zero layer) to reach the film. The film is then moved laterally (parallel to the axis) at a speed and in a direction that are coupled to the rotation speed and direction. In order to discover the appearance of the resultant pattern on a film, consider the Ewald construction (Fig. 9.4). In the figure attention is fixed on a particular row of lattice points in the zero layer ($n(h\mathbf{a}^* + k\mathbf{b}^*)$ with $n = 0, 1, 2, \ldots$) with the crystal initially with the particular $h, k, 0$ planes horizontal and the $n(h\mathbf{a}^* + k\mathbf{b}^*)$ reciprocal vectors vertical. As the crystal and the reciprocal lattice rotate, the reciprocal lattice points intersect the Ewald sphere and diffraction occurs. The vertical distance (ℓ_F) between the film base line, established, by the undiffracted beam, and the diffraction spot on the film is proportional to $\theta_{hk\ell}$. The amount the crystal has rotated in order to bring the crystal into the diffraction orientation is also proportional to $\theta_{hk\ell}$ (is equal to $2\theta_{hk\ell}$ given the specified initial orientation). The distance the film moves laterally, since it is coupled to the rotation, is also proportional to $\theta_{hk\ell}$, and thus vertical and lateral distance are proportional to each other when the diffractions correspond to a given lattice row, and thus the diffractions fall on a straight line on the film. The slope of this line is determined by the radius of the film cylinder and the coupling of the lateral motion of the film to the rotation of the crystal. These experimental parameters are chosen so that the height-to-lateral distance ratio is 2:1, and $1{:}2{:}\sqrt{5}$ triangular measuring device can be used to simultaneously measure the polar coordinates of the reciprocal lattice points from the diffraction peaks on a Weissenberg film (Fig. 9.5).

At each setting of the measuring triangle all points falling on the $\sqrt{5}$ edge have the same angular polar coordinate (i.e., fall on a lattice row) in reciprocal space, and when the triangle is moved laterally the polar angle is changed by an amount proportional to the distance moved. The length of the reciprocal vector is a function of the distance along the $\sqrt{5}$ edge. From Fig. 9.4 it is apparent that

$$360\ell_F/2\pi R = 2\theta_{hk\ell} \tag{6}$$

or

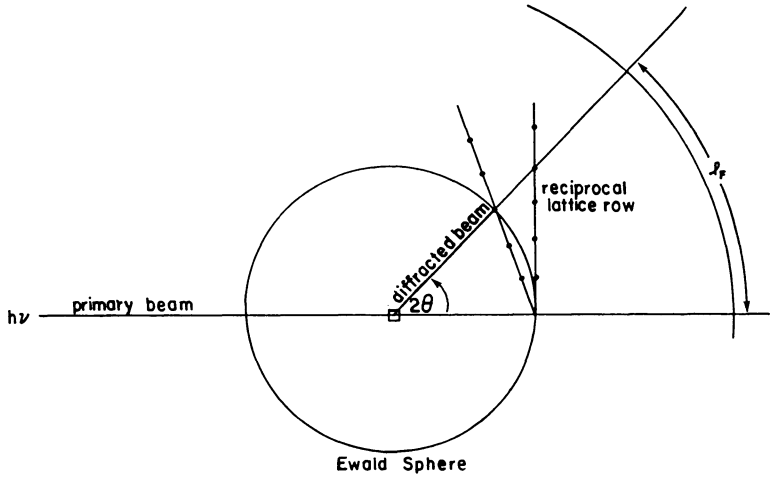

Fig. 9.4. The zero-level Weissenberg experiment.

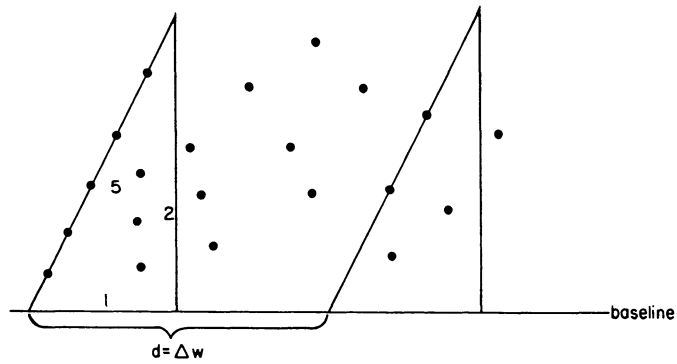

Fig. 9.5. Interpretation of the zero-layer Weissenberg.

$$|\mathbf{K}_{hk\ell}| = \frac{2\pi}{d} = \frac{4\pi}{\lambda} \sin\left[\frac{90\ell_F}{\pi R}\right] \tag{7}$$

and thus a nonlinear scale that will yield $|\mathbf{K}_{hk\ell}|$ directly from the distance along the $\sqrt{5}$ edge can be devised.

The zero-level reciprocal lattice can be plotted using the polar coordinates measured as described above, and the reflections can be indexed. A similar procedure can be used for higher levels, but some modifications are usually required by the equi-inclination technique used to avoid missing some low angle data (Fig. 9.6). These modifications are considered in detail in texts on crystallography (see the bibliography to this chapter).

One result of a complete Weissenberg investigation is the determination of a reciprocal, and thus also a real, lattice type. This lattice might be the conventional lattice, but is not necessarily so. The possibility of an alternative, conventional lattice can be considered in two ways. One is to check the symmetry of the pattern, as discussed in the next section, and to determine whether the pattern symmetry and lattice symmetry are consistent. A second method is to reduce the cell, if possible, and to determine the conventional cell from the conventional reduced cell.

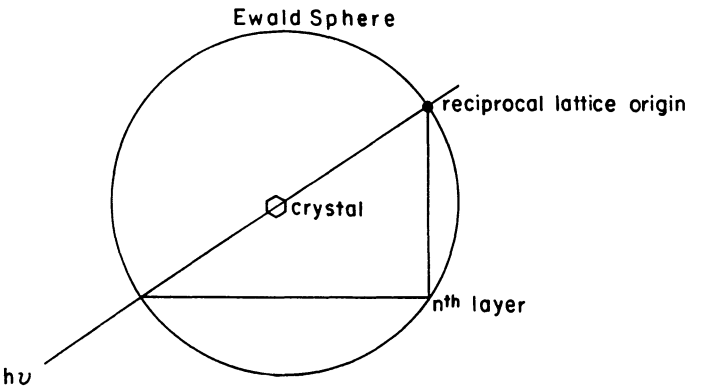

Fig. 9.6. Equi-inclination diffraction.

9.5. Symmetry of Single-Crystal Diffraction Patterns

Some of the symmetry elements of diffraction will be apparent if the axis of rotation is a symmetry axis of the crystal. For example, if the Weissenberg patterns repeat every $2\pi/n$, then an n-fold rotational symmetry is demonstrated. On the other hand, since inversion carries F into its complex conjugate, and since the diffraction intensity is proportional to FF^*, all

diffraction patterns are centrosymmetric (provided there is no anomalous scattering, to be discussed later). The centrosymmetricity of X-ray diffraction is called Friedel's law, and it means that the diffraction symmetry is the symmetry of the crystal class plus the addition of inversion symmetry. The crystal classes that cannot be distinguished from diffraction symmetry alone are called the Laue classes, and these are listed in Table 9.1.

Table 9.1. The Laue classes.

Laue class	Crystal class
$\bar{1}$	$1, \bar{1}$
$2/m$	$2, m, 2/m$
mmm	$mm2, 222, mmm$
$4/m$	$4, \bar{4}, 4/m$
$4/mmm$	$422, 4mm, (\bar{4}2m, \bar{4}m2), 4/mmm$
$\bar{3}$	$3, \bar{3}$
$\bar{3}m1$ *or* $\bar{3}1m$	$(321, 312), (3m1, 31m), (\bar{3}m1, \bar{3}1m)$
$6/m$	$6, \bar{6}, 6/m$
$6/mmm$	$622, 6mm, (\bar{6}m2, \bar{6}2m)6/mmm$
$m3$	$23, m3$
$m3m$	$432, \bar{4}3m, m3m$

The structure factor is a sum over the unit cell, thus it includes terms from atoms that are related by symmetry. For example, C_{2z} takes x, y, z into $\bar{x}, \bar{y}, z$. Thus, $|F|^2$ for h, k, ℓ and $\bar{h}, \bar{k}, \ell$ are equal and the diffraction pattern has two-fold symmetry in the sense that $|F_{hk\ell}|^2 = |F_{\bar{h}\bar{k}\ell}|^2$, and by Friedel's law the pattern has $2/m$ symmetry.

Furthermore, a 2_1 axis along **c** takes x, y, z into $\bar{x}, \bar{y}, z + 1/2$ and thus each term $\exp 2\pi i(hx + ky + \ell z)$ into $(\exp i\pi\ell) \exp 2\pi i(-hx - ky + \ell z)$ and again $|F_{hk\ell}|^2 = |F_{\bar{h}\bar{k}\ell}|^2$. In this case $0,0,\ell$ reflections are absent when ℓ is odd because for each term in the sum for F, $f_j \exp 2\pi i\ell z_j$, there is another $-f_j \exp 2\pi i\ell z_j$, and $F \equiv 0$. Thus, a 2_1 axis makes it presence known by $2/m$ diffraction symmetry coupled with extinction of the $0,0,\ell$ reflections with odd ℓ.

Glide planes also give rise to systematic absences. For example, an a glide perpendicular to **c** takes x, y, z into $x + 1/2, y, \bar{z}$ and thus $|F|^2$ is zero

for $h\,k\,0$ reflections when h is odd, as can be seen from

$$F_{hk0} = \ldots f_j \exp 2\pi i(hx_j + ky_j) + \cdots + f_j \exp 2\pi i(h(x_j + 1/2) + ky_i) + \ldots \quad (8)$$

This effect can also be analyzed as follows: the $h, k, 0$ reflections are determined by the projection of the structure onto the $h, k, 0$ plane, and this projection, by virtue of the a glide, has half the translation period of the lattice along the a direction. In general, a glide plane creates a submultiple of a translation period in the glide direction for the projection of the structure onto the glide plane, and thus the diffraction data exhibit systematic absences in the data corresponding to that projection. This is also true for screw axes, i.e., $0, 0, \ell$ data correspond to a projection of the structure onto the c-axis and a screw axis creates a submultiple period in the projection onto the axis.

In general, when systematic absences demonstrate that an even-fold screw axis is perpendicular to a glide plane, a centrosymmetric crystal symmetry can be inferred from diffraction data in spite of Friedel's law. For example, the following conditions for observation of diffractions: $0, k, \ell, k = 2n$; $h, 0, \ell, \ell = 2n$; $h, k, 0, h + k = 2n$ yield *Pbcn* as the only orthorhombic space group consistent with the data. Each pair of glide operations, implied by the systematic absences, implies a two-fold operation perpendicular to the third glide, which in turn assures us that the space-group is centrosymmetric.

On the other hand, with the conditions for observation: $h, k, 0, h = 2n$ and $0, k, \ell, k + \ell = 2n$ an a glide perpendicular to **c** and a n glide perpendicular to **a** are demonstrated and, by Friedel's law, either *Pnma* or $Pn2_1a$ is a possible space-group symmetry.

9.6. Anomalous Scattering

The scattering of X-rays by atoms results in no phase difference from atom to atom unless the energy of the scattered radiation is close to the energy of an atomic transition. On the other hand, if the atom is excited into a virtual state during the scattering there is some phase shift and the scattering can be resolved into a real and an imaginary part. The scattering factor is then of the form $f + \Delta f' + i\Delta f''$ ($\Delta f'$ and $\Delta f''$ are the real and imaginary contributions to the scattering that result from the interaction between the atom (as opposed to just the electrons in the atom) and the radiation). The

small imaginary contribution to the scattering factor introduces a small, but sometimes measurable, noncentrosymmetricity into the diffraction by noncentrosymmetric structures.

9.7. Fourier Series

Consider the integral (n_1 and n_2 different integers):

$$\int_0^1 (\exp 2\pi i n_1 x)(\exp -2\pi i n_2 x)dx = \frac{[\exp 2\pi i(n_1 - n_2)x]_0^1}{2\pi i(n_1 - n_2)} = 0 . \quad (9)$$

On the other hand, if $n_1 = n_2$, then the integral has a value 1. On this basis the set of functions $\exp 2\pi i n x$ for $n = 1, 2, 3 \ldots$ are said to form an orthonormal set. They are orthogonal in the sense that

$$\int_0^1 f(n_1) f^*(n_2) dx = 0 \quad (10)$$

when $n_1 \neq n_2$ and normalized in the sense that the integral is unity when $n_1 = n_2$.

Suppose a one-dimensional electron density, $\rho(x)$, is expanded in a Fourier series:

$$\rho(x) = \sum_n C_n \exp -2\pi i n x . \quad (11)$$

Multiplying on both sides by $\exp 2\pi i h x$, where h is an integer, and integrating yields, by the orthonormality of $\{\exp -2\pi i n x\}$,

$$\int_0^1 (\exp 2\pi i h x)\rho(x) dx = C_n , \quad (12)$$

and thus, given $\rho(x)$, the Fourier coefficients C_n be evaluated.

9.8. The Phase Problem

In three dimensions

$$\rho(x, y, z) = \sum_n \sum_m \sum_p C_{nmp} \exp -2\pi i[nx + my + pz] \quad (13)$$

and multiplying by $\exp 2\pi i(hx + ky + \ell z)$ and integrating,

$$C_{hk\ell} = \int_0^1 \int_0^1 \int_0^1 \rho(x, y, z) \exp 2\pi i(hx + ky + \ell z) dx dy dz . \quad (14)$$

If the units of measure in the three directions are a, b, c (i.e., $x = x/a$, etc.), then $C_{hk\ell} = F_{hk\ell}$, i.e., the Fourier coefficients of the electron density expansion are the structure factors. It is possible to determine $|F_{hk\ell}|$ from measured intensities, however the electron densities cannot be calculated without the phases associated with the $F_{hk\ell}$ values. Thus, the problem of structure solution, which is the problem of determining $\rho(x, y, z)$, is solved when $|F_{hk\ell}|$ values have been determined experimentally and the phases to be assigned to the $F_{hk\ell}$'s have been determined. For this reason, structure solution given diffraction data has been called the phase problem. When a structure is centrosymmetric and f_j is real, for each term in $F_{hk\ell}$ of the type $f_j \exp 2\pi i(hx+ky+\ell z)$ there occurs its complex conjugate, $f_j \exp -2\pi i(hx+hy+\ell z)$, and thus, $F_{hk\ell}$ is real and its phase is either 0 or π, i.e, $F_{hk\ell} = |F_{hk\ell}|$ or $F_{hk\ell} = -|F_{hk\ell}|$. Hence, for centrosymmetric structure solution the phase problem is one of assigning signs to observed $|F_{hk\ell}|$ values.

9.9. The Direct Method

Direct methods are based upon the assumption that the electron density of the structure to be solved is so distributed that the structure factors approximate an assumed distribution. Here the assumption is of a normal distribution.[3] The validity of a structure solution is determined by the fit between calculated F's obtained from the refined solution and the observed F's, a determination that is divorced from the method of structure solution. Thus, the validity of the assumed distribution is not a matter of concern. If the assumption is more-or-less valid and the method works a structure is found, if not then other methods must be attempted.

It is helpful to remove, insofar as it is possible to do so, the Bragg angle dependence of the atomic scattering factors. This is done by defining

$$n_j = f_j / \sum f_j \tag{15}$$

and n_j is principally angle independent since the angular dependencies of the f_j's are quite similar. The *unitary structure factors* are defined as

$$U_k = \sum_j n_j \exp 2\pi i(hx_j + ky_j + \ell z_j)\,, \tag{16}$$

and these are essentially structure factors with the angular decay due to intra-atomic interference removed, i.e., they are structure factors appropriate to point atoms that scatter with the number of electrons appropriate

to the actual atom. First it is useful to find the average value of the magnitudes of U_h squared, i.e., $\langle |U_h|^2 \rangle$.

$$U_h U_h^* = \sum n_j \exp i\mathbf{K}_h \cdot \mathbf{r}_j \sum n_k \exp -i\mathbf{K}_h \cdot \mathbf{r}_k \tag{17}$$

$$|U_h|^2 = \sum n_j^2 + \sum_{n_j} \sum_{n_k \neq n_j} n_j n_k \exp i\mathbf{K}_h(\mathbf{r}_j - \mathbf{r}_k) \tag{18}$$

To find $\langle |U_h|^2 \rangle$ Eq. 18 is summed over h (all $\mathbf{K} \in \{\mathbf{K}\}$) and divided by N. For each $\mathbf{K}_h$ in the sum there is a $-\mathbf{K}_h$, thus

$$\sum_h |U_h|^2 = \sum_h \sum_j n_h^2 + 2 \sum_h^{N/2} \sum_j \sum_{k \neq j} n_j n_k \cos \mathbf{K}_h(\mathbf{r}_j - \mathbf{r}_k) . \tag{19}$$

The second term on the right, given an appropriate distribution of scatterers, will contain terms that are positive and negative in approximately equal numbers and will not accumulate, whereas the first term on the right, when summed over h, has only positive contributions. Thus,

$$\langle |U_h|^2 \rangle \cong \sum_h n_j^2 , \tag{20}$$

and Σn_j^2 is given the symbol ε.

To proceed with a direct method solution, it is necessary to estimate, at least approximately, $|U_h|$ values using the observed $|F_h|$ data. This is accomplished as follows: the $|F_h|$ data are grouped into annular intervals in reciprocal space (Δd^{-1} intervals). These intervals (e.g., $0.1 < \sin\theta < 0.3$, $0.2 < \sin\theta < 0.4$, etc.) are approximately associated with their mean $\sin\theta$ values (e.g., $\sin\theta = 0.2$, $\sin\theta = 0.3$, etc.) and the values of Σn_j^2 appropriate to the interval are calculated from tabulated f_j values and the known or assumed unit cell contents. For each interval the average magnitude of F squared, $\langle |F_h|^2 \rangle$, is calculated from the observed data. Then $\varepsilon = \Sigma n_j^2$ and $\langle |F_h|^2 \rangle$ at each median $\sin\theta$ are used to calculate ϕ^2:

$$\phi^2 = \varepsilon / \langle |F_h|^2 \rangle \tag{21}$$

and ϕ is plotted versus $\sin\theta$. From this plot ϕ is interpolated for the $\sin\theta$ value corresponding to a particular $|F_h|$ and

$$|U_h| = \phi |F_h| , \tag{22}$$

and thus a list of $|F_h|$'s is converted into a list of $|U_h|$'s.

The direct method deals extensively with correlated triples (ct) of U_h's, i.e.,

$$U_{ct} = U_{-h} U_{h'} U_{h-h'} \,. \tag{23}$$

Again, the average value can be estimated

$$U_{ct} = \sum_j n_j \exp -i\mathbf{K}_h \cdot \mathbf{r}_j \sum_k n_k \exp i\mathbf{K}_{h'} \mathbf{r}_k \sum_\ell n_\ell \exp i(\mathbf{K}_h - \mathbf{K}_{h'})\mathbf{r}_\ell \tag{24}$$

$$= \sum_j \sum_k \sum_\ell n_j n_k n_\ell \exp i[\mathbf{K}_h(\mathbf{r}_\ell - \mathbf{r}_j) + \mathbf{K}_{h'}(\mathbf{r}_k - \mathbf{r}_\ell)] \,, \tag{25}$$

and summing over all values of h and $h' \neq h$

$$\sum_h^N \sum_{h' \neq h}^N U_{ct} = \sum_h \sum_{h' \neq h} \sum_j \sum_k \sum_\ell n_j n_k n_\ell \exp i[\mathbf{K}_h(\mathbf{r}_\ell - \mathbf{r}_j) + \mathbf{K}_{h'}(\mathbf{r}_k - \mathbf{r}_\ell)] \,. \tag{26}$$

In this sum when $j = k = \ell$ the quantity n_j^3 is contributed and the remainder, since $-\mathbf{K}_h$ and $-\mathbf{K}h'$ are included in the sum, will be (sum over half the $\mathbf{K}$'s)

$$2 \sum_h \sum_{h'} n_j n_k n_\ell \cos(\mathbf{K}_n \cdot (\mathbf{r}_\ell - \mathbf{r}_j) + (\mathbf{K}_{h'}(\mathbf{r}_k - \mathbf{r}_\ell)] \,, \tag{27}$$

which will have approximately equal numbers of positive and negative terms and will not accumulate. Thus,

$$\langle U_{ct} \rangle = \sum_j n_j^3 = \varepsilon_3 \,. \tag{28}$$

Thus, it follows that the phases of the U_{ct} values have a proportionately larger number of positive real components than negative real components and the imaginary components sum to zero.

The second moment[3] of U_{ct} about the origin is given by

$$\mu_2' = \langle U_{ct} U_{ct}^* \rangle = \langle |U_{-h}|^2 |U_{h'}|^2 |U_{h-h'}|^2 \rangle = \varepsilon^3 \tag{29}$$

and the variance is the second moment about the origin minus the square of the average value[3]

$$\sigma^2 = \varepsilon^2 - \varepsilon_3^2 \,. \tag{30}$$

If the U_{ct}'s are distributed normally about their mean value, then

$$P(z) = (1/2\pi)^{1/2} \exp -(z^2/2) \tag{31}$$

where

$$z = (U_{ct} - \varepsilon_3)/(\varepsilon^3 - \varepsilon_3^2)^{1/2} . \tag{32}$$

From the diffraction data $|U_{ct}| = |U_{-h}||U_{h'}||U_{h-h'}|$ can be readily found. If the structure is centrosymmetric, the problem is to assign signs to the $|U_h|$ values. In the case of a centrosymmetric structure, $U_h = U_{-h}$, and thus U_{ct} can be taken to be $U_h U_{h'} U_{h-h'}$. As will be shown in the next section it is possible to assign some signs arbitrarily in order to position the origin, and the signs of the U_{ct}'s can then be used to find additional signs. The probabilities that a U_{ct} is positive ($U_{ct} = |U_{ct}|$) or negative ($U_{ct} = -|U_{ct}|$) can be obtained from the Eqs. 31 and 32

$$P(U_{ct} = |U_{ct}|) = (1/2\pi)^{1/2} \exp -(|U_{ct}| - \varepsilon_3)^2/(2(\varepsilon^2 - \varepsilon_3^2)) \tag{33}$$

and

$$P(U_{ct} = -|U_{ct}|) = (1/2\pi)^{1/2} \exp -(|U_{ct}| + \varepsilon_3)^2/(2(\varepsilon^2 - \varepsilon_3^2)) . \tag{34}$$

Thus

$$\frac{P(U_{ct} = |U_{ct}|)}{P(U_{ct} = -|U_{ct}|)} = \exp \left[\frac{2\varepsilon_3 |U_{ct}|}{(\varepsilon^3 - \varepsilon_3^2)} \right] \tag{35}$$

and

$$\ell n \left[\frac{P(U_{ct} = |U_{ct}|)}{P(U_{ct} = -|U_{ct}|)} \right] = \left[\frac{2\varepsilon_3 |U_{ct}|}{\varepsilon^3 - \varepsilon_3^2} \right] . \tag{36}$$

For example, suppose a structure has m equal atomic number atoms,

$$\varepsilon = \sum m^{-2} = m^{-1} , \tag{37}$$

$$\varepsilon_3 = \sum m^{-3} = m^{-2} \tag{38}$$

and

$$\ell n \left[\frac{P(U_{ct} = |U_{ct}|)}{P(U_{ct} = -|U_{ct}|)} \right] = \frac{2m^2}{(m-1)} |U_{ct}| , \tag{39}$$

and taking $P(U_{ct} = |U_{ct}|) = 0.999$. Thus $P(U_{ct} = -|U_{ct}|) = 0.001$ yields the values of Table 9.2.

Assuming that the U_h values are distributed normally about a mean value of zero, Eq. 31 yields $P(U_h)$ with $Z = U_h/(2\varepsilon^{1/2})$, i.e., $Z = m^{1/2}U_h/2$ for the m equal atom structure. Using these values and the values of the cube roots of $|U_{ct}|$ from Table 9.2, the probability that $|U_h|$ is large enough to contribute equally to $|U_{ct}|$ such that $U_{ct} = |U_{ct}|$ with a probability of 0.999 can be calculated using Eq. 31 and is given in column 3 of Table 9.2. What is apparent from this table is that a declining fraction of $|U_{ct}|$'s can be assigned a positive sign at a given confidence level as the size of the structure increases. Therefore, there is a limit on the size of a structure that can be solved using the U_{ct}'s to assign signs.

Table 9.2. Values of $\sqrt[3]{U_{ct}}$ for 99.9% probability that $U_{ct} = |U_{ct}|$ vs. m, the number of equivalent atoms in an equal atom structure.

m	$\sqrt[3]{U_{ct}}$	$P(\|U\| > \sqrt[3]{U_{ct}})$
5	0.82	0.36
10	0.68	0.28
20	0.55	0.22
40	0.44	0.165
80	0.35	0.12

In some cases there is more than one relationship involving the same h, i.e., $|U_hU_{h'}U_{h-h'}|$ and $|U_hU_{h''}U_{h-h''}|$ and the number of such relationships might be sufficiently large that they give a probability for $U_{ct} = |U_{ct}|$ that is greater than 1/2. These probabilities are independent and thus (π denotes product)

$$\frac{P(U_h = |U_h|)}{P(U_h = -|U_h|)} = \frac{\pi P_{h'}(U_h = |U_h|)}{\pi P_{h'}(U_h = -|U_h|)} \tag{40}$$

or

$$\frac{P(U_h = |U_h|)}{P(U_h = -|U_h|)} = \exp\left(\frac{2\varepsilon_3}{\varepsilon^2 - \varepsilon_3^2}\right)|U_h| \sum_{h'} U'_h U_{h-h'} \,. \tag{41}$$

Thus, although $|U_h|$ may not be sufficiently large that any single U_{ct} can be shown to be positive with sufficient confidence, nonetheless the sign of U_h can be reliably related to the signs of a number of correlated pairs.

For example, suppose that some $|U_h|$'s and some signs are known as given in Table 9.3. Since if $h - h' = \bar{3}, \bar{1}, 2$ and $h' = 1, 1, \bar{1}$, then $h = \bar{2}, 0, 1,$

and if $h - h' = \bar{3}, \bar{1}, 2$ and $h' = 4, 2, \bar{2}$, then $h = 1, 1, 0$, these data yield two separate probabilities for $U_{\bar{3},\bar{1},2} = |U_{\bar{3},\bar{1},2}|$, 0.93 and 0.98 (Eq. 35). These probabilities are not sufficient to accept the sign of $U_{\bar{3},\bar{1},2}$ at the 99.9% confidence level on the basis of either alone, however

$$\frac{P(U_h = |U_h|)}{P(U_h = -|U_h|)} = \exp(82(-0.049 - 0.032))$$

$$= 0.001 \tag{42}$$

and $P(U_h = -|U_h|) = 0.999$ based upon the two independent probabilities.

Table 9.3. Some U_h and $|U_h|$ values for a structure with $2\varepsilon_3/(\varepsilon^3 - \varepsilon_3^2) = 82(m = 40$ in Eqs. 37 and 38).

h	$\|U_h\|$	sign
$1, 1, \bar{1}$	0.63	+
$\bar{2}, 0, 1$	0.52	−
$4, 2, \bar{2}$	0.48	+
$1, 1, 0$	0.44	−
$\bar{3}, \bar{1}, 2$	0.15	?

9.10. Sign Assignment and Origin Location

In the case of a centrosymmetric structure the origin can always be arbitrarily shifted by a vector between centers of inversion. Without loss of generality, suppose the origin to be located on a center of inversion. In the general case the origin could be shifted by 1/2, 1/2, 0; 1/2, 0, 1/2; 0, 1/2, 1/2; 1/2, 0, 0; 0, 1/2, 0; 0, 0, 1/2; and 1/2, 1/2, 1/2, i.e., there are eight alternative sites at which the origin could be located. If $\mathbf{r}_s$ is the vector by which the origin is shifted, then a new F, F_N, is related to an old, F_0, by

$$F_N = F_0 \exp i\mathbf{r}_s \cdot (h\mathbf{a}^* + k\mathbf{b}^* + \ell\mathbf{c}^*) \tag{43}$$

and the effects of the various origin shifts are shown in Table 9.4.

It follows that some phases (signs) can be assigned to U's in order to fix the origin. In the case of eight different locations, three ($2^3 = 8$) signs can be arbitrarily assigned, but the three must be chosen in accordance with the following: (1) the signs of even h, even k, even ℓ (eee) reflections do

Table 9.4. Sign changes in F as the result of origin shifts.

$\mathbf{r}_s$	eee	oee	eoe	eeo	eoo	oeo	ooe	ooo
1/2,0,0	+	−	+	+	+	−	−	−
0,1/2,0	+	+	−	+	−	+	−	−
0,0,1/2	+	+	+	−	−	−	+	−
1/2,0,1/2	+	−	+	−	−	+	−	+
1/2,1/2,0	+	−	−	+	−	−	+	+
0,1/2,1/2	+	+	−	−	+	−	−	+
1/2,1/2,1/2	+	−	−	−	+	+	+	−

not change with a change of origin by any of the $\mathbf{r}_s$ values of Table 9.4, and therefore *eee* reflections have signs that are *structure invariant* and these signs cannot be arbitrarily chosen, and (2) the product of the signs of $U_{h'}U_{h'}$ and $U_{h-h'}$ are structure invariant (and thus can be determined as in the preceding section) as can be seen by multiplying any three columns of Table 9.4 that combine to form *eee* (e.g., *eoo*, *oeo* and *ooe*). Thus, it is possible to fix the origin by specifying the signs of an *eoo*, an *oeo*, and say, an *ooo* reflection, but *not* by specifying an *eoo*, an *oeo* and an *ooe* reflection. At any rate some signs can be arbitrarily specified, and these can then be combined as $U_{h'}U_{h-h'}$ (generally, using relationships among U's (F's) that arise from the symmetry), and combined with the implied U_h's to find high probability sign assignments. For example, suppose that in $P4/mmm$ the reflections 2, 1, 3 and 5, 2, 3 are assigned signs. The International Tables list $F(hk\ell) = F(\bar{h}\bar{k}\ell) = F(\bar{h}k\ell) = F(h\bar{k}\ell) = F(hk\bar{\ell}) = F(kh\ell)$. In this case all the combinations $\bar{7},\bar{3},\bar{6}$; $3,1,\bar{6}$; $3,\bar{3},\bar{6}$; $\bar{7},1,0$; $\bar{7},\bar{3},0$; $\bar{4},\bar{6},6$; $0,4,\bar{6}$; $0,\bar{6},\bar{6}$; $\bar{4},4,\bar{6}$; $\bar{4},\bar{6},0$ arise from $h-h'$ with $h = 2,1,3$ and $h'' = 5,2,3$; $\bar{5},\bar{2},3$; $\bar{5},2,3$; $5,\bar{2},3$; $5,2,\bar{3}$, $2,5,3$; $\bar{2},\bar{5},3$; $\bar{2},5,3$; $2,\bar{5},3$; $2,5,\bar{3}$, and their remaining combinations with $hk\ell$ values equivalent to 213!

9.11. The Effect of Centered Cells

If a lattice is indexed on the basis of a face, body or end centered cell, there are systematic absences. The conditions that U_h be nonzero are given in Table 9.5. It follows that there is one possible symmetry inequivalent origin shift in face-centered cells and only the sign of one *ooo* reflection can be

arbitrarily specified in this case, while in the body-centered case there are four possible origins and any two of e, o, o; o, e, o or o, o, e reflections can be arbitrarily assigned signs. In the case of an end-centered cell 3 signs can be arbitrarily fixed subject to the parity restraints given in Section 9.10.

Table 9.5. Conditions for observation of U's in centered cells.

Face-centered	*eee; ooo*
Body-centered	*eee; eeo; eoe; o, e, e*
End-centered	only in projection

9.12. Other Uses of Symmetry in Sign Assignment

It was found above that if $|U_h|$, $|U_{h'}|$ and $|U_{-h-h'}|$ are all sufficiently large, then it is highly probable that $U_h U_{h'} U_{-h-h'} = |U_h||U_{h'}|U_{-h-h'}|$. In a centrosymmetric structure with the origin at a center of symmetry $U_h = U_{-h}$ and thus

$$U_{-h} U_{h'} U_{h-h'} = U_h U_{h'} U_{h-h'}$$

is positive with high probability if $|U_h|, |U_{h'}|$ and $|U_{h-h'}|$ are sufficiently large. This is the form in which the triple product sign relation is usually given.

If symmetry implies that $F_h = F_{h'}$ (or $F_h = -F_{h'}$), then in the first case

$$U_h U_{h'} U_{h-h'} = -U_{h-h'} U_h^2 , \tag{44}$$

and in the second

$$U_h U_{h'} U_{h-h'} = -U_{h-h'} U_h^2 . \tag{45}$$

In either case it can be determined at the probability level given by $|U_{ct}|$ (Eq. 31) that $U_{h-h'} = |U_{h-h'}|$ in the first case and that $U_{h-h'} = -|U_{h-h'}|$ in the second. Furthermore, since $U_h U_{-h} U_{2h}$ is a U_{ct}, it can be determined that U_{2h} is positive at the confidence level corresponding to $|U_{2h} U_h^2|$.

9.13. Thermal Motion

The general expression to account for thermal motion of a single atom in a crystal is

$$T = \exp -1/2(U_{11} h^2 a^{*2} + U_{22} k^2 b^{*2} + U_{33} \ell^2 c^{*2} + 2U_{12} hk a^* b^* + 2U_{13} h\ell a^* c^* + 2U_{23} k\ell b^* c^*) , \tag{46}$$

where the U_{ik}'s have the significance that the mean square vibration in the direction of the vector: $\ell_1\mathbf{a}^*/a^* + \ell_2\mathbf{b}^*/b^* + \ell_3\mathbf{c}^*/c^*$ with $\ell_1^2 + \ell_2^2 + \ell_3^2 = 1$ is

$$\overline{U}^2_{\ell_1\ell_2\ell_3} = \sum_{i=1}^{3}\sum_{j=1}^{3} \ell_i \ell_j U_{ij} \,. \tag{47}$$

For example, if two atoms are located at x_1, y_1, z_1 and x_2, y_2, z_2, then the vector between them is

$$\mathbf{V} = (x_2 - x_1)\mathbf{a} + (y_2 - y_1)\mathbf{b} + (z_2 - z_1)\mathbf{c} \tag{48}$$

and the vibration of an atom along this interatomic direction has mean square vibration given by Eq. 47 with

$$\ell_1 = \frac{x_2 - x_1}{a^*\left[\left(\frac{x_2 - x_1}{a^*}\right)^2 + \left(\frac{y_2 - y_1}{b^*}\right)^2 + \left(\frac{z_2 - z_2}{c^*}\right)^2\right]^{1/2}}, \tag{49}$$

$$\ell_2 = \frac{y_2 - y_1}{b^*\left[\left(\frac{x_2 - x_1}{a^*}\right)^2 + \left(\frac{y_2 - y_1}{b^*}\right)^2 + \left(\frac{z_2 - z_1}{c^*}\right)^2\right]^{1/2}} \tag{50}$$

and

$$\ell_3 = \frac{z_2 - z_1}{c^*\left[\left(\frac{x_2 - x_1}{a^*}\right)^2 + \left(\frac{y_2 - y_1}{b^*}\right)^2 + \left(\frac{z_2 - z_1}{c^*}\right)^2\right]^{1/2}}. \tag{51}$$

Bibliography

1. D. McKie and C. McKie, *Essentials of Crystallography* (Blackwell Scientific Publications, Boston, 1980).
2. M. M. Woolfson, *Direct Methods in Crystallography* (Oxford at the Clarendon Press, Oxford, 1961).
3. J. E. Freund and R. E. Walpole, *Mathematical Statistics*, Third Ed. (Prentice-Hall, Englewood Cliffs, New Jersey, 1962).
4. G. H. Stout and L. H. Jensen, *X-Ray Structure Determination* (The Macmillan Company, London, 1968).
5. N. F. M. Henry and K. Lensdale, Eds., *Int. Tables for X-Ray Crystallography* (The Kynoch Press, Birmingham, England, 1969).

Problems

1. An orthorhombic crystal is oriented so that $\mathbf{a}^* + \mathbf{b}^*$ is vertical at the zero point of a Weissenberg film. Calculate the horizontal and vertical coordinates of the 2, 2, 0 reflection if $\mathbf{a} = 5.00$ Å, $b = 6.00$ Å, the film translates 1 mm for each 2 degrees of crystal rotation, $\lambda = 1.54$ Å and the camera diameter is 57.3 mm.
2. Give the Laue class for each of the following space groups: $I\bar{4}$, $R\bar{3}m$, $P6_3/mmc$, $P4_232$, $Pn3$, $I4cm$.
3. How are the Laue classes $m3$ and $m3m$ distinguished?
4. Find the space groups consistent with:

Laue Symmetry	Condition for Observation
mmm	$\ell = 2n$ for $0k\ell$ and $h0\ell$
mmm	$k = 2n$ for $0k\ell$ $\ell = 2n$ for $h0\ell$ $h + k = 2n$ for $hk0$
$m3$	$k + \ell = 2n$ for $0k\ell$
$\bar{3}m1$	$\ell = 3n$ for 0,0,0,ℓ
$4/m$	none
$4/mmm$	$h + k = 2n$ for $h, k, 0$ $\ell = 2n$ for $0, k, \ell$

5. If diffraction from a centrosymmetric structure has all U_h positive and with the same magnitude, what is the structure? Treat the structure as though atoms were point atoms (i.e., take f to be the number of electrons at all θ).
6. Find the mean square vibration of S along a perpendicular to the Tm-S direction and in the $y = 0$ plane, where

$$x = 0.039\ 29\,, \quad y = 0\,, \quad z = -0.274\ 0 \text{ for } Tm\,,$$
$$x = 0.052\ 7\,, \quad y = 0\,, \quad z = 0.503\ 0 \text{ for } S$$

and $U_{11} = 0.14$, $U_{22} = 0.014$, $U_{33} = 0.023$, $U_{12} = 0$, $U_{13} = 0.053$ and $U_{33} = 0$ Å^2 for S. The lattice is monoclinic with $a = 38.395$, $b = 3.8421$ and $c = 11.141$ Å and $\beta = 91.02°$.

CHAPTER 10

ELECTRONIC STRUCTURE

10.1. Bloch Functions

As developed in Section 5.1 the basis functions for the translational subgroup are of the form $\exp i(\mathbf{k}+\mathbf{K})\cdot\mathbf{r}$ ($\mathbf{K}$ variable and $\mathbf{k}$ fixed for a given irreducible representation), and a complete set is considered if all $\mathbf{k}$'s within a unit cell (the Brillouin zone) are considered. Since the Hamiltonian for a single electron commutes with any translational symmetry operator, these plane waves are also eigenfunctions of the Hamiltonian as far as translational symmetry is concerned. In order to obtain functions that are bases for both the translations and the rotations these plane waves can be multiplied by functions, $\phi(\mathbf{r})$, that transform as basis functions for the essential operations of the space group, i.e.,

$$\Phi_{\mathbf{k}}(\mathbf{r}) = \phi(\mathbf{r}) \sum_{\mathbf{K}} C_{\mathbf{k}} \exp i(\mathbf{k}+\mathbf{K})\cdot\mathbf{r} \tag{1}$$

with the set of $\mathbf{K}$'s over which the sum is carried including any subset (including the empty set) of $\{\mathbf{K}\}$.

10.2. Boundary Conditions

A problem with these functions as electron wave functions, however, is that the wave vectors, $\mathbf{k}$, have been defined such that they are continuously distributed within the *BZ*, and thus mathematically there are infinitely many $\Phi_k(\mathbf{r})$ functions within any interval $\Delta\mathbf{k}$. This is not physically realistic and this lack of realism can be viewed as arising from the lack of boundary conditions. The real lattice of a finite crystal is not infinite in extent and this fact implies boundary restraints that divide the *BZ* into a very large

but finite number of volumes associated with discrete wave vectors. Since the bulk electrical properties of a macroscopic crystalline solid do not depend upon the shape or size of the crystal, it is clear that while boundary conditions are necessary to avoid the infinity mentioned above, the exact nature of the boundary conditions is not physically important. Therefore, it is possible to be arbitrary about the nature of the boundary conditions, and for many years it has been generally agreed that the boundary conditions be adopted that require that the wave functions be in phase with themselves at the boundaries, i.e., that

$$\exp i\boldsymbol{k} \cdot \mathbf{r} = \exp i\mathbf{k} \cdot (\mathbf{r} + n_1\mathbf{a}) \tag{2}$$

where $n_1\mathbf{a}$ is an edge of the crystal (and similarly for **b** and **c**). Thus, if

$$\mathbf{k} = \mu\mathbf{a}^* + \nu\mathbf{b}^* + \omega\mathbf{c}^*, \tag{3}$$

then $\mu n_1, \nu n_2$ and ωn_3 are integers. Suppose, for example, that a crystal is 10^5 a units long in the **a** direction, i.e., $n_1 = 10^5$. Then $10^5\mu =$ an integer means that $\mu = 1 \times 10^{-5}, 2 \times 10^{-5}, \ldots$ but $1 \times 10^{-5} < \mu < 2 \times 10^{-5}$ is not allowed. Thus, these cyclic boundary conditions quantize reciprocal space. The crystal volume is $n_1\mathbf{a} \cdot n_2\mathbf{b} \times n_3\mathbf{c} = n_1 n_2 n_3\, V_{\text{cell}}$, and thus the Brillouin zone is divided into small volumes

$$\frac{\mathbf{a}^*}{n_1} \cdot \frac{\mathbf{b}^*}{n_2} \times \frac{\mathbf{c}^*}{n_3} = \frac{V_{BZ}}{n_1 n_2 n_3} \tag{4}$$

and there are as many discrete wave vectors (one for each small volume) as there are unit cells in the crystal volume.

10.3. Energy Values for Plane Waves Solutions. The Free Electron Model

The free electron model is the idealized case for which there is no potential and the electron energy is purely translational. This model contains an inherent contradiction, for the wave functions are assumed to be the $\Phi_{\mathbf{k}}(\mathbf{r})$'s, but these wave functions are found by using the lattice periodicity which is imposed by the periodic potential of the crystal. We will therefore find some anomalies that are introduced by this model, and they will be removed by considering the periodic potential as a perturbation.

In the free electron case the Hamiltonian is

$$H = -\frac{\hbar^2}{2m}\left[\frac{\partial^2}{\partial x^2} + \frac{\partial^2}{\partial y^2} + \frac{\partial^2}{\partial z^2}\right] \tag{5}$$

where x, y, z are cartesian coordinates, or

$$H = -\frac{\hbar^2}{2m}\left[\frac{1}{a^2}\frac{\partial^2}{\partial x^2} + \frac{1}{b^2}\frac{\partial^2}{\partial y^2} + \frac{1}{c^2}\frac{\partial^2}{\partial z^2}\right] \tag{6}$$

where x, y, z are the coordinates in units of the unit cell dimensions in an orthogonal system. Taking a second partial derivative of $\exp i\mathbf{k}\cdot\mathbf{r}$ ($\mathbf{k}$ as in Eq. 3),

$$\begin{aligned}\frac{\partial^2 \exp i\mathbf{k}\cdot\mathbf{r}}{\partial x^2} &= \exp 2\pi i\nu y \exp 2\pi i\omega z \frac{\partial^2 \exp 2\pi i\mu x}{\partial x^2} \\ &= -(2\pi\mu)^2 \exp i\mathbf{k}\cdot\mathbf{r}\end{aligned} \tag{7}$$

and similarly for the derivatives with respect to y and z. Thus,

$$H \exp i\mathbf{k}\cdot\mathbf{r} = \frac{h^2}{2m}\left[\frac{\mu^2}{a^2} + \frac{\nu^2}{b^2} + \frac{\omega^2}{c^2}\right] \exp i\mathbf{k}\cdot\mathbf{r}\,, \tag{8}$$

or

$$E(\mathbf{k}) = E(\mu,\nu,\omega) = \frac{h^2}{2m}\left[\frac{\mu^2}{a^2} + \frac{\nu^2}{b^2} + \frac{\omega^2}{c^2}\right] = \frac{h^2|\mathbf{k}|^2}{2m}\,. \tag{9}$$

Letting the dimensions of the crystal be $L_x = n_1 a$, $L_y = n_2 b$, $L_z = n_3 c$, and $\mu = P_1/n_1$, $\nu = P_2/n_2$ and $\omega = P_3/n_3$ (P_i = integer less than or equal to n_i),

$$E(\mathbf{k}) = \frac{h^2}{2m}\left[\frac{P_1^2}{L_x^2} + \frac{P_2^2}{L_y^2} + \frac{P_3^2}{L_z^2}\right].$$

Thus, the energies are quantized and there are $n_1 n_2 n_3$ free electron states in a crystal containing $n_1 n_2 n_3$ unit cells. These states form a quasicontinuum for any reasonably sized crystal, and Eq. 9 means that $E(\mathbf{k})$ is quadratic in $|\mathbf{k}|$ as shown in Fig. 10.1.

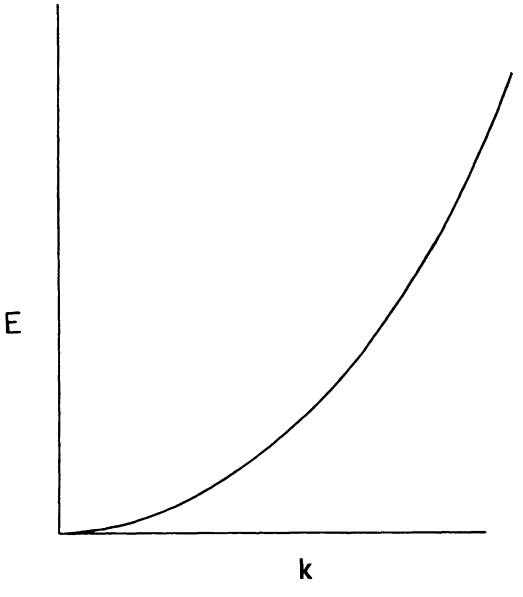

Fig. 10.1. Free electron E vs. $\mathbf{k}$.

10.4. $E(\mathbf{k})$ in the *BZ*. The Nearly Free Electron Model

The origin of the $\Phi(\mathbf{k})$ curve is a reciprocal lattice point. Taking $\mu\mathbf{a}^*$ as a direction yields the result of Fig. 10.2. These curves emphasize the periodic nature of reciprocal space. The zone boundary at $\mathbf{a}^*/2$ is of particular interest, for it is at this point that evidence of the anomalous nature of these curves mentioned in Section 10.3 appears. The functions $\exp i\pi x$ and $\exp -i\pi x$ are both eigenfunctions of the translational subgroup at $\mathbf{k} = \mathbf{a}^*/2$ and they introduce an artificial double degeneracy at this point. A potential (which must be present if there is periodicity) introduces a mixing of $\exp i\pi x$ and $\exp -i\pi x$ to produce symmetric ($\cos \pi x$) and antisymmetric ($\sin \pi x$) combinations which remove the degeneracy. The energy eigenvalues can, for purposes other than counting of states, be taken to be analytic functions at $\mathbf{k}$ (since as L_x, L_y and L_z increase, the quasicontinuum continuously approaches a continuum) and thus the slope of G vs. $\mathbf{k}$ must vary continuously. Since $\exp i\mu x$ and $\exp -i\mu x$ correspond to the same energy there is reflection symmetry through the point $\mathbf{a}^*/2$, as

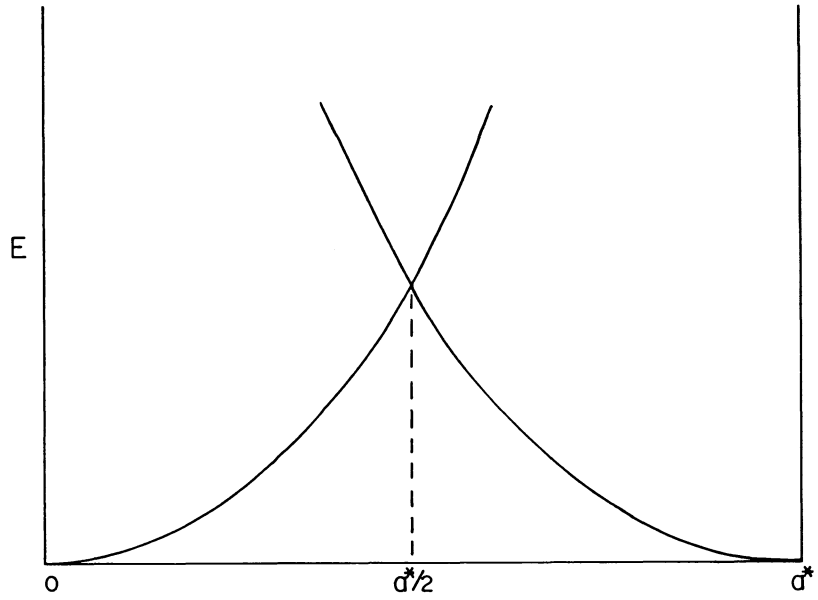

Fig. 10.2. Free electron E vs. $\mathbf{k}$, two adjacent BZ's.

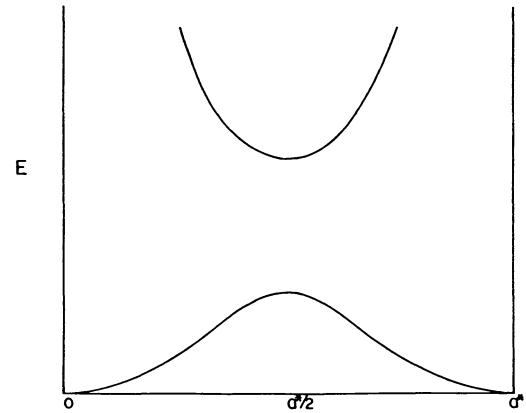

Fig. 10.3. Nearly free electron E vs. $\mathbf{k}$.

shown in Fig. 10.2. The lifting of the degeneracy, the continuity of the slope of $G(\mathbf{k})$ and the reflection symmetry yield an $E(\mu)$ vs. $\mu\mathbf{a}^*$ curve as shown in Fig. 10.3. In Section 5.2 it was shown that if there is a 2_1 axis parallel to $\mathbf{a}$ and perpendicular to a reflection plane, then there is a two-dimensional irreducible representation at $\mathbf{k} = \mathbf{a}^*/2$. Thus, in this case the degeneracy is not lifted by the mixing that is appropriate for $2/m$ symmetry along $\mathbf{a}$.

10.5. E vs. k: Bonding and Antibonding Interactions

In order to get a first idea about $\phi(\mathbf{r})$ in Eq. 1, it is frequently helpful to think of these functions as atomic orbitals centered on the lattice positions. Such a model is appropriate to the cases such as elemental metals with atoms located at the lattice sites (e.g., *fcc*, *bcc*, *hcp*). For example, consider the $s\sigma, p\sigma, p\pi, d\sigma$ and $d\pi$ interactions for $\mathbf{k} = 0$ as shown in Fig. 10.4. The σ interactions of the g-symmetry orbitals and π interactions of the u-symmetry orbitals are bonding in character, and antibonding for the σ

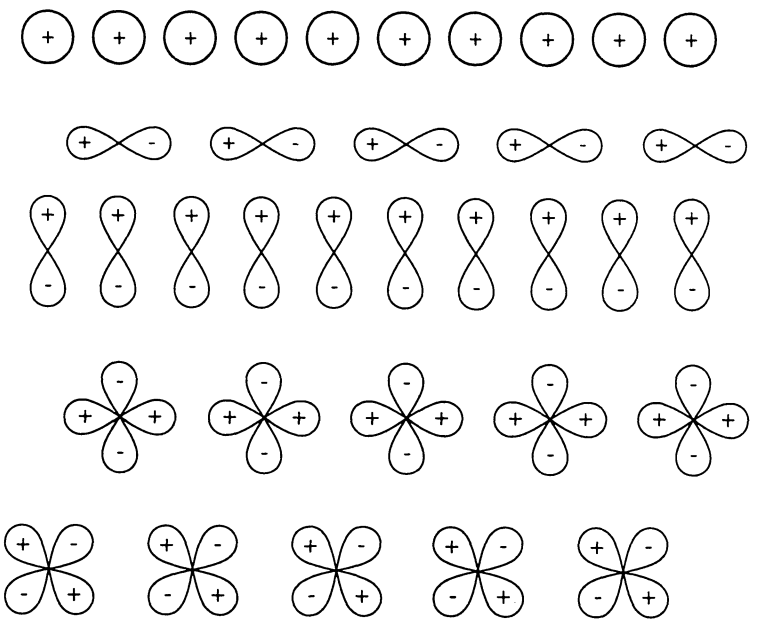

Fig. 10.4. Spherical harmonic orbitals at $\mathbf{k} = 0$.

interactions of u-symmetry orbitals and the π interactions of g-symmetry orbitals. This result stems from the fact that at $\mathbf{k} = 0$,

$$\Phi_{\mathbf{k}}(\mathbf{r}) = \Phi_{\mathbf{k}}(\mathbf{r} + \mathbf{T})$$

and thus

$$\phi(\mathbf{r}) = \phi(\mathbf{r} + \mathbf{T}),$$

each function must be in phase for all translations. On the other hand, at the zone boundary, say at $\mathbf{k} = \mathbf{a}^*/2$, the crystal wave functions that are symmetric with respect to translation by $\mathbf{a}$ at $\mathbf{k} = 0$ have transformed continuously with changing $\mu(\mathbf{k} = \mu\mathbf{a}^*)$ to functions that are antisymmetric with respect to translation by $\mathbf{a}$ (and symmetric with respect to translation by $2\mathbf{a}$), and thus the functions that are bonding at the Γ point are antibonding at $\mathbf{a}^*/2$ and vice-versa (see Fig. 10.5).

It follows that E vs. $\mathbf{k}$ from Γ to X for $s\sigma$, $p\pi$ and $d\sigma$ are increasing functions of μ, whereas for $p\sigma$ and $d\pi$ they are decreasing functions (Fig. 10.6).

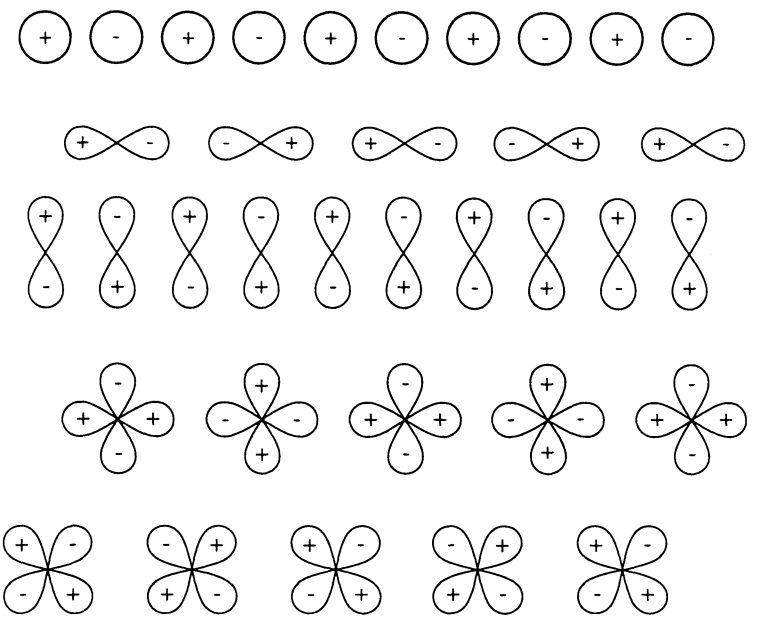

Fig. 10.5. Spherical harmonic orbitals at $\mathbf{k} = \mathbf{a}^*/2$.

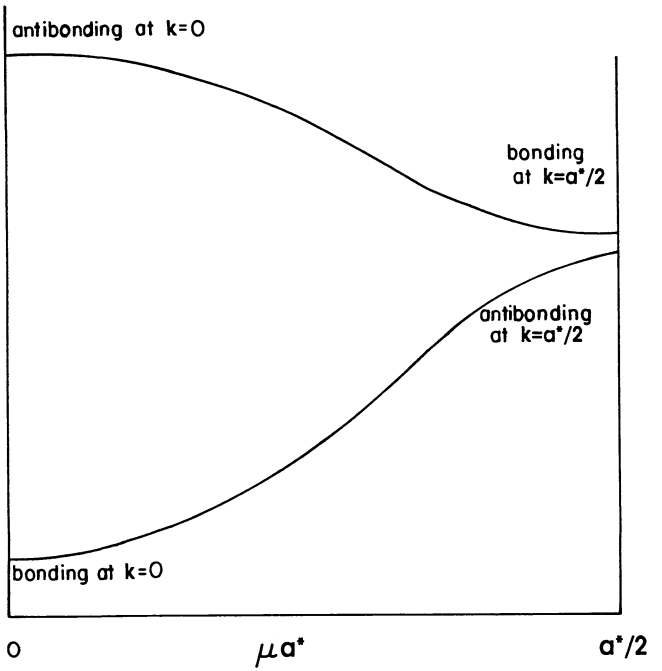

Fig. 10.6. Bonding and antibonding interactions at the zone center and zone boundary.

Figure 10.6 schematically contains many of the essential features of a band diagram (an E vs. $\mathbf{k}$ diagram). First, as mentioned previously, although the states are discrete, there are so many states within the interval that the function can be considered to be continuous for many purposes. Second, the curves are roughly parabolic in shape but with extrema at the zone boundary (except in special cases of doubly degenerate small representations at the zone boundary). Furthermore, those curves which are bonding at the zone center are antibonding at the zone boundary and E vs. $\mathbf{k}$ is increasing, while those that are antibonding at the center are bonding at the boundary and E vs. $\mathbf{k}$ is decreasing. It is also true that curves with the same symmetry will avoid crossing and that this behavior will lead to maxima and minima between the zone center and the zone boundary.

It is a very rough approximation to take $\phi(\mathbf{r})$ to be an atomic orbital centered on a lattice site. In many cases it would be better to take a hybrid mixture, with the amount of mixing varying with $\mathbf{k}$. Thus, the fraction of s, p or d contribution to bonding depends upon $\mathbf{k}$ and overall contributions can be obtained only by integrating over an asymmetrical unit of the *BZ*.

10.6. Peierl's Distortion

Second-order phase transitions were discussed in Chapters 6 and 7. One mechanism giving rise to such a transition involves the lowering of the conduction electron energy as the result of symmetry breaking. Suppose that in some direction of $\mathbf{k}$ space, e.g., the $\mathbf{a}^*$ direction, an energy band is half-filled half-way to the *BZ* boundary (i.e., at $\mathbf{a}^*/4$, see Fig. 10.7a). If a continuous transition occurs so as to double the period along $\mathbf{a}$ a new zone boundary will be created at $\mathbf{a}^*/4 = \mathbf{a}_N^*/2$, and this can open an gap (Fig. 10.7b) and thus lower the Fermi energy and stablize the symmetry lowered structure. Inherent in this idea is the fact that the density-of-states (DOS $= dN/dE$) is inversely proportional to the slope of E vs. $\mathbf{k}$ which follows directly from the fact that the number of states is proportional to

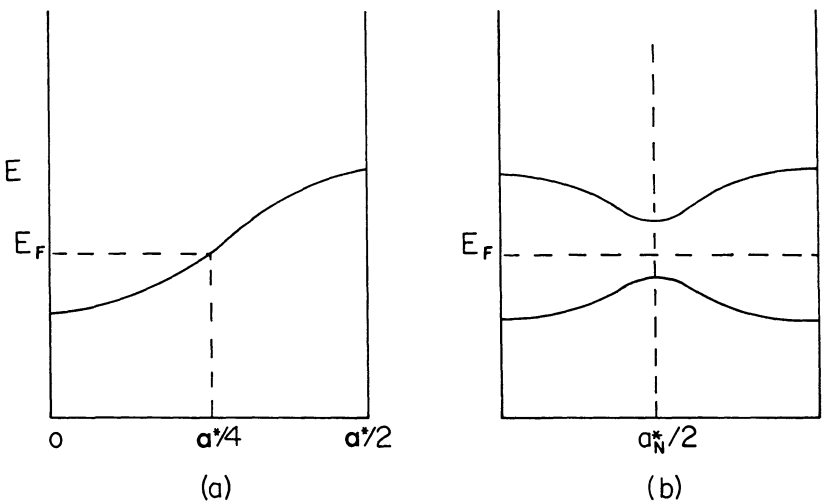

Fig. 10.7. Peierl's distortion.

$\Delta\mathbf{k}$. Thus, when the new zone boundary is created by symmetry breaking and $dE/dk = 0$ at the new zone boundary, it follows that the DOS is increased for states below the old Fermi energy, and thus the Fermi energy in the low-symmetry structure is reduced relative to that in the high-symmetry structure.

This type of energetic instability is present in all conducting solids, but not always at $\mathbf{k}$ points that double a period and sometimes at $\mathbf{k}$ points that would lead to incommensurate structure (i.e., not at special points of the *BZ*). However, it is generally the case that other competing energies (e.g., Madelung energy) favor the high symmetry form and thus permit these structures to remain stable even down to *O* K. Transitions of the Peierl's type are favored by nearly isolated linear conducting chains, for these can distort without excessively impacting upon other energetic factors.

10.7. Compatibility

When two bands have a point in common at a special point but are separated at other points in the neighborhood (Fig. 10.8), then the special point is a point of a higher degeneracy that is lowered when $\mathbf{k} = \mathbf{k}_0 + \delta\mathbf{k}$. It is sometimes of interest to know into what bands and of what degeneracy a high degeneracy band at a special point evolves with changing $\mathbf{k}$. This is a problem in compatibility, for example one asks, say in $m3m$, what symmetries at $\delta\mathbf{a}^*$ are compatible with the T_{2g} band at $\mathbf{k} = 0$? To answer this question examine the character tables of the point groups of the wave vector ($g^\circ(\mathbf{k} = 0)) = O_h$ and $g^\circ(\delta\mathbf{a}^*) = C_{4v}$, for $m3m$) Tables 10.1 and 10.2). The last row of Table 10.2 shows the characters, deduced by continuity, of the reducible representation in C_{4v} (at $\delta\mathbf{a}^*$) that is compatible with the T_{2g} representation in O_h (at $\mathbf{k} = 0$). Since the Γ^4 and Γ^5 rows sum to yield the T_{2g} row (in Table 10.2), it follows the representation labelled T_{2g} in C_{4v} is reducible to $\Gamma^4 + \Gamma^5$. This means that the triply degenerate irreducible representation at $\mathbf{k} = 0$ is compatible with the doubly degenerate Γ^5 irreducible representation and the singly degenerate Γ^4 representation at $\delta\mathbf{a}^*$, and the triply degenerate band at $\mathbf{k} = 0$ will split into a doubly degenerate and a singly degenerate band along $\mathbf{a}^*$. This fits, for example, with the T_{2g} orbitals transforming as xy, yz and xz, and since the $\mathbf{a}^*$ direction differentiates x from y and z, this change in period along this direction differentiates yz from xz and xy.

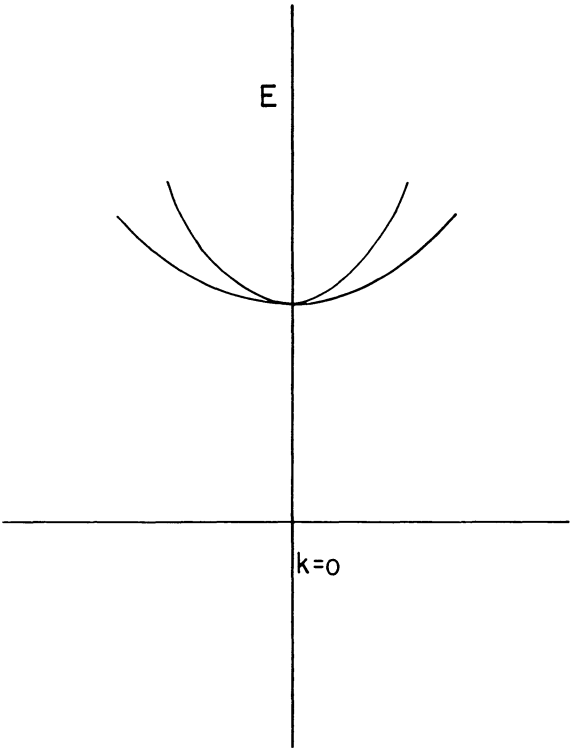

Fig. 10.8. E vs. $\mathbf{k}$ for bands which are degenerate at $\mathbf{k} = 0$.

Table 10.1. Character table of T_{2g} in O_h.

# of operations	1	8	3	6	6	1	8	3	6	6
class	E	C_3	C_{2h}	C_4	C_{2d}	i	$\overline{C}_3$	σ_v	$\overline{C}_4$	σ_d
χ	3	0	−1	−1	1	3	0	−1	−1	1

Table 10.2. Character table of C_{4v}.

# of operations	1	2	1	2	2
class	E	C_4	C_2	σ_v	σ_d
Γ^1	1	1	1	1	1
Γ^2	1	1	1	−1	−1
Γ^3	1	−1	1	1	−1
Γ^4	1	−1	1	−1	1
Γ^5	2	0	−2	0	0
T_{2g}	3	−1	−1	−1	1

Bibliography

1. R. Hoffmann, *Solids and Surfaces: A Chemist's View of Bonding in Extended Structures* (VCH Publishers, New York, 1988).
2. J. F. Cornwell, *Group Theory and Electronic Energy Bands in Solids* (North-Holland Publishing, London, 1969).
3. M. Hamermesh, *Group Theory and Its Application to Physical Problems* (Addison-Wesley, New York, 1962).
4. M. Tinkham, *Group Theory and Quantum Mechanics* (McGraw-Hill, New York, 1964).
5. T.-H. Nguyen, H. Franzen and B. N. Harmon, The Electronic Structure of Zirconium Monosulfide, *J. Chem. Phys.* **73**, No. 1, 425–437 (1980).

Problems

1. Calculate the speed of a free electron with wave vector $\mathbf{a}^*/2$ in an orthorhombic crystal with lattice parameter $\mathbf{a} = 10$ Å. Find the corresponding quantum number in a crystal 10^6 Å on an edge.
2. (a) For a band in one-dimension what is the relationship between the DOS and dE/dk?
   (b) What happens to the DOS in the vicinity of the zone boundary if the bands avoid each other?
3. Is it possible for bands to be degenerate at the $\mathbf{c}^*/2$ special point of the *BZ* for $P4_2/m$?
4. Using the character tables for $Fm3m$ (given below) determine the degeneracies of the bands at $\delta(\mathbf{a}^* + \mathbf{b}^* + \mathbf{c}^*)$ that connect with the triply degenerate T_{1u} band at $\mathbf{k} = 0$.

T_{1u}

#	1	8	3	6	6	1	8	3	6	6
class	E	C_3	C_{2h}	C_4	C_{2d}	i	$\overline{C}_3$	σ_h	$\overline{C}_4$	σ_d
χ	3	0	−1	1	−1	−3	0	1	−1	1

at $\mathbf{k} = \delta(\mathbf{a}^* + \mathbf{b}^* + \mathbf{c}^*)$

#	1	2	3
class	E	C_3	σ_d
Γ^1	1	1	1
Γ^2	1	1	−1
Γ^3	2	−1	0

5. (a) What happens to these bands at the *L* point (character table given below)?

#	1	2	3	1	2	3
class	E	C_3	C_{2d}	i	$\overline{C}_3$	σ_d
Γ^1	1	1	1	1	1	1
Γ^2	1	1	1	−1	−1	−1
Γ^3	1	1	−1	1	1	−1
Γ^4	1	1	−1	−1	−1	1
Γ^5	2	−1	0	2	−1	0
Γ^6	2	−1	0	−2	1	0

(b) Discuss the bonding-antibonding character of these bands at Γ and L (see Fig. 10.9). Sketch a plausible atomic orbital picture for these bands at L if Zr at the origin contributes principally d orbitals, S at 1/2, 0, 0 contributes principally p orbitals and nearest neighbor interactions predominate.

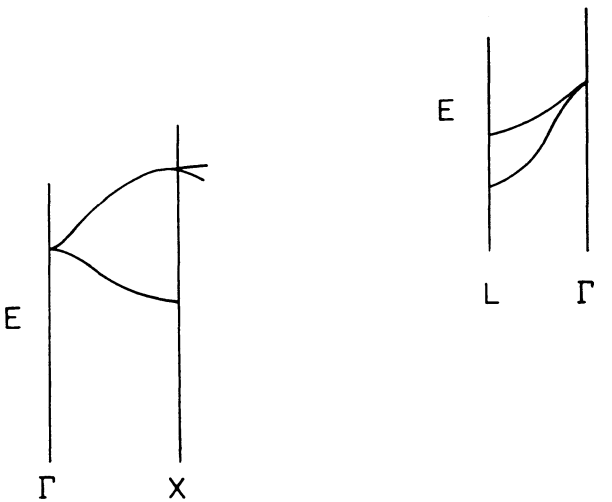

Fig. 10.9. E vs. **k** for ZrS($Fm3m$).

6. Discuss the behavior of the T_{2g} band of NaCl-type ZrS along the δ**a** direction for $0 \leq \delta \leq 1/2$. Assume it to be 100% d_{xy}, d_{yz}, d_{xz}.

CHAPTER 11

ORDER-DISORDER TRANSITIONS

11.1. The $\beta - \beta'$ Brass Transition

Order-disorder transitions in crystalline solids generally occur as the result of a long-range average change in the fractional occupation of some subset of atom positions within the solid. A classic example is the $\beta - \beta'$ brass transition in which the high-symmetry, high-temperature form is the *bcc* structure (equal long-range occupation of the sites at 0, 0, 0 and 1/2, 1/2, 1/2 by two kinds of metals, most notably Cu and Zn) and the low-temperature, ordered form is CsCl-type (unequal occupation of the sites at 0, 0, 0 and 1/2, 1/2, 1/2 of a cubic cell). The symmetry change is from $Im3m$ to $Pm3m$ and the broken symmetries are $\varepsilon|(\mathbf{a}+\mathbf{b}+\mathbf{c})/)2$ (translational symmetry is lost and the $Pm3m$ structure is a superstructure of the $Im3m$ structure) and the operations associated with this translation in $Im3m$, e.g., $C_{4x}|(\mathbf{a}+\mathbf{b}+\mathbf{c})/2$, $C_{2x}|(\mathbf{a}+\mathbf{b}+\mathbf{c})/2$, $i|(\mathbf{a}+\mathbf{b}+\mathbf{c})/2$, etc.

The T–X phase diagram (Fig. 11.1) shows the two symmetries separated by a T–X line, meaning that $\Delta X = 0$. This line has nonzero slope (for 44.8 percent Zn the transition occurs at 454 °C, for 48.2 percent Zn it occurs at 468 °C). Thus,

$$\left(\frac{\partial T}{\partial X}\right)_P \neq 0 \tag{1}$$

and it follows from the Gibbs-Konovalow equation (Section 7.16) that $\Delta S = 0$ and the transition is second-order. Not all order-disorder transitions occur as second-order processes. In order for the transition to occur with continuous structure change, the two phases must meet the Landau conditions (Chapter 6), and even then the transition could occur as a first-

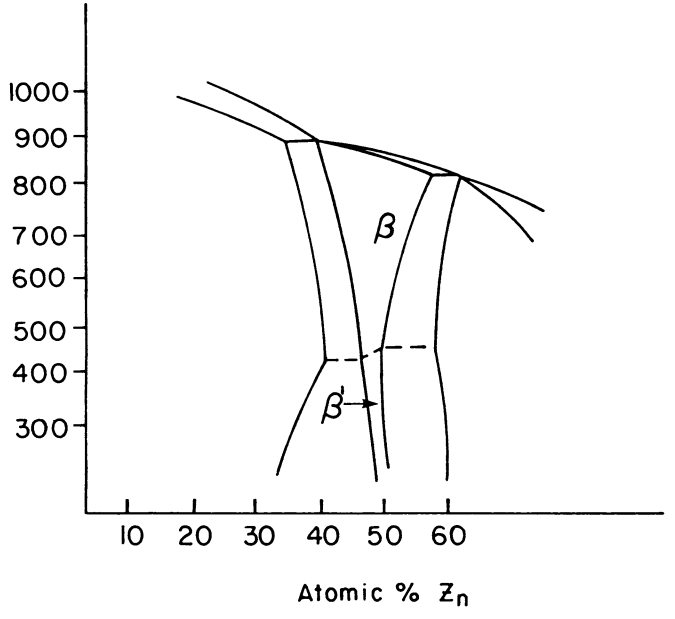

Fig. 11.1. Cu–Zn phase diagram.

order process since the Landau conditions are necessary but not sufficient for a second-order transition.

In the case of the $\beta - \beta'$ brass transition, the star to which the process corresponds is the star of $\mathbf{a}^*$, which consists of $\mathbf{a}^*$ alone (although rotations carry $\mathbf{a}^*$ into $\mathbf{b}^*$ and $\mathbf{c}^*$, they are all equal modulo reciprocal lattice vectors, e.g., $\mathbf{a}^* = \mathbf{b}^* \bmod(\mathbf{a}^* - \mathbf{b}^*)$ and $(\mathbf{a}^* - \mathbf{b}^*) \in \{\mathbf{k}\}$. Since $\mathbf{a}^*$ is in a star by itself, $g(\mathbf{a}^*)$ is isomorphic with O_h, and the transition $Im3m \rightarrow Pm3m$ corresponds to the totally symmetric small representation of $Im3m$ at $\mathbf{a}^*$. The difference particle density

$$\Delta\rho = \eta\phi \tag{2}$$

thus is antisymmetric with respect to translation by $(\mathbf{a}^* + \mathbf{b}^* + \mathbf{c}^*)/2$ and hence η transforms into $-\eta$ under this translation. That is, addition of the function that corresponds to the addition of Cu and subtraction of Zn at 0, 0, 0 and to the opposite at 1/2, 1/2, 1/2 is equivalent to subtraction of that function with an irrelevant origin shift by 1/2, 1/2, 1/2.

Thus, two equivalent distortions have

$$G = G^{\circ} + A\eta^2 + B\eta^3 + C\eta^4 + \ldots \tag{3}$$

and

$$G = G^{\circ} + A\eta^2 - B\eta^3 + C\eta^4 + \ldots , \tag{4}$$

and since the distortions are equivalent, their Gibbs free energies are equal and $B = -B$, or $B \equiv 0$ by symmetry. Thus, there is no third-order term and it is confirmed that the transition meets Landau's conditions.

Since inversion belongs to the point group of the wave vector, the transition meets the Lifshitz condition also. Thus, the $\beta - \beta'$ brass transition, according to Landau theory, can occur as a second-order process and according to the Gibbs-Konovalow equation and experiment (Fig. 11.1) does in fact do so.

11.2. *L* Point Ordering in NaCl-Type Solids

Solids that contain vacancies also exhibit the potential for long-range ordering. In fact the third-law of thermodynamics, if it is interpreted to mean that solids transform to remove configurational entropy with decreasing temperature, implies that all disordered solids, including those in which vacancies and atoms are randomized on sites, will have a tendency to order with decreasing temperature. Of course, diffusion is an essential kinetic feature of order-disorder processes, and the thermodynamic tendency may be manifest at a temperature that is too low for the ordering rate to be significant. In this case upon cooling the system would remain upon the uppermost curves of Fig. 7.7 or 7.8 when the temperature is lowered through T_t.

Two monosulfides, ScS and ZrS, are known to occur with large fractions (ca. 25%) of their metal sites vacant and with the average structure of NaCl-type at high temperatures (above about 1 250 °C)[1,2]. Thus, the high-temperature diffraction pattern is that of a NaCl-type material ($|F|^2 = 16(f_m + f_s)^2$ for h, k, ℓ even and $|F|^2 = 16(f_m - f_s)^2$ for h, k, ℓ (odd) but with f_m equal to the atomic scattering factor for the metal reduced by a factor corresponding to the fractional occupancy of the sites.

When the temperature of $Zr_{0.75}S$ is reduced below 1 250 °C the X-ray diffraction pattern is altered relative to that at higher temperatures by the

addition of weak diffraction maxima (superstructure lines) and by splitting of some of the substructure lines. The refined structure at room temperature (refined by the Rietveld least-squares treatment) can be described as NaCl-type with 25% of the metal sites vacant, and the vacancies ordered in every order 1, 1, 1 plane along the body-diagonal direction. The ordering transition has the appearance of occurring by a continuous ordering of the vacancies, i.e., without nucleation and growth of a second phase, but rather by the continuous increase and decrease of metal occupation of adjacent 1, 1, 1 planes. As discussed in Sections 6.12 and 6.13, there are four wave vectors in the star at the L point, and three possible minima in G vs. η. One minimum corresponds to $R\bar{3}m$ symmetry, another to $Fm3m$ (with twice the lattice parameter of the NaCl-type structure) and a third to $Fd3m$ (again with $a = 2a_0$).

The structure with vacancies ordered in alternate 1, 1, 1 planes has $R\bar{3}m$ symmetry with $a = \sqrt{3}/2a_{\mathrm{NaCl}}$ and $\alpha = \cos^{-1}(5/6)$ (Fig. 11.2) and is the $R\bar{3}m$ structure found by minimization of $G(\gamma_1, \gamma_2, \gamma_3, \gamma_4)$. A second cubic superstructure has also been found for $Zr_{1-x}S$ (Fig. 11.3) with a somewhat larger value of x, and this has been found to refine in the $Fd3m$ type structure. This structure splits the metal atom positions (in the cubic cell with $a = 2a_{\mathrm{NaCl}}$) into two 16-fold positions at 0, 0, 0 and 1/2, 1/2, 1/2, and one of the sites is preferentially occupied, the other is preferentially depleted. The sulfur atoms in the $Fd3m$ superstructure are in 32-fold

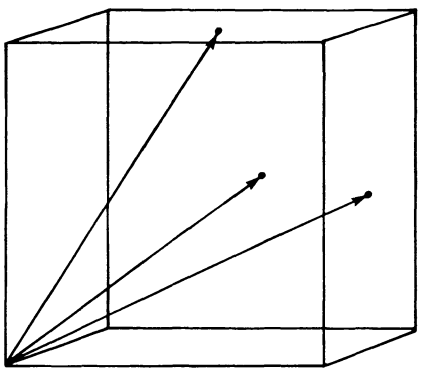

Fig. 11.2. Rhombohedral superlattice for $Sc_{1-x}S$ and $Zr_{1-x}S$.

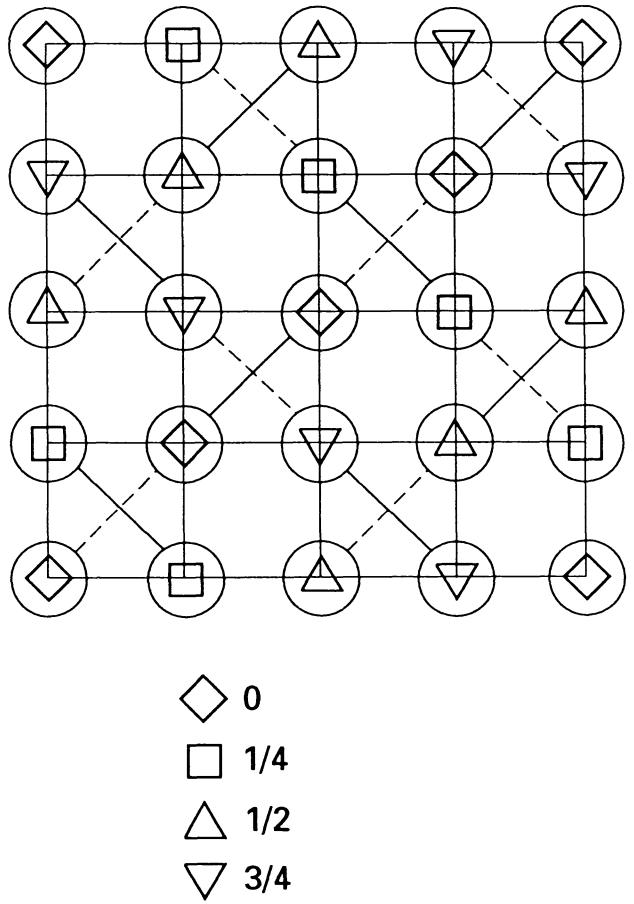

Fig. 11.3. $Fd3m$ ordering in $Zr_{1-x}S$.

positions at $1/4+\delta$, $1/4+\delta$, $1/4+\delta$, i.e., they are free to move parallel to the body diagonal.

The configuration entropy in both cases ($R\bar{3}m$ and $Fd3m$) decreases with ordering from the random value:

$$0.562R = -[3/4\,\ell n\,3/4 + 1/4\,ln\,1/4]R \tag{5}$$

to the ordered (insofar as possible with two equal-fold positions) value of

$$0.347R = -[1/4\,\ell n\,1/2 + 1/4\,\ell n\,1/2]R\,. \tag{6}$$

The configurational entropy corresponding to x (one minus the fractional occupancy of the more highly occupied site and the fractional occupancy of the less occupied site minus 0.50) is, per total mole of $Zr_{1-x}S$:

$$-S/R = 1/2[(1-x)\ell n(1-x) + x\ell nx] + 1/2[(1/2+x)\ell n(1/2+x) + (1/2-x)\ell n(1/2-x)] \quad (7)$$

(see Fig. 11.4) and as T approaches T_t, x approaches 0.25 and the configurational entropy of the defect solid approaches the random value.

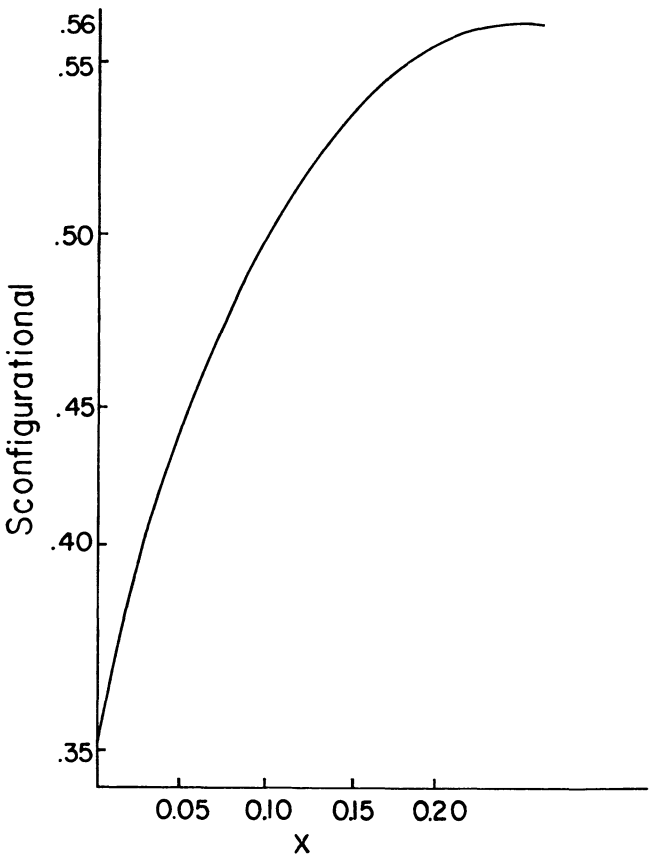

Fig. 11.4. Configurational entropy vs. fractional occupancy.

The G expansion (from Section 6.13) is

$$G = G^{\circ} + A\eta^2 + [C_1 + C_2[\gamma_1^4 + \gamma_2^4 + \gamma_3^4 + \gamma_4^4] + C_3\gamma_1\gamma_2\gamma_3\gamma_4]\eta^4 \quad (8)$$

and this has a minimum for $\gamma_1 = 1, \gamma_2 = \gamma_3 = \gamma_4 = 0$ when $C_2 < -|C_3|/12$ and a minimum for $\gamma_1 = \gamma_2 = \gamma_3 = -\gamma_4 = 1/2$ when $C_2 > -|C_3|/12$ and $C_3 > 0$. Thus, one can schematically represent a phase diagram in terms of the conditions $A(T, \mathrm{S/Zr}) = 0$ and $12C_2(T, \mathrm{S/Zr}) = -|C_3(T, \mathrm{S/Zr}|$ (see Fig. 11.4). The region separating the $Fd3m$ and $R\bar{3}m$ superstructures is necessarily a two-phase region because neither space-group is a subgroup of the other, and therefore, by the Landau conditions, a second-order transition is not allowed, and by the Gibbs-Konovalow equation (Section 7.16) a two-phase region must separate the two phases when they coexist.

The point of intersection of the T vs. S/Zr curves implied by $A = 0$ and $C_2 = -|C_3|/12$ is a critical point at which all three phases have the same stability. A system which is cooled too rapidly through a state near to this critical point will tend to have mixtures of ordering of the various kinds allowed by the minima in G. Thus, phases that correspond to different stable solutions consistent with the star of the wave vectors will mix and yield a complex mixture of domains unless the sample is cooled slowly. The resultant crystal will exhibit a widespread twinning and confused superstructure crystallinity superimposed upon the coherent substructure lattice.

That this does in fact occur is suggested by the fact that the single crystal structures do not always correspond to known bulk phases in a system. For example, a strange structure was found for $Zr_{0.77}S$ that had been quenched from high temperature.[3] The structure was reported to have $C2/m$ symmetry with $a = 2a_{\mathrm{NaCl}}$, $b = 2a_{\mathrm{NaCl}}$ and $c = \sqrt{2}a_{\mathrm{NaCl}}$ with $\beta = 135.06°$. The lattice was very little distorted relative to cubic (Table 11.2). There were six independent Zr atom sites in the structure and these were determined to be fractionally occupied as shown in Table 11.2. This structure has never been found to correspond to a bulk sample as observed by powder diffraction. It therefore seems likely that this structure occurred for a small region of a sample that was quenched through a point in the neighborhood of the critical point discussed above, and that other different metastable regions of the solid occur in other regions of the structure.

The occurrence of such nonequilibrium order-disorder multiple twins is expected when a sample which orders according to a star containing more

Table 11.1. Lattice parameters for $Zr_{0.77}S$.

$a/(2a_{NaCl})$	1.003
$b/(2a_{NaCl})$	0.999
$c/(\sqrt{2}a_{NaCl})$	1.004
β/β_{NaCl}	1.000 4

Table 11.2. Fractional occupancy of Zr sites in $Zr_{0.77}S$.

Wycott notation	% occupancy
a	107 ± 8
b	27 ± 8
c	63 ± 8
d	79 ± 8
e	69 ± 7
f	85 ± 7

than one wave-vector is quenched through a transition region close to the critical point. The effect can be checked for comparing the powder pattern calculated using the single-crystal structure with that observed from a bulk sample. The most powerful comparison is accomplished using a full-profile (Rietveld) least squares calculation.

11.3. Incommensurate Structure

It has been observed in both $Sc_{1-x}S$ and $Zr_{1-x}S$ that there is a tendency for the vacancies to further order by tripling or nearly tripling the period perpendicular to the body diagonal.[2] A $\bar{1}, 1, 0$ tripling would give rise to a monoclinic structure with C_2 symmetry and

$$\begin{pmatrix} \mathbf{a} \\ \mathbf{b} \\ \mathbf{c} \end{pmatrix}_{cm} = \begin{pmatrix} 1/2 & 1/2 & \bar{1} \\ \bar{3}/2 & 3/2 & 0 \\ 2 & 2 & 2 \end{pmatrix} \begin{pmatrix} \mathbf{a} \\ \mathbf{b} \\ \mathbf{c} \end{pmatrix}_{NaCl} . \tag{9}$$

However, in $Sc_{1-x}S$ the period is not exactly tripled. The near tripling occurs in the following way: the vacancies order so as to triple the period along the $1, \bar{1}, 0$ direction, but with *nearly* periodic disruption of the tripling by faults. Thus, the ordering occurs such that two adjacent planes have

increased occupancy followed a third with decreased occupancy, i.e., $++-+++-++-\ldots$, but occasionally a $-+-$ fault appears (see Fig. 11.6a). This can be mathematically modeled by the function shown in Fig. 11.6b. The distance L is not exactly 3 times the interplanar spacing and thus the function is *incommensurate* with the planes. If the planes were incremented and decremented in exact accordance with the math function of Fig. 11.6b, however, the disruption of the tripling would be periodic, although with a rather long period. On the basis of the experimental results discussed below, as well as on the basis of the fact that a tripling in this direction would not correspond to a special point and thus by Landau theory is not expected to yield a commensurate structure, this ordering was assumed

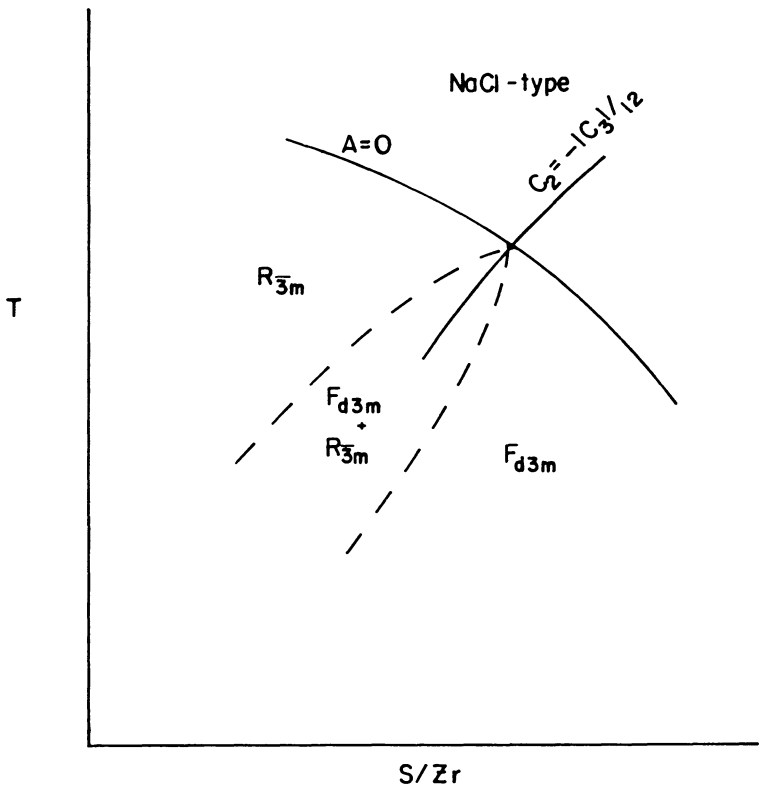

Fig. 11.5. Schematic phase diagram for L-point ordering in $Zr_{1-x}S$.

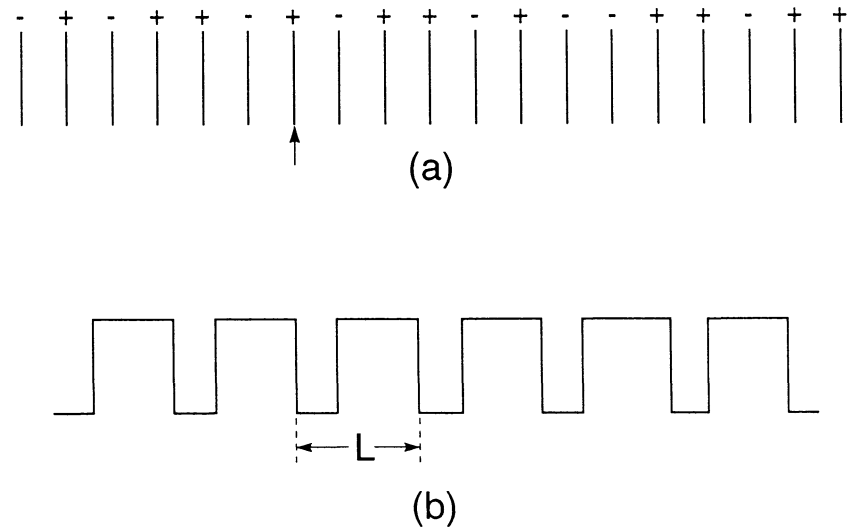

Fig. 11.6. Incommensurate population wave for $Sc_{1-x}S$.

to be incommensurate by virtue of an aperiodic character of the ordering function of Fig. 11.6b.

The experimental consequences of a vacancy order such as mathematically modeled in Fig. 11.6b can be discovered by modulating the atomic scattering factor by that function. The function can be expressed as a Fourier series.

$$\phi(x) = \frac{\phi_1 + 2\phi_2}{3} + \sum_{m=0}^{\infty} 2\frac{(\phi_1 - \phi_2)}{m\pi} \sin\left(\frac{m\pi}{3}\right) \cos\left(\frac{2m\pi x}{L}\right). \tag{10}$$

To consider the effect of this (nearly) incommensurate population wave upon diffraction, it is only necessary to modulate the atomic scattering factor of the metal atoms by $\phi(n)$ where n corresponds to the row number (an integer) and where the sum is over the planes and thus is the type discussed in Section 8.1. Thus,

$$FF^* = \left| \sum_{n=1}^{N-1} \phi(n) f_{Sc} \exp 2\pi i n h \right|^2 \tag{11}$$

and using $\cos(2m\pi x/L) = 1/2[\exp(i2m\pi x/L) + \exp -(i2m\pi x/L)]$,

$$FF^* = \left| \sum_{n=1}^{N-1} \frac{\phi_1 + 2\phi_2}{3} f_{Sc} \exp(2\pi inh) \right.$$

$$+ \sum_{m=1}^{\infty} \frac{\phi_1 - \phi_2}{m\pi} f_{Sc} \sin\left(\frac{m\pi}{3}\right) \sum_{n=1}^{N-1} (\exp[2\pi in(h + m/L)]$$

$$\left. + \exp -[2\pi in(h - m/L)]) \right|^2 \tag{12}$$

This expression can be analyzed as follows. First if $L = 3$, then this becomes the condition for constructive interference for the commensurate superstructure and could be straightforwardly obtained by the methods of Chapter 8. Second, if $L \neq 3$ exactly, then the value cf h corresponding to constructive interference is given by

$$h \pm m/L = \text{integer} \tag{13}$$

and the superstructure diffraction is shifted off the integral positions expected for an exact tripling of the period by m/L. Third, in the diffraction pattern only diffractions corresponding to $m = 1$ are observed.

This third point probably derives from the fact that the **k** point to which the ordering corresponds is not a special point, i.e., is not fixed by symmetry, and thus varies with thermodynamic state. In this case the prediction of Eq. 12 is too precise, the long range period that arises from the domains of $\cdots + + - + + - + + - \cdots$ ordering via $\cdots + - + \cdots$ faults (antidomain boundaries) is not precise — the faults occur fairly regularly, but not with the precision required to yield higher order diffraction reflections (as are predicted by Eq. 12). The characteristic feature of an incommensurate structure is that the period varies with thermodynamic state. Landau theory shows that this is the expected behavior when a superstructure does not meet the condition that there exist no vector invariants that transform as the irreducible representation to which the superstructure corresponds. Thus, in principle it is anticipated that a superstructure that triples the period, such as observed in $Sc_{1-x}S$, will occur with domain structure that is incommensurate with the substructure lattice except by chance. Of course, it may be that the energetics of ordering strongly favor a very nearly commensurate structure and the domain structure may therefore be inconsequential.

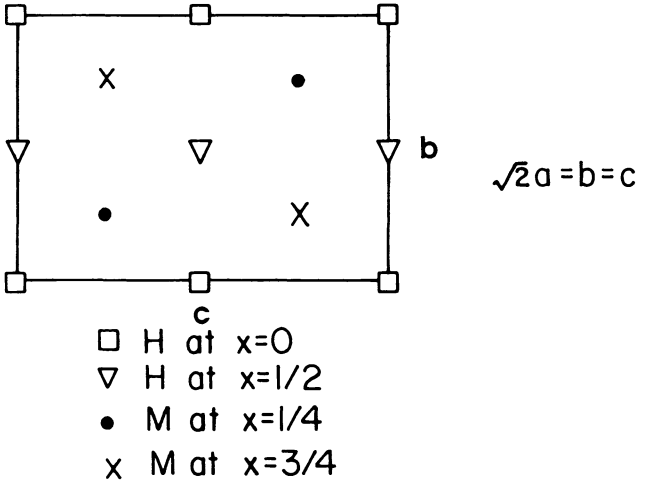

Fig. 11.7. Hydride ordering.

Bibliography

1. S. J. Kim, T. H. Nguyen and H. F. Franzen, The Homogeneity Ranges, Order-Disorder Transition and Structures of the Nonstoichiometric Monosulfides of Zirconium, *J. Solid State Chem.* **70**, 88–92 (1987).
2. H. F. Franzen, R. T. Tuenge and L. Eyring, Vacancy Ordering in $Sc_{1-x}S$, *J. Solid State Chem.* **46**, 206–214 (1983).
3. B. R. Conard and H. F. Franzen, *The Crystal Structures of ZrS and $Zr_{0.77}S$, in The Chemistry of Extended Defects in NonMetallic Solids*, LeRoy Eyring and Michael O'Keefe, Eds. (North-Holland Publishing, London, 1970), 207–219.
4. S. J. Kim, J. W. Anderegg and H. F. Franzen, Structure of a New Intermediate $Lu_{2+x}S_3$ Phase, *J. Less-Common Met.* **157**, 133–138 (1990).

Problems

1. Sketch the clusters of one set of equivalently occupied positions in the $a = 2a_{\mathrm{NaCl}}$, $Fd3m$ superstructure.
2. Find two ordered superlattices that correspond to the W point of $Fd3m$.
3. To what star would a $\sqrt{3} \times \sqrt{3}$ superstructure of hexagonal correspond.
4. Find the star to which ordering on the faces (as opposed to the corners) of *fcc* occurs. Are there other ordered superstructures corresponding to the same star?
5. If atoms and vacancies are random in a square net parallel to c in $P4/mmm$, what space group results and to what wave vector does it correspond if the vacancies preferentially locate in sites along one of the basal directions (e.g., a)? Is there another ordering corresponding to the same star?
6. The structure of Fig. 11.7 is that of an ordered hydride.
   (a) What is the spacing group?
   (b) What is the space group if all H atoms are randomized on all tetrahedral positions?
   (c) Can the transition be second order? The irr. reps. of D_{2h} are

ε	C_{2z}	$C_{2(y-x)}$	$C_{2(x+y)}$	i	σ_z	σ_{y-x}	σ_{x+y}
1	1	1	1	1	1	1	1
1	1	1	1	−1	−1	−1	−1
1	−1	1	−1	1	−1	1	−1
1	−1	1	−1	−1	1	−1	1
1	1	−1	−1	−1	−1	1	1
1	−1	−1	1	1	−1	−1	1
1	−1	−1	1	−1	1	1	−1

This page is intentionally left blank

APPENDIX I

SOLUTIONS TO PROBLEMS

Chapter 1

1. The group consists of $\varepsilon, C_{3v}, C_{3v}^2$. Since $2^2 = 4 > 3$ there msut be 3 1-dimensional irr. reps. One is the totally symmetric. For the remaining two

$$\chi(\varepsilon) + \chi(C_{3v}) + \chi(C_{3v}^2) = 0$$

by orthogonality to the totally symmetric irr. rep. and since $\chi(\varepsilon) = 1$,

$$\chi(C_{3v}) + \chi(C_{3v}^2) = -1\,.$$

Furthermore, $\chi(C_{3v}^2) = \chi^2(C_{3v})$, thus

$$\chi^2(C_{3v}) + \chi(C_{3v}) + 1 = 0$$

and

$$\chi(C_{3v}) = -\frac{1 \pm \sqrt{1-4}}{2} = -1/2 \pm \frac{2\sqrt{3}i}{2}\,.$$

Thus,

ε	C_{3v}	C_{3v}^2
1	1	1
1	$\exp(2\pi i/3)$	$\exp -(2\pi i/3)$
1	$\exp -(2\pi i/3)$	$\exp(2\pi i/3)$

2. See Fig. AI.1.

$x = \ell \cos\alpha$

$y = \ell \sin\alpha$

$x' = -\ell \cos(60 - \alpha) = -\ell(\cos 60 \cos\alpha + \sin 60 \sin\alpha)$

$y' = \ell \sin(60 - \alpha) = \ell(\sin 60 \cos\alpha - \cos 60 \sin\alpha)$

$$\varepsilon : \begin{pmatrix} 1 & 0 & 0 \\ 0 & 1 & 0 \\ 0 & 0 & 1 \end{pmatrix} \begin{pmatrix} x \\ y \\ z \end{pmatrix} = \begin{pmatrix} x' \\ y' \\ z' \end{pmatrix} \qquad \chi = 3$$

$$C_{3v} : \begin{pmatrix} -1/2 & -\frac{\sqrt{3}}{2} & 0 \\ \frac{\sqrt{3}}{2} & -1/2 & 0 \\ 0 & 0 & 1 \end{pmatrix} \begin{pmatrix} x \\ y \\ z \end{pmatrix} = \begin{pmatrix} x' \\ y' \\ z' \end{pmatrix} \qquad \chi = 0$$

$$C_{3v}^2 : \begin{pmatrix} -1/2 & -\frac{\sqrt{3}}{2} & 0 \\ \frac{\sqrt{3}}{2} & -1/2 & 0 \\ 0 & 0 & 1 \end{pmatrix} \begin{pmatrix} x \\ y \\ z \end{pmatrix} = \begin{pmatrix} x' \\ y' \\ z' \end{pmatrix} \qquad \chi = 0$$

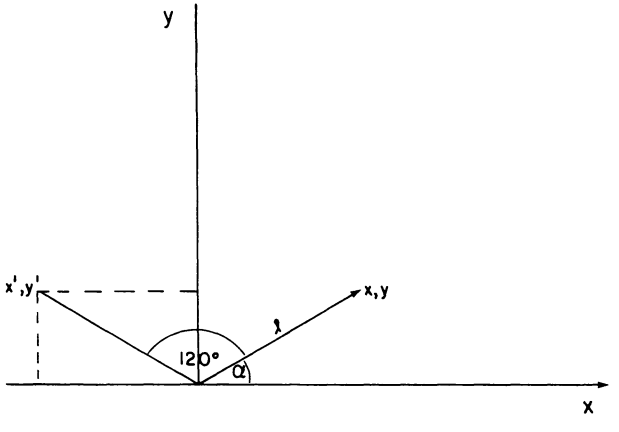

Fig. AI.1. Rotation by 120°.

	ε	C_{3v}	C_{3v}^2
Γ_1	1	1	1
Γ_2	1	$\exp(2\pi i/3)$	$\exp -(2\pi i/3)$
Γ_3	1	$\exp -(2\pi i/3)$	$\exp(2\pi i/3)$
Γ_3	3	0	0

$\Gamma_{\text{red}} = \Gamma_1 + \Gamma_2 + \Gamma_3$

3. (a) $dH = TdS + VdP$

$$dS = \left(\frac{\partial S}{\partial T}\right)_P dT + \left(\frac{\partial S}{\partial P}\right)_T dP$$

$$= C_p/T\, dT + T\left(\frac{\partial V}{\partial T}\right)_P dP$$

$$\Delta\overline{H} = \int \left(\overline{V} + T\left(\frac{\partial \overline{V}}{\partial T}\right)_P\right) dP$$

$$\frac{1}{V}\left(\frac{\partial \overline{V}}{\partial P}\right)_T = -1.87 \times 10^{-7}$$

$$\overline{V} = \overline{V} \exp -(1.87 \times 10^{-7}(P-1)) = 3.419 \exp -1.87 \times 10^{-7} P$$

$$\left(\frac{\partial \overline{V}}{\partial T}\right)_P = 2.7 \times 10^{-6}\overline{V}$$

$$\Delta\overline{H} = \int (\overline{V} + 7.4 \times 10^{-4}\overline{V})\, dP \cong \int \overline{V}\, dP$$

$$\int_1^{1\,000} \overline{V} dP = 3.419 \int_1^{1\,000} \exp -(1.87 \times 10^{-7} P)\, dP = 34\ 150J$$

$$\Delta\overline{U} = \Delta\overline{H} - \Delta(P\overline{V}) = 34\ 150 - 10\left[3\ 419e^{-1.87\times10^{-4}} - 3.419e^{-1.87\times10^{-7}}\right]$$

$$= 34\ 150 - 34\ 149 \cong 0.$$

(b) $dH = TdS + VdP$

$$= CpdT$$

$$\Delta\overline{H} = 6.11[1\ 000 - 298] = 4\ 290\ \text{J mol}^{-1}$$

$$\overline{V} = \overline{V}^0 \exp(2.7 \times 10^{-6}(T - 298))$$

$$\Delta\overline{V} = 3.419(e^{1.9\times10^{-3}} - 1) = 6.5 \times 10^{-3}\text{cm}^3$$

$$\Delta\overline{U} = \Delta\overline{H} - \Delta(P\overline{V}) = \Delta\overline{H} - P\Delta\overline{V} = 4\,290 - 6.5\times10^{-2} = 4\,290\ \text{J mol}^{-1}$$

4. $dU = TdS - PdV + \Sigma\mu_i dn_i$ open system

   $dU = TdS - PdV$ closed system

   if the open and closed pass through the same states (i.e., if the $dn_i = v_i d\xi$'s of the closed system are imitated in the open system), then dU, TdS and PdV are the same in each and

$$\Sigma\mu_i dn_i = 0\,.$$

5. $c = 2$

   $f = c - p + 2 = 2 - 3 + 2 = 1$

   $\therefore T = T(P)$

6. $$\sum_{n=1}^{\infty} \exp(in\pi/10) = \sum_{n=1}^{20} \exp(in\pi/10) + \sum_{n=21}^{40} \exp(in\pi/10) + \ldots$$

   but $\exp i((20+m)\pi/10) = \exp(2\pi i)\exp(im\pi/10)$

   $$= \exp(im\pi/10)$$

   $$\therefore \sum_{n=1}^{\infty} \exp(in\pi/10) = \sum_{n=1}^{20} \exp(in\pi/10) + \sum_{n=1}^{20} \exp(in\pi/10) \ldots$$

   and

   $$\sum_{n=1}^{20} \exp(in\pi/10) = \sum_{n=1}^{10} \exp(in\pi 10) + \sum_{n=11}^{20} \exp(in\pi/10)$$

   $$= \sum_{n=1}^{10} (\exp(in\pi/10) + \exp i\pi \exp(in\pi 10))$$

   $$= 0.$$

7. $|F|^2 = FF^*$

$= (6\exp(i\pi/3) + 8\exp(i\pi/6))(6\exp(-i\pi/3) + 8\exp(-i\pi/6))$

$= 36 + 64 + 48(\exp(i\pi/3)\exp(-i\pi/6) + \exp(i\pi/6)\exp(-i\pi/3))$

$= 36 + 64 + 48(\exp(i\pi(1/3 - 1/6) + \exp(i\pi(1/6 - 1/3)))$

$= 36 + 64 + 48[\exp(i\pi/6) + \exp(-i\pi/6)]$

$= 36 + 64 + 48 \cdot 2 \cdot \cos(\pi/6)$

$= 183.14$

$|F| = \sqrt{183.14} = 13.53.$

8.

$x\ y\ z$	$\bar{y}\ x\ z$	$\bar{x}\ \bar{y}\ z$	$y\ \bar{x}\ z$
$\sin \pi x$	$-\sin \pi y$	$-\sin \pi x$	$\sin \pi y$
$\sin \pi y$	$\sin \pi x$	$-\sin \pi y$	$-\sin \pi x$

r_{red}	$\begin{pmatrix} 1 & 0 \\ 0 & 1 \end{pmatrix}$	$\begin{pmatrix} 0 & \bar{1} \\ 1 & 0 \end{pmatrix}$	$\begin{pmatrix} \bar{1} & 0 \\ 0 & \bar{1} \end{pmatrix}$	$\begin{pmatrix} 0 & 1 \\ \bar{1} & 0 \end{pmatrix}$
χ_{red}	2	0	-2	0
χ_1	1	i	-1	$-i$
χ_2	1	$-i$	-1	i

(χ_1 and χ_2 from Table 1.6)

Chapter 2

1. $V = \mathbf{a} \cdot \mathbf{b} \times \mathbf{c} = \mathbf{b} \cdot \mathbf{c} \times \mathbf{a}$

$|\mathbf{c} \times \mathbf{a}| = ac \sin \beta$

$\mathbf{b} \cdot \mathbf{c} \times \mathbf{c} = |\mathbf{b}||\mathbf{c} \times \mathbf{a}| = abc \sin \beta.$

2. C_{2v} consists of two vertical reflection planes and a 2-fold axis along their intersection, but all lattices have inversion symmetry through each lattice point and a vertical 2-fold means a 2-fold through each lattice point. Therefore, vertical two-folds pass through inversion centers implying horizontal mirrors.

3. See Fig. AI.2.
   The body-centers (x's at $z = 1/2$) destroy the $6/mmm$ symmetry — mmm symmetry remains and the lattice is *fco*.

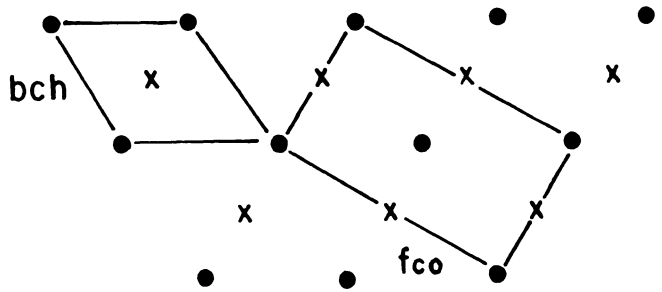

Fig. AI.2. *bch* equals *fco*.

4. (a) See Fig. AI.3.

4. (b) See Fig. AI.4, the result is primitive rhombohedral.

5. $\mathbf{a}_r = (a_{bcc}/2)(-\mathbf{i}+\mathbf{j}+\mathbf{k})$

   $\mathbf{b}_r = (a_{bcc}/2)(\mathbf{i}-\mathbf{j}+\mathbf{k})$

   $\mathbf{a}_r \cdot \mathbf{a}_r = a_r^2 = (a_{bcc}^2/4)(1+1+1)$

   $a_r = (\sqrt{3}/2)a_{bcc}$

   $\mathbf{a}_{rh} \cdot \mathbf{b}_{rh} = (a_{bcc}^2/4)(-1-1+1) = -(a_{bcc}^2/4)$

   $= a_r^2 \cos\alpha = (3/4)a_{bcc}^2 \cos\alpha$

   $\cos\alpha = -1/3, \alpha = 109.47°$.

6. See Fig. AI.5.

7. $$\begin{pmatrix} 1 & 0 & 0 \\ 0 & \bar{1} & 0 \\ 0 & 0 & \bar{1} \end{pmatrix} \times \begin{pmatrix} 0 & 1 & 0 \\ 1 & 0 & 0 \\ 0 & 0 & \bar{1} \end{pmatrix} = \begin{pmatrix} 0 & 1 & 0 \\ \bar{1} & 0 & 0 \\ 0 & 0 & 1 \end{pmatrix}$$

   $$\begin{pmatrix} 0 & 1 & 0 \\ \bar{1} & 0 & 0 \\ 0 & 0 & 1 \end{pmatrix} \times \begin{pmatrix} 0 & 1 & 0 \\ \bar{1} & 0 & 0 \\ 0 & 0 & 1 \end{pmatrix} \times \begin{pmatrix} 0 & 1 & 0 \\ \bar{1} & 0 & 0 \\ 0 & 0 & 1 \end{pmatrix} = \begin{pmatrix} 0 & \bar{1} & 0 \\ 1 & 0 & 0 \\ 0 & 0 & 1 \end{pmatrix}$$

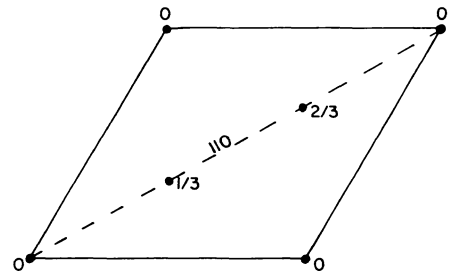

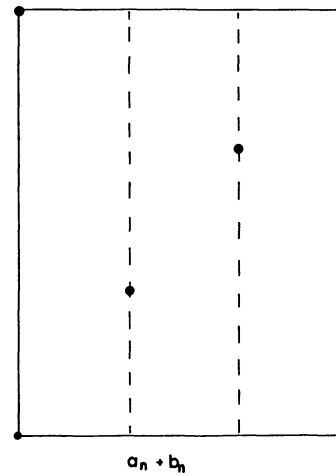

Fig. AI.3. The 110 hexagonal plane for a rhombohedral lattice.

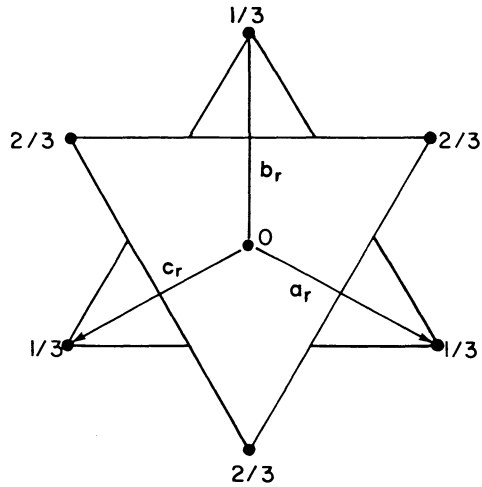

Fig. AI.4. *bcr* = *pr*.

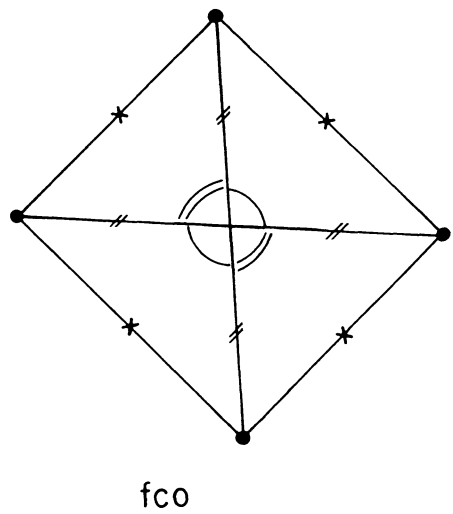

Fig. AI.5. *fco* vis distortion of pt.

8. $$\begin{pmatrix}\mathbf{a}\\ \mathbf{b}\\ \mathbf{c}\end{pmatrix}_r = \begin{pmatrix}-1/2 & 1/2 & 1/2\\ 1/2 & -1/2 & 1/2\\ 1/2 & 1/2 & -1/2\end{pmatrix}\begin{pmatrix}\mathbf{a}\\ \mathbf{b}\\ \mathbf{c}\end{pmatrix}$$

$$\begin{pmatrix}\mathbf{a}\\ \mathbf{b}\\ \mathbf{c}\end{pmatrix}_h = \begin{pmatrix}\bar{1} & 1 & 0\\ 0 & \bar{1} & 1\\ 1 & 1 & 1\end{pmatrix}\begin{pmatrix}\mathbf{a}\\ \mathbf{b}\\ \mathbf{c}\end{pmatrix}_r$$

$$\begin{pmatrix}\mathbf{a}\\ \mathbf{b}\\ \mathbf{c}\end{pmatrix}_r = \begin{pmatrix}-2/3 & -1/3 & 1/3\\ 1/3 & -1/3 & 1/3\\ 1/3 & 2/3 & 1/3\end{pmatrix}\begin{pmatrix}\mathbf{a}\\ \mathbf{b}\\ \mathbf{c}\end{pmatrix}_h$$

$$\mathbf{a}_r = \frac{-2\mathbf{a}_h - \mathbf{b}_h + \mathbf{c}_h}{3} = \text{stacking vector}$$

$$\mathbf{c}_h = \mathbf{a}_r + \mathbf{b}_r + \mathbf{c}_r = \frac{\mathbf{a}_c + \mathbf{b}_c + \mathbf{c}_c}{2}$$

$$|\mathbf{c}_h| = (\sqrt{3}/2)a_{bcc}$$

$$\mathbf{a}_h = \mathbf{b}_r - \mathbf{a}_r = \mathbf{a}_c - \mathbf{b}_c$$

$$|\mathbf{a}_h| = \sqrt{2}a_{bcc}$$
$$|\mathbf{c}_h| = (\sqrt{3}/(2\sqrt{2}))|\mathbf{a}_h|$$

$$\text{stacking vector} = \frac{-2\mathbf{a}_h - \mathbf{b}_h}{3} + \frac{\mathbf{c}_h}{3}$$

$$\mathbf{c}_h = \frac{\mathbf{a}_h \times \mathbf{b}_h \cdot |\mathbf{c}_h|}{|\mathbf{a}_h|^2 \sin 120} = \frac{\mathbf{a}_h \times b_h \cdot \sqrt{3}|\mathbf{a}_h|}{|a_h|^2(\sqrt{3}/2)\cdot 2\sqrt{2}}$$
$$= \frac{\mathbf{a}_h \times \mathbf{b}_h}{\sqrt{2}|\mathbf{a}_h|}$$

$$\text{stacking vector} = \frac{-2\mathbf{a}_h - \mathbf{b}_h}{3} + \frac{\mathbf{a}_h \times \mathbf{b}_h}{3\sqrt{2}|\mathbf{a}_h|}.$$

9. $$a^* = \frac{2\pi \mathbf{b}_r \times \mathbf{c}_r}{V} = \frac{\frac{2\pi[\mathbf{i}-\mathbf{j}+\mathbf{k}}{2} \times \frac{\mathbf{i}+\mathbf{j}-\mathbf{k}]}{2} a^2}{a^3/2}$$

$$= (2\pi/a)[\mathbf{j}+\mathbf{k}]$$

$$\mathbf{b}^* = \frac{2\pi \mathbf{c}_r \times \mathbf{a}_r}{V} = (2\pi/a)(\mathbf{i}+\mathbf{k})$$

$$\mathbf{c}^* = \frac{2\pi \mathbf{a}_r \times \mathbf{b}_r}{V} = (2\pi/a)(\mathbf{i}+\mathbf{j})$$

$$K_{2,3,5} = (2\pi/a)[2\mathbf{j}+2\mathbf{k}+3\mathbf{i}+3\mathbf{k}+5\mathbf{i}+5\mathbf{j}]$$

$$= (2\pi/a)[8\mathbf{i}+7\mathbf{j}+5\mathbf{k}]$$

$$\mathbf{K}\cdot\mathbf{K} = (4\pi^2/d^2) = (4\pi 2)[64+25+49]$$

$$d = \frac{a}{\sqrt{138}}$$

10. (a) For cubic

$$\mathbf{a}^* = 2\pi\mathbf{i}/a, \quad \mathbf{b}^* = 2\pi\mathbf{j}/a, \quad \mathbf{c}^* = 2\pi\mathbf{k}/a$$

thus, by the above

$$\mathbf{K}_{2,3,5} = 8\mathbf{a}^*_{bcc} + 7\mathbf{b}^*_{bcc} + 5\mathbf{c}^*_{bcc}$$

and the planes are the cubic 8,7,5 planes.

(b) $$\begin{pmatrix} 0 & 1 & 1 \\ 1 & 0 & 1 \\ 1 & 1 & 0 \end{pmatrix} \begin{pmatrix} 2 \\ 3 \\ 5 \end{pmatrix} = \begin{pmatrix} 8 \\ 7 \\ 5 \end{pmatrix}$$

(c) $$\begin{pmatrix} 0 & 1 & 1 \\ 1 & 0 & 1 \\ 1 & 1 & 0 \end{pmatrix} \begin{pmatrix} \overline{1/2} & \underline{1/2} & 1/2 \\ 1/2 & \underline{1/2} & \underline{1/2} \\ 1/2 & 1/2 & \overline{1/2} \end{pmatrix} = \begin{pmatrix} 1 & 0 & 0 \\ 0 & 1 & 0 \\ 0 & 0 & 1 \end{pmatrix}$$

11. $$\begin{pmatrix} 0 & 1 & 1 \\ 1 & 0 & 1 \\ 1 & 1 & 0 \end{pmatrix} \begin{pmatrix} 1/8 \\ 3/8 \\ 5/8 \end{pmatrix} = \begin{pmatrix} 1 \\ 3/4 \\ 1/2 \end{pmatrix}$$

12. $r_{11} = 15.25$

$r_{22} = 25.00$

$r_{33} = 22.25$

$r_{12} = 9.00$

$r_{13} = 6.25$

$r_{23} = 16.00$

$r_{22}/2 = 12.5 > 9.00 = r_{12}$ $\therefore$ **b** can be reduced by **a**, i.e., $\mathbf{b}_1 = \mathbf{b}_0 - \mathbf{a}_0$

$r_{11} = 15.25$

$r_{22} = b_0^2 + a_0^2 - 2\mathbf{a}_0 \cdot \mathbf{b}_0 = 25 + 15.25 - 18.00 = 22.25$

$r_{33} = 22.25$

$r_{12} = (\mathbf{b}_0 - \mathbf{a}_0) \cdot \mathbf{a}_0 = 9.00 - 15.25 = -6.25$

$r_{13} = 6.25$

$r_{23} = (\mathbf{b}_0 - \mathbf{a}_0) \cdot \mathbf{c}_0 = 16.00 - 6.25 = 9.75$

This cannot be further reduced but it is not in a standard setting since two r_{ij}'s are positive and c is not less than band a. Transforming according to line 13 of Table 2.5.

$r_{11} = 22.25$

$r_{22} = 22.25$

$r_{33} = 15.25$

$r_{12} = 9.75$

$r_{13} = -6.25$

$r_{23} = -6.25$

which according to Appendix II is *fco*. To find the reduced cell for *fco*

$$\mathbf{a} = (a_{fco}/2)\mathbf{i} + (b_{fco}/2)\mathbf{j}$$
$$\mathbf{b} = (b_{fco}/2)\mathbf{j} + (c_{fco}/2)\mathbf{k}$$
$$\mathbf{c} = (a_{fco}/2)\mathbf{i} + (\mathbf{c}_{fco}/2)\mathbf{k}\,.$$

$$r_{11} = 1/4(a_{fco}^2 + b_{fco}^2)$$
$$r_{22} = 1/4(b_{fco}^2 + c_{fco}^2)$$
$$r_{33} = 1/4(a_{fco}^2 + c_{fco}^2)$$
$$r_{12} = b_{fco}^2/4$$
$$r_{13} = a_{fco}^2/4$$
$$r_{23} = c_{fco}^2/4.$$

If $c_{fco} > b_{fco} > a_{fco}$, then

$$1/2r_{22} = 1/8(b_{fco}^2 + c_{fco}^2) > 1/4b_{fco}^2 = r_{12}$$

and b can be reduced by a:

$$\mathbf{b} = 1/2(b_{fco}\mathbf{j} + c_{fco}\mathbf{k} - a_{fco}\mathbf{i} - b_{fco}\mathbf{j})$$
$$= 1/2(c_{fco}\mathbf{k} - a_{fco}\mathbf{i})$$

and

$$r_{11} = 1/4(a_{fco}^2 + b_{fco}^2)$$
$$r_{22} = 1/4(a_{fco}^2 + c_{fco}^2)$$
$$r_{33} = 1/4(a_{fco}^2 + c_{fco}^2)$$
$$r_{12} = 1/4(c_{fco}\mathbf{k} - a_{fco}\mathbf{i}) \cdot (a_{fco}\mathbf{i} + b_{fco}\mathbf{j}) = -1/4a_{fco}^2$$
$$r_{13} = 1/4a_{fco}^2$$
$$r_{23} = 1/4(c_{fco}\mathbf{k} - a_{fco}\mathbf{i}) \cdot (a_{fco}\mathbf{i} + c_{fco}\mathbf{k}) = 1/4(c_{fco}^2 - a_{fco}^2)$$

Now $r_{11} < r_{22} = r_{33}$ and standard form requires $r_{33} < r_{11} = r_{22}$ thus transform according to line 13 of Table 2.5

$$r_{11} = 1/4(a_{fco}^2 + c_{fco}^2)$$
$$r_{22} = 1/4(a_{fco}^2 + c_{fco}^2)$$
$$r_{33} = 1/4(a_{fco}^2 + b_{fco}^2)$$
$$r_{12} = -1/4(c_{fco}^2 + a_{fco}^2)$$
$$r_{13} = -1/4a_{fco}^2$$
$$r_{23} = -1/4a_{fco}^2$$

Thus, $a_{fco}^2 + c_{fco}^2 = 4 \cdot 22.25 = 89$

$a_{fco}^2 + b_{fco}^2 = 4 \cdot 15.25 = 61$

$c_{fco}^2 - a_{fco}^2 = 4 \cdot 9.75 = 39$

$a_{fco}^2 = 4 \cdot 6.25 = 25$

and $a = 5.00$ Å, $b = 6.00$ Å and $c = 8.00$ Å.

Chapter 3

1. If $C_{5z}|\mathbf{c}/5 + \mathbf{t}_\perp$ were a sym. op., then also would $C_{5z}^{-1}| - \mathbf{c}/5 - C_{5z}^{-1}\mathbf{t}_\perp$ (its inverse) be, and then if $\varepsilon|\mathbf{T}$ is any pure transition so too is

$$C_{5z}|\mathbf{C}/5 + \mathbf{t}_1 \cdot \varepsilon|\mathbf{T} \cdot C_{5z}^{-1}| - \mathbf{c}/5 - C_{5z}^{-1}\mathbf{t}_\perp = C_{5z}|\mathbf{T}.$$

Let $\mathbf{T}_{\min}$ be the shortest translation in a plane perpendicular to $\mathbf{c}$. Then (Fig. AI.6)

$$|\mathbf{T}_{\min}|[1 - 2\cos 72°] < |\mathbf{T}_{\min}|.$$

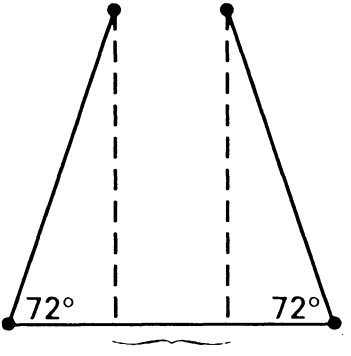

Fig. AI.6. Rotation by C_5 is incompatible with translational periodicity.

2. $$\begin{pmatrix} 0 & 1 & 0 & t_1 \\ 1 & 0 & 0 & t_2 \\ 0 & 0 & 1 & t_3 \\ 0 & 0 & 0 & 1 \end{pmatrix} \begin{pmatrix} 0 & 1 & 0 & t_1 \\ 1 & 0 & 0 & t_2 \\ 0 & 0 & 1 & t_3 \\ 0 & 0 & 0 & 1 \end{pmatrix} = \begin{pmatrix} 1 & 0 & 0 & t_2 + t_1 \\ 0 & 1 & 0 & t_2 + t_1 \\ 0 & 0 & 1 & 2t_3 \\ 0 & 0 & 0 & 1 \end{pmatrix}$$

$t_1 + t_2 = 1/2$ and $2t_3 = 1/2$.

The origin can be placed in the mirror plane in which case $t_1 - t_2 = 0$ and thus $t_1 = t_2 = t_3 = 1/4$. The origin could also be shifted by $t_1 - t_2 = 1/2$, in which case $t_1 = 1/2, t_2 = 0$ and $t_3 = 1/4$.

3. Without loss of generality let the mirror operation be $\sigma_x|0$. Then

$$\varepsilon|(\mathbf{a}+\mathbf{b}+\mathbf{c})/2 \cdot \sigma_x|0 = \sigma_x|(\mathbf{a}+\mathbf{b}+\mathbf{c})/2$$

which is the operation of an n-glide at $x = 1/4$. Also

$$\varepsilon|\mathbf{a} \cdot \sigma_x|0 = \sigma_x|\mathbf{a}$$

is the operation of a mirror at $x = 1/2$.

4. $$\begin{pmatrix} \bar{1} & 0 & 0 & t_x \\ 0 & 1 & 0 & 1/2 \\ 0 & 0 & 1 & 0 \\ 0 & 0 & 0 & 1 \end{pmatrix} \begin{pmatrix} 1 & 0 & 0 & 0 \\ 0 & \bar{1} & 0 & t_y \\ 0 & 0 & 1 & 1/2 \\ 0 & 0 & 0 & 1 \end{pmatrix} \begin{pmatrix} 1 & 0 & 0 & 1/2 \\ 0 & 1 & 0 & 1/2 \\ 0 & 0 & \bar{1} & t_z \\ 0 & 0 & 0 & 1 \end{pmatrix} = \begin{pmatrix} \bar{1} & 0 & 0 & t_x - 1/2 \\ 0 & \bar{1} & 0 & t_y \\ 0 & 0 & \bar{1} & t_z + 1/2 \\ 0 & 0 & 0 & 1 \end{pmatrix}$$

placing the origin at the inversion center: $t_x = 1/2, t_y = 0, t_z = 1/2$:

$$\sigma_x|(\mathbf{a}+\mathbf{b})/2, \quad \sigma_y|\mathbf{c}/2, \quad \sigma_z|(\mathbf{a}+\mathbf{b}+\mathbf{c})/2,$$

$$i|0, \quad C_{2x}|(\mathbf{a}+\mathbf{b})/2, \quad \sigma_y|\mathbf{c}/2, \quad \sigma_z|(\mathbf{a}+\mathbf{b}+\mathbf{c})/2$$

1. b-glide $\perp$ to $\mathbf{a}$ at $x = 1/4$, 2. c-glide $\perp$ to $\mathbf{b}$ at $y = 0$, 3. n-glide $\perp$ to $\mathbf{c}$ at $z = 1/4$, 4. inversion at origin, 5. 2_1 parallel to $\mathbf{a}$ at $y = 1/4, z = 0$, 6. 2 parallel to $\mathbf{b}$ at $x = 0, z = 1/4$, 7. 2_1 parallel to $\mathbf{c}$ at $x = y = 1/4$.

5. $C2/c$:$2/m$, $Pna2_1$:$mm2$, $Cmcm$:mmm, $I4$:4, $P4cc$:$4mm$, $P4_2/mcm$:$4/mmm$, $P6_322$:622, $I2_13$:23, $P\bar{4}3n$:$\bar{4}3m$.

6. (a) a 4_1 axis implies $C_{2z}|\mathbf{c}/2+\mathbf{t}_\perp$ body-centering implies $\varepsilon|(\mathbf{a}+\mathbf{b}+\mathbf{c})/2$.

$$\varepsilon|(\mathbf{a}+\mathbf{b}+\mathbf{c})/2 \cdot C_{2z}|\mathbf{c}/2+\mathbf{t}_\perp = C_{2z}|\mathbf{t}'_\perp$$

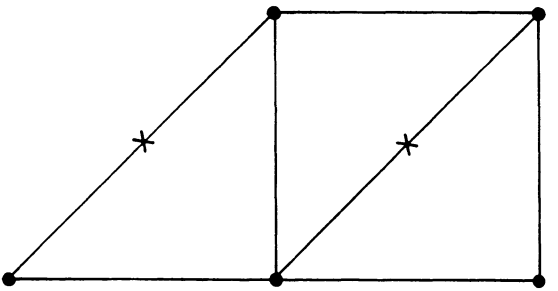

Fig. AI.7. $I2/a$ equivalent to $C2/c$.

(b) a-glide perpendicular to **c**.

$\therefore I2/1 \approx C2/c$ (see Fig. AI.7).

7. C_{3h}: $C_{3z}, C_{3z}^2, \overline{C}_6, \sigma_z, \overline{C}_6^5$

in $P6_3/mmc$: $C_{3z}|0$, $C_{3z}^2|0$, $\sigma_z|\mathbf{c}/2$, $\overline{C}_6|\mathbf{c}/2$, $\overline{C}_6^5|\mathbf{c}/2$

origin shift by $\mathbf{c}/2$ yields $P\bar{6}$.

8. $\bar{x}+1/2, y+1/2, z$

$x, \bar{y}, z+1/2$

$x+1/2, y+1/2, \bar{z}+1/2$

$\bar{x}, \bar{y}, \bar{z}$

$x+1/2, \bar{y}+1/2, \bar{z}$

$\bar{x}, y, \bar{z}+1/2$

$\bar{x}+1/2, \bar{y}+1/2, \bar{z}+1/2.$

9. See Fig. AI.8.

$$\mathbf{a} = \mathbf{a}_{fcc} + (\mathbf{b}_{fcc} + \mathbf{c}_{fcc})/2$$

$$\mathbf{b} = \mathbf{b}_{fcc} + (\mathbf{a}_{fcc} + \mathbf{c}_{fcc})/2$$

$$\mathbf{c} = \mathbf{c}_{fcc} + (\mathbf{a}_{fcc} + \mathbf{b}_{fcc})/2$$

$$a = \sqrt{\mathbf{a} \cdot \mathbf{a}} = \sqrt{3/2}\, a_{fcc}$$

$$= b = c$$

$$\mathbf{a} \cdot \mathbf{b} = (3/2)a_{fcc}^2 \cos\alpha = a_{fcc}^2(\mathbf{i} + (\mathbf{j} + \mathbf{k})/2) \cdot (\mathbf{j} + (\mathbf{i} + \mathbf{k})/2)$$

$$= a_{fcc}^2(1/2 + 1/2 + 1/4) = (5/4)a_{fcc}^2$$

$$\cos\alpha = 5/6$$

$$\alpha = 33.56°$$

Space group: $R\bar{3}m$

Superstructure order is expressed in terms of the primitive cell. (See Fig. AI.9)

$$\mathbf{a}_r = \mathbf{a}_p + \mathbf{b}_p$$

$$\mathbf{b}_r = \mathbf{b}_p + \mathbf{c}_p$$

$$\mathbf{c}_r = \mathbf{c}_p + \mathbf{a}_p$$

$$\text{order} = \begin{vmatrix} 1 & 1 & 0 \\ 0 & 1 & 1 \\ 1 & 0 & 1 \end{vmatrix} = 2.$$

10. See Fig. AI.10.

hex	ortho
$\varepsilon\|0$	$\varepsilon\|0$
$\sigma_{2x+y}\|0$	$\sigma_x\|0$
$\sigma_y\|\mathbf{c}/2$	$\sigma_y\|\mathbf{c}/2$
$\sigma_z\|0$	$\sigma_z\|0$

subgroups: combinations of $\sigma_x|0$, $\sigma_x|(\mathbf{a}+\mathbf{b})/2$, $\sigma_y|\mathbf{c}/2$, $\sigma_y|(\mathbf{a}+\mathbf{b}+\mathbf{c})/2$, $\sigma_z|0$, $\sigma_z(\mathbf{a}+\mathbf{b})/2$

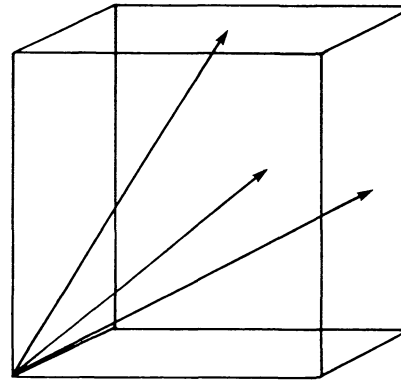

Fig. AI.8. Rhombohedral superstructure of *fcc*.

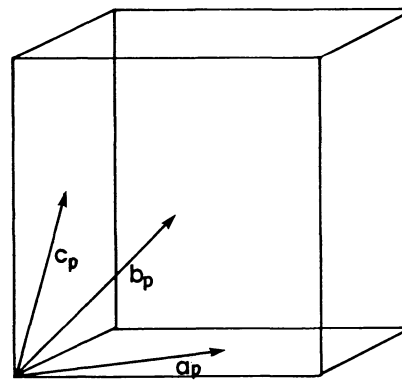

Fig. AI.9. *pr* for *fcc*.

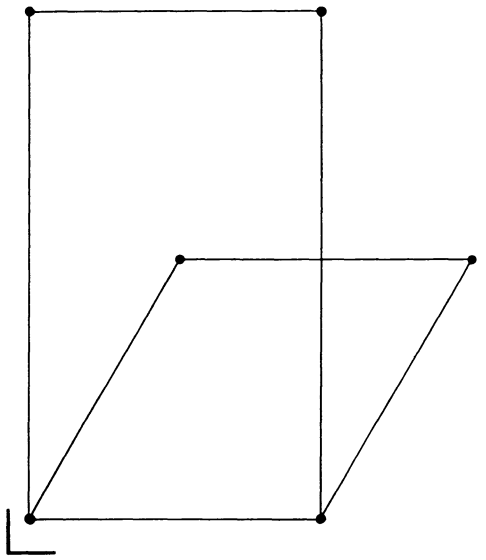

Fig. AI.10

Combinations	Conventional Setting*
Pmcm	*Pmma*
Pmnm	*Pmmn*
Pmcn	*Pnma*
Pmnn	*Pnnm*
Pbcm	*Pbcm*
Pbnm	*Pnma*
Pbcm	*Pbcn*
Pbnn	*Pnna*

*From Int. Tables for X-Ray Cryst. Vol. 1 (1969) Table 6.2.1 of Appendix 6.

11. $\begin{vmatrix} 2 & 1 & 0 \\ 0 & 1 & 0 \\ 0 & 0 & 1 \end{vmatrix} = 2.$

12. Using Table 3.5 we can find the 16 point operations of $D_{4h}(\varepsilon, C_{2x}, C_{2y}, C_{2z}, C_{2(y-x)}, C_{2(x+y)}, C_{4z}, C_{4z}^3, i, \sigma_x, \sigma_y, \sigma_z, \sigma_{y-x}, C_{4z}, \overline{C}_{4z}^3, \sigma_{x+y})$. Among these σ_x, σ_y and σ_z correspond to diamond glides in $Fd3m$. Since it is conventional to describe tetragonal as *bct* and not *fct*, the axes are transformed converting σ_x and σ_y to σ_{x+y} and σ_{y-x} and vice versa (Fig. AI.11). Thus,

$\sigma_x|(\mathbf{a}+\mathbf{b})/4$ becomes $\sigma_z|\mathbf{a}/2$,

$\sigma_x|(\mathbf{b}+\mathbf{c})/4$ becomes $\sigma_{x+y}|(\mathbf{a}+\mathbf{b}+\mathbf{c})/4$,

$\sigma_{x+y}|0$ becomes $\sigma_x|0$.

Thus, the lattice is I and the intersecting planes are *amd*. Now

$$\begin{pmatrix} \bar{1} & 0 & 0 & 0 \\ 0 & 1 & 0 & 1/4 \\ 0 & 0 & 1 & 1/4 \\ 0 & 0 & 0 & 1 \end{pmatrix} \begin{pmatrix} 0 & 1 & 0 & 0 \\ 1 & 0 & 0 & 0 \\ 0 & 0 & 1 & 0 \\ 0 & 0 & 0 & 1 \end{pmatrix} = \begin{pmatrix} 0 & \bar{1} & 0 & 0 \\ 1 & 0 & 0 & 1/4 \\ 0 & 0 & 1 & 1/4 \\ 0 & 0 & 0 & 1 \end{pmatrix}$$

$\sigma_z|(\mathbf{b}+\mathbf{c})/4 \cdot \sigma_{y-x}|0 = C_{4z}|(\mathbf{b}+\mathbf{c})/4$.

Which is the operation of a 4_1 axis and the full symbol is $I4_1/amd$.

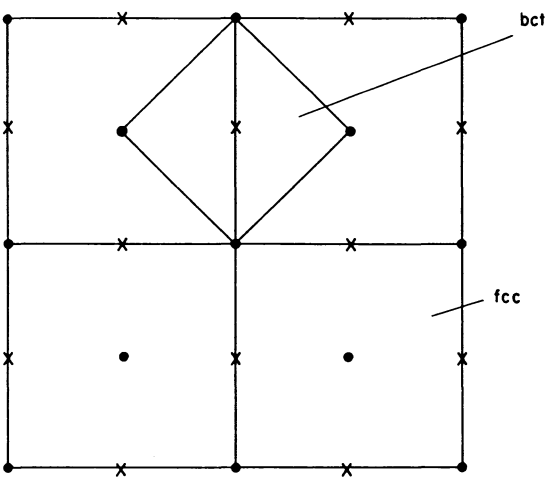

Fig. AI.11. *fcc* equivalent to *bct*.

Chapter 4

1. A star consists of $\mathbf{a}^*/2$, $\mathbf{b}^*/2$ and $(\mathbf{a}^* - \mathbf{b}^*)/2$ (Fig. 4.3). The operations of D_{6h} (Table 3.6) that take $\mathbf{a}^*/2$ into $\pm\mathbf{a}^*/2$ are: ε, C_{2z}, C_{2y}, $C_{2(2x+y)}$, i, σ_z, σ_{2x+y}, thus,

   $$g^0(\mathbf{a}^*/2) = D_{2h}$$

   and $g(\mathbf{a}^*/2) = \{\varepsilon|0, \sigma_x|0, \sigma_y|\mathbf{c}/2, \sigma_x|0, i|0, C_{2x}|0, C_{2y}|\mathbf{c}/2, C_{2z}/0, \varepsilon|\mathbf{T}\}$.

2. A star consists of:

   $$\mathbf{a}^* + \mathbf{b}^*/2,\ \mathbf{a}^* + \mathbf{c}^*/2,\ \mathbf{b}^* + \mathbf{a}^*/2,\ \mathbf{b}^* + \mathbf{c}^*/2,\ \mathbf{c}^* + \mathbf{a}^*/2,\ \mathbf{c}^* + \mathbf{b}^*/2.$$

   Note that $\pm\mathbf{a}^* \pm \mathbf{b}^*/2$ are not equivalent mod $\mathbf{k}$ because $2\mathbf{a}^* + \mathbf{b}^*$ is not a reciprocal lattice vector (Section 2.18) however

   $$-\mathbf{a}^* - \mathbf{b}^*/2 + \mathbf{a}^* + \mathbf{b}^* + \mathbf{c}^* = \mathbf{c}^* + \mathbf{b}^*/2$$

   and thus the negative of the vectors are included mod $\mathbf{K}$.

3. The operations of O_h (Table 3.5) that carry $\mathbf{a}^* + \mathbf{b}^*/2$ into itself mod $\mathbf{K}$ are those that carry x into $\pm x$ and y into itself or x into $\pm z$ and z into $\pm x$ and y into $-y$ (since $\pm\mathbf{c}^* - \mathbf{b}^*/2$ equals $\mathbf{a}^* + \mathbf{b}^*/2$ modulo $-\mathbf{a}^* - \mathbf{b}^* + \mathbf{c}^*$ or $-\mathbf{a}^* - \mathbf{b}^* - \mathbf{c}^*$). Thus, the operations in $g(\mathbf{a}^* + \mathbf{b}^*/2)$ are $\varepsilon|0$, $C_{2y}|0$, $C_{2(z-x)}|0$, $C_{2(x+y)}|0$, $\sigma_x|0$, $\sigma_z|0$, $\overline{C}_{4y}|0$, and $C_{4y}^3|0$ i.e., $g(\mathbf{a}^* + \mathbf{b}^*/2) = \bar{4}m2$.

4. The star contains $(\mathbf{a}^* + \mathbf{b}^* + \mathbf{c}^*)/2$, $(\mathbf{a}^* + \mathbf{b}^* - \mathbf{c}^*)/2$, $(\mathbf{a}^* - \mathbf{b}^* + \mathbf{c}^*)/2$, $(-\mathbf{a}^* + \mathbf{b}^* + \mathbf{c}^*)/2$, and operations to which $(\mathbf{a}^* + \mathbf{b}^* + \mathbf{c}^*)/2$ remains invariant are those which permute x, y, and z without sign change, or with all signs changed. According to Table 3.5 these are ε, $C_{3(x+y+z)}^2$, $C_{3(x+y+z)}$, $C_{2(y-x)}$, $C_{2(z-y)}$, $C_{2(z-x)}$, i, $\overline{C}_{3(x+y+z)}$, $\overline{C}_{3(x+y+z)}$, σ_{y-x}, σ_{z-y}, σ_{z-x}. These are the operations of $R\bar{3}m$.

5. $g(\mathbf{a}^*/2)$ is given in the solution of Problem 1 and is *Pmcm*. Each of the symmetry operations can be replaced by itself together with $(\mathbf{a} + \mathbf{b})/2$, i.e., *mcm*, *bcm*, *bnm*, *bnn*, *mmm*, *mnn*, *mcn*.

6. $$\mathbf{K} \cdot \mathbf{r} = (\mathbf{a}^* + 2\mathbf{b}^* + 3\mathbf{c}^*) \cdot (x\mathbf{a} + y\mathbf{b} + z\mathbf{c})$$
   $$= 2\pi(x + 2y + 3z)$$

   Translation by $\mathbf{T} = m\mathbf{a} + n\mathbf{b} + p\mathbf{c}$ takes $x + 2y + 3z$ into $x + 2y + 3z + m + 2n + 3p$ and thus

$\exp i\mathbf{K}\cdot\mathbf{r} = \exp 2\pi i(x+y+3z)$ into $\exp 2\pi i(m+2n+3p)\exp 2\pi i(x+2y+3z)$

and

$\exp 2\pi i(m+2n+3p) = 1.$

7. $\mathbf{k}\cdot\mathbf{r} = (\mathbf{a}^*/3)\cdot(x\mathbf{a}+y\mathbf{b}+z\mathbf{c}) = 2\pi x/3$

   and $x+x+3m$ takes $\cos(2\pi x/3)$ into $\cos((2\pi x/3)+2\pi m) = \cos(2\pi x/3)$.

8. $I4_1/amd$ is in the crystal class $4/mmm(D_{4h})$, therefore it has lattice symmetry D_{4h} and this is, therefore, the symmetry of the BZ.

9. D_{4h} contains the symmetry elements in Table 3.5 that carry z into $\pm z$, i.e., ε, C_{2x}, C_{2y}, C_{2z}, $C_{2(y-x)}$, C_{4z}, C_{4z}^3, $C_{2(x+y)}$, i, σ_x, σ_y, σ_z, σ_{y-x}, $\overline{C}_{4z}^3$, $\overline{C}_{4z}$, σ_{x+y}. Among these ε, C_{2x}, C_{2y}, C_{2z}, i, σ_x, σ_y, σ_z carry $\mathbf{a}^*/2$ into $\pm\mathbf{a}^*/2$, i.e., into $(\mathbf{a}^*/2)$ mod $\mathbf{a}^*$. Thus $g^0(\mathbf{a}^*/2) = D_{2h}$. The corresponding space group operations in $I4_1/amd$ are generated by $\sigma_x|0$, $\sigma_y|0$, and $\sigma_2|\mathbf{a}/2$, thus $g(\mathbf{a}^*/2) = Imma$.

10. Special points arise because some operations in $g^0(\mathbf{k})$ take $\mathbf{k}$ into $\mathbf{k}$ mod $\mathbf{K}$ at that point, but not at neighboring points.

    σ_x, i, C_{2x} and C_{2y} take $\mathbf{c}^*/2$ into $\mathbf{c}^*/2$ mod $\mathbf{c}^*$

    σ_x, i, C_{2y} and C_{2z} take $\mathbf{a}^*/2$ into $\mathbf{a}^*/2$ mod $\mathbf{a}^*$

    σ_y, i, C_{2x} and C_{2y} take $\mathbf{b}^*/2$ into $\mathbf{b}^*/2$ mod $\mathbf{b}^*$

    σ_x, σ_y, σ_z, i, C_{2x} and C_{2y}, C_{2z}, take $(\mathbf{a}^*+\mathbf{b}^*)/2, (\mathbf{b}^*+\mathbf{c}^*)/2$, $(\mathbf{a}^*+\mathbf{c}^*)/2$ and $(\mathbf{a}^*+\mathbf{b}^*+\mathbf{c}^*)/2$ into themselves mod $\mathbf{K}$.

    Special Points: 0, $\mathbf{a}^*/2$, $\mathbf{b}^*/2$, $\mathbf{c}^*/2$, $(\mathbf{a}^*+\mathbf{b}^*)/2$, $(\mathbf{b}^*+\mathbf{c}^*)/2$, $(\mathbf{a}^*+\mathbf{c}^*)/2$ and $(\mathbf{a}^*+\mathbf{b}^*+\mathbf{c}^*)/2$.

11.

$$V^* = \mathbf{a}^* \cdot \mathbf{b}^* \times \mathbf{c}^*$$

$$= 8\pi^3 \frac{\mathbf{b} \times \mathbf{c} \cdot (\mathbf{c} \times \mathbf{a}) \times (\mathbf{a} \times \mathbf{b})}{V^3}$$

$$= 8\pi^3 \mathbf{b} \times \mathbf{c} \cdot \frac{[(\mathbf{c} \times \mathbf{a} \cdot \mathbf{b})\mathbf{a} - (\mathbf{c} \times \mathbf{a} \cdot \mathbf{a})\mathbf{b}]}{V^3}$$

$$= \frac{8\pi^3 (\mathbf{b} \times \mathbf{c} \cdot \mathbf{a})(\mathbf{c} \times \mathbf{a} \cdot \mathbf{b})}{V^3} = 8\pi^3/V$$

12. See Fig. AI.12.

$$\mathbf{a}^*_{eco} = 2\pi\mathbf{j}/a_{eco}, b^*_{eco} = 2\pi\mathbf{i}/b_{eco}$$

$$\mathbf{a}_p = \frac{\mathbf{a}_{eco} + \mathbf{b}_{eco}}{2} = \frac{(a_{eco}\mathbf{i} + b_{eco}\mathbf{j})}{2}$$

$$\mathbf{b}_p = \frac{\mathbf{b}_{eco} - \mathbf{a}_{eco}}{2} = \frac{(b_{eco}\mathbf{j} - a_{eco}\mathbf{i})}{2}$$

$$\mathbf{a}^*_p \cdot \mathbf{b}_p = 0 = (a^*_1\mathbf{i} + a^*_2\mathbf{j}) \cdot (b_{eco}\mathbf{j} - a_{eco}\mathbf{i})/2$$

$$0 = a^*_1 a_{eco} - a^*_2 b_{eco}$$

$$\mathbf{a}^*_p \cdot \mathbf{a}_p = 2\pi = (a^*_1\mathbf{i} + a^*_2\mathbf{j}) \cdot (a_{eco}\mathbf{i} - b_{eco}\mathbf{j})/2$$

$$2\pi = a^*_i a_{eco} + a^*_2 b_{eco}$$

Solving, $a^*_1 = 2\pi/a_{eco}, a^*_2 = 2\pi/b_{eco}$

$$\mathbf{a}^*_p = 2\pi(\mathbf{i}/a_{eco} + \mathbf{j}/b_{eco})$$

Thus,

$$\mathbf{b}^*_p = 2\pi(-\mathbf{i}/a_{eco} + \mathbf{j}/b_{eco})$$

$$\mathbf{K} = 2\pi\{[h_p(\mathbf{i}/a_{eco} + \mathbf{j}/b_{eco})] + [k_p(-\mathbf{i}/a_{eco} + \mathbf{j}/b_{eco})]\}$$

$$= 2\pi\{(h_p - k_p)\mathbf{i}/a_{eco} + (h_p + k_p)\mathbf{j}/b_{eco}\}$$

$$= 2\pi\{h_{eco}\mathbf{i}/a_{eco} + k_{eco}\mathbf{j}/b_{eco}\}$$

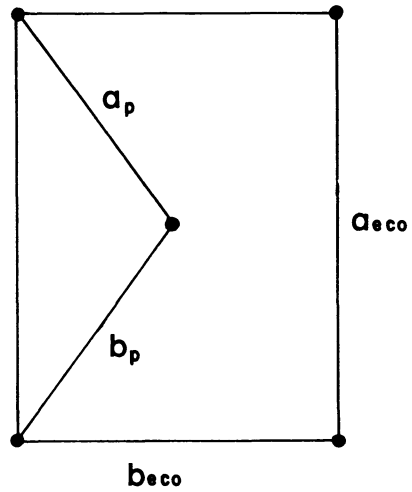

Fig. AI.12. Primitive vectors for *eco*.

and

$$h_{eco} = h_p - k_p \text{ and } k_{eco} = h_p - k_p$$

and

$$h_{eco} + k_{eco} = 2h_p.$$

Thus the recip. lattice is rectangular with $h + k$ even.

Chapter 5

1. A translational operation takes x into $x + m$ and thus

   $\cos \pi x$ into $\cos \pi(x + m)$,

   $\sin \pi x$ into $\sin \pi(x + m)$.

   In both cases $f(x)$ goes into $-f(x)$ when m is odd and into itself when m is even.

2. $P2/m$ is symmorphic. Therefore, the small representations are the same as the irr. reps. of C_{2h} and the irr. reps. of the translations are $\exp i\mathbf{k}\cdot\mathbf{T}$

$\varepsilon\|0$	$C_{2y}\|0$	$i\|0$	$\sigma_y\|0$	$\varepsilon\|\mathbf{T}$
1	1	1	1	$\exp i\mathbf{k}\cdot\mathbf{T}$
1	−1	1	−1	$\exp i\mathbf{k}\cdot\mathbf{T}$
1	−1	−1	1	$\exp i\mathbf{k}\cdot\mathbf{T}$
1	1	−1	−1	$\exp i\mathbf{k}\cdot\mathbf{T}$

3. $P2_1/c$: $\varepsilon|0$, $C_{2y}|(\mathbf{b}+\mathbf{c})/2$, $i|0$, $\sigma_y|(\mathbf{b}+\mathbf{c})/2$

$$\begin{aligned}
\hat{\Gamma}(C_{2y})\hat{\Gamma}(C_{2y}) &= \exp-[(\mathbf{c}^*/2)\cdot(C_{2y}\cdot(\mathbf{b}+\mathbf{c})/2-(\mathbf{b}+\mathbf{c})/2)]\hat{\Gamma}(\varepsilon)\\
&= \exp-[(\mathbf{c}^*/2)\cdot((\mathbf{b}-\mathbf{c})/2-(\mathbf{b}+\mathbf{c})/2)]\hat{\Gamma}(\varepsilon)\\
&= -\hat{\Gamma}(\varepsilon)\\
\hat{\Gamma}(C_{2y})\hat{\Gamma}(i) &= \hat{\Gamma}(\sigma_y)\\
\hat{\Gamma}(i)\hat{\Gamma}(C_{2y}) &= \exp-[(\mathbf{c}^*/2)\cdot((-\mathbf{b}-c)/2-(\mathbf{b}+\mathbf{c})/2)]\hat{\Gamma}(\sigma_y)\\
&= -\hat{\Gamma}(\sigma_y)
\end{aligned}$$

	ε	C_{2y}	i	σ_y
ε	$\hat{\Gamma}(\varepsilon)$	$\hat{\Gamma}(C_{2y})$	$\hat{\Gamma}(i)$	$\hat{\Gamma}(\sigma_y)$
C_{2y}	$\hat{\Gamma}(C_{2y})$	$-\hat{\Gamma}(\varepsilon)$	$\hat{\Gamma}(\sigma_y)$	$-\hat{\Gamma}(i)$
i	$\hat{\Gamma}(i)$	$-\hat{\Gamma}(\sigma_y)$	$\hat{\Gamma}(\varepsilon)$	$-\hat{\Gamma}(C_{2y})$
σ_y	$\hat{\Gamma}(\sigma_y)$	$\hat{\Gamma}(i)$	$\hat{\Gamma}(C_{2y})$	$\hat{\Gamma}(\varepsilon)$

4. Some do not commute — must be 2-D.

$$\hat{\Gamma}(\varepsilon)=\begin{pmatrix}1&0\\0&1\end{pmatrix}$$

$$\hat{\Gamma}(C_{2y})\hat{\Gamma}(C_{2y})=\begin{pmatrix}-1&0\\0&-1\end{pmatrix}=\begin{pmatrix}0&1\\-1&0\end{pmatrix}\begin{pmatrix}0&1\\-1&0\end{pmatrix}$$

$$\hat{\Gamma}(C_{2y})\hat{\Gamma}(i)=\begin{pmatrix}0&1\\-1&0\end{pmatrix}\begin{pmatrix}0&1\\1&0\end{pmatrix}=-\hat{\Gamma}(i)\hat{\Gamma}(C_{2y})$$

$$=-\begin{pmatrix}0&1\\1&0\end{pmatrix}\begin{pmatrix}0&1\\-1&0\end{pmatrix}$$

$$\hat{\Gamma}(\sigma_y)=\hat{\Gamma}(C_{2y})\hat{\Gamma}(i)=\begin{pmatrix}1&0\\0&-1\end{pmatrix}$$

1. $\hat{\Gamma}(\varepsilon|0) = \hat{\Gamma}(\varepsilon) = \begin{pmatrix} 1 & 0 \\ 0 & 1 \end{pmatrix}$

2. $\Gamma(C_{2y}|(\mathbf{b}+\mathbf{c})/2) = \exp -i(\mathbf{c}^*/2)\cdot(\mathbf{b}+\mathbf{c}/2)\hat{\Gamma}(C_{2y})$
$= -i\begin{pmatrix} 0 & 1 \\ -1 & 0 \end{pmatrix} = \begin{pmatrix} 0 & -i \\ i & 0 \end{pmatrix}$

3. $\Gamma(\sigma_y|(\mathbf{b}+\mathbf{c})/2) = -i\begin{pmatrix} 1 & 0 \\ 0 & -1 \end{pmatrix} = \begin{pmatrix} -i & 0 \\ 0 & i \end{pmatrix}$

4. $\Gamma(i|0) = \hat{\Gamma}(i) = \begin{pmatrix} 0 & 1 \\ 1 & 0 \end{pmatrix}$

5. $\Gamma(\varepsilon|0) = \hat{\Gamma}(\varepsilon) = \begin{pmatrix} 1 & 0 \\ 0 & 1 \end{pmatrix}$

$\Gamma(C_{2x}|\mathbf{c}/2) = \exp -i(\mathbf{c}^*/2)\cdot(\mathbf{c}/2)\hat{\Gamma}(C_{2x}) = \exp -(\pi i/2)\hat{\Gamma}(C_{2x})$
$= -i\begin{pmatrix} i & 0 \\ 0 & -i \end{pmatrix} = \begin{pmatrix} 1 & 0 \\ 0 & \bar{1} \end{pmatrix}$

$\Gamma(C_{2z}|\mathbf{c}/2) = -i\begin{pmatrix} 0 & i \\ -i & 0 \end{pmatrix} = \begin{pmatrix} 0 & 1 \\ -1 & 0 \end{pmatrix}$, etc.

6. From Table 3.5.

$$\overline{C}_{4z}|0\cdot C_{2(x+y)}|0 \equiv \begin{pmatrix} 0 & \bar{1} & 0 \\ 1 & 0 & 0 \\ 0 & 0 & \bar{1} \end{pmatrix}\begin{pmatrix} 0 & 1 & 0 \\ 1 & 0 & 0 \\ 0 & 0 & \bar{1} \end{pmatrix} = \begin{pmatrix} \bar{1} & 0 & 0 \\ 0 & 1 & 0 \\ 0 & 0 & 1 \end{pmatrix} \equiv \sigma_x|0$$

check: $\begin{pmatrix} -i & 0 \\ 0 & i \end{pmatrix}\begin{pmatrix} 0 & -i \\ i & 0 \end{pmatrix} = \begin{pmatrix} 0 & -1 \\ -1 & 0 \end{pmatrix} = \Gamma(\sigma_x|0)$

and

$$\sigma_y|0\cdot\overline{C}_{4z}^3|0 \equiv \begin{pmatrix} 1 & 0 & 0 \\ 0 & \bar{1} & 0 \\ 0 & 0 & 1 \end{pmatrix}\begin{pmatrix} 0 & \bar{1} & 0 \\ 1 & 0 & 0 \\ 0 & 0 & \bar{1} \end{pmatrix} = \begin{pmatrix} 0 & \bar{1} & 0 \\ \bar{1} & 0 & 0 \\ 0 & 0 & \bar{1} \end{pmatrix} \equiv C_{2(y-z)}$$

check: $\begin{pmatrix} 0 & 1 \\ 1 & 0 \end{pmatrix}\begin{pmatrix} i & 0 \\ 0 & -i \end{pmatrix} = \begin{pmatrix} 0 & -i \\ i & 0 \end{pmatrix} = \Gamma(C_{2(y-z)})$

Chapter 6

1. *Pcmn*: $\sigma_x|\mathbf{c}/2 + t_1\mathbf{a}$, $\sigma_y|t_2\mathbf{b}$, $\sigma_z|(\mathbf{a}+\mathbf{b})/2 + t_3\mathbf{c}$

The corresponding essential symmetry operations of $P6_3/mmc$ (in terms of the orthorhombic axes, Table 5.7) are $\sigma_x|\mathbf{c}/2$, $\sigma_y|0$, $\sigma_z|\mathbf{c}/2$. The translation $(\mathbf{a}+\mathbf{b})/2$ is $\mathbf{a}_h$ and $\Gamma(\mathbf{a}_{\text{hex}}) = -1$, thus we want an irr. rep. for which $\Gamma(\sigma_x|\mathbf{c}/2) = 1$, $\Gamma(\sigma_x|0) = 1$, $\Gamma(\sigma_z|\mathbf{c}/2) = -1$ (so that $\Gamma(\sigma_x|(\mathbf{a}+\mathbf{b}+\mathbf{c})/2 = 1)$ and thus from Table 5.6 (relative to the functions of Table 5.8) we want R_8:

$\varepsilon\|0$	$C_{2x}\|\mathbf{c}/2$	$C_{2y}\|0$	$C_{2z}\|\mathbf{c}/2$	$i\|0$	$\sigma_x\|\mathbf{c}/2$	$\sigma_y\|0$	$\sigma_z\|\mathbf{c}/2$
1	−1	−1	1	−1	1	1	−1

and $P6_3/mmc \rightarrow Pcmn$ does correspond to a single irr. rep.

There are 3 vectors in the star: $\mathbf{a}^*/2$, $\mathbf{b}^*/2$, $(\mathbf{a}^*+\mathbf{b}^*)/2$ and since the small representations are 1-dimensional, the irr. rep. is 3-dimensional and

$$\rho = \rho^\circ + [\gamma_1\phi_1 + \gamma_2\phi_2 + \gamma_3\phi_3]\eta\,.$$

Each of the functions is antisymmetric with respect to inversion and thus no odd order invariants can be formed. The forth order term is:

$$C_1(\gamma_1^4 + \gamma_2^4 + \gamma_3^4) + C_2(\gamma_1^2\gamma_2^2 + \gamma_1^2\gamma_3^2 + \gamma_2^2\gamma_3^2)$$

and since $\Sigma\gamma_1^2 = 1$, this can be written as

$$C_1 + (C_2 - 2C_1)(\gamma_1^2\gamma_2^2 + \gamma_1^2\gamma_3^2 + \gamma_2^2\gamma_3^2)\,.$$

Finding the extrema subject to the restraint $\Sigma\gamma_i^2 = 1$,

$$\frac{\partial}{\partial\gamma_i}[\gamma_1^2\gamma_2^2 + \gamma_1^2\gamma_3^2 + \gamma_2^2\gamma_3^2 - \lambda\Sigma\gamma_1^2] = 0$$

or

$$2\gamma_1(\gamma_2^2 + \gamma_3^2) - 2\lambda\gamma_1 = 0$$
$$2\gamma_2(\gamma_1^2 + \gamma_3^2) - 2\lambda\gamma_2 = 0$$
$$2\gamma_3(\gamma_2^2 + \gamma_1^2) - 2\lambda\gamma_3 = 0$$

and if $\gamma_1 \neq 0$, $\gamma_2 \neq 0$, $\gamma_3 \neq 0$, then

$$\lambda = \gamma_2^2 + \gamma_3^2 = 1 - \gamma_1^2$$
$$\lambda = \gamma_1^2 + \gamma_3^2 = 1 - \gamma_2^2$$
$$\lambda = \gamma_2^2 + \gamma_3^2 = 1 - \gamma_3^2$$

$\gamma_1^2 = \gamma_2^2 = \gamma_3^2$ and thus $\gamma_1 = \gamma_2 = \gamma_3 = \pm 1/\sqrt{3}$. Since all sign combinations yield the same value of G (the γ_i's enter only in even order), they correspond to the same possible stable structure, i.e.,

$$\rho = \rho^0 + [\phi_1 + \phi_2 + \phi_3]\eta/\sqrt{3}\,.$$

This structure has $P6_3mc$ symmetry with $a = 2a^0$. If $\gamma_1 \neq 0$, $\gamma_2 \neq 0$, $\gamma_3 = 0$ the "solution" is $\gamma_1 = \gamma_2 = 1/\sqrt{2}$, and this is a saddle point solution. If $\gamma_1 \neq 0$, $\gamma_2 = \gamma_3 = 0$, then $\gamma_1 = 1, \gamma_2 = \gamma_3 = 0$ solves the minimization equations and another solution

$$\rho + \rho^0 + \eta\phi_1$$

with $Pcmn$ symmetry is found.

2. There are 48 essential symmetry operations in $Fm3m$ and there are 16 essential symmetry operations in $R\bar{3}m$. Thus, such a distortion cannot correspond to a 1-D small rep., which would halve the number of essential symmetry operations. The e_g rep. has a third-order invariant and the e_u yields a tetragonal or orthorhombic symmetry. This leaves the T reps. T_{1g} has a third-order invariant. Only T_{2g}, T_{1u} and T_{2u} remain. These can yield a rhombohedral distortion, but with $\bar{3}$, 32 or $3m$ symmetry.

3. The structure described has $Pm3m$ symmetry. The allowed tetragonal symmetries by second-order transition are 422 (e_u), $4/m$ (T_{2g}) $\bar{4}m2$ (T_{1u}) and $4mm$ (T_{2u}). These do not include $4/mmm$.

4. The tetragonal structure has $P4/mmm$ symmetry. The reps of this symmorphic space group at $\mathbf{k} = 0$ are the same as the irr. reps. of D_{4h}. Among the 16 operations of D_{4h} there are eight ($\varepsilon, C_{2z}, C_{2(y-x)}, C_{2(x+y)}$, i, σ_x, σ_y, σ_z that remain after distortion, namely the elements of D_{2h}. This distortion corresponds to the irr. rep.

ε	C_{4z}	C_{2z}	C_{4z}^3	C_{2y}	C_{2z}	$C_{2(y-x)}$	$C_{2(y+x)}$
1	-1	1	-1	-1	-1	1	1
i	$\overline{C}_{4z}$	σ_z	$\overline{C}_{4z}^3$	σ_y	σ_z	σ_{y-x}	σ_{y+z}
1	-1	1	-1	-1	-1	1	1

Since this is a 1-D irr. rep. and since a corresponding basis function changes sign under some symmetry operations, there can be no third-order invariant. Since $i \in g^\circ(\mathbf{k})$, the $\mathbf{k}$ point meets the Lifshitz condition

5. The ordering yields $R\bar{3}m$ symmetry with

$$\mathbf{a}_r = \mathbf{a}_{fcc} + (\mathbf{b}_{fcc} + \mathbf{c}_{fcc})/2$$

$$\mathbf{b}_r = \mathbf{b}_{fcc} + (\mathbf{a}_{fcc} + \mathbf{c}_{fcc})/2$$

$$\mathbf{c}_r = \mathbf{c}_{fcc} + (\mathbf{a}_{fcc} + \mathbf{b}_{fcc})/2.$$

There are four equivalent structures corresponding to the four body diagonals. In each case the operation $(\mathbf{a} + \mathbf{b})/2$ (for example) is lost, thus all four basis functions change sign under this symmetry operation. Thus, no odd-order terms appear in G and there is no third-order term. As shown in Section 6.13, $\gamma_1 = 1, \gamma_2 = \gamma_3 = \gamma_4$ corresponds to a possible minimum.

6. The space group is either $Fm3m$ (with $a = 2a^\circ$) or $Fd3m$ (with $a = 2a^\circ$), as shown in Section 6.15. There are $2^3 = 8$ times as many metal atom positions in the superstructure as in the small structure, and thus 32 positions. The positions in $Fd3m$ are: 0,0,0; 0,1/4,1/4; 1/4,0,1/4; 1/4,1/4,0 (a 16-fold position) and 1/2, 1/2, 1/2; 1/2,1/4,1/4; 1/4,1/2,1/4; 1/4,1/4,1/2; another 16-fold position. The nonmetal positions are x, x, x (32-fold position) with $x \cong 1/2$.

Chapter 7

1.

	La_2O_3	O_2	SO	La_2S_3	La_2O_2S	SO_2
La	2	0	0	2	2	0
O	3	2	1	0	2	2
S	0	0	1	3	1	1

Row reduction yields

$$\begin{array}{cccccc} 1 & 0 & 0 & 1 & 1 & 0 \\ 0 & 1 & 0 & \bar{3} & \bar{1} & 1/2 \\ 0 & 0 & 1 & 3 & 1 & 1 \end{array}$$

Thus,

$$-\Delta n_{La_2O_3} = \Delta n_{La_2S_3} + \Delta n_{La_2O_2S}$$

$$-\Delta n_{O_2} = -3\Delta n_{La_2S_3} - \Delta n_{La_2O_2S} + 1/2\Delta n_{SO_2}$$

$$-\Delta n_{SO_2} = 3\Delta n_{La_2S_3} + \Delta n_{La_2O_2S} + \Delta n_{SO_2}$$

and

$$SO_2 = SO + 1/2O_2$$

$$O_2 + La_2O_2S = SO + La_2O_3$$

$$3O_2 + La_2S_3 = 3SO + La_2O_3.$$

2.

	O (in s.s.)	C (in s.s.)	Ti (in s.s.)	CO (g)	O_2 (g)	TiO (g)	Ti (g)
O	1	0	0	1	2	1	0
C	0	1	0	1	0	0	0
Ti	0	0	1	0	0	1	1

rank = 3, there are 7 − 3 = 4 independent net reactions.

$$-\Delta n_{O(ss)} = \Delta n_{CO} + 2\Delta_{O_2} + \Delta n_{TiO}$$

$$-\Delta n_{O(ss)} = \Delta n_{CO}$$

$$-\Delta n_{Ti(ss)} = \Delta n_{TiO} + 2\Delta n_{Ti(g)}$$

$$Ti\,(ss) = Ti\,(g)$$

$$O\,(ss) + Ti\,(ss) = TiO\,(g)$$

$$2O\,(ss) = O_2\,(g)$$

$$C\,(ss) + O\,(ss) = CO\,(g).$$

3. $n^{\circ}_{La_2O_2S} = 3n_{La_2S_3} + n_{La_2O_2S} + n_{SO} + n_{SO_2}$

$2n^{\circ}_{La_2O_2S} = 3n_{La_2O_3} + 2n_{La_2O_2S} + n_{SO} + 2n_{SO_2} + 2n_{O_2}$

$2n^{\circ}_{La_2O_2S} = 2n_{La_2O_3} + 2n_{La_2S_3} + 2n_{La_2O_2S}$

elimination of $n^{\circ}_{La_2O_2S}$ yields

$$2n_{SO} + 2n_{O_2} + 3n_{SO_2} = 0$$

which implies a restraint eq.

$$2P_{SO} + 2P_{O_2} + 3P_{SO_2} = 0$$

$$f = c - \rho - p + 2 = 3 - 1 - 4 + 2 = 0$$

4. The first question to be answered is, "Is ThN (s) stable with respect to disproportionation at 2 000 K"? That is, is $\Delta G > 0$ for

$$4\text{ThN (s)} = \text{Th}_3\text{N}_4\text{ (s)} + \text{Th (s)}\,?$$

At 2 000 K, $\Delta G = -630.0 + 4(206.4) = 195.6$ kJ mol^{-1} and the answer is yes. Thus, either ThN (s) coexists with Th (s) or ThN (s) coexists with Th_3N_4 (s) (unless the system is on the stoichiometry of one of the phases).

$$n^{\circ}_{N_2} = \frac{1}{28.0} = 0.0357 \text{ mol}$$

$$n^{\circ}_{Th} = \frac{16}{232.0} = 0.0690 \text{ mol}$$

Since $N/Th = 2 \cdot 0.0357/0.0690 = 1.03 > 1$, first guess is ThN (s) coexists with Th_3N_4 (s) and N_2 (g)

$$n_{Th} = 0.0690 = n_{ThN} + 3n_{Th_3N_4}$$
$$n_N = 0.0714 = n_{ThN} + 4n_{Th_3N_4} + 2n_{N_2}$$

for the reaction

$$\text{Th}_3\text{N}_4\text{ (s)} = 3\text{ThN (s)} + 1/2\text{N}_2\text{ (g)}$$

$$\Delta G^{\circ} = 3(-206.0) + 630.0 = 12 \text{ kJ mol}^{-1}$$

$$-8.314 \cdot 2\,000 \ell\text{n}K = 1\,200$$
$$K = 0.486 = P_{N_2}^{1/2}$$
$$P_{N_2} = 0.24 \text{ bar}$$
$$n_{N_2}(g) = \frac{0.24 \cdot 0.500}{.083\,14 \cdot 2\,000} = 0.000\,7$$

thus, $n_{ThN} + 3n_{Th_3N_4} = 0.069\ 0$

$$n_{ThN} + 4n_{Th_3N_4} = 0.071\ 4 - 0.001\ 4 = 0.070\ 0$$

$$n_{Th_3N_4} = 0.001\ 0$$
$$n_{ThN} = 0.066\ 0$$
$$n_{N_2} = 0.000\ 7$$

and since all n's are positive the assumption was correct.

5. First it must be determined whether ZrAl(s) is stable with respect to disproportionation, i.e., is $\Delta G > 0$ for

$$7\,ZrAl(s) = Zr_2Al_3(s) + Zr_5Al_4(s)$$

$\Delta H = (7/2)(369.7) - 372.8 = 921.15$ kJ mol^{-1}

$\Delta S = (7/2)(115.5) - 118.4 = 285.85$ kJ mol^{-1}

$\Delta G = 921\ 150 - 1\ 500(285.85) = 492\ 400$ J

and the answer is yes, either Zr_2Al_3 coexists with ZrAl(s) or Zr_5Al_4 does.

Try ZrAl and Zr_5Al_4, assume Al(g) negligible

$$\frac{n_{ZrAl} + 5n_{Zr_5Al_4}}{2n_{ZrAl} + 9n_{Zr_5Al_4}} = 0.55$$

$$n_{Zr_5Al_4} = 0.00160 \qquad n_{ZrAl} = 0.0080$$

check on moles Al(g):

$$5\,ZrAl(s) = Zr_5Al_4(s) + Al(g)$$

$\Delta H^\circ = (7/2)(369.7) - (5/2)(372.8) = 361.95$ kJ mol^{-1}

$\Delta S^\circ = (7/2)(115.5) - (5/2)(118.4) = 108.25$ kJ mol^{-1}

$\Delta G^\circ = 199,\ 600$ J mol^{-1}

$$P_{Al} = \exp -(\Delta G^\circ/RT) = 9 \times 10^{-10} \text{ bar}$$

which checks.

6. (a) $X_A d\mu_A + X_B d\mu_B = 0$

$$X_A\{RT/X_A - 2wX_B]dX_A + X_B dX_B = 0$$

$$X_A + X_B = 1 \rightarrow dX_A = -dX_B$$

$$X_B d\mu_B = RT dX_B + 2wX_{13} + 2wX_B X_A dX_A$$

$$\int_{\text{pure } B}^{\text{soln}} d\mu_B = \int_{X_B=1}^{X_B} \frac{RT dX_B}{X_B} + \int_{X_A=0}^{X_A} 2wX_A dX_A$$

$$\mu_B = \mu_B^\circ + RT\ell nX_B + wX_A^2$$

(b) $\overline{G} = X_A\mu_A + X_B\mu_B$

$$= X_A\mu_A^\circ + x_B\mu_B^\circ + RT[X_A\ell nX_A + X_B\ell nX_B] + w[X_A X_B^2 + X_B X_A^2]$$

$$= X_A\mu_A^\circ + X_B\mu_B^\circ + RT[X_A\ell nX_A + X_B\ell nX_B] + wX_A X_B$$

$$\left\{\frac{\partial\overline{G}}{\partial X_A}\right\}_T = \mu_A^\circ - \mu_B^\circ + RT\ell n(X_A/X_B) + w[X_B - X_A]$$

$$\left\{\frac{\partial^2\overline{G}}{\partial X_A^2}\right\}_T = \frac{RT}{X_A} + \frac{RT}{X_B} - 2w = (RT/(X_A X_B)) - w$$

$X_A X_B$ has a maximum at $X_A = X_B = 1/2$ and therefore so long as $2w < 4RT$

$$\left\{\frac{\partial^2\overline{G}}{\partial X_A^2}\right\}_T > 0$$

and $\overline{G}$ vs. X_A is concave up. However, at

$$T = w/2R,$$

$\left\{\frac{\partial^2\overline{G}}{\partial X_A^2}\right\}_T = 0$ at $X_A = X_B = 1/2$, and for $T < w/2R$ $\left\{\frac{\partial^2\overline{G}}{\partial X_A^2}\right\}_T > 0$ and $\overline{G}$ vs. X_A is concave down at $X_A = X_B = 1/2$. However, $\overline{G} \rightarrow \infty$ as $X_A \rightarrow 0$ and also as $X_B \rightarrow 0$, therefore, $\overline{G}$ vs. X_A becomes concave up between $X_A = 1/2$ and $X_A = 0$ and also between $X_A = 1/2$ and $X_A = 1$. Thus, there must be a tangent line common to two different concave upward portions of $\overline{G}$ vs. X_A (see Fig. AI.13) and thus by the argument of Section 7.12 two phases coexist for $T < w/2R$ whereas a single solution exists for $T > w/2R$ (see Fig. AI.14).

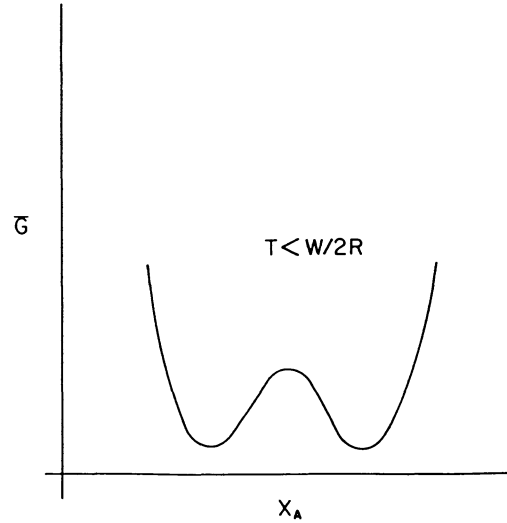

Fig. AI.13. Double minimum in $\overline{G}$ for a regular solution.

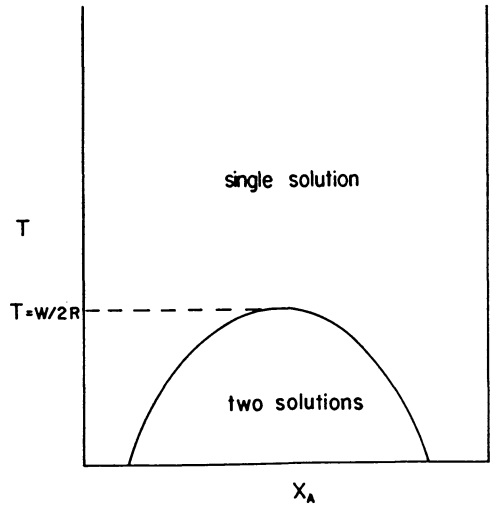

Fig. AI.14. Miscibility gap in a regular solution.

Chapter 8

1. (a) *fcc* h,k,ℓ all even or all odd: 1,1,1; 2,0,0; 3,1,1; 2,2,2; 4,0,0

$d^{-1} = \left(\sqrt{h^2 + k^2 + \ell^2}\right)/a$

$|F|^2 = |6[40 + 16]^2$ for *eee*

$|F|^2 = |6[40 - 16]^2$ for *ooo*

$hk\ell$	θ	M	$\lvert F\rvert^2$	$I \alpha M\lvert F\rvert^2$
111	14.97	8	9 216	12
200	17.35	6	50 176	50
220	24.95	12	50 176	100
311	29.65	24	9 216	36
222	31.11	8	50 176	67
400	36.62	6	50 176	50

(b)

$hk\ell$	I
111	6
200	50
220	100
311	19
222	67
400	50

$|F|^2 = 16[(3/4)\ 40 + 16]^2$ *eee*

$|F|^2 = 16[(3/4)\ 40 - 16]^2$ *ooo*

(c) $F = 40 + 20\cos\pi(h+k+\ell) + 32\cos((\pi/2)(h+k+\ell))$

$(hk\ell)_{fcc}$	$hk\ell$	$\lvert F\rvert^2$	M	θ	I
	111	380	2	7.42	2
	100	380	6	14.40	5
111	222	702	2	14.97	3
$11\bar{1}$	110	702	6	15.05	9
200	211	8 190	6	17.42	100
	221	380	6	19.03	5
220	332	8 190	6	25.00	100
$\bar{2}20$	$\bar{1}10$	8 190	6	25.11	100
	210	380	6	26.32	5
	$\bar{1}11$	380	6	29.46	5
311	433	702	6	29.69	9
$3\bar{1}1$	312	702	12	29.78	17
$3\bar{1}\bar{1}$	200	8 190	6	29.83	9
	etc.				

(d)

$hk\ell$	M	$\lvert F\rvert^2$	θ	I
100	6	2 304	14.26	3
110	12	18 496	20.39	50
111	8	2 304	25.25	4
200	6	18 496	29.51	25
210	24	2 304	33.42	12
211	24	18 496	37.11	100

$F = 92 + 44 = 136$ for $h + k + \ell$ even.

$F = 92 - 44 = 48$ for $h + k + \ell$ odd.

(e)

$(hk\ell)_{\text{cubic}}$	$hk\ell$	M	$\lvert F\rvert^2$	I	θ
100	100	4	2 304	3	10.51
001	001	2	2 304	1.5	13.29
110	110	4	18 496	25	14.95
101	101	8	18 496	50	17.06
111	111	8	2 304	6	20.22
200	200	4	18 496	25	21.40
210	210	8	2 304	6	24.08
201	201	8	2 304	6	25.55
002	002	2	18 496	12.5	27.37
211	211	16	18 496	100	27.92
102	102	8	2 304	6	29.64
112	112	8	18 496	50	31.81

(f) End-centered orthorhombic (see Fig. AI.15)

$(hk\ell)_t$	$hk\ell$	M	I	Θ
100	110	4	6	10.50
001	001	2	3	13.29
110	200	2	25	14.84
	020	2	25	15.04
101	111	8	100	17.06
111	201	4	6	20.13
	021	4	6	20.29
200	220	4	50	21.39
210	310	4	6	23.93
	130	4	6	24.19
201	221	8	12	25.54
002	002	2	25	27.38
211	311	8	100	27.78
	131	8	100	28.02
102	112	8	12	29.65
112	202	4	50	31.76
	022	4	50	31.87

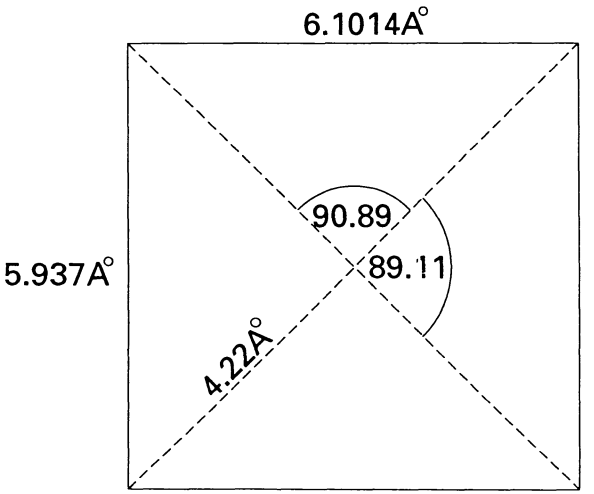

Fig. AI.15. *eco* distortion of *sc*.

(g) V in 0,0,0 and 0,0,1/2

S in 1/3,2/3,1/4 and 2/3,1/3,3/4

$F = 23[1 + \cos \pi\ell] + 32[\cos 2\pi(h + 2k)/3 + \ell/4)]$

$hk\ell$	Θ	$\lvert F\rvert^2$	M	I
002	15.30	196	2	1
100	15.44	900	6	12
101	17.29	768	12	20
102	22.01	3 844	12	100
110	27.46	6 084	6	79
103	28.49	768	12	20
004	31.84	6 084	2	26
112	32.10	196	12	5
200	32.18	900	6	12
201	33.28	768	12	20
104	36.23	900	12	23
202	36.46	3 844	12	100

$$\text{(h)}\quad \begin{pmatrix} h \\ k \\ \ell \end{pmatrix}_0 = \begin{pmatrix} 2 & 1 & 0 \\ 0 & 1 & 0 \\ 0 & 0 & 1 \end{pmatrix} \begin{pmatrix} h \\ k \\ \ell \end{pmatrix}_h$$

$(hk\ell)_h$	$hk\ell$		I
002	002	2	3
100	200	2	6
	110	4	12
101	201	4	11
	111	8	20
102	202	4	50
	112	8	100
110	310	4	80
	020	2	41
103	203	4	11
	113	8	20
004	004	2	40
112	312	8	5
	022	4	3
200	400	2	6
	220	4	12
201	401	4	10
	221	8	20
104	204	4	12
	114	8	23
202	402	4	50
	222	8	100

2. $N = 511/5.162 = 99$

$$\sum_{n_1=1}^{97} \exp i[n_1(\mathbf{K} + \delta\mathbf{k}) \cdot \mathbf{a}/\lambda] \sum_{n_2=1}^{97} \exp i[n_2(\mathbf{K} + \delta\mathbf{k}) \cdot \mathbf{b}/\lambda]$$

$$\sum_{n_3=1}^{97} \exp i[n_3(\mathbf{K} + \delta\mathbf{K}) \cdot \mathbf{c}/\lambda]$$

$$= \frac{\sin[100h + \delta h)\pi]}{\sin[(h + \delta h)\pi]} \frac{\sin[100(k + \delta k)\pi]}{\sin((k + \delta k)\pi]} \frac{\sin[100(\ell + \delta \ell)\pi]}{\sin[(\ell + \delta \ell)\pi]}$$

$$= \left(\frac{\sin[100\delta h\pi]}{\sin[\delta h\pi]}\right)^3$$

From Table 8.9, $\delta h = 256 \times 10^{-5}$ when $\left(\frac{\sin[100\delta h\pi]}{\sin \delta h\pi}\right)^3 = 0.51$

$$\delta\theta = \frac{\lambda(h + k + \ell)[\delta h + \delta k + \delta \ell]}{2 \cdot a \cdot (h^2 + k^2 + \ell^2)^{1/2} \cos\theta} = 1.8 \times 10^{-3} \text{ radians}$$

$= 0.10$ degrees

3.

0.056 18						
0.088 80	0.031 82					
0.112 38	0.056 20	0.024 38				
0.145 13	0.088 95	0.057 13	0.032 75			
0.201 13	0.144 95	0.113 13	0.088 75	0.056 00		
0.224 67	0.168 49	0.136 67	0.112 29	0.079 54	0.023 54	
0.280 45	0.224 27	0.192 45	0.168 07	0.135 32	0.079 32	0.055 78
0.313 50	0.257 32	0.225 50	0.201 12	0.168 37	0.112 37	0.088 83
0.356 44	0.300 26	0.268 44	0.244 06	0.211 31	0.155 31	0.131 77
0.369 01	0.312 83	0.281 01	0.256 63	0.223 88	0.167 88	0.144 34
0.412 44	0.356 26	0.324 44	0.300 06	0.267 31	0.211 31	0.187 77

$0.112\ 45 \pm 0.000\ 07$ occurs 3x

$0.056\ 16 \pm 0.000\ 01$ occurs 2x

together these suggest trying $a^{-2} = 0.056\ 19$

0.056 18	100
0.088 80	
0.112 38	110
0.145 13	
0.201 13	
0.224 67	200
0.280 45	210
0.313 50	
0.356 44	
0.369 01	
0.412 44	

Now either 0.088 80 is 00ℓ, in which case $c^{-2} = 0.088\ 0/\ell^2$ or it is 10ℓ, in which case $c^{-2} = 0.032\ 61/\ell^2$.

Try $0.088\ 80 = c^{-2}, 0.056\ 19 = a^{-2}$,

0.056 18	100
0.088 80	001
0.112 38	110
0.145 13	101
0.201 13	111
0.224 67	200
0.280 45	210
0.313 50	201
0.356 44	002
0.369 01	211
0.412 44	102

4. Let $A = a^{-2}, C = c^{-2}$

$$\Sigma r_i^2 = \Sigma(d_i^{-2} - A(h_i^2 + k_i^2) - C\ell_i^2)^2$$

$$= \Sigma d_i^{-4} + A\Sigma(h_i^2 + k_i^2)^2 + C\Sigma\ell_i^4 - 2A\Sigma d_i^{-2}(h_i^2 + k_i^2)$$

$$-2C\Sigma d_i^{-2}\ell_i^2 + 2AC\Sigma\ell_i^2(h_i^2 + k_i^2)$$

$$\frac{\partial\Sigma r_i^2}{\partial A} = 0 = 2A\Sigma(h_i^2 + k_i^2) - 2\Sigma d_i^2(h_i^2 + k_i^2) + 2C\Sigma\ell_i^2(h_i^2 k_i^2)$$

$$\frac{\partial\Sigma r_i^2}{\partial C} = 0 = 2C\Sigma\ell_i^4 - 2\Sigma d_i^2\ell_i^2 + 2A\Sigma\ell_i^2(h_i^2 + k_i^2)$$

d^{-2}	$hk\ell$	h^2+k^2	$(h^2+k^2)^2$	$\ell^2(h^2+k^2)$	$d^{-2}(h^2+k^2)$	$d^{-2}\ell^2$	ℓ^4
0.056 18	100	1	1	0	0.056 18	0	0
0.088 80	001	0	0	0	0	0.088 80	1
0.112 38	110	2	4	0	0.224 76	0	0
0.145 13	101	1	1	1	0.145 13	0.145 13	1
0.201 13	111	2	4	2	0.402 26	0.201 13	1
0.224 67	200	4	16	0	0.898 68	0	0
0.280 45	210	5	25	0	1.402 25	0	0
0.313 50	201	4	16	4	1.254 0	0.313 50	1
0.356 44	002	0	0	0	0	1.425 76	16
0.369 01	211	5	25	5	1.845 05	0.369 01	1
0.412 44	102	1	1	4	0.412 44	1.649 76	16
			93	16	6.640 75	4.193 09	37

$$93A + 16C = 6.640\ 75$$

$$16A + 37C = 4.193\ 09$$

$$a = 4.223\ \text{Å}, c = 3.350\ \text{Å}$$

5. $a_h = 6.319\ 4\sqrt{2 - 2\cos 33.377} = 3.6294\ \text{Å}$

$c_h = 6.319\ 4\sqrt{3 + 6\cos 33.377} = 17.886\ \text{Å}$

$$\begin{pmatrix} \mathbf{a} \\ \mathbf{b} \\ \mathbf{c} \end{pmatrix}_h = \begin{pmatrix} 1 & 0 & \bar{1} \\ \bar{1} & 1 & 0 \\ 1 & 1 & 1 \end{pmatrix} \begin{pmatrix} \mathbf{a} \\ \mathbf{b} \\ \mathbf{c} \end{pmatrix}_r$$

$$\begin{pmatrix} h \\ k \\ \ell \end{pmatrix}_h = \begin{pmatrix} 1 & 0 & \bar{1} \\ \bar{1} & 1 & 0 \\ 1 & 1 & 1 \end{pmatrix} \begin{pmatrix} h \\ k \\ \ell \end{pmatrix}_r$$

$(hk\ell)_r$	$(hk\ell)_h$
1 1 1	0 0 3
1 0 0	1 $\bar{1}$ 1
2 2 2	0 0 6
1 1 0	1 0 2
2 1 1	1 $\bar{1}$ 4

etc.

6. $R_d/d = (\text{cotan}\ \theta) r_\theta$

   $r_\theta = \pm(1.8 \times 10^{-3})/2$ radians

   $R_d/d = 0.9 \times 10^{-3} \cdot \text{cotan}\ 24.95° = 0.002$

   $\ell n\, d - \ell n \sin\theta = \text{const.} \rightarrow R_d/d = (R_{\sin\theta})/\sin\theta = 0.002\ R_{\sin\theta} = 8 \times 10^{-4}$.

7. Interatomic vector:

   $\mathbf{V}_{TmS} = (0.052\ 7 - 0.039\ 3)\mathbf{a} + (0.503\ 0 + 0.274\ 0)\mathbf{c}$

   $= 0.013\ 4\mathbf{a} + 0.229\ 0\mathbf{c}$

   A unit vector perpendicular to $\mathbf{V}_{TmS}$ is defined as $x_p\mathbf{a} + y_p\mathbf{c}$ where

$$(x_p\mathbf{a} + y_p\mathbf{c}) \cdot (0.013\ 4\mathbf{a} + 0.229\ 0\mathbf{c}) = 0$$

   and

$$(x_p\mathbf{a} + y_p\mathbf{c}) \cdot (x_p\mathbf{a} + y_p\mathbf{c}) = 1\,.$$

   From the first

$$0 = 0.013\ 4\, x_p a^2 + 0.229\ 0\, z_p c^2 + 0.013\ 4 \cdot 0.229\ 0\, ac\, x_p z_p \cos 91.02°$$

   or

$$19.75\, x_p + 28.42\, z_p - 0.023\ 4\, x_p z_p = 0$$

   and from the second

$$1\ 474\, x_p^2 + 124.1\, z_p^2 - 7.61\, x_p z_p = 1.$$

   Solving by neglecting $x_p z_p$, then using $x_p z_p$ as a perturbation

$$x_p = -0.025\ 49$$

$$z_p = 0.017\ 71.$$

To express in terms of $\mathbf{a}^*$ and $\mathbf{c}^*$,

$$-0.025\ 49\,\mathbf{a} + 0.017\ 71\,\mathbf{c} = \ell_1\mathbf{a}^*/\mathbf{a}^* + \ell_3\mathbf{c}^*/\mathbf{c}^*$$

$$-0.025\ 49\,(\mathbf{a}\cdot\mathbf{a}^*) = \ell_1\mathbf{a}^* + \ell_3\mathbf{a}^*\cos\beta^*$$

$$\text{or } \frac{-0.025\ 49(2\pi)}{a^*} = \ell_1 + \ell_3\cos\beta^*$$

and similarly

$$\frac{0.017\ 71(2\pi)}{c^*} = \ell_1\cos\beta^* + \ell_3$$

$$a^* = \frac{2\pi|\mathbf{b}\times\mathbf{c}|}{V_{\text{cell}}} = \frac{2\pi}{38.395}$$

$$c^* = \frac{2\pi}{c} = \frac{2\pi}{11.141}$$

$$\beta^* = 180 - 91.02 = 88.98°$$

Thus,

$$(-0.025\ 49)\cdot(38.395) = \ell_1 + 0.017\ 8\ell_3$$

$$(0.017\ 71)\cdot(11.141) = 0.017\ 8\ell_1 + \ell_3$$

$$\ell_1 = -0.983$$

$$\ell_2 = 0.180$$

and

$$\overline{U}^2 = (0.983)^2\cdot 0.14 + (0.180)(0.014)^2 + (0.180)(0.983)0.053$$

$$= 0.135\ \text{Å}^2$$

$$U_{\text{rms}} = 0.368\ \text{Å}$$

Chapter 9

1. $\mathbf{K}_{220} = 2\mathbf{a}^* + 2\mathbf{b}^*$

$$|\mathbf{K}_{220}| = \sqrt{4|\mathbf{a}^*| + 4|\mathbf{b}^*|^2} = 4\pi\sqrt{1/25 + 1/36}$$

$$= (4\pi/\lambda)\sin(90\ell_F/(28.65\pi))$$

$$\ell_F = 23.63\ \text{mm} = \text{vertical distance}$$

horizontal distance $= \Theta/2$

$$\theta = \sin^{-1}(\lambda/2d) = 23.63°$$

$$\theta/2 = 11.815\ \text{mm}.$$

2. $4/m$; $\bar{3}$; $6/mmm$; $m3m$; $m3$; $4mm$

3. In $m3m$ $|F_{hk\ell}|$ is the same for all permutations of h, k, ℓ in $m3$ $|F_{hk\ell}| \neq |F_{khl}|$.

4. (a) $Pccm, Pcc2$

   (b) $Pbcn$

   (c) $Pn3$

   (d) $P3_121, P3_221$

   (e) $P4/m, P\bar{4}, P4$

   (f) $P4_2/nnm$

Chapter 10

1. $$E = \frac{h^2\mu^2}{2ma^2} = \frac{1}{2}mc^2$$

$$c = \frac{h\mu}{ma} = \frac{6.63 \times 10^{-3} \times 1/2}{9.11 \times 10^{-31} \times 10 \times 10^{-10}} = 3.64 \times 10^5 \text{ ms}^{-1}$$

$\mu/a = P/L \rightarrow (2 \times 10)^{-1} = P/10^6$ and $P = 5 \times 10^4$

2. (a) $k = P/L$

$$\frac{dP}{dk} = L$$

$$\frac{dE}{dk} \cdot \frac{dP}{dE} = L$$

$$\frac{dE}{dk} = \frac{L}{dp/dE}$$

(b) $\dfrac{dE}{dk} \rightarrow 0 \rightarrow \dfrac{dP}{dE} \rightarrow \infty$

3. The essential sym. ops. are: $C_{4z}|\mathbf{c}/2$; $C_{2z}|0$; $C_{4z}^2|\mathbf{c}/2$; $\sigma_z|0$; $i|0$; $\overline{C}_{4z}|\mathbf{c}/2$; $\overline{C}_{4z}^3|\mathbf{c}/2$ and multiplying loaded reps:

$$\hat{\Gamma}(C_{4z})\hat{\Gamma}(\sigma_z) = \hat{\Gamma}(\overline{C}_{4z}^3)$$

and

$$\hat{\Gamma}(\sigma_z)\hat{\Gamma}(C_{4z}) = \exp -((\mathbf{c}^*/2)\cdot(\sigma_z\mathbf{c}/2 - \mathbf{c}/2)\hat{\Gamma}(C_{4z}^3)$$
$$= -\hat{\Gamma}(\overline{C}_{4z}^3)$$

$\therefore$ loaded reps. do not commute and the irr. reps. must be at least 2-D. Since $3^2 = 9 > 8$, there can be no 3-D irr. rep. and thus there are two 2-D irr. reps.

4. $\chi(\tau_1) + \chi(\tau_3) = \chi(\tau_{\text{red}})$

$\therefore$ it splits into a doubly degenerate band and a singly degenerate band.

5. (a) τ_1 and τ_3 at $\delta(\mathbf{a}^* + \mathbf{b}^* + \mathbf{c}^*)$ are compatible with τ_1 and τ_4 at the L point and thus the bands remain one doubly and the other singly degenerate.

   (b) The bands become more bonding as δ in $\delta(\mathbf{a}^* + \mathbf{b}^* + \mathbf{c}^*)$ increases from 0 to 1/2 (Fig. AI.16).

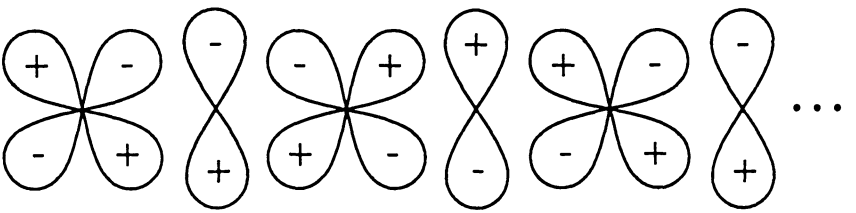

Fig. AI.16. Zone boundary combination of metal d and nonmetal p orbitals in NaCl-type structures.

   (c) At $\mathbf{k} = 0$ there are 3 basis functions each of which is antisymmetric with respect to inversion at the origin and at $\mathbf{a}/2$ — since the d orbitals have g symmetry they cannot contribute to the T_{1u} band and at $\mathbf{k} = 0$ it is nonbonding. At $\mathbf{k} = \mathbf{a}^*/2$, $\mathbf{k}\cdot\mathbf{a} = \pi$ and thus $\varepsilon/\mathbf{a}$ carries each function into its negative — the 2-D irr. rep. for $i|0$ has character 2 and thus carries each function into itself, whereas

$i|\mathbf{a}$ has character -2 and carries each function into its negative, (see Fig. 10.9 for $\mathbf{a}^*/2$).

6. The behavior of xy, yz and xz is summarized;

	ε	C_3	C_{2d}	i	$\overline{C}_3$	σ_d
	xyz	zxy	$yx\bar{z}$	$\bar{x}\bar{y}\bar{z}$	$\bar{z}\bar{x}\bar{y}$	$\bar{y}\bar{x}z$
xy	xy	zx	xy	xy	xz	xy
xz	xz	yz	$-yz$	xz	yz	$-yz$
yz	yz	xy	xy	xy	xz	$-xz$

Thus, xy, yz and xz form a basis for τ_{red} with characters:

τ_{red}	3	0	1	3	0	1
τ_6	2	-1	0	2	-1	0
τ_1	1	1	1	1	1	1

which reduces to τ_1 and τ_6. Using projection operators we find

$$xy + \varepsilon xz + \varepsilon^2 yz$$
$$xy + \varepsilon^2 xz + \varepsilon yz$$

as bases for τ_6, and $xy + xz + yz$ as a basis for τ_1. The functions $P_z(x = 1/2)$, $P_y(z = 1/2)$, $P_z(y = 1/2)$ also form a basis for a reducible rep. which reduces to a τ_6 with

$$x + \varepsilon^2 y + \varepsilon z$$
$$x + \varepsilon y + \varepsilon^2 z$$

and a τ_1 with $x + y + z$ as basis.

(a) First consider $\mathbf{a}^*$ (in Fig. AI.17) vertical. As $\mathbf{k}$ increases along $\mathbf{a}^*$, the interactions between yz orbitals at $x = 0$ and those at $x = 1/2$ take on increasing bonding character. The pi interactions are exactly out of phase at $\mathbf{k} = 0$ and shift to $\pi/2$ phase difference at $\mathbf{k} = \mathbf{a}^*/2$. There is no change in the σ interactions within the $x = 0$ and $x = 1/2$ planes.

(b) Consider **a*** horizontal in Fig. AI.17. As **k** increases, one half of the π interactions become increasingly less antibonding (i.e., the phase difference changes from π toward $\pi/2$ for Zr at 0,0,0 interacting with Zr at $1/2, 0, 1/2$, but remains the same for Zr at 0,0,0 and 0,1/2,1/2); however, the σ interactions (e.g., between 0,0,0 and 1/2,1/2,0) become increasingly out of phase.

Thus, the singly degenerate yz interaction becomes more bonding along $\Gamma - X$, whereas the doubly degenerate xz and xy lose bonding character due to loss of σ bonding.

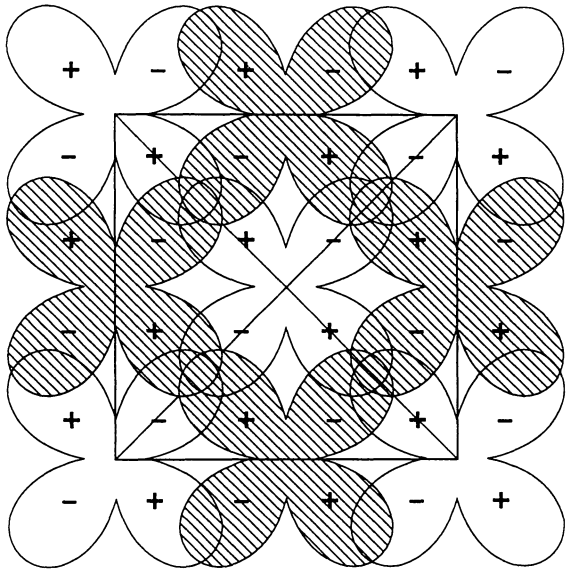

Fig. AI.17. *d–d* interactions in NaCl-type structures.

Chapter 11

1. $Fd3m$ 16: 0,0,0; 0,1/4,1/4; 1/4,0,1/4; 1/4,1/4,0 (+ 1/2,1/2,0; + 1/2,0,1/2; + 0,1/2,1/2)

2. W point: 1,1/2,0; 1/2,1,0; 0,1,1/2; 0,1/2,1; 1/2,0,1; 0,1/2,1.

T	k · T
1/2, 0, 1/2	π
1/2, 1/2, 0	$3\pi/2$
0, 1/2, 1/2	$\pi/2$
0, 0, 1	0
0, 1, 0	π
1, 0, 0	2π
1/2, 1, 1/2	2π
0, 2, 0	2π

(see Fig. AI.18)

(b) 1,1/2,0 + 0,1,1/2 + 1/2,0,1

T	$(a^* + b^*/2) \cdot T$	$(b^* + c^*/2) \cdot T$	$(c^* + a^*/2) \cdot t$
0, 0, 2	0	2π	4π
0, 2, 0	2π	4π	0
2, 0, 0	4π	0	2π

pc with $a = 2a°$

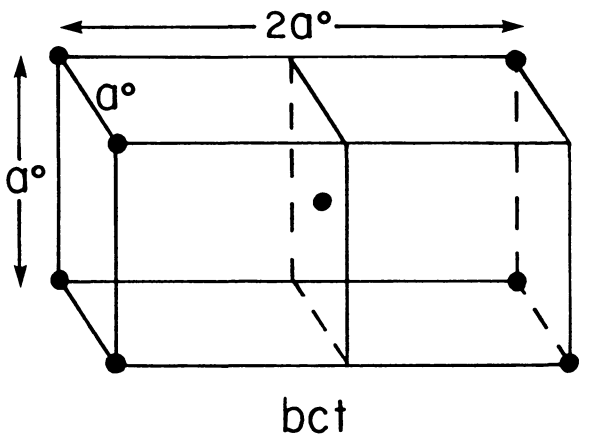

Fig. AI.18. Tetragonal superstructure of *fcc* corresponding to $\mathbf{k} = \mathbf{a}^* + \mathbf{c}^*/2$.

3. See Fig. AI.19.

in	out
300	100
210	200
$1\bar{1}0$	110
	$2\bar{1}0$

$\pm\mathbf{k} = (\mathbf{a}^* + \mathbf{b}^*)/3, (2\mathbf{b}^* + \mathbf{a}^*)/3, (\mathbf{b}^* - 2\mathbf{a}^*)/3.$

4. (a) See Fig. AI.20.

$\mathbf{a}^*, \mathbf{b}^*, \mathbf{c}^*$

$\phi_1 = \cos 2\pi x$

$\phi_2 = \cos 2\pi y$

$\phi_3 = \cos 2\pi z$

$\Delta\rho = \eta(\phi_1 + \phi_2 + \phi_3)$

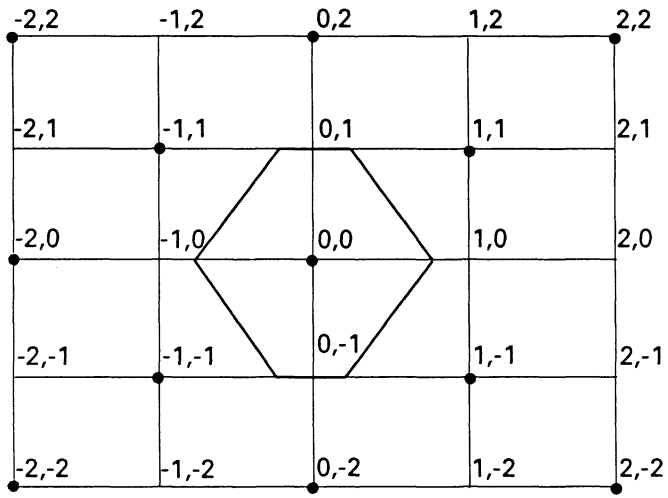

Fig. AI.19. *BZ* for *eco*.

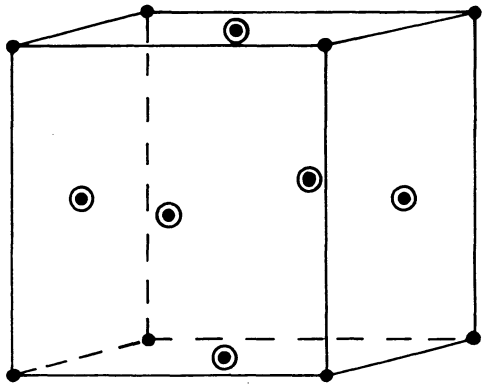

Fig. AI.20. Ordering in *fcc* corresponding to $\mathbf{k} = \mathbf{a}^*$.

(b) Yes, for example $\mathbf{k} = \mathbf{c}^*$, st with $a = a^\circ/\sqrt{2}$.

5. $\mathbf{k} = \mathbf{a}^*/2$

$P4/mmm \rightarrow Pmmm$

$\mathbf{a}_0 = 2\mathbf{a}_t, \mathbf{b}_0 = \mathbf{b}_t, \mathbf{c}_0 = \mathbf{c}_t$

$\mathbf{a}^*/2$ and $\mathbf{b}^*/2$ are in the star

$\phi_1 = \cos \pi x, \phi_2 = \cos \pi y$

x, y	$\cos \pi x + \cos \pi y$
1,0	0
0,1	0
1,1	−2
2,0	2
0,2	2
2,1	0
2,2	2

Ans: t with $a = 2a^\circ$.

6. (a) *Cccm*

   (b) The M atoms are in a *bcc* substructure and the H atoms are ordered in tetrahedral sites (expressing the structure in terms of *bcc*, the M atoms are the 0,0,0, 2-fold positions, and the H atoms are ordered in the 1/2,0,1/4 12-fold positions of $Im3m$.

   (c) Does $Im3m \rightarrow Cmmc$ where $\sqrt{2}a = b = c = \sqrt{2}a_{bcc}$ meet the Landau criteria?

   If the transition corresponds to a single irr. rep. than either $\sigma_z|0$ or $\sigma_z|(\mathbf{a}+\mathbf{b}+\mathbf{c})/2$ and either $\sigma_{y-x}|0$ or $\sigma_{y-x}|(\mathbf{a}+\mathbf{b}+\mathbf{c})/2$ and either $\sigma_{x-y}|0$ or $\sigma_{x+y}|(\mathbf{a}+\mathbf{b}+\mathbf{c})/2$ remain. The axial transformations to *Cccm* are

$$\mathbf{a}_0 = \mathbf{a}_c$$
$$\mathbf{b}_0 = (\mathbf{b}_c - \mathbf{a}_c)$$
$$\mathbf{a}_0 = (-\mathbf{a}_c - \mathbf{b}_c)$$

   Thus, the corresponding operations in C_{cmm} would be

$$\sigma_x|0 \text{ or } \sigma_x|(\mathbf{c}_0 + \mathbf{a}^0)/2$$
$$\sigma_y|0 \text{ or } \sigma_y|(\mathbf{c}_0 + \mathbf{a}^0)/2$$
$$\sigma_z|0 \text{ or } \sigma_z|(\mathbf{c}_0 + \mathbf{a}^0)/2$$

   In C_{ccm} the symmetry planes are parallel to n-glides, i.e., C_{ccm} is equivalent to C_{nnn}, or C_{cnm}, etc. Now,

   $\sigma_x|(\mathbf{c}_0 + \mathbf{a}^0)/2$ is the operation of a c-glide perpendicular to $\mathbf{a}$

   $\sigma_y|(\mathbf{c}_0 + \mathbf{a}^0)/2$ is the operation of a n-glide perpendicular to $\mathbf{b}$

   $\sigma_z|0$ is the operation of a minor perpendicular to $\mathbf{c}$

   Thus, if there exists in irr. rep. of $Im3m$ at $\mathbf{k} = (\mathbf{a}^* + \mathbf{b}^*+)/2$ for which $\sigma_z|0$ and $\sigma_{y-x}|0$ (in $Im3m$) have character -1 and $\sigma_z|0$ has character $+1$, then the transition corresponds to a single irr. rep. This is the case (see the next to the last row of the character table given for D_{2h}).

   Next it must be determined whether there is a third-order invariant. A basis function is:

$$\phi_1 = (\sin 2\pi z)(\sin \pi(x + y))$$

and the irr. rep. is 6-D, i.e.,

$$\phi_1 = (\sin 2\pi z)(\sin \pi(x + y))$$
$$\phi_2 = (\sin 2\pi y)(\sin \pi(z - x))$$
$$\phi_3 = (\sin 2\pi x)(\sin \pi(y - z))$$
$$\phi_4 = (\sin 2\pi z)(\sin \pi(x - y))$$
$$\phi_5 = (\sin 2\pi y)(\sin \pi(x + z))$$
$$\phi_6 = (\sin 2\pi x)(\sin \pi(y + x))$$

By the methods of group theory (the antisymmetric cube contains the identity) it is found that there exists a 3rd-order invariant for the rotations of $Im3m$, and by the method of Section 6.11 it is determined to be

$$\phi_1\phi_2\phi_6 + \phi_1\phi_3\phi_5 + \phi_2\phi_3\phi_4 + \phi_4\phi_5\phi_6.$$

Under the translation $(\mathbf{a} + \mathbf{b} + \mathbf{c})/2$,

$$\phi_1 \rightarrow \phi_1$$
$$\phi_2 \rightarrow -\phi_2$$
$$\phi_3 \rightarrow -\phi_3$$
$$\phi_4 \rightarrow -\phi_4$$
$$\phi_5 \rightarrow \phi_6$$
$$\phi_6 \rightarrow \phi_5$$

and thus the third-order term is not invariant under translation by $(\mathbf{a} + \mathbf{b} + \mathbf{c})/2$.

APPENDIX II

A. $r_{11} = r_{22} = r_{33}$ (all signed permutations of Table 2.5 are possible).

r_{12}	r_{13}	r_{23}	
O	O	O	*c*
O	$-r_{11}/2$	$-r_{11}/2$	*fcc*
$r_{11}/2$	$-r_{11}/2$	$-r_{11}/2$	*fcc*
r_{12}	r_{12}	r_{12}	*r*
$-r_{11}/3$	$-r_{11}/3$	$-r_{11}/3$	*bcc*
r_{12}	$-(r_{12}+r_{11})/2$	$-(r_{12}+r_{11})/2$	*bct*
r_{12}	r_{13}	$-(r_{12}+r_{13}+r_{11})/2$	*bco*

B. $r_{11} = r_{22} \neq r_{33}$ (all signed interchanges of **a** and **b** are possible).

0	0	0	*t*
$r_{11}/2$	0	0	*h*
r_{12}	0	0	*eco*
$r_{33}/4$	$-r_{33}/2$	$-r_{33}/2$	*bct*
r_{12}	$-r_{33}/2$	$-r_{33}/2$	*bco*
$(r_{11}-r_{33})/2$	$-r_{33}/2$	$-r_{33}/2$	*r*
r_{12}	r_{13}	r_{13}	*ecm*
$-(r_{11}+r_{13})/2$	r_{13}	r_{13}	*fco*

C. $r_{11} = r_{33} \neq r_{22}$ (all signed interchanges of a and c are possible).

0	0	0	t
0	$-r_{11}/2$	0	h
0	r_{13}	0	eco
$r_{11}/2$	0	$-r_{11}/2$	bct
r_{12}	r_{13}	r_{12}	ecm
$r_{11}/2$	$-r_{11}/2$	$-r_{11}/2$	r
r_{12}	$-(r_{11}+2r_{12})$	r_{12}	fco
r_{12}	$-(r_{12}+r_{23}+r_{11})$	r_{23}	ecm

D. $r_{11} \neq r_{22} \neq r_{33}$ (pairs of sign changes are possible).

0	0	0	0
$r_{11}/2$	0	0	eco
r_{12}	0	0	m
0	$-r_{33}/2$	0	eco
0	r_{13}	0	m
r_{12}	$-r_{33}/2$	0	ecm
0	0	$-r_{33}/2$	eco
r_{23}	0	0	m
$r_{11}/2$	0	$-r_{33}/2$	bco
r_{12}	0	$-r_{33}/2$	ecm
$-r_{11}/2$	0	r_{23}	ecm
$r_{33}/4$	$-r_{33}/2$	$-r_{33}/2$	fco
r_{12}	$-r_{33}/2$	$-r_{33}/2$	ecm
$-r_{13}/2$	r_{13}	$-r_{33}/2$	ecm
$r_{11}/2$	r_{13}	$r_{13}/2$	ecm
$-r_{33}/2$	$-r_{33}/2$	r_{23}	ecm
$(-r_{13}-r_{11})/2$	r_{13}	$(-r_{13}+r_{33})/2$	ecm
r_{12}	r_{13}	r_{23}	tr

APPENDIX III

The relationship between Axial and Miller Index Transformations.

Let two vector sets be related by

$$\begin{pmatrix} w_{11} & w_{12} & w_{13} \\ w_{21} & w_{22} & w_{23} \\ w_{31} & w_{32} & w_{33} \end{pmatrix} \begin{pmatrix} \mathbf{a}_1 \\ \mathbf{b}_1 \\ \mathbf{c}_1 \end{pmatrix} = \begin{pmatrix} \mathbf{a}_2 \\ \mathbf{b}_2 \\ \mathbf{c}_3 \end{pmatrix},$$

and the reciprocal vectors in the two sets by

$$\frac{2\pi}{V_1}[h_1(\mathbf{b}_1 \times \mathbf{c}_1) + k_1(\mathbf{c}_1 \times \mathbf{a}_1) + \ell_1(\mathbf{a}_1 \times \mathbf{b}_1)]$$

$$= \frac{2\pi}{V_2}[h_2(\mathbf{b}_2 \times \mathbf{c}_2) + k_2(\mathbf{c}_2 \times \mathbf{a}_2) + \ell_2(\mathbf{a}_2 \times \mathbf{b}_2)].$$

Then by substitution

$$\frac{V_1}{V_2}\begin{pmatrix} (w_{22}w_{33} - w_{23}w_{32}) & (w_{23}w_{31} - w_{21}w_{33}) & (w_{21}w_{32} - w_{22}w_{31}) \\ (w_{32}w_{13} - w_{33}w_{12}) & (w_{33}w_{11} - w_{13}w_{31}) & (w_{13}w_{12} - w_{32}w_{11}) \\ (w_{12}w_{23} - w_{13}w_{22}) & (w_{13}w_{21} - w_{11}w_{23}) & (w_{11}w_{22} - w_{21}w_{12}) \end{pmatrix}\begin{pmatrix} h_2 \\ k_2 \\ \ell_2 \end{pmatrix} = \begin{pmatrix} h_1 \\ k_1 \\ \ell_1 \end{pmatrix}$$

Now

$$\begin{pmatrix} w_{11} & w_{12} & w_{13} \\ w_{21} & w_{22} & w_{33} \\ w_{31} & w_{32} & w_{33} \end{pmatrix}\begin{pmatrix} (w_{32}w_{33} - w_{23}w_{32}) & (w_{23}w_{31} - w_{21}w_{33}) & (w_{21}w_{32} - w_{22}w_{31}) \\ (w_{32}w_{13} - w_{33}w_{12}) & (w_{33}w_{11} - w_{13}w_{31}) & (w_{13}w_{12} - w_{32}w_{11}) \\ (w_{12}w_{23} - w_{13}w_{22}) & (w_{13}w_{21} - w_{11}w_{23}) & (w_{11}w_{22} - w_{21}w_{12}) \end{pmatrix}$$

$$= \begin{pmatrix} V_2/V_1 & 0 & 0 \\ 0 & V_2/V_1 & 0 \\ 0 & 0 & V_2/V_1 \end{pmatrix}$$

and thus

$$\begin{pmatrix} w_{11} & w_{12} & w_{13} \\ w_{21} & w_{22} & w_{33} \\ w_{31} & w_{32} & w_{33} \end{pmatrix} \begin{pmatrix} h_1 \\ k_1 \\ \ell_1 \end{pmatrix} = \begin{pmatrix} h_2 \\ k_2 \\ \ell_2 \end{pmatrix}.$$

This page is intentionally left blank

INDEX

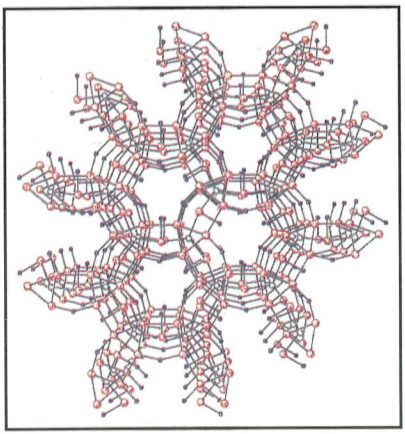

1816 hc

ISBN 981–02–1153–8